Stem Cells International

Challenges in Translating Germinal Stem Cell Research and Therapy

Guest Editors: Irma Virant-Klun, Hong-Thuy Bui, and Mariusz Z. Ratajczak

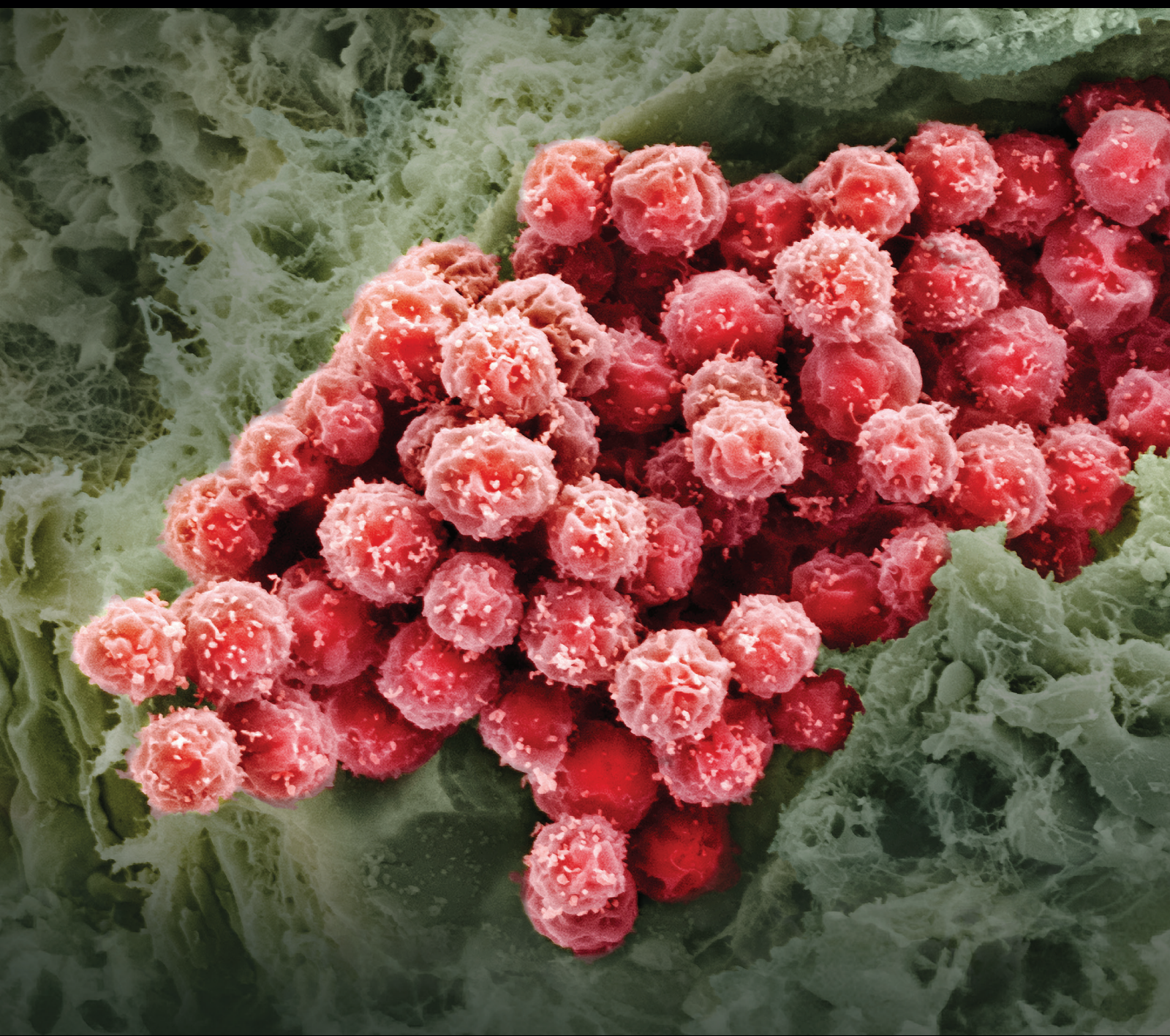

Challenges in Translating Germinal Stem Cell Research and Therapy

Stem Cells International

Challenges in Translating Germinal Stem Cell Research and Therapy

Guest Editors: Irma Virant-Klun, Hong-Thuy Bui, and Mariusz Z. Ratajczak

Editorial Board

Contents

Hindawi Publishing Corporation
Stem Cells International
Volume 2016, Article ID 4687378, 2 pages
http://dx.doi.org/10.1155/2016/4687378

Editorial

Challenges in Translating Germinal Stem Cell Research and Therapy

Irma Virant-Klun,[1] Hong-Thuy Bui,[2] and Mariusz Z. Ratajczak[3]

[1]*Department of Obstetrics and Gynaecology, University Medical Centre Ljubljana, SI-1000 Ljubljana, Slovenia*
[2]*Department of Biotechnology, School of Biotechnology, International University, Vietnam National University, Ho Chi Minh City 70000, Vietnam*
[3]*Stem Cell Institute, James Graham Brown Cancer Center, University of Louisville, Louisville, KY 40202, USA*

Correspondence should be addressed to Irma Virant-Klun; irma.virant@kclj.si

Received 31 August 2015; Accepted 31 August 2015

The field of stem cells research is one of the most exciting and fast developing fields with a great potential to heal different degenerative diseases in regenerative medicine, to better understand cancer and to improve quality of human life. In spite of great enthusiasm and effort, there are several general obstacles and questions about stem cells, which still need to be resolved to enable safe and efficient treatment of degenerative diseases in the future. There are more interesting types of stem cells in humans, as also evidenced by thirteen manuscripts published in this special issue.

Very small embryonic-like stem cells (VSELs) represent one of the most interesting types of stem cells in humans. These small stem cells are suggested to originate in epiblast of an embryo and to persist in a quiescent state in adult human tissues and organs (e.g., bone marrow) from embryonic period of life. They are mobilized into peripheral blood to regenerate the damaged area. It is not excluded that they are involved in tumor formation at inappropriate condition. They have been proven to be multipotent with a degree of pluripotency and able to differentiate into different cell types of all three germ layers. In the manuscript by H. Sovalat et al. it is shown that VSELs have been present in the peripheral blood of healthy volunteers in the same numbers regardless of their age, ranging from 20 to 70 years. Interestingly, endurance exercise such as long-distance running mobilizes VSELs into peripheral blood and increases their number in bone marrow in favor of regeneration, as found by K. Marycz et al. The VSELs have also been identified in bone marrow of other mammalian species such as rat (A. Labedz-Maslowska et al.). Moreover, the VSELs have been proposed by D. Bhartiya et al. to exist in adult mammalian ovaries and to participate in primordial follicle assembly and postnatal oogenesis under the regulation of follicle-stimulating hormone (FSH). This idea has been experimentally supported by M. Zbucka-Kretowska et al. who evidenced the effective release of VSELs into peripheral blood of women treated by FSH hormonal therapy to retrieve the oocytes in the in vitro fertilization program.

The VSELs are related to germinal lineage, especially primordial germ cells (PGCs), and it is not excluded that they are related to germinal stem cells (GSCs) and may be even their progenitors. The PGCs, precursors of gametes, can be generated from stem cells, thereafter, result in birth of mouse pups, and represent an exciting new tool to treat infertility in the future, as reviewed by A. Nikolic et al. The female GSCs, namely, oogonial stem cells, can be efficiently isolated from adult mouse ovaries by a new method provided by Z. Lu et al. and might be also applied to human ovaries. B. Fereydouni et al. have demonstrated the development of oocyte-like cells in long-term cell cultures of neonatal marmoset monkey ovary expressing several genes related to the germinal lineage. The ovarian GSCs are very interesting to regenerate the nonfunctional ovaries although also some other types of cells such as human amniotic epithelial cells can express a beneficial paracrine effect on function of chemotherapy-treated ovaries in a mouse model (X. Yao et al.). The GSCs can also be

retrieved from adult human testicles but are heterogeneous and, along with genes related to the germinal lineage, express more or less pluripotency, as reported by S. Conrad et al. In a mouse model, derivation of embryonic-like stem cells from spermatogonial stem cells (SSCs) depends on animal age (up to 7 weeks of age) and special time window in long-term SSC cultures (H. Azizi et al.). Not only reproductive tissues but also parthenogenetic embryos may represent an interesting source of pluripotent stem cells after activation of nonfertilized oocytes from the in vitro fertilization program, as reviewed by A. Bos-Mikich et al.

Last but not least, the microRNAs, noncoding RNA molecules mediating the translational suppression and post-transcriptional control of gene expression, have been exposed by I. Virant-Klun et al. as extremely important regulators of developmental processes, pluripotency, differentiation, and also shift to cancer.

The manuscripts published in this special issue bring an important new knowledge to the field and arise some new interests and challenges for the future.

Irma Virant-Klun
Hong-Thuy Bui
Mariusz Z. Ratajczak

Hindawi Publishing Corporation
Stem Cells International
Volume 2016, Article ID 2480298, 17 pages
http://dx.doi.org/10.1155/2016/2480298

Research Article

Long-Term Oocyte-Like Cell Development in Cultures Derived from Neonatal Marmoset Monkey Ovary

Bentolhoda Fereydouni,[1] Gabriela Salinas-Riester,[2] Michael Heistermann,[3] Ralf Dressel,[4] Lucia Lewerich,[1] Charis Drummer,[1] and Rüdiger Behr[1]

[1]*Stem Cell Biology Unit, German Primate Center-Leibniz Institute for Primate Research, Kellnerweg 4, 37077 Göttingen, Germany*
[2]*Microarray and Deep-Sequencing Core Facility, University Medical Center Göttingen (UMG), Justus-von-Liebig-Weg 11, 37077 Göttingen, Germany*
[3]*Endocrinology Laboratory, German Primate Center-Leibniz Institute for Primate Research, Kellnerweg 4, 37077 Göttingen, Germany*
[4]*Department of Cellular and Molecular Immunology, University of Göttingen, Humboldtallee 34, 37073 Göttingen, Germany*

Correspondence should be addressed to Rüdiger Behr; rbehr@dpz.eu

Received 28 May 2015; Revised 28 July 2015; Accepted 28 July 2015

Academic Editor: Irma Virant-Klun

We use the common marmoset monkey (*Callithrix jacchus*) as a preclinical nonhuman primate model to study reproductive and stem cell biology. The neonatal marmoset monkey ovary contains numerous primitive premeiotic germ cells (oogonia) expressing pluripotent stem cell markers including OCT4A (POU5F1). This is a peculiarity compared to neonatal human and rodent ovaries. Here, we aimed at culturing marmoset oogonia from neonatal ovaries. We established a culture system being stable for more than 20 passages and 5 months. Importantly, comparative transcriptome analysis of the cultured cells with neonatal ovary, embryonic stem cells, and fibroblasts revealed a lack of germ cell and pluripotency genes indicating the complete loss of oogonia upon initiation of the culture. From passage 4 onwards, however, the cultured cells produced large spherical, free-floating cells resembling oocyte-like cells (OLCs). OLCs strongly expressed several germ cell genes and may derive from the ovarian surface epithelium. In summary, our novel primate ovarian cell culture initially lacked detectable germ cells but then produced OLCs over a long period of time. This culture system may allow a deeper analysis of early phases of female primate germ cell development and—after significant refinement—possibly also the production of monkey oocytes.

1. Introduction

It is a long-held opinion in reproductive biology that in females of most species, including the human, the postnatal germ cell pool is limited in number and cannot be replenished or even expanded. Early studies in the rat showed that oogonia, the proliferating female germ line progenitor cells that enter meiosis to produce oocytes, were found only during fetal development [1]. Human females are also thought to be born with a nonrenewable pool of germ cell follicles which declines with age [2]. In postnatal human ovaries, oogonia were found only very sporadically and were undetectable by the age of two years [3]. A lack of evidence for postnatal germ cell proliferation in human ovaries was also reported by Liu et al. [4]. Instead, by far most of the proliferation-competent oogonia in the human ovary entered meiosis by the end of the second trimester of gestation [5, 6]. Recent studies using transgenic mice and nonhuman primates also reported a lack of evidence for germ cell proliferation in adult mouse [7, 8] and monkey [9] ovaries. However, these data supporting the view of a fixed postnatal female germ cell pool are profoundly challenged by reports starting a decade ago [10, 11], suggesting replenishment of the ovarian germ cell pool in mice. The existence of mitotically active germ line stem cells in postnatal mouse and human ovaries was suggested by the isolation, molecular characterization, and transplantation of cell populations [10, 12]. Probably the strongest evidence so far for a germ line stem cell pool in the ovary was provided by Zou et al. [13], who generated mouse female germ line stem cells (FGSCs) with

the ability to reconstitute oogenesis and produce offspring after transplantation. Other authors reported the production of oocyte-like cells *in vitro* from cultures of adult ovarian surface epithelium (OSE) [14–16]. In summary, currently there are several apparently contradictory reports which provide data supporting or negating generation of new oocytes in the postnatal rodent and primate—including the human—ovary. Adding to this complex situation, Dyce et al. [17] reported that even fetal porcine skin cells can form oocyte-like cells (OLCs) *in vitro*.

We use the common marmoset monkey (*Callithrix jacchus*) as a nonhuman primate model to study reproductive and stem cell biology. In contrast to other species used in reproductive biology, the marmoset monkey still has numerous oogonia in the neonatal ovary, which robustly express the pluripotency associated markers OCT4A, LIN28, and SALL4, the germ cell marker VASA, and the proliferation marker KI-67 [18]. Therefore, these oogonia in the neonatal marmoset ovary share important pluripotency markers with marmoset monkey embryonic stem (ES) cells [19]. We failed to detect this proliferating and pluripotency-marker-positive cell population in the one-year-old and adult ovary [18] indicating a fast postnatal oogonial clearing also in this nonhuman primate species. Here, we report studies on the culture of neonatal marmoset ovarian cells. We originally aimed at culturing the proliferating marmoset monkey oogonia exhibiting a pluripotency signature similar to marmoset monkey embryonic stem cells. Hence, we established a mouse embryonic fibroblast- (MEF-) based cell culture system, which allowed the long-term culture of ovarian cells. However, germ cell and pluripotency marker expression was lost in the first passages indicating the complete loss of the oogonia. After a few passages, however, germ cell marker expression recovered, and we observed in later passages the development of large spherical, free-floating cells which we called oocyte-like cells (OLCs) due to their morphological resemblance with the cells reported by Dyce et al. [17]. OLCs had a diameter up to ~40 μm and strongly expressed several germ cell markers. This study demonstrates the development of oocyte-like cells in long-term ovarian cell cultures from a translational and experimentally accessible nonhuman primate species.

2. Materials and Methods

2.1. Animals. Marmoset monkeys (*Callithrix jacchus*) for this study were obtained from the self-sustaining breeding colony of the German Primate Center (Deutsches Primatenzentrum; DPZ). The German Primate Center is registered and authorised by the local and regional veterinary governmental authorities (Reference number 122910.3311900, PK Landkreis Göttingen). Health and well-being of the animals were controlled daily by experienced veterinarians and animal care attendants. The legal guidelines for the use of animals and the institutional guidelines of the DPZ for the care and use of marmoset monkeys were strictly followed. The animals were pair-housed in a temperature- (25 ± 1°C) and humidity-controlled (65 ± 5%) facility. Illumination was provided by daylight and additional artificial lighting on a 12.00 : 12.00-hour light : dark cycle. The animals were fed ad libitum with a pelleted marmoset diet (ssniff Spezialdiäten, Soest, Germany). In addition, 20 g mash per animal was served in the morning and 30 g cut fruits or vegetables mixed with noodles or rice was supplied in the afternoon. Furthermore, once per week mealworms or locusts were served in order to provide adequate nutrition. Drinking water was always available.

In captivity, marmosets sometimes give birth to triplets or even quadruplets. However, the mother is usually able to feed and rear only two neonates, which is the normal litter size of free-living marmosets. Therefore, the neonates from triplet births were used to collect organs for this study. Marmoset monkey ovaries were obtained from six neonatal animals (postnatal days 1–5). All animals were narcotized with Pentobarbital (Narcoren; 0.05 mL intramuscular) and euthanized by an experienced veterinarian with an intracardial injection of 0.5 mL Pentobarbital before a lack of nourishment caused suffering of the animals. Wherever applicable, the ARRIVE guidelines were followed.

2.2. Numbers of Animals. Altogether, ovaries from 6 neonatal marmosets were used in this study: 5 pairs for culture and one pair as reference for transcriptome analysis.

2.3. Neonatal Common Marmoset Monkey Ovarian Cell Cultures. Neonatal ovaries (approximate dimensions 2 mm × 1 mm × 1 mm; see also [18]) were first collected and washed in a Petri dish containing cold DPBS. Fat and blood cells were removed and the whole ovary including the OSE was transferred to fresh buffer and minced with sterile scissors. Minced ovaries were then transferred to a 15 mL falcon tube. After gentle centrifugation, DPBS was removed and ovarian tissue fragments were resuspended in DMEM/F12 medium containing collagenase (Sigma #C2674) and DNase and kept for 45 minutes at 37°C. Every 5 to 10 min the ovaries were gently pipetted to disintegrate the tissue. Finally, 10% FBS was added to inactivate the enzyme. In order to remove larger undigested tissue fragments, the cells were passed through 70 μm strainer (BD, USA) and were centrifuged at 200 g for 10 min. Then the supernatant was removed and the cells were resuspended in culture medium and transferred on a prepared feeder layer of mouse embryonic fibroblast (MEF) feeder at a concentration 3–5 × 10^5 cells per 5 cm well. After one week large colonies were individually picked with a microprobe (FST, Heidelberg, Germany, #10032-13) and digested with Accutase (Life Technologies, Germany) for 4 min. Then the cells were centrifuged at 300 g for 10 minutes and resuspended in the culture medium for further passages. Cultures were maintained at 37°C under 5% CO_2 and 5% oxygen in a humidified incubator.

2.4. Culturing Neonatal Common Marmoset Ovaries. Different cell culture conditions were tested. Finally this condition was selected: DMEM/F12 supplemented with FBS (10%), Pen/Strep, amphotericin B, and human LIF (10 μg/mL) on an irradiated mouse embryonic fibroblast (MEF) feeder cell layer. For further passages (usually after 7–10 days) colonies

were mechanically removed with a sterile probe, digested with Accutase, and placed on a newly prepared MEF layer.

2.5. Culturing Marmoset Monkey Embryonic Stem Cells. Marmoset monkey ES cells were basically cultured as described previously [20]. Only for passaging of the ES cells, StemPro Accutase (Life Technologies) was used instead of trypsin-EDTA with subsequent mechanical dissociation.

2.6. Immunofluorescence Staining. For immunofluorescence staining, medium was removed and cell colonies were washed twice in PBS and then fixed in 4% PFA for 15 minutes. Cells were permeabilized by 0.1% Triton X-100 in PBS for 10 minutes at room temperature. Primary antibody (VASA, R&D Systems, AF2030) was diluted in 3% BSA-PBS, and colonies were incubated for 1 h at 37°C. Cells were washed twice in PBS. The secondary antibody, which was diluted in 3% BSA-PBS, was added to the cells and incubated for 20 minutes in a dark box at 37°C. Cells were washed again twice in PBS and 5% DAPI-PBS was added. Cells were washed again with PBS and mounted with CitiFluor (Science Services AF1, Glycerol/PBS solution). For negative controls, the primary antibody was (i) omitted or (ii) replaced by IgG isotopes. DAPI staining of the OLCs was performed in 5% DAPI-PBS for 5 minutes followed by two washes in PBS.

2.7. Histology and Immunohistochemistry Staining. Histology of the colonies was performed after mechanically detaching of whole MEF layer including the ovarian cell colonies from the cell culture well. After detachment, the randomly arranged MEF layer was fixed in Bouin's solution for 3 hours, washed several times for at least 24 h in 70% EtOH, and then embedded in paraffin wax. The resulting cell culture conglomerate was randomly sectioned. Due to the large number of colonies sufficient sections of ovarian cell colonies in different orientations were available for histological analysis. Immunohistochemistry was performed as described recently [18] using the following primary antibodies: OCT4A (#2890S, Cell Signaling Technology, Germany; 1 : 100), LIN28A (#3978S, Cell Signaling Technology; 1 : 100–1 : 200), SALL4 (#ab57577, Abcam, UK; 1 : 200), and VASA (DDX4; #AF2030, R&D Systems, Germany; 1 : 100).

2.8. Western Blot Analysis. Western blotting was performed according to standard procedures. In brief, 20 mg of frozen tissue per sample was used. Proteins were isolated by mechanical destruction of the tissue in a TissueLyser at 50 HZ (Qiagen, Hilden, Germany). The samples were denatured for 5 minutes at 95°C. Samples were then run on a 10% SDS-page gel in Tris HCl buffer, pH 8.8, and then semi-dry-blotted onto a PVDF membrane (150 mA for 1 h). Blocking of unspecific binding was achieved by incubating the membrane in 5% skim milk powder diluted in TBS for 1 h. Primary antibodies against VASA (#AF2030, R&D Systems; 1 : 2000) and β-actin (Santa Cruz, SC-1616-R; 1 : 5000) were diluted in blocking buffer. Membranes were incubated in primary antibody solutions for 16 hours at 4°C and then washed three times with blocking solution supplemented with Tween 20. After incubation with the horseradish peroxidase-coupled secondary antibody (1 h at 20°C) the membrane was washed again. Detection of bound antibody was performed using the Amersham ECL Western Blotting Detection Reagents Kit (RPN2106). Signals were detected and documented using the ChemoCam Imager (INTAS, Göttingen, Germany).

2.9. Transcriptome Analysis. For transcriptome analysis, two neonatal marmoset ovaries, colonies from P4 from two different individual animals (100–300 colonies per sample), marmoset skin fibroblasts, and marmoset ES cells were analyzed. Primary fibroblasts were obtained and cultured as described recently [21]. RNA was isolated using the TRIzol Reagent (Life Technologies) according to the manufacturer's instructions. RNA quality was assessed by measuring the RIN (RNA Integrity Number) using an Agilent 2100 Bioanalyzer (Agilent Technologies, Palo Alto, CA). Library preparation for RNA-Seq was performed by using the TruSeq RNA Sample Preparation Kit (Illumina, Cat. number RS-122-2002) starting from 500 ng of total RNA. Accurate quantitation of cDNA libraries was performed by using the QuantiFluor dsDNA System (Promega). The size range of final cDNA libraries was determined applying the DNA 1000 chip on the Bioanalyzer 2100 from Agilent (280 bp). cDNA libraries were amplified and sequenced by using the cBot and HiSeq2000 from Illumina (SR; 1 × 50 bp; 5-6 GB ca. 30–35 million reads per sample). Sequence images were transformed with Illumina software BaseCaller to bcl files, which were demultiplexed to fastq files with CASAVA v1.8.2. Quality check was done via fastqc (v. 0.10.0, Babraham Bioinformatics). The alignment was performed using Bowtie2 v2.1.0 to the cDNA for *Callithrix jacchus*. Data were converted and sorted by samtools 0.1.19 and reads per gene were counted via htseq version 0.5.4.p3. Data analysis was performed by using R/Bioconductor (3.0.2/2.12) loading DESeq, gplots, and goseq packages. Candidate genes were filtered to a minimum of 4x fold change and FDR-corrected p value < 0.05. The data discussed in this paper were generated in compliance with the MIAME guidelines and have been deposited in NCBI's Gene Expression Omnibus and are accessible through GEO Series accession number GSE 64966.

2.10. Quantitative Reverse Transcriptase Polymerase Chain Reaction (RT-qPCR) Analysis. RT-qPCR was carried out as described previously [18]. Total RNA was extracted from different passages of colony-forming cells. Around 50–100 colonies per passage were pooled and analyzed. Three independent cultures (derived from three different animals) were analyzed. Each RNA sample was analyzed in triplicate. As positive controls, neonatal marmoset ovary and marmoset embryonic stem cells were used. Marmoset monkey fibroblasts served as a biological negative control for pluripotency and germ cell markers. Primers are listed in Supplementary Table 1 in Supplementary Material available online at http://dx.doi.org/10.1155/2016/2480298. For oocyte-like cell RNA extractions, altogether 28 cells from different

Table 1: Primer sequences, sizes of amplicons, and concentration of respective primers.

Primer	Primer sequence	PCR product size (bp)	Concentration [nM]
Cj_*GAPDH*_Fw	5′-TGCTGGCGCTGAGTATGTG-3′	64	300
Cj_*GAPDH*_Re	5′-AGCCCCAGCCTTCTCCAT-3′		50
Cj_*LIN28*_Fw	5′-GACGTCTTTGTGCACCAGAGTAA-3′	67	300
Cj_*LIN28*_Re	5′-CGGCCTCACCTTCCTTCAA-3′		50
Cj_*SALL4*_Fw	5′-AAGGCAACTTGAAGGTTCACTACA-3′	77	900
Cj_*SALL4*_Re	5′-GATGGCCAGCTTCCTTCCA-3′		50
Cj_*VASA*_Fw	5′-TGGACATGATGCACCACCAGCA-3′	210	50
Cj_*VASA*_Re	5′-TGGGCCAAAATTGGCAGGAGAAA-3′		900
Cj_*OCT4A*_Fw	5′-GGAACAAAACACGGAGGAGTC-3′	234	300
Cj_*OCT4A*_Re	5′-CAGGGTGATCCTCTTCTGCTTC-3′		50
Cj_*PRDM1*_Fw	5′-ATGAAGTTGCCTCCCAGCAA-3′	147	50
Cj_*PRDM1*_Re	5′-TTCCTACAGGCACCCTGACT-3′		50
Cj_*PRDM14*_Fw	5′-CGGGGAGAAGCCCTTCAAAT-3′	91	50
Cj_*PRDM14*_Re	5′-CTCCTTGTGTGAACGTCGGA-3′		50
Cj_*DAZL*_Fw	5′-GAAGAAGTCGGGCAGTGCTT-3′	70	50
Cj_*DAZL*_Re	5′-AACGAGCAACTTCCCATGAA-3′		50
Cj_*DPPA3*_Fw	5′-GCGGATGGGATCCTTCTGAG-3′	129	50
Cj_*DPPA3*_Re	5′-GAGTAGCTTTCTCGGTCTGCT-3′		50
Cj_*NOBOX*_Fw	5′-GAAGACCACTATCCTGACAGTG-3′	320	50
Cj_*NOBOX*_Re	5′-TCAGAAGTCAGCAGCATGGGG-3′		50
*Cj_SCP3*_Fw	5′-TGGAAAACACAACAAGATCA-3′	60	50
*Cj_SCP3*_Re	5′-GCTATCTCTTGCTGCTGAGT-3′		50

passages were collected and randomly divided into two groups. The RNA was isolated with the RNeasy MICRO kit (Qiagen) according to the manufacturer's instructions. To analyze the relative gene expression level changes during the culture within one passage, colonies from P7 were seeded into 8 separate wells. The cells from two wells were harvested for analysis at days 2, 4, 6, and 8. Primer sequences, sizes of PCR products and primer concentrations are given in Table 1.

2.11. Hormone Measurements. Measurement of progesterone in the selected cell culture medium samples after at least 3 days of conditioning was performed using an enzyme immunoassay (EIA) using antiserum raised in sheep against progesterone-11-hemisuccinate-BSA as described by Heistermann and colleagues [22]. Fresh medium was used as control. Estradiol-17β was determined using an EIA according to Heistermann et al. [23] with the exception that 17β-estradiol-6-horse-radish-peroxidase was used as label. Both steroid measurements were performed in undiluted samples and fresh medium was used as control.

2.12. Cell Transplantation Assay. In order to test the cultured ovarian cells for their regenerative and tissue neomorphogenesis potential, we subcutaneously injected ~10^6 cells per mouse. The cells were obtained from Accutase-treated ovarian cell colonies from the 5th passage. Four female adult RAG2$^{-/-}\gamma c^{-/-}$ mice lacking B, T, and NK cells were used. The technical procedure has been described previously for neonatal testis tissue [24].

3. Results

3.1. General Observations and Morphology of the Primary Cell Cultures. We established a long-term primary culture of ovarian cells. This included passaging as well as expansion of the cells. Five individual primary cultures of neonatal marmoset ovaries were performed and run up to 6 months with very similar morphology and kinetics. The maximum passage number was 23. Then the cells stopped proliferation. Initially, relatively small ovarian cell colonies (OCCs) formed which could be distinguished from the MEFs by the morphology of the cells and the colonies' boundaries (Figure 1(a)). The OCCs quickly increased in size forming big colonies with diameters up to 1000 μm (Figure 1(b)) within a few days. The cells forming the OCCs exhibited an epitheloid phenotype as judged from morphology (Figure 1(d)); that is, they are apparently polar with apical nuclei, and no intracellular matrix was visible between the cells forming the colonies by light microscopy. However, the cells lacked typical epithelial markers such as E-cadherin (CDH1). For further details, see below. In higher passages the individual OCCs became smaller (compare Figures 1(b) and 1(c)). Some OCCs developed in their centers a second layer of cells on top of the primary cell layer (Figure 1(c)). The morphology of the colonies was faintly reminiscent of primate ES cell colonies [20] (Figure 1(e)). Colonies with the morphology of OCCs were never observed in pure mouse embryonic feeder cell cultures.

3.2. OCCs Lack a Germ Cell Population in Early Passages. In order to initially compare the neonatal ovary-derived cell

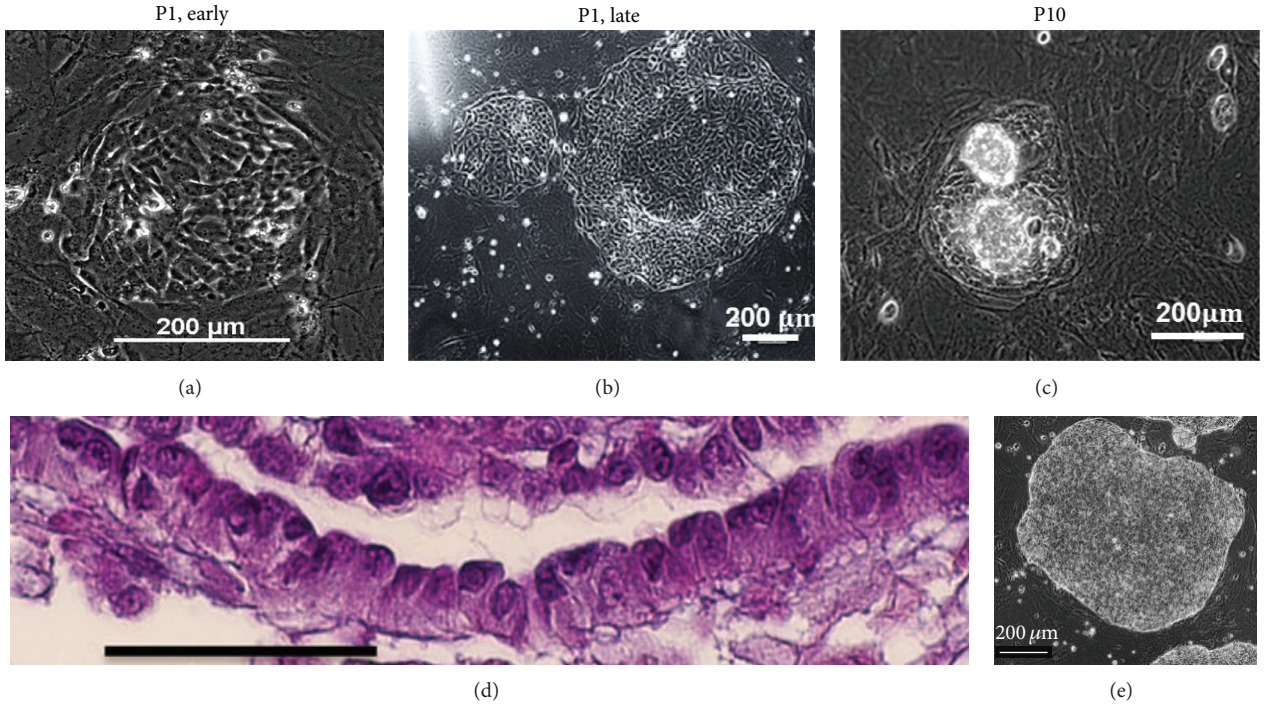

Figure 1: Morphology of ovarian cell colonies (OCCs). (a–c) Morphology of cell colonies in the first passage and in higher passages. (d) H&E staining of cross sections of colonies. Cells have an epitheloid morphology with rather apical nuclei. (e) Morphology of a marmoset monkey ES cell colony.

colonies on the transcriptome level with reference samples we performed a comprehensive transcriptome analysis of OCCs by deep sequencing and compared the data set with the transcriptomes of neonatal ovaries, which served as starting material and contained oogonia, marmoset ES cells as a reference for pluripotent cells, and skin fibroblasts, which represent prototypic mesenchymal cells. Each individual sample's transcriptome was represented by at least 12 Mio. reads (Supplementary Figure 1). About 40.000 different transcripts were detected in each individual sample (Supplementary Figure 2). We used low passage number samples (passage 4) in order to obtain data from cells without extensive cell culture adaptation artefacts. Due to the very limited material, only two independent OCC samples and two neonatal ovaries could be analyzed. However, already this small set of samples provided valuable insights (Figure 2). The OCC samples were clearly distinct from native ovary and fibroblasts (Figure 2(a)). In contrast, the differences between the OCCs' and the ES cells' transcriptomes were smaller. Importantly, the PCA plot (Figure 2(a)) indicates fundamental differences between the transcriptomes of ovaries and OCCs. Notably, the top 50 differentially expressed genes between native ovaries and OCCs revealed two major facts (Figure 2(b)). (1) Almost all differentially expressed genes were overrepresented in the native ovary. This suggests that the OCCs generally represent a subpopulation of the whole cell population constituting the native ovary and that no completely different or novel cell type developed in culture, at least not in detectable quantities. (2) Among the top 50 differentially expressed genes are numerous germ-cell-specific genes like *MAEL*, *RNF17*, *TEX12*, *TDRD9*, *MOV10L1*, *NOBOX*, *ZP3*, *FIGLA*, *SOHLH2*, *DAZL*, and *SYCP2*. In fact, several germ cell genes, including *DAZL*, *MAEL*, *RNF17*, *TEX12*, *TEX101*, and *TDRD*, were totally undetectable in the transcriptomes of the OCCs. Other transcripts like *OCT4*, *LIN28*, and *VASA* were also extremely low or absent. This strongly indicates the complete loss of the typical neonatal ovarian germ cell population, including postmigratory PGCs, oogonia, and oocytes in the cell culture.

The comparison between the OCCs and the fibroblasts revealed an increased expression of many genes in the OCCs (Figure 2(c)). The upregulated genes include *COL2A1*, the keratin gene *KRT36*, and *VCAM1*. Importantly, however, no germ cell gene was found upregulated in OCCs compared to fibroblasts, further substantiating the absence of germ cells from the OCC cultures. The comparison of the top 50 differentially expressed genes between the OCCs and the ES cells showed that most genes were upregulated in ES cells, like *TDGF1*, *LIN28A*, *OCT4* (*POU5F1*), and *NANOG*. Only a few genes including the dual specificity phosphatase 13 (*DUSP13*) and the serine peptidase inhibitor, Kazal type 1 (SPINK1), were upregulated in OCCs (Figure 2(d)).

The detailed cellular identity of the OCCs could not be determined so far. Many of the cells of the OCCs were proliferation marker Ki-67-positive (Supplemental Figure S3). Although the cells had an epitheloid shape, we failed to detect E-cadherin in the transcriptome data as well as by IHC (data not shown). Also cytokeratins as characteristic proteins of epithelial cells were only barely represented in the transcriptomes. Vimentin as typical protein of cells of mesenchymal origin was expressed at medium levels (~50% of neonatal ovary levels and 30% of fibroblast levels). However,

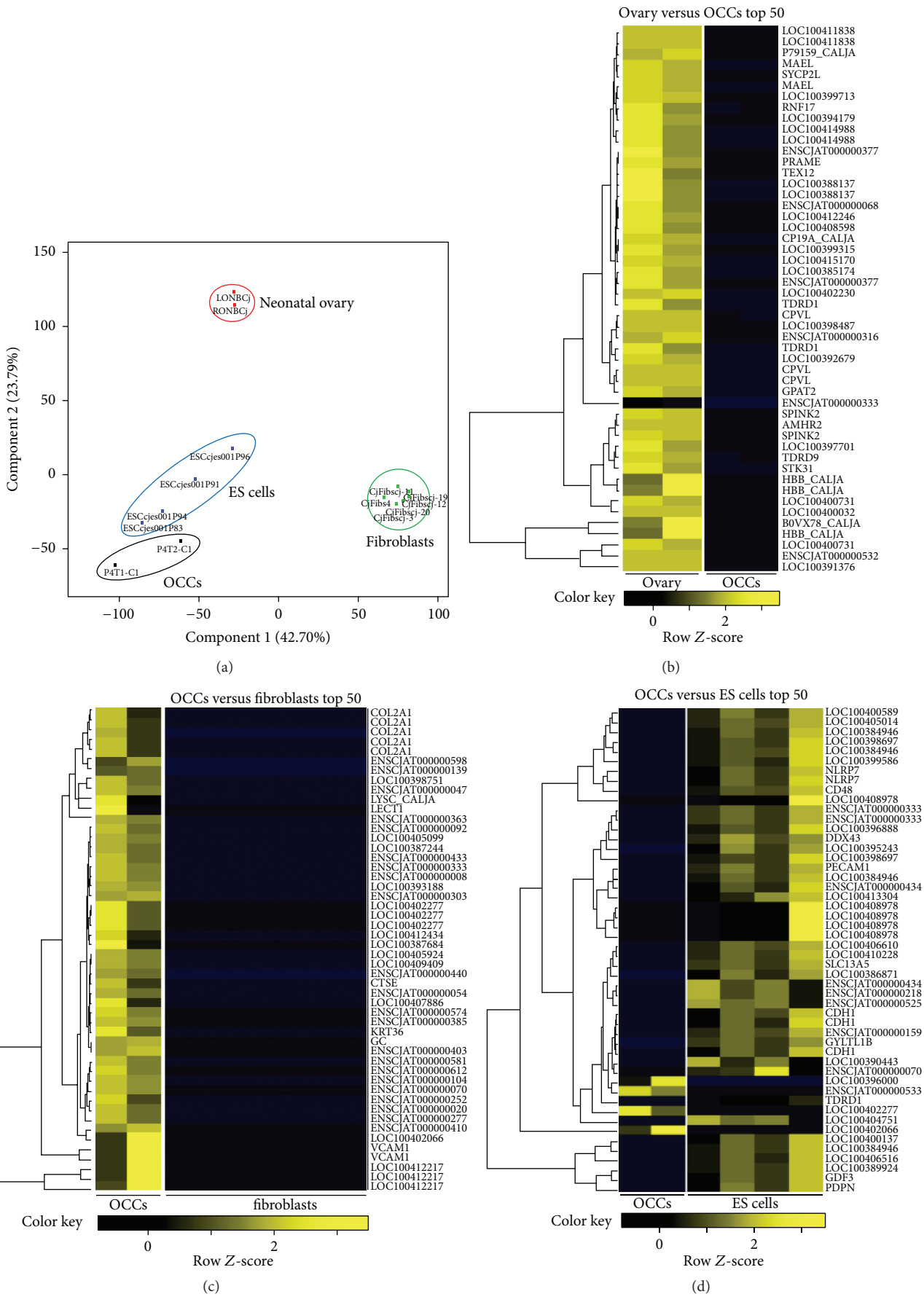

Figure 2: Continued.

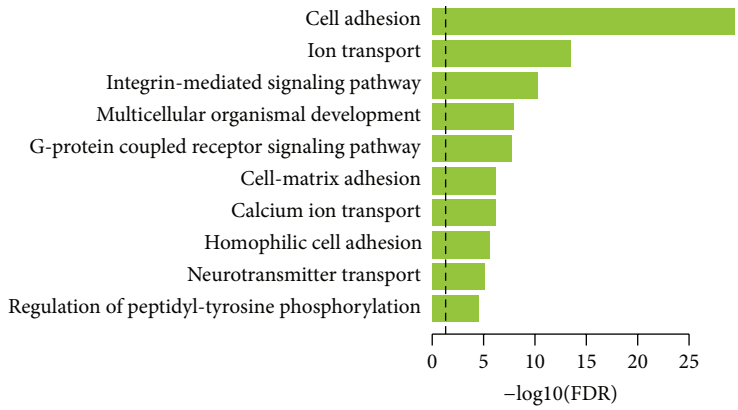

(e)

Figure 2: Transcriptome analysis of OCCs. (a) Principal component analysis of the transcriptome analyses of ovarian cell colonies (OCCs), neonatal ovaries, which served as starting material for OCC cultures, embryonic stem cells, and fibroblasts. The latter two served as reference samples. OCC transcriptomes differ from the neonatal ovaries' transcriptomes. However, ovaries, ES cells, and OCCs are more similar among each other than to fibroblasts (see component 1, relative weight of 38.54%). (b) Top 50 differentially expressed genes between native neonatal ovary and OCCs. For gene bank and Ensembl identifiers, see Table 1 of Supplementary Material. (c) Top 50 differentially expressed genes between OCCs and fibroblasts. (d) Top 50 differentially expressed genes between OCCs and ES cells. (e) Gene ontology analysis of OCCs versus native ovary. Cell adhesion, ion and neurotransmitter transporters, and signaling pathways are predominantly upregulated in OCCs compared to the native ovary.

other cadherins such as CDH2 (at similar levels in cultured ovarian cells compared to ovaries, fibroblasts, and ES cells) and CDH22 (the same range as neonatal ovaries, 10–20% of fibroblasts, and 50% of ES cells) were expressed by the OCCs. Hence, the phenotypical and molecular indicators of the status of the cells constituting the OCCs are not congruent. In order to initially characterize the features of the OCCs we performed a gene ontology analysis based on the genes upregulated in OCCs compared to native ovary (Figure 2(e)). This shows that particularly cell adhesion, ion and neurotransmitter transport, and signaling pathways are upregulated in the OCCs.

In summary, the transcriptome data indicate that germ cells are absent from the OCCs. However, the detailed identity of the OCCs remains unclear so far. Due to the limited number of samples ($n = 2$) and the fact that we could analyze only one time point by deep sequencing, we further investigated specific genes by RT-qPCR in different passages to obtain also longitudinal data over the course of the OCC culture.

We have recently shown that the neonatal marmoset monkey ovary contains primitive proliferating germ cells expressing the germ cell and pluripotency markers OCT4A, SALL4, LIN28, and the general germ cell marker VASA (DDX4) [18]. All these markers are only very poorly represented in the transcriptomes of the early passage OCCs or were even absent. We also failed to detect OCT4A, LIN28, or VASA on the protein level in early passage OCC samples by a well-established immunohistochemistry protocol [18] (data not shown). In order to quantify the expression of selected key marker genes in OCCs in relation to ES cells, skin fibroblasts, and neonatal ovaries by an independent method and also at higher (>4) passages, we performed RT-qPCR for a number of pluripotency and (premeiotic) germ cell markers including *OCT4A* [25], *NANOG* [25], *SALL4* [26], *LIN28* [27], *VASA* [28, see also Figure 5], *DAZL* [29], *NOBOX* [30], *DPPA3/STELLA/PGC7* [31, 32], *PRDM1* [33], and *PRDM14* [34, 35]. Figure 3 shows the exemplary RT-qPCR data of one culture from passage 1 to passage 13. These data confirm that the most indicative pluripotency factors *OCT4A* and *NANOG* were not expressed in all OCC samples analyzed (Figure 3). In contrast, *SALL4*, *LIN28*, and *VASA* were induced in passages ≥P4 except for SALL4 and LIN28 in P9. In order to further substantiate these findings, we also tested the expression of *PRDM1, PRDM14, DAZL, DPPA3, NOBOX*, and *SCP3* in the OCCs from different passages (Figure 4). *DAZL, DPPA3, NOBOX*, and *SCP3* as specific germ cell genes were absent or very low at low passages, which is in concordance with the data shown in Figure 3. In later stages, however, all markers were detectable at variable levels. In contrast, *PRDM1* and *PRDM14*, early germ cell specification genes but not specific to germ cells, were robustly expressed in all cell culture samples. These data suggest that our culture supports the survival and probably also the selection of cells that have the potential to (re)express a set of premeiotic and female germ cell marker genes.

3.3. The OCCs Generate Oocyte-Like Cells. OCCs generated large, free-floating spherical cells, which we termed oocyte-like cells (OLCs; [17]). OLCs had a morphology resembling immature oocytes. Their diameter ranged from 20 to ~40 μm (Figure 5(a)). We sometimes also observed small structures slightly resembling polar bodies (Figure 5(a), right picture). However, we never observed *Zona pellucida* nor follicle-like structures as described by Dyce et al. [17]. For comparison of the OLCs with real marmoset monkey oocytes, see Figure 5(b). Importantly, OLCs developed even after 20

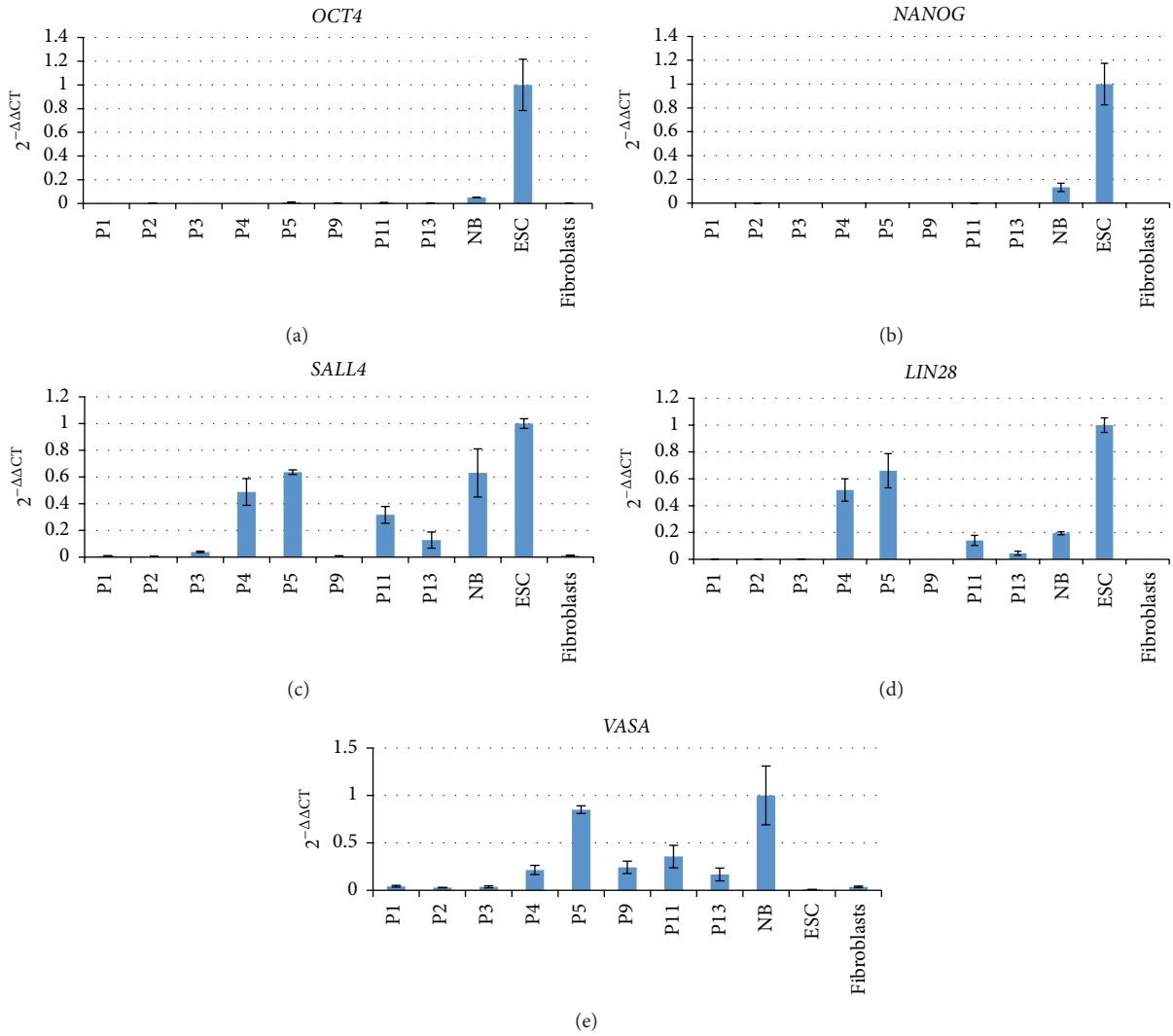

Figure 3: RT-qPCR analysis of OCCs in different passages. Real-time quantitative RT-PCR analysis of selected key pluripotency and germ cell markers in OCCs. *OCT4, NANOG, SALL4*, and *LIN28* are all robustly expressed in pluripotent stem cells as well as in primitive germ cells. In contrast *OCT4* and *NANOG* are absent from OCCs. *SALL4* and *LIN28* were absent or very low at low passages and increased in expression at higher passages. *VASA* is a general germ cell marker and was detected in later OCC passages and in the neonatal ovary.

passages and more than 5 months of culture but were not observed in passages < 4. We also observed OLCs neither in MEF-only cell cultures nor in ESC cultures which are also based on MEFs. This strongly indicates that the OLCs indeed derive from the OCCs. To initially characterize the OLCs, we tested the expression of key pluripotency and germ cell markers by RT-qPCR. We collected 28 OLCs and randomly allocated the cells to one of two groups (termed OLCs1 and OLCs2), which were then analyzed. *OCT4A, NANOG*, and *LIN28* were low in OLCs compared to ES cells and neonatal ovaries (Figures 5(c)–5(e)). *SALL4* was robustly expressed (Figure 5(f)) in the range of the controls. In contrast, *PRDM14, DPPA3, DAZL*, and *VASA* were much higher in OLCs than in neonatal ovary indicating very robust expression of these germ cell markers in OLCs (Figures 5(g)–5(j)). *NOBOX* was in a similar range as in the neonatal ovary. Importantly, *DAZL, VASA*, and *NOBOX* are specific germ line markers and are all not expressed by ES cells and fibroblasts (Figures 5(i)–5(k)). As a marker of meiosis, we also tested *SCP3*. This mRNA was also detected in OLCs, although at lower levels compared to the neonatal ovary (Figure 5(l)). *SCP3* was undetectable in ES cells and fibroblasts. A good indicator of meiosis is chromatin condensation in preparation of the reduction division (Figure 5(m), left). However, we did not see a comparable chromatin condensation in OLCs. In contrast, the OLCs showed a homogenous DAPI signal throughout the nucleus (Figure 5(m), right). Although there was no evidence for meiosis, the expression of the markers strongly indicates a germ cell identity of the OLCs. In order to further corroborate the germ line identity of the OLCs we aimed at detecting also VASA protein in the OLCs. First we characterized the VASA antibody to prevent misleading antibody-based results as we [36] and others [37] recently described. In western blot analysis a

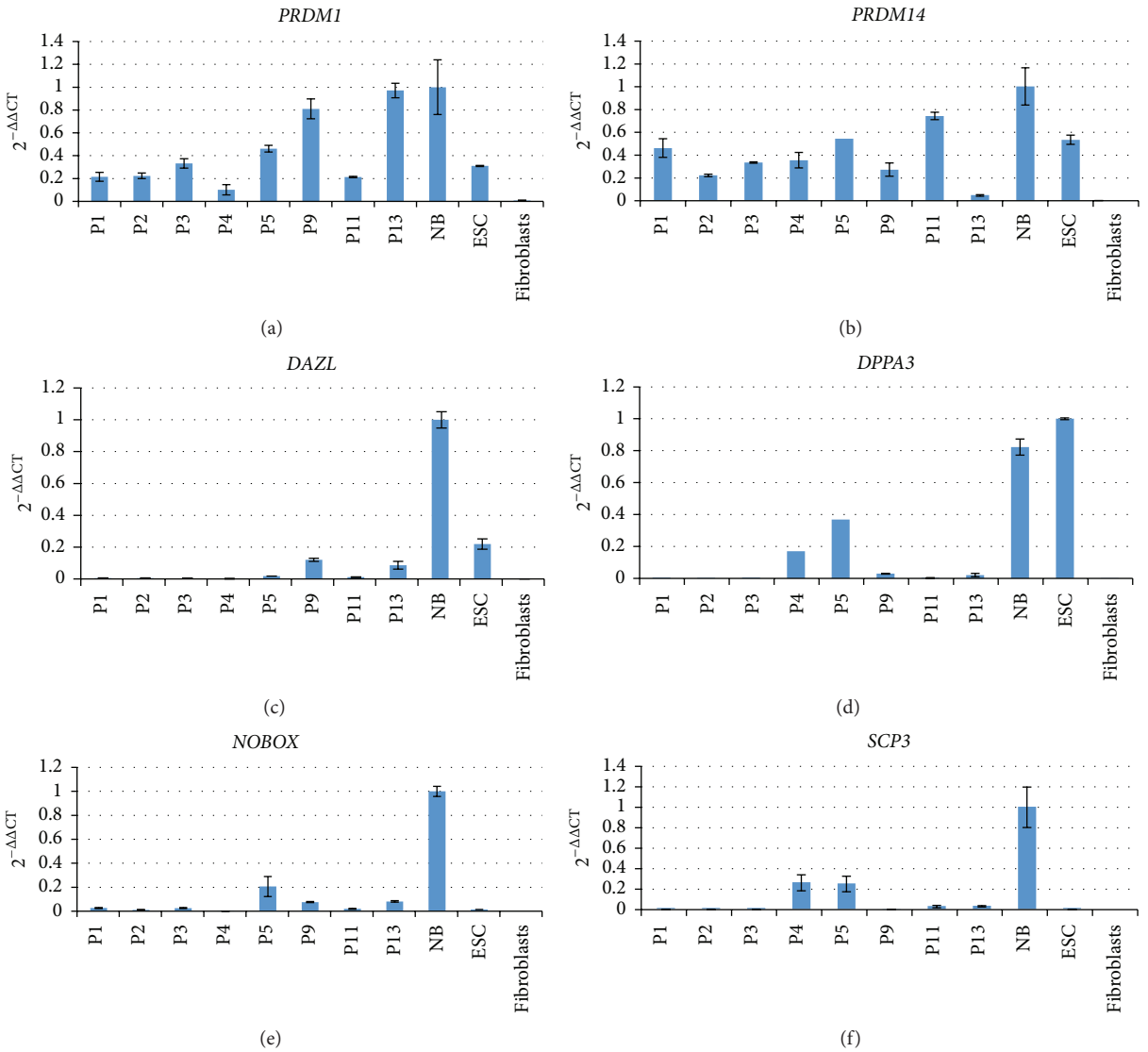

Figure 4: Expression of additional germ cell markers in OCCs. *PRDM1* and *PRDM14* are necessary for germ cell specification and are expressed in all OCC passages in the range of the controls. *DAZL* and *DPPA3* are also necessary for germ cell specification and were detectable only in few samples. *NOBOX* is a female-specific germ cell marker and was detectable at relatively low levels in most samples. *SCP3* is a meiosis marker and was detectable only in some samples at variable levels. In general, the germ-cell-specific markers were very low or absent during the first three passages.

very intense and prominent band of the expected size of ~85 kDa was detected in testis indicating a high specificity of the VASA antibody (Figure 6(a)). Lack of a VASA signal in the ovary was due to the fact that the ovary was from an old monkey with an almost exhausted ovarian germ cell reserve. Hence, VASA was below the detection limit in the protein homogenate of the aged ovary. We also tested the VASA antibody in immunohistochemistry on tissue sections from adult marmoset testis and ovary (Figures 6(b) and 6(c)). In both sexes, the antibody very robustly and specifically detected an epitope in germ cells resulting in clear cytoplasmic germ cell labeling. The nongerm cells were not stained or showed only faint background staining. These findings demonstrate the specificity of the antibody also for marmoset VASA protein. We then used this antibody to detect potential OLCs in OCCs. When we fixed OCCs of the 5th passage *in situ*, large cells with strongly condensed chromatin, as indicated by strong DAPI fluorescence in Figure 6(d), were labeled by the VASA antibody (Figure 6(e)). Whether the signal of the surrounding cells is only background staining or whether it highlights small germ cell progenitor cells cannot be decided at present. The diameter of the large labeled cell was approximately 35 μm like the diameter of the OLCs shown in Figure 5(a). We also detached the cell cultures from the culture dish and processed them—like the testis and ovary shown in Figures 6(b) and 6(c)—for immunohistochemistry. We detected large isolated cells that were strongly stained for VASA (Figures 6(f) and 6(g)). The control where VASA was replaced by the corresponding IgG showed only very faint background signals (Figure 6(h)). These data demonstrate

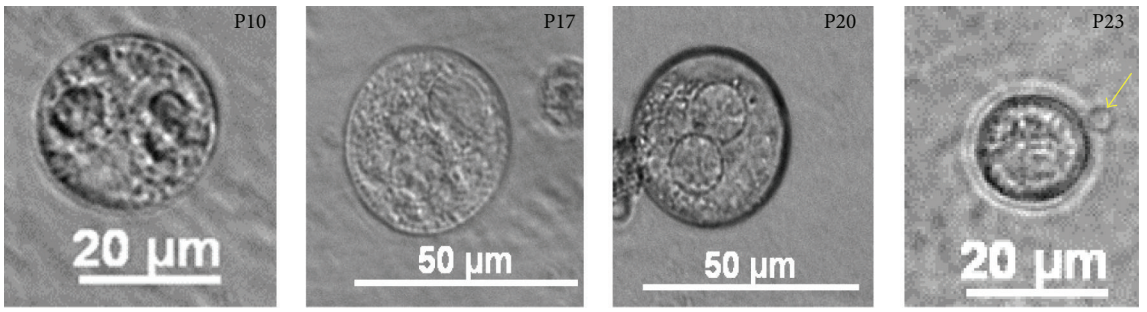

(a)

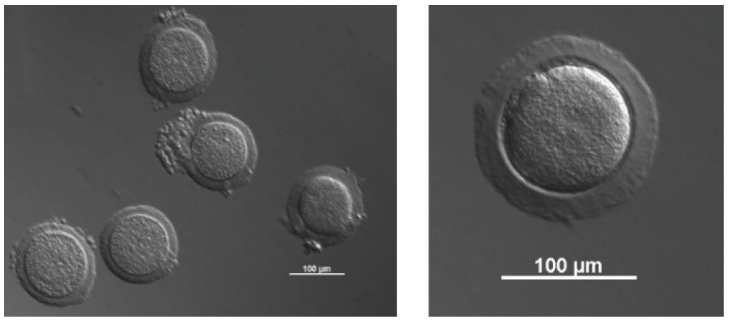

(b)

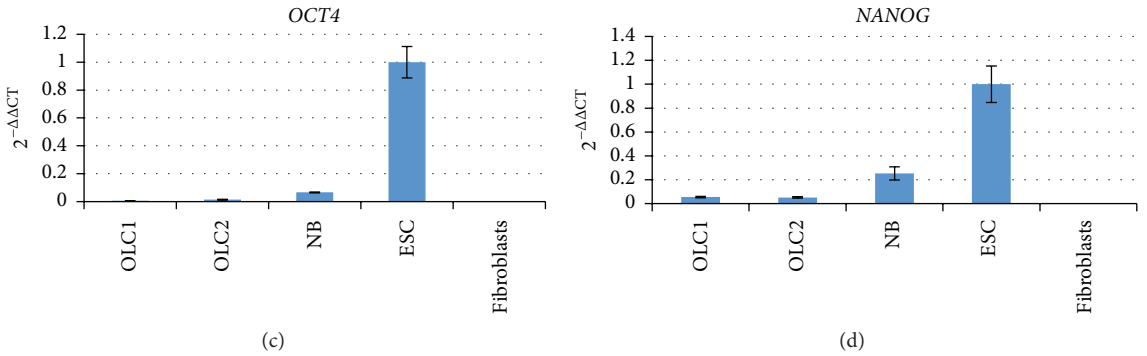

(c) (d)

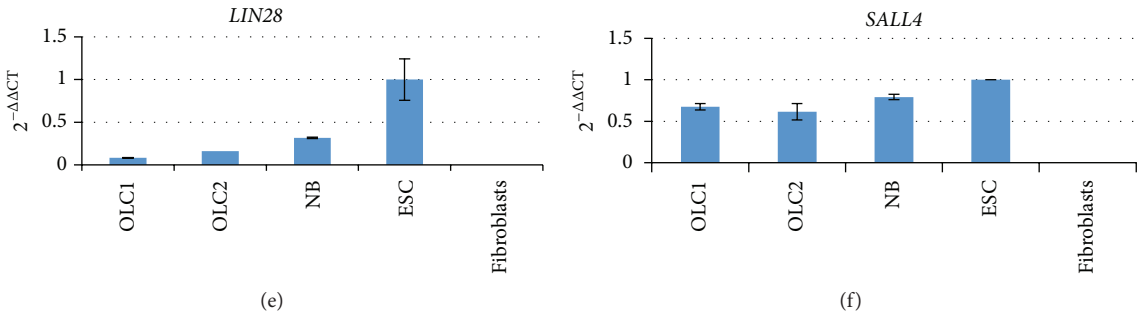

(e) (f)

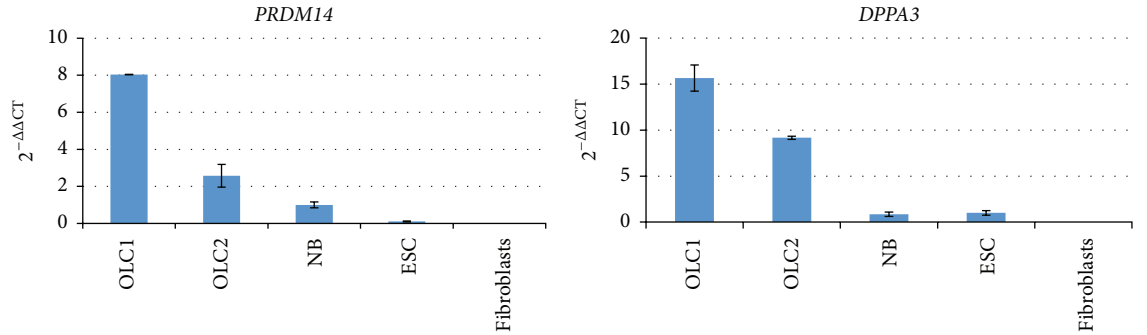

(g) (h)

Figure 5: Continued.

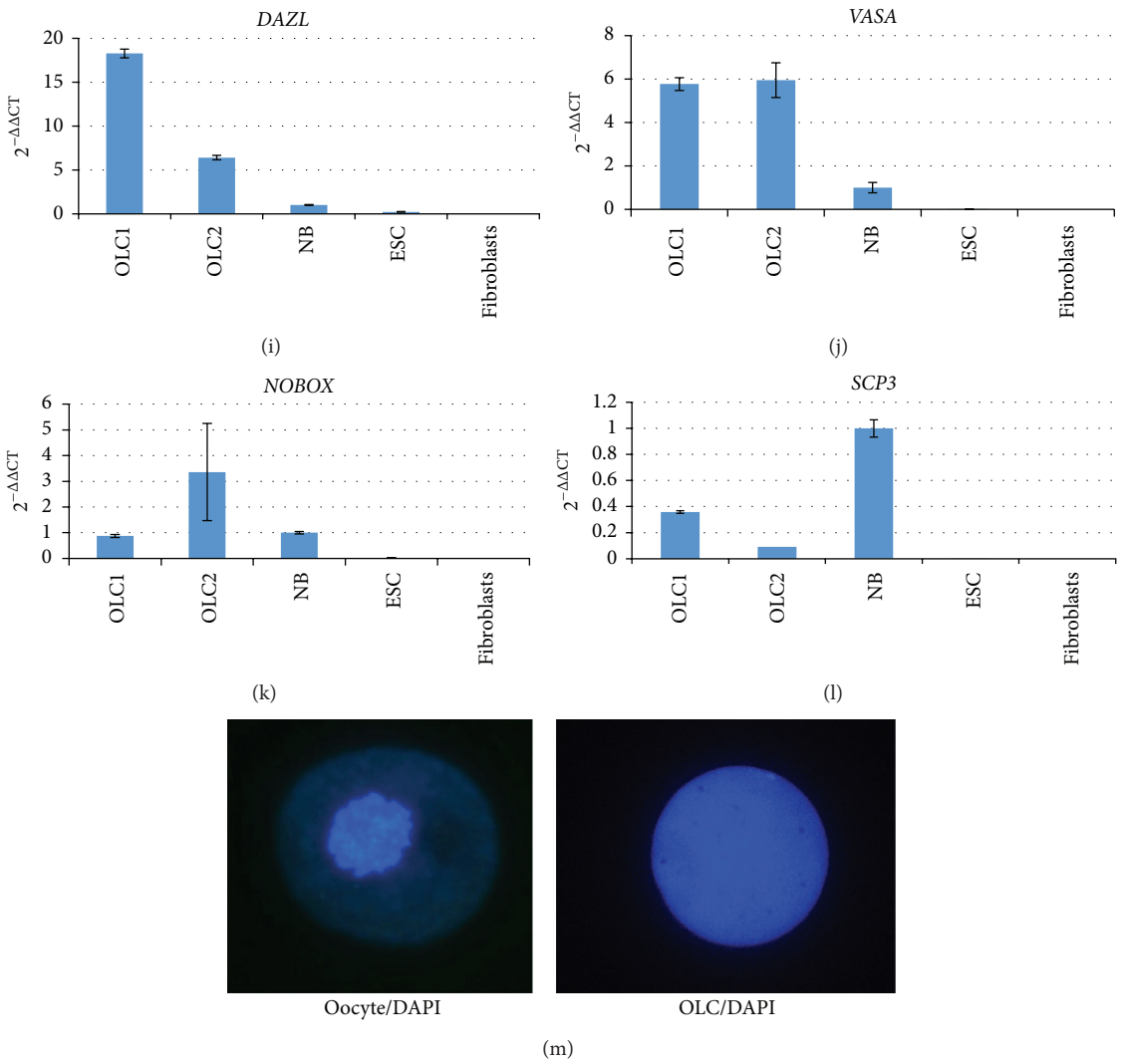

Figure 5: Oocyte-like cells derived from OCCs highly express germ cell markers. (a) Oocyte-like cells that spontaneously developed even in high cell culture passages. The cells were freely floating in the cell culture medium and had a diameter of approximately 40 μm. The passage number is indicated in the upper right corner of each picture. Sometimes small spherical structures attached to the OLCs could be seen slightly resembling polar bodies (arrow). (b) Left: a group of natural marmoset monkey oocytes. Some oocytes are still associated with granulosa cells. Right: higher magnification of a marmoset monkey oocyte with a robust *Zona pellucida*. (c–l) Oocyte-like cells express pluripotency and germ cell markers. Relative mRNA levels of selected pluripotency and germ cell markers in oocyte-like cells as revealed by real-time quantitative RT-PCR. For *OCT4A*, *SALL4*, and *LIN28*, ES cells were used as positive control. Neonatal ovary was used as positive control for the germ cell markers. Fibroblasts served as biological negative control. (m) DAPI staining of a natural oocyte (left) and of an OLC. While the oocyte shows strongly compacted chromatin, the DAPI staining of the OLC is homogenous indicating a different chromatin state in OLCs and natural oocytes.

that there are isolated VASA protein-positive oocyte-like cells in the cultures derived from neonatal marmoset monkey ovary.

3.4. The Relative Marker Abundance Is Decreasing within One Passage. To obtain initial information on the transcript abundance of the markers during the OCC development over time within one passage, we isolated RNA from duplicate samples from OCCs after 2, 4, 6, and 8 days. *OCT4A*, *NANOG*, and *LIN28* were very low or absent (Figures 7(a)–7(c)). In contrast, *SALL4* and *VASA* were robustly detectable in all samples (Figures 7(d) and 7(e)). Both markers exhibited a high abundance at day 2. Later time points (days 4–8) showed a decrease in transcript abundance relative to *GAPDH* probably reflecting a higher proliferation rate of the marker-negative (but *GAPDH* expressing) cells compared to the marker-positive cells leading to a dilution effect of the *VASA*- and *SALL4*-positive cells.

3.5. No Production of Sex Steroids by the OCCs. We were wondering whether the OCCs have the ability to produce female sex steroids like specific cells of the ovary *in vivo*. Therefore, we tested medium samples from low and high culture passages after several days without medium change. Samples were analyzed for estradiol, which is primarily produced by ovarian granulosa cells, and progesterone, which

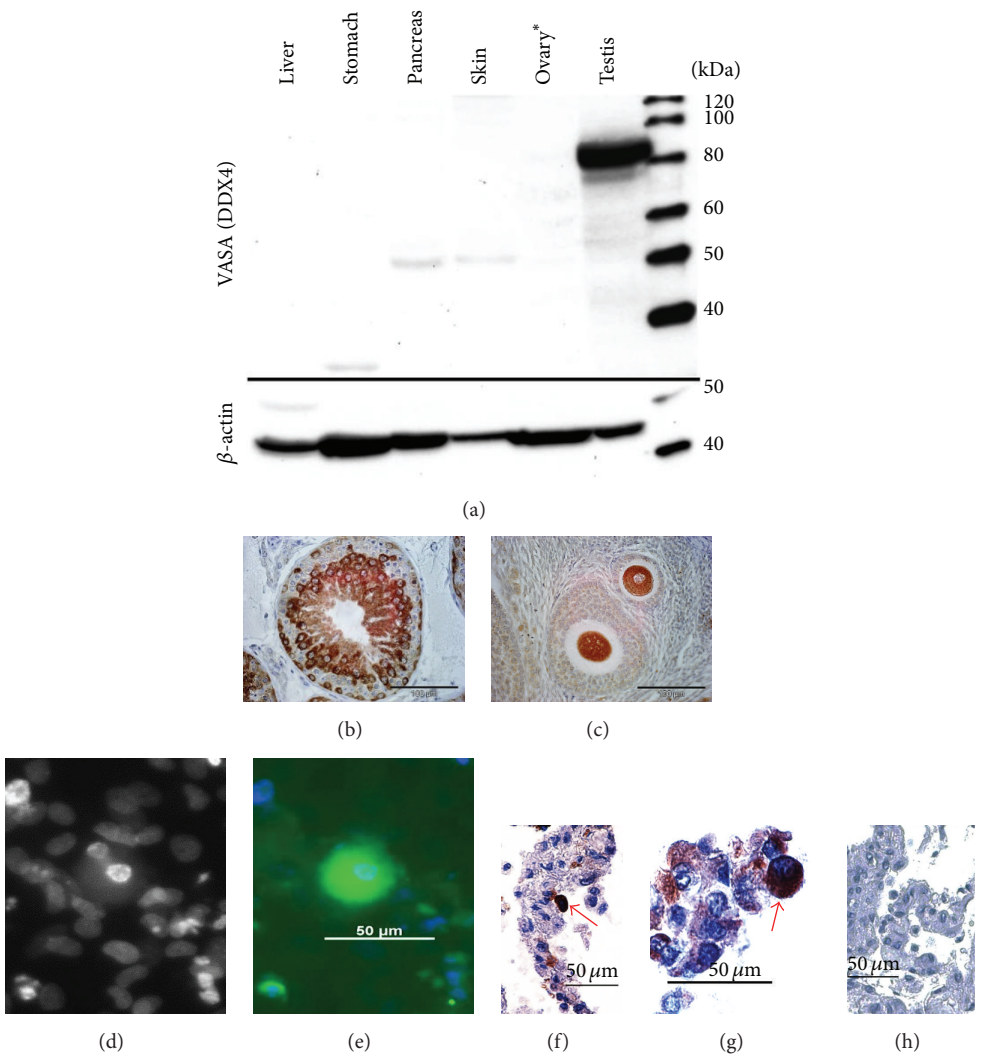

Figure 6: Characterization of the VASA antibody and detection of VASA-positive cells in OCCs. (a) Western blot analysis using marmoset monkey protein samples demonstrates the specificity of the VASA antibody. ∗ indicates that the ovary was from an aged animal. The ovarian germ cell pool was therefore most likely strongly reduced or even exhausted leading to undetectable VASA protein concentrations in the sample. (b and c) Immunohistochemical application of the VASA antibody to marmoset gonads showed germ-cell-specific labeling in the adult testis and the adult ovary. (d) DAPI staining of a part of an OCC. Note the intensely stained nucleus in the central part. (e) The same area shown in (d). The large cell containing the intensely stained nucleus strongly stains for VASA. The signal is blurry due to the fact that the picture was taken through the bottom of a normal cell culture dish. (f, g) Examples of isolated VASA-positive cells in sections of paraffin-embedded OCCs.

is synthetized by the cells of the *Corpus luteum*. Neither estradiol nor progesterone was detected in medium samples. Moreover, *FSHR* transcripts were undetectable in OCC samples by deep sequencing and *LH/CGR* abundance was lower than in neonatal ovary, fibroblasts, and ES cells (data not shown). Hence, the colonies do not consist of functional endocrine cells of the ovary.

3.6. Neither Teratoma Nor Ovarian Tissue Formation in a Subcutaneous Transplantation Assay. Subcutaneous transplantation of cells into immune-deficient mice is a useful approach to assay cells with regard to their differentiation capabilities, for example, the teratoma formation assay. Moreover, we have recently shown that single-cell suspensions derived from dissociated neonatal monkey testis can reconstitute complex testis tissue after transplantation into immune-deficient mice [24]. In order to test whether the OCCs have the ability to form ovarian tissue under the "*in vivo*" conditions after transplantation, we injected ~10^6 cells per mouse from the 5th passage subcutaneously into 4 female adult NOD-SCID mice. Tissues from the injection site were collected for histological analysis after 15 weeks. Neither ovary-like tissue nor teratoma or any other conspicuous tissue was found (data not shown).

4. Discussion

A controversial debate on the presence of mitotically active germ line stem cells in the postnatal ovary characterized

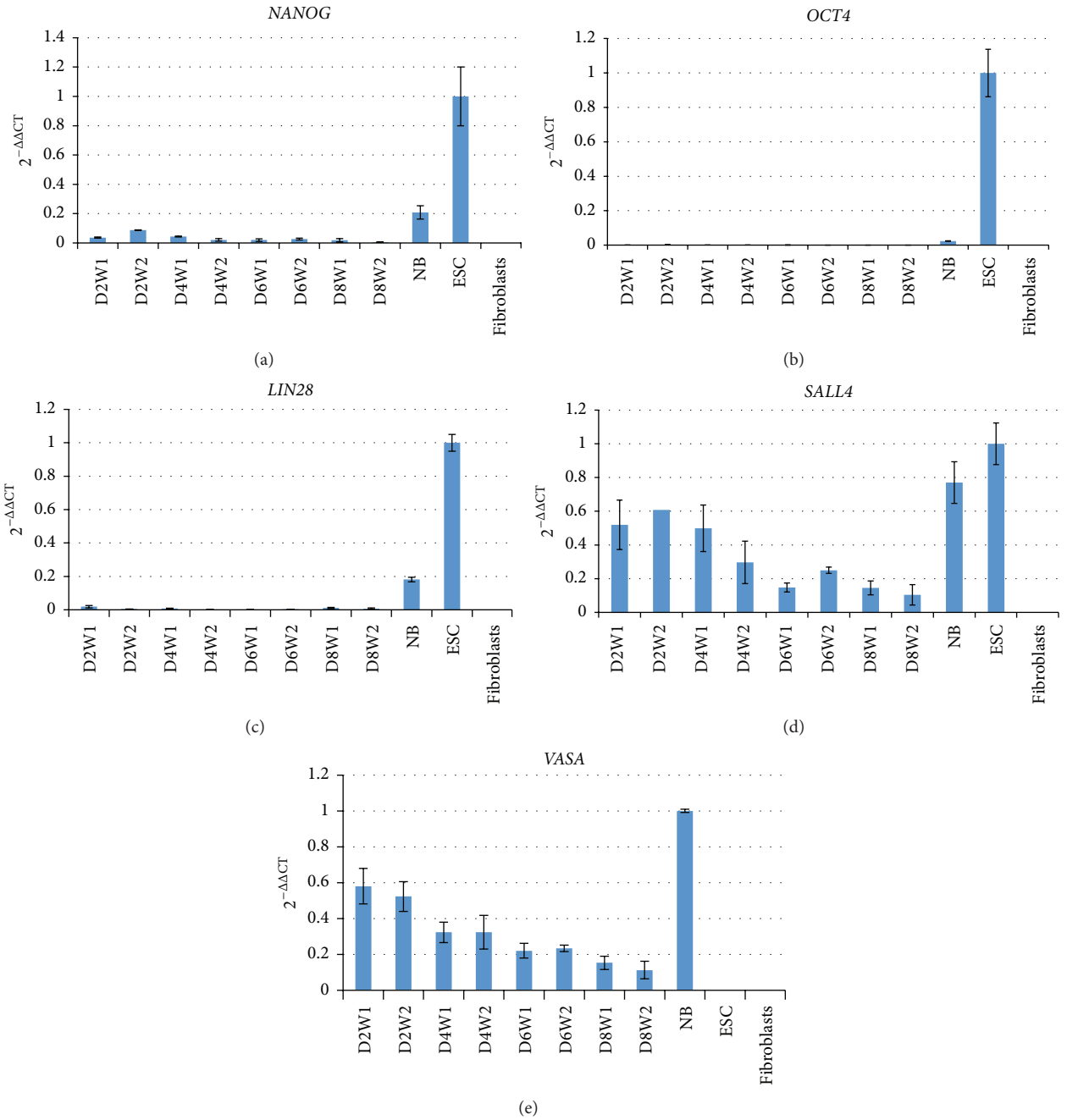

Figure 7: Pluripotency and germ cell marker mRNA abundance during the development of OCCs within one passage as revealed by real-time quantitative PCR. Positive controls for *OCT4A*, *SALL4*, and *LIN28* were ES cells. Neonatal ovary was used as positive control for the germ cell marker *VASA*. *NANOG* was very low and *OCT4A* and *LIN28* were absent at all time points analyzed. Relative abundance of *SALL4* and *VASA* generally decreased with time during the culture period. D: days of culture. W: well for cell culture. NB: newborn ovary.

the last decade of ovarian germ cell research in mammals. Several reports provided data supporting the presence of ovarian germ line stem cells in postnatal mouse ovaries, for example, [10, 13, 38], while other studies failed to identify female germ line stem cells, for example, [7, 8], thereby supporting the classical view of ovarian biology [1]. In primates including humans, the published data are similarly controversial and still not fully conclusive. Byskov et al. [3] failed to detect oogonia, which may be candidate cells for ovarian stem cells, in the postnatal human ovary older than two years, and even in younger postnatal ovaries the stem cell marker OCT4 was detectable only very rarely. We recently also failed to detect pluripotency and stem cell marker-positive cells in marmoset ovaries at one year of age [18]. On the other hand, White et al. [12] isolated mitotically active cells from human adult ovarian cortex that had the potential to form oocyte-like cells *in vitro* and to form ovarian follicles in a combined alloxenografting approach. Recently, however,

Yuan et al. [9] failed to provide evidence for mitotically active germ line stem cells in rhesus monkeys (*Macaca mulatta*) and mice concluding that adult ovaries do not undergo germ cell renewal. Furthermore, almost ten years ago, Dyce et al. [17] reported that not only ovarian cells have the potential to develop female germ cells, but also fetal porcine skin cells have. They formed oocyte-like cells *in vitro* which were extruded from hormone-responsive follicle-like aggregates.

We have established a long-term cell culture system for neonatal marmoset monkey ovarian cells. Seeding of the marmoset monkey ovarian cell suspension onto the MEF cells resulted in the development of cell colonies morphologically resembling colonies which have been observed previously by different other groups for human [39] and mouse [38, 40] ovarian cell cultures. However, while these studies reported the robust expression of pluripotency markers such as OCT4 and NANOG and therefore claimed an ES cell-like character of the cells [40], we failed to detect these core pluripotency markers in marmoset ovarian cell cultures on the transcript and on the protein level (the latter not shown), although our starting material, that is, neonatal ovary, was positive for these factors. In fact, marmoset monkey primordial germ cells [19] and oogonia [18] robustly express OCT4. This discrepancy between the native premeiotic germ cells and the cultured ovarian cells shows that the marmoset OCCs did not contain remaining ("contaminating") primordial germ cells or oogonia. All our data point to the fact that premeiotic germ cells were absent from the early passages of the cultured ovarian cells. This is also in contrast to a publication on pig ovarian stem cells. Bui and colleagues [41] derived putative stem cells from adult pig ovary that gave rise to germ cell-like cells corresponding to primordial germ cells. However, these cells, unlike the cells described in our present study, also robustly expressed pluripotency factors such as *OCT4* and *NANOG*. Moreover, the phenotype of the pig cells in culture was different from the colonies observed in this study and other studies, for example, [40]. Interestingly, however, despite the clearly different starting conditions, both our and Bui's cell culture systems resulted in the development of large oocyte-like cells.

In addition to the absence of the pluripotency factors, we did not detect even a single *DAZL, MAEL, RNF17, TEX12, TEX101*, or *TDRD1* transcript in OCCs of the 4th passage by deep sequencing, while all these germ cell transcripts were abundant in the neonatal ovary samples further supporting the absence of germ cells from the marmoset ovarian cell cultures at low passages. Hence, we conclude that marmoset monkey OCCs are neither germ cells nor pluripotent stem cells. The exact identity of the OCCs will be analyzed in future studies. However, despite showing morphology resembling an epithelium, the OCCs lacked characteristic proteins of epithelia like E-cadherin and cytokeratins. However, from OCC passage 4 onwards, we observed the development of individual oocyte-like cells strongly expressing the germ cell genes *VASA, DAZL, NOBOX, DPPA3*, and *SALL4*. Furthermore, also the meiotic marker *SCP3* was expressed in OLCs even though at moderate levels. In contrast, *OCT4A, NANOG*, and *LIN28* were low in OLCs. In addition to the marker expression data on the mRNA level we wanted to confirm VASA also on the protein level. We detected robust VASA protein expression in OLCs. Altogether, this marker profile suggests that the OLCs may correspond to a late premeiotic stage. These characteristics are partly similar to those of the OLCs described by Dyce et al. [17]. However, Dyce and colleagues showed that OLCs developed from cell aggregates that detached from the cell culture surface and formed hormone-responsive follicle-like structures. Then, the OLCs were extruded from the follicles and released into the medium. From ~500,000 skin cells approximately 6–70 large cells were extruded. Our findings were in the same range with typically 5–10 large OLCs per well and passage. But we never observed follicle-like structures. Moreover, we did not obtain any evidence for an endocrine regulation of OLC development in the marmoset monkey ovarian cell cultures.

Since we originally intended to culture oogonia, we spun down the cells down primary cells at 200 g. This may be insufficient to quantitatively collect those cells in the pellet that were cultured in previous studies, where the ovarian germ line stem cells were sedimented at 300 g [13] or 1000 g [14], respectively. Based on this, we hypothesize that we collected in the present study oogonia (and other larger somatic cells) using a force of 200 g but only marginal amounts of the progenitors of the OLCs, which probably are a subpopulation of the OSE [14]. The oogonia apparently did not survive in our culture system. Therefore, we were unable to detect pluripotency markers in our culture and germ cell markers in the early passages. However, we further hypothesize that despite the low *g* force applied in our study some OSE cells with stem cell capacity were still present in the culture. They were hypothetically able to develop into OLCs after more than three passages.

We also tested magnetic activated cell sorting (MACS) to enrich putative stem cells. However, MACS using, for example, TRA-1-81 antibodies was not successful. It must be noted, however, that the neonatal marmoset ovary is extremely tiny and that its availability is very limited. Indeed, the size of the neonatal ovary is only about 2 mm × 1 mm × 1 mm. Hence, experimental refinement and cell enrichment approaches are extraordinarily challenging. Therefore, we decided in the present study to culture the unsorted cell population obtained after tissue digestion.

In summary, we have established a long-term neonatal marmoset monkey ovarian cell culture system. However, we failed to detect pluripotent stem and premeiotic germ cell markers in low OCC passages. From passage 4 onwards, however, OLCs developed and were still developing at high passages (>20) after more than 5 months of culture. Considering the marker expression data, the view of a germ cell identity of the OLCs appears justified. An essential prerequisite of gamete formation is meiosis [42]. Except for the expression of SCP3, which is an essential protein for meiotic synaptonemal complex formation, we obtained no evidence for meiotic entry of the OLCs except the formation of some structures morphologically resembling polar bodies. We also never observed a *Zona pellucida*. Altogether, OLCs generated in this culture system appear to be germ line cells, but they are neither functional female gametes nor do they represent meiotic germ cell stages.

Currently it remains to be proven from which progenitor cells the OLCs develop in our culture system. So far, we were not able to identify these cells in the marmoset. However, a candidate tissue for the presence of ovarian stem cells with germ line potential could be the ovarian surface epithelium, which is discussed to be a multipotent tissue possibly harboring a stem or progenitor cell type [43]. In this regard, also the concept of the very small embryonic-like stem cells (VSELs) should be taken into account [16].

5. Conclusion and Outlook

In conclusion, we have established a nonhuman primate cell culture system that allows the long-term culture and development of OLCs from a nonhuman primate species. The vast majority of the cultured cells in this study, however, are neither pluripotent stem cells nor germ (line stem) cells, as has been suggested or shown in previous reports [38–40]. Future experiments should aim at resolving this discrepancy and test whether this is a species-specific phenomenon.

Future experiments will also aim at the identification and functional characterization of the stem/progenitor cell population in the marmoset culture system. Furthermore, protocols are needed that support the entry of the OLCs into meiosis potentially giving rise to mature oocytes in the future. Besides functional testing of these cells, their correct epigenetic state needs to be confirmed. In the future, a refined culture system based on the one described here may allow more detailed *in vitro* studies on early phases of primate germ cell development and on the molecular and cellular identity of OLCs and their progenitors in an experimentally accessible NHP system. In the long term, this may also contribute in the future to the development of novel therapeutic approaches of female infertility.

Conflict of Interests

The authors declare that there is no conflict of interests that could be perceived as prejudicing the impartiality of the research reported.

Authors' Contribution

Bentolhoda Fereydouni carried out conception and design, collection and assembly of data, data analysis and interpretation, paper writing, and final approval of paper. Gabriela Salinas-Riester carried out collection and assembly of data, data analysis and interpretation, paper writing, and final approval of paper. Michael Heistermann carried out collection and assembly of data, data analysis and interpretation, and final approval of paper. Ralf Dressel carried out financial support, collection and/or assembly of data, and final approval of paper. Lucia Lewerich carried out collection and/or assembly of data, data analysis and interpretation, and final approval of paper. Charis Drummer carried out provision of study material and final approval of paper. Rüdiger Behr carried out conception and design, financial support, collection and/or assembly of data, data analysis and interpretation, paper writing, and final approval of paper.

Acknowledgments

The authors appreciate the excellent assistance and the support of Nicole Umland, Angelina Berenson, and Gesche Spehlbrink. They are also very thankful to Erika Sasaki for providing the ES cells, Katharina Debowski for ES cell culture, and the members of the animal facility for excellent animal husbandry. They thank Ellen Wiese for administrative support. The support of Bentolhoda Fereydouni by the scholarship of the Deutscher Akademischer Austauschdienst (DAAD) is gratefully acknowledged. Bentolhoda Fereydouni is on a scholarship of the Deutscher Akademischer Austauschdienst (DAAD). The work was mainly supported by institutional resources and marginally by a grant of the Deutsche Forschungsgemeinschaft (DFG; Be2296-6) entitled "Pluripotent cells from marmoset testis" to Rüdiger Behr. The cell injection assays in mice performed by Ralf Dressel were supported by a Collaborative Research Centre from the Deutsche Forschungsgemeinschaft (SFB1002, TP C05).

References

[1] S. Zuckerman, "The number of oocytes in the mature ovary," *Recent Progress in Hormone Research*, vol. 6, pp. 63–108, 1951.

[2] A. G. Byskov, M. J. Faddy, J. G. Lemmen, and C. Y. Andersen, "Eggs forever?" *Differentiation*, vol. 73, no. 9-10, pp. 438–446, 2005.

[3] A. G. Byskov, P. E. Høyer, C. Yding Andersen, S. G. Kristensen, A. Jespersen, and K. Møllgård, "No evidence for the presence of oogonia in the human ovary after their final clearance during the first two years of life," *Human Reproduction*, vol. 26, no. 8, pp. 2129–2139, 2011.

[4] Y. Liu, C. Wu, Q. Lyu et al., "Germline stem cells and neo-oogenesis in the adult human ovary," *Developmental Biology*, vol. 306, no. 1, pp. 112–120, 2007.

[5] E. Bendsen, A. G. Byskov, C. Y. Andersen, and L. G. Westergaard, "Number of germ cells and somatic cells in human fetal ovaries during the first weeks after sex differentiation," *Human Reproduction*, vol. 21, no. 1, pp. 30–35, 2006.

[6] H. Stoop, F. Honecker, M. Cools, R. de Krijger, C. Bokemeyer, and L. H. J. Looijenga, "Differentiation and development of human female germ cells during prenatal gonadogenesis: an immunohistochemical study," *Human Reproduction*, vol. 20, no. 6, pp. 1466–1476, 2005.

[7] H. Zhang, W. Zheng, Y. Shen, D. Adhikari, H. Ueno, and K. Liu, "Experimental evidence showing that no mitotically active female germline progenitors exist in postnatal mouse ovaries," *Proceedings of the National Academy of Sciences of the United States of America*, vol. 109, no. 31, pp. 12580–12585, 2012.

[8] L. Lei and A. C. Spradling, "Female mice lack adult germline stem cells but sustain oogenesis using stable primordial follicles," *Proceedings of the National Academy of Sciences of the United States of America*, vol. 110, no. 21, pp. 8585–8590, 2013.

[9] J. Yuan, D. Zhang, L. Wang et al., "No evidence for neo-oogenesis may link to ovarian senescence in adult monkey," *Stem Cells*, vol. 31, no. 11, pp. 2538–2550, 2013.

[10] J. Johnson, J. Canning, T. Kaneko, J. K. Pru, and J. L. Tilly, "Germline stem cells and follicular renewal in the postnatal mammalian ovary," *Nature*, vol. 428, no. 6979, pp. 145–150, 2004.

[11] J. Johnson, J. Bagley, M. Skaznik-Wikiel et al., "Oocyte generation in adult mammalian ovaries by putative germ cells in bone marrow and peripheral blood," *Cell*, vol. 122, no. 2, pp. 303–315, 2005.

[12] Y. A. R. White, D. C. Woods, Y. Takai, O. Ishihara, H. Seki, and J. L. Tilly, "Oocyte formation by mitotically active germ cells purified from ovaries of reproductive-age women," *Nature Medicine*, vol. 18, no. 3, pp. 413–421, 2012.

[13] K. Zou, Z. Yuan, Z. Yang et al., "Production of offspring from a germline stem cell line derived from neonatal ovaries," *Nature Cell Biology*, vol. 11, no. 5, pp. 631–636, 2009.

[14] A. Bukovsky, M. Svetlikova, and M. R. Caudle, "Oogenesis in cultures derived from adult human ovaries," *Reproductive Biology and Endocrinology*, vol. 3, article 17, 2005.

[15] I. Virant-Klun, N. Zech, P. Rožman et al., "Putative stem cells with an embryonic character isolated from the ovarian surface epithelium of women with no naturally present follicles and oocytes," *Differentiation*, vol. 76, no. 8, pp. 843–856, 2008.

[16] S. Parte, D. Bhartiya, J. Telang et al., "Detection, characterization, and spontaneous differentiation in vitro of very small embryonic-like putative stem cells in adult mammalian ovary," *Stem Cells and Development*, vol. 20, no. 8, pp. 1451–1464, 2011.

[17] P.-W. Dyce, L. Wen, and J. Li, "In vitro germline potential of stem cells derived from fetal porcine skin," *Nature Cell Biology*, vol. 8, no. 4, pp. 384–390, 2006.

[18] B. Fereydouni, C. Drummer, N. Aeckerle, S. Schlatt, and R. Behr, "The neonatal marmoset monkey ovary is very primitive exhibiting many oogonia," *Reproduction*, vol. 148, no. 2, pp. 237–247, 2014.

[19] N. Aeckerle, C. Drummer, K. Debowski, C. Viebahn, and R. Behr, "Primordial germ cell development in the marmoset monkey as revealed by pluripotency factor expression: suggestion of a novel model of embryonic germ cell translocation," *Molecular Human Reproduction*, vol. 21, no. 1, pp. 66–80, 2015.

[20] T. Müller, G. Fleischmann, K. Eildermann et al., "A novel embryonic stem cell line derived from the common marmoset monkey (*Callithrix jacchus*) exhibiting germ cell-like characteristics," *Human Reproduction*, vol. 24, no. 6, pp. 1359–1372, 2009.

[21] K. Debowski, R. Warthemann, J. Lentes et al., "Non-viral generation of marmoset monkey iPS cells by a six-factor-in-one-vector approach," *PLoS ONE*, vol. 10, no. 3, 2015.

[22] M. Heistermann, S. Tari, and J. K. Hodges, "Measurement of faecal steroids for monitoring ovarian function in new world primates, callitrichidae," *Journal of Reproduction and Fertility*, vol. 99, no. 1, pp. 243–251, 1993.

[23] M. Heistermann, M. Finke, and J. K. Hodges, "Assessment of female reproductive status in captive-housed Hanuman langurs (*Presbytis entellus*) by measurement of urinary and fecal steroid excretion patterns," *American Journal of Primatology*, vol. 37, no. 4, pp. 275–284, 1995.

[24] N. Aeckerle, R. Dressel, and R. Behr, "Grafting of neonatal marmoset monkey testicular single-cell suspensions into immunodeficient mice leads to *ex situ* testicular cord neomorphogenesis," *Cells Tissues Organs*, vol. 198, no. 3, pp. 209–220, 2013.

[25] R. M. Perrett, L. Turnpenny, J. J. Eckert et al., "The early human germ cell lineage does not express SOX2 during in vivo development or upon in vitro culture," *Biology of Reproduction*, vol. 78, no. 5, pp. 852–858, 2008.

[26] K. Eildermann, N. Aeckerle, K. Debowski et al., "Developmental expression of the pluripotency factor sal-like protein 4 in the monkey, human and mouse testis: restriction to premeiotic germ cells," *Cells Tissues Organs*, vol. 196, no. 3, pp. 206–220, 2012.

[27] N. Aeckerle, K. Eildermann, C. Drummer et al., "The pluripotency factor LIN28 in monkey and human testes: a marker for spermatogonial stem cells?" *Molecular Human Reproduction*, vol. 18, no. 10, Article ID gas025, pp. 477–488, 2012.

[28] D. H. Castrillon, B. J. Quade, T. Y. Wang, C. Quigley, and C. P. Crum, "The human VASA gene is specifically expressed in the germ cell lineage," *Proceedings of the National Academy of Sciences of the United States of America*, vol. 97, no. 17, pp. 9585–9590, 2000.

[29] Y. Lin, M. E. Gill, J. Koubova, and D. C. Page, "Germ cell-intrinsic and -extrinsic factors govern meiotic initiation in mouse embryos," *Science*, vol. 322, no. 5908, pp. 1685–1687, 2008.

[30] A. Rajkovic, S. A. Pangas, D. Ballow, N. Suzumori, and M. M. Matzuk, "NOBOX deficiency disrupts early folliculogenesis and oocyte-specific gene expression," *Science*, vol. 305, no. 5687, pp. 1157–1159, 2004.

[31] Y.-J. Liu, T. Nakamura, and T. Nakano, "Essential role of DPPA3 for chromatin condensation in mouse oocytogenesis," *Biology of Reproduction*, vol. 86, no. 2, article 40, 2012.

[32] M. Sato, T. Kimura, K. Kurokawa et al., "Identification of PGC7, a new gene expressed specifically in preimplantation embryos and germ cells," *Mechanisms of Development*, vol. 113, no. 1, pp. 91–94, 2002.

[33] Y. Ohinata, B. Payer, D. O'Carroll et al., "Blimp1 is a critical determinant of the germ cell lineage in mice," *Nature*, vol. 436, no. 7048, pp. 207–213, 2005.

[34] M. Yamaji, Y. Seki, K. Kurimoto et al., "Critical function of Prdm14 for the establishment of the germ cell lineage in mice," *Nature Genetics*, vol. 40, no. 8, pp. 1016–1022, 2008.

[35] F. Sugawa, M. J. Arauzo-Bravo, J. Yoon et al., "Human primordial germ cell commitment *in vitro* associates with a unique PRDM14 expression profile," *The EMBO Journal*, vol. 34, no. 8, pp. 1009–1024, 2015.

[36] R. Warthemann, K. Eildermann, K. Debowski, and R. Behr, "False-positive antibody signals for the pluripotency factor OCT4A (POU5F1) in testis-derived cells may lead to erroneous data and misinterpretations," *Molecular Human Reproduction*, vol. 18, no. 12, pp. 605–612, 2012.

[37] R. Ivell, K. Teerds, and G. E. Hoffman, "Proper application of antibodies for immunohistochemical detection: antibody crimes and how to prevent them," *Endocrinology*, vol. 155, no. 3, pp. 676–687, 2014.

[38] J. Pacchiarotti, C. Maki, T. Ramos et al., "Differentiation potential of germ line stem cells derived from the postnatal mouse ovary," *Differentiation*, vol. 79, no. 3, pp. 159–170, 2010.

[39] M. Stimpfel, T. Skutella, B. Cvjeticanin et al., "Isolation, characterization and differentiation of cells expressing pluripotent/multipotent markers from adult human ovaries," *Cell and Tissue Research*, vol. 354, no. 2, pp. 593–607, 2013.

[40] S. P. Gong, S. T. Lee, E. J. Lee et al., "Embryonic stem cell-like cells established by culture of adult ovarian cells in mice," *Fertility and Sterility*, vol. 93, no. 8, pp. 2594.e9–2601.e9, 2010.

[41] H.-T. Bui, N. Van Thuan, D.-N. Kwon et al., "Identification and characterization of putative stem cells in the adult pig ovary," *Development*, vol. 141, no. 11, pp. 2235–2244, 2014.

[42] M. A. Handel, J. J. Eppig, and J. C. Schimenti, "Applying 'gold standards' to in-vitro-derived germ cells," *Cell*, vol. 157, no. 6, pp. 1257–1261, 2014.

[43] A. Bukovsky, M. R. Caudle, I. Virant-Klun et al., "Immune physiology and oogenesis in fetal and adult humans, ovarian infertility, and totipotency of adult ovarian stem cells," *Birth Defects Research Part C: Embryo Today: Reviews*, vol. 87, no. 1, pp. 64–89, 2009.

Hindawi Publishing Corporation
Stem Cells International
Volume 2016, Article ID 8216312, 13 pages
http://dx.doi.org/10.1155/2016/8216312

Research Article

Derivation of Pluripotent Cells from Mouse SSCs Seems to Be Age Dependent

Hossein Azizi,[1,2,3] Sabine Conrad,[4] Ursula Hinz,[1] Behrouz Asgari,[2] Daniel Nanus,[1] Heike Peterziel,[5] Akbar Hajizadeh Moghaddam,[6] Hossein Baharvand,[2,7] and Thomas Skutella[1]

[1] *Institute for Anatomy and Cell Biology, Medical Faculty, University of Heidelberg, Im Neuenheimer Feld 307, 69120 Heidelberg, Germany*
[2] *Department of Stem Cells and Developmental Biology at the Cell Science Research Center, Royan Institute for Stem Cell Biology and Technology, P.O. Box 19395, Tehran 4644, Iran*
[3] *Faculty of Veterinary Medicine, Amol University of Special Modern Technologies, P.O. Box 49767, Amol 49767, Iran*
[4] *P.O. Box 12 43, 72072 Tübingen, Germany*
[5] *Division of Signal Transduction and Growth Control, DKFZ/ZMBH Alliance, Heidelberg, Germany*
[6] *Department of Biology, Faculty of Basic Sciences, University of Mazandaran, Babolsar, Iran*
[7] *Department of Developmental Biology, University of Science and Culture, ACECR, Tehran, Iran*

Correspondence should be addressed to Thomas Skutella; skutella@ana.uni-heidelberg.de

Received 20 May 2015; Revised 25 July 2015; Accepted 27 July 2015

Academic Editor: Mariusz Z. Ratajczak

Here, we aimed to answer important and fundamental questions in germ cell biology with special focus on the age of the male donor cells and the possibility to generate embryonic stem cell- (ESC-) like cells. While it is believed that spermatogonial stem cells (SSCs) and truly pluripotent ESC-like cells can be isolated from adult mice, it remained unknown if the spontaneous conversion of SSCs to ESC-like cells fails at some age. Similarly, there have been differences in the literature about the duration of cultures during which ESC-like cells may appear. We demonstrate the possibility to derive ESC-like cells from SSC cultures until they reach adolescence or up to 7 weeks of age, but we point out the impossibility to derive these cells from older, mature adult mice. The inability of real adult SSCs to shift to a pluripotent state coincides with a decline in expression of the core pluripotency genes Oct4, Nanog, and Sox2 in SSCs with age. At the same time genes of the spermatogonial differentiation pathway increase. The generated ESC-like cells were similar to ESCs and express pluripotency markers. *In vitro* they differentiate into all three germ lineages; they form complex teratomas after transplantation in SCID mice and produce chimeric mice.

1. Introduction

Pluripotent stem cells (PSCs) are undifferentiated cells which have the potential for proliferation, self-renewal, and differentiation into ectodermal, mesodermal, and endodermal cells of all three embryonic germ layers *in vitro* and *in vivo* [1]. So far, several different approaches were used for the generation of PSCs, including ESCs obtained after fertilization from the inner cell mass of an embryo at the blastocyst stage [1, 2]. They were also procured by enforced expression of pluripotency genes in somatic cells, giving rise to the so-called induced pluripotent stem cells (iPSCs) [3, 4]; one of the promising methods for a more natural and ethical unproblematic establishment of PSCs is SSCs, especially for therapeutic approaches in human medicine [5–11]. SSCs are present in a small number in the testis, but they can be isolated and expanded *in vitro* [5]. Although they are unipotent stem cells under the environmental control of their stem cell niche, under specific culture conditions outside the niche and without any exogenous pluripotency genes, they are able to convert to ESC-like cells at different times after the initiation of culture or isolation of SSCs [5, 9, 10].

The generation of PSCs of mouse testis cells dates back to 2004 by Kanatsu-Shinohara et al. [5], when they generated ESC-like cells in SSC culture from two-day-old pups and obtained these cells 4–7 weeks after the initiation of culture. Guan et al. [9] obtained ESC-like cells from populations of STRA8-GFP positive cells of 4–7-week-old adult mice. Ko et al. repeated the induction of pluripotency in 5-week- to 7-month-old Oct-4 GFP positive adult SSCs and described the dependence of the induction on the initial number of plated SSCs and the length of culture time of Oct-4-positive cells without splitting [7]. On the other hand, this group worked in the later published protocol of conversion of SSCs into pluripotent stem cells only with SSCs of mice from postnatal day 35 (5 weeks old) [8].

Also Seandel et al. generated adult spermatogonial-derived stem cells from GPR125-positive cells in 3-week- to 8-month-old mice, but these cells were only multipotent [10].

In our experiments, we identified the spontaneous conversion of SSCs in ESC-like cells from neonate and nearly adult testis up to 7-week-old mice. On the contrary, it was impossible to generate ESC-like cells from mice older than 7 weeks. According to the NIH criteria (http://www.researchgate.net/post/At_what_age_are_laboratory_mice_considered_adult2), mice are considered adult after 8 weeks of age. The sexual activity of mice starts between 5 and 6 weeks of age [12]. According to Finlay and Darlington [13], mice should be considered mature adult between 3 and 6 months of age.

The potential generation of pluripotent cells from SSCs can apparently only be realized up to the age of 7 weeks. Therefore, it is a debatable point whether generation of pluripotent SSCs depends on their development status in correlation with the completion of puberty. The possibility of generating ESC-like cells from this cell type seems to stall before donor mice are fully matured adults.

2. Material and Methods

2.1. Isolation of SSCs and Establishment and Culture of ESC-Like Cells. All animal experiments were confirmed to the local and international guidelines for the use of experimental animals and were approved by the Royan Institutional Review Board and Institutional Ethical Committee (Tehran, Iran) and by the regional authorities in Germany (Regierungspräsidium Karlsruhe). Testis cells were isolated from C57BL/6, 129/Sv mouse strains of 6-day- to 6-month-old transgenic Oct4-GFP-reporter mice. After removing the tunica albuginea, the seminiferous tubules were separated and placed in a digestion solution which contained collagenase IV (0.5 mg/mL, Sigma), DNAse I (0.5 mg/mL, Sigma), and Dispase I (0.5 mg/mL, Roche) in HBSS buffer with Mg^{++} and Ca^{++} (PAA) at 37°C for 8 minutes. Digestion enzymes were stopped with 10% ESC-qualified FBS (Invitrogen) and additionally the cell suspension was triturated by pipetting to obtain a single cell suspension. After centrifugation, the cell pellet was washed with DMEM/F12 (PAA), filtered through a 70 μm cell strainer, and centrifuged again for 10 minutes at 1200 rpm. The supernatant was completely removed and the cells were resuspended in mouse SSC medium (StemPro-34 medium, N2-supplement, D+ glucose, bovine serum albumin, L-glutamine, β-mercaptoethanol, penicillin/streptomycin, MEM vitamins, NEAA, estradiol, progesterone, EGF, FGF, GDNF, LIF, ES-FBS, ascorbic acid, pyruvic acid, and DL-lactic acid) and plated onto 0.1% gelatin-coated culture dishes (5×10^5 cells per 9.6 cm^2 for neonate and 5×10^5 cells per 9.6 cm^2 for adult mice). About 3–7 days later, cultures of cells from neonate mice and 7–14 days later from adult mice, GFP-positive SSC colonies were manually selected from the primary culture and plated on a mouse embryonal feeder (MEF) layer in at least four 24-well plates (approximately 500 cells per well) per group. Cells were passaged 1 : 1–1 : 4 every 3-4 weeks. At the beginning, SSCs expressed Oct4-GFP especially from neonate mice and much weaker in mice older than 7 weeks. But this signal was downregulated after 2-3 weeks after the initiation of culture. During SSC cultivation we screened daily for colonies which were similar to mouse ESCs, ESC-like cells that re-expressed a high level of Oct4-GFP.

These generated ESC-like cells were manually selected and subcultured on a MEF feeder layer in mouse ESC (mESC) medium with KO-DMEM, (Invitrogen) 15% ESC-qualified FBS (Invitrogen), 1% NEAA (PAA), 1% L-glutamine (PAA), 1% Pen-Strep (PAA), 0.1% β-mercaptoethanol (Invitrogen), and LIF (ESGRO, Millipore) at a final concentration of 1000 U/mL. ESC-like colonies were grown in mESCs media and were passaged every 3-4 days.

In the supplementary method section (in Supplementary Material available online at http://dx.doi.org/10.1155/2016/8216312), we describe in more detail the material and methods of RNA extraction and RT-PCR analysis, gene expression analyses (Fluidigm Biomark), immunofluorescence staining (IMH), electrophysiology, FACS analysis, alkaline phosphatase assay, embryoid body (EB) formation, neuronal differentiation, cardiomyocyte differentiation production of teratoma and chimeric mice, and the statistical analysis.

3. Results

3.1. Isolation and Expansion of SSCs. After mild digestion with collagenase, the seminiferous testicular tubules from neonatal, 7-week-old, and 12-week-old mice were separated and could be microscopically investigated under UV-light. The Oct4-GFP signal was clearly observable in the freshly isolated seminiferous tubules of neonate mouse testis (Figure 1(a)), while in adult mice the number and intensity of Oct4-GFP signals were much lower and very low in 12-week-old mice (Figure 1(b)). After digesting and plating, the expression of the Oct4-GFP signal was detectable in both neonate and adult SSCs, although in adult SSCs to a much lower extend and with lower intensity (data not shown). All the isolated Oct4-GFP SSCs were positive for DDX4 (Vasa) and negative for Vimentin immunocytochemistry (data not shown). The morphology of SSCs was similar, irrespective of the age of the mice and the days of the culture. Representative examples of spermatogonial cultures are shown in Figure 1.

Up to 14–21 days after initiation of the primary testis cultures with SSC medium, SSCs with a positive Oct4-GFP signal were observed during the culture of neonate but were observed very rarely during the culture of adult mice (Figures

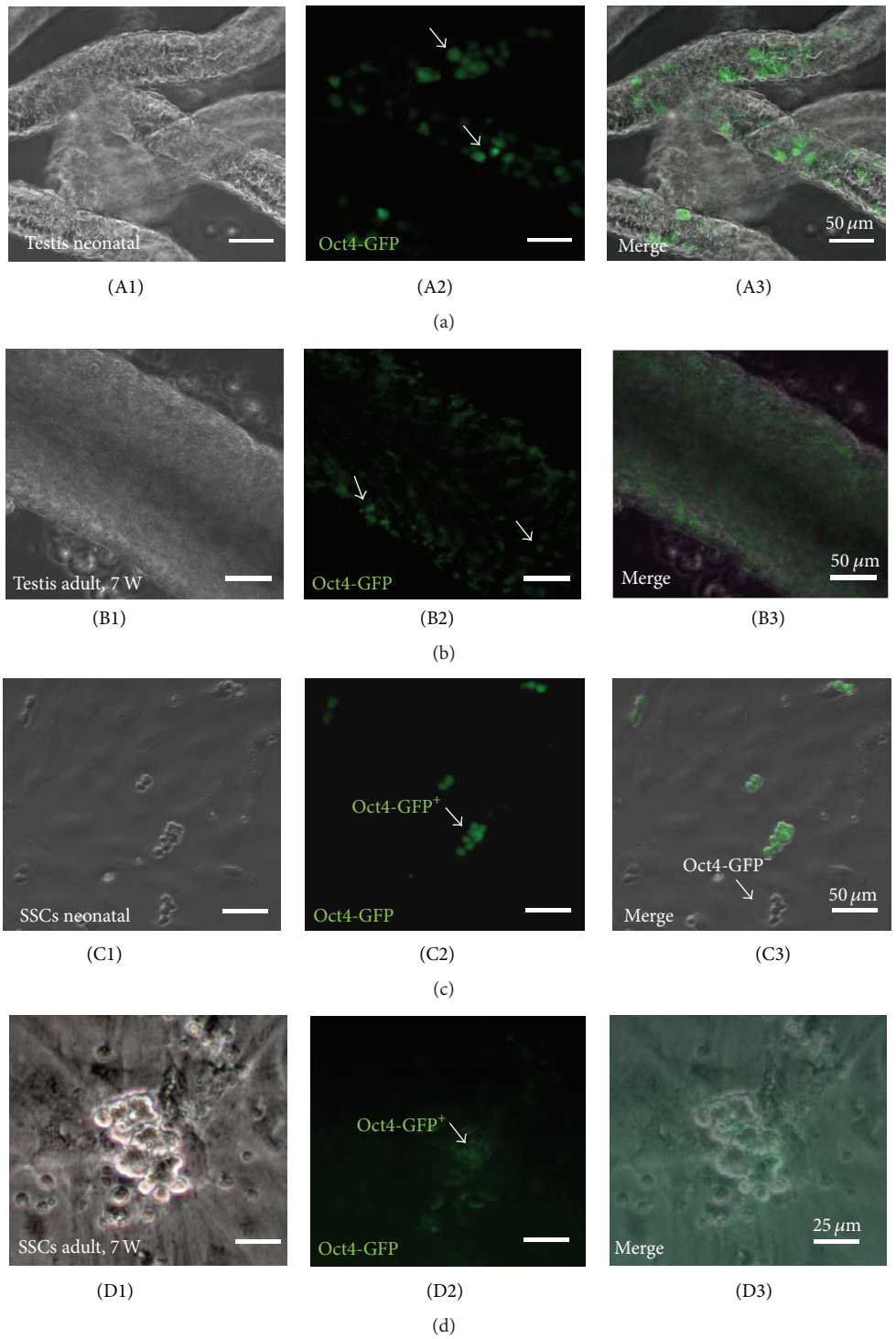

Figure 1: Number and intensity of GFP signals in the neonate and adult mouse testicular tubules (a, b) and SSC cultures (c, d) from transgenic Oct4-GFP reporter mice. (A1–A3) In the freshly dissected testicular tubules, the number of Oct4-GFP positive cells and the intensity of the Oct-GFP signal were higher and stronger in neonate mice than in adult mice >7 weeks (B1–B3). (C1–C3) Oct4-GFP positive SSCs were clearly present during initial cultures from neonate mice, while in adult mice >7 weeks SCCs Oct4-GFP signals were much weaker from the beginning (D1–D3). SSC colonies were grown on MEF feeder layers. (A1–D1) bright field; (A2–D2) green fluorescence for Oct4-GFP; (A3–D3) merged images. Scale bars: (a)–(c) 50 μm, (d) 25 μm.

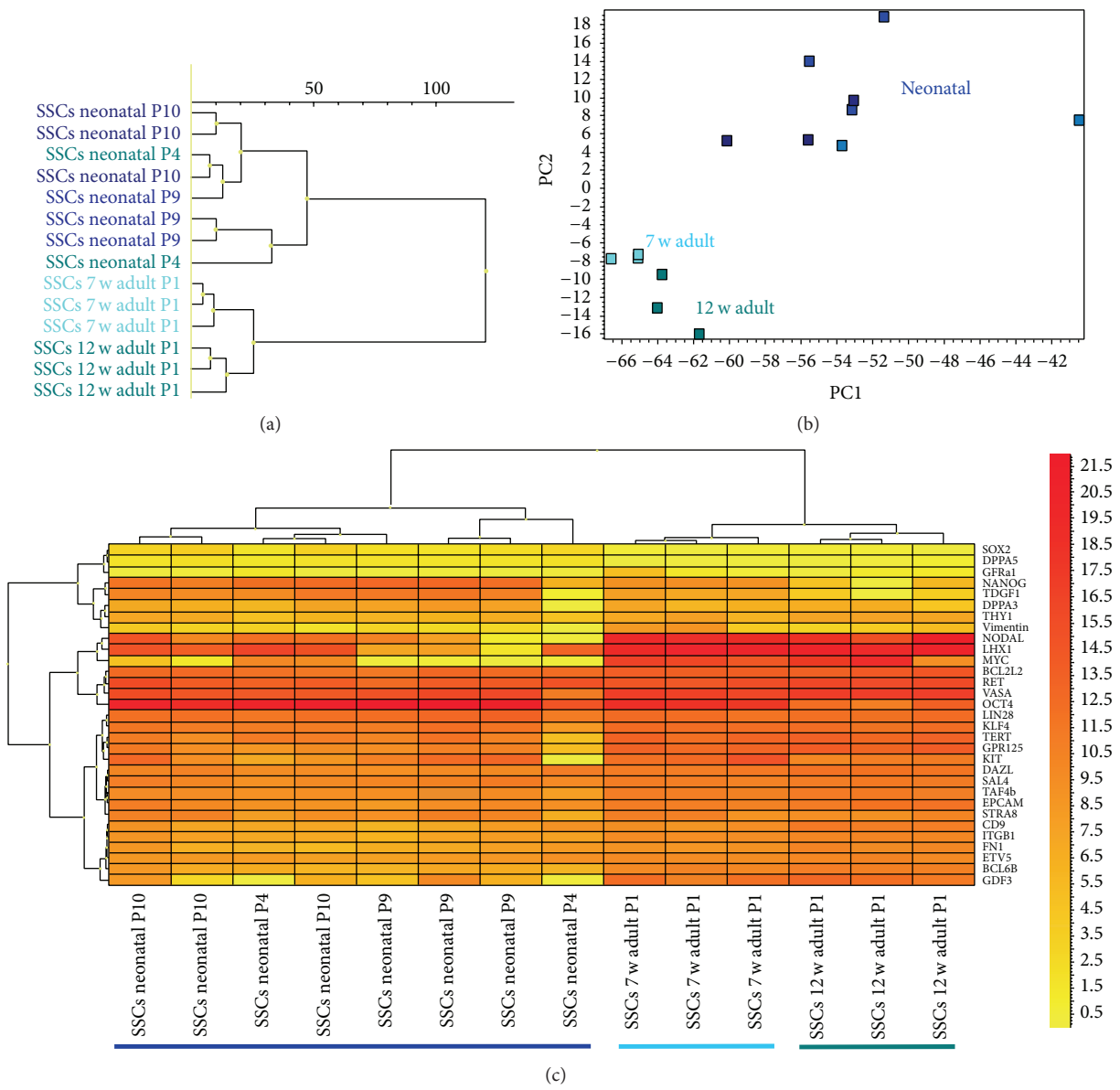

Figure 2: Different gene expression profiles of neonatal and adult SSCs with germ cell-enriched and pluripotency associated genes. Adult SSCs were obtained from 7- and 12-week-old mice. (a) Dendrogram and (b) PCA demonstrate that neonate and adult SSCs are distinct and localize in separated trees in the dendrogram or areas in the PCA. (c) Heat map shows array of pluripotency and germ cell associated genes with a cluster of different populations of neonatal SSCs (coloured dark blue), while adult SSCs cluster from 7- and 12-week-old mice in a separate tree (coloured light blue and green).

1(c) and 1(d)). After three weeks, the Oct4-GFP signal was completely downregulated and in the near of not observable during long-term culture (data not shown). The SSCs were passaged for more than 22 times and could be cultivated up to one year and longer.

3.2. Gene Expression Profiling of SSCs from Neonatal and Adult Mice. We quantified and analyzed the expression of important germ cell-enriched genes (*LHX1, Stella, VASA, DAZL, CD9, EPCAM, GPR125, GDF3, THY1, STRA8, GFRa1, 1ITGB1, TAF4b, KIT, ETV5,* and *BCL6B*) and pluripotency associated genes (*Oct4, Nanog, Sox2, TDGF1, KLF4, MYC, LIN28, SALL4, DPPA3,* and *DPPA5*) in neonatal and adult SSCs, which were obtained from 7- and 12-week-old mice by real-time PCR with Fluidigm nanofluid technology.

Hierarchical clustering (dendrogram) and principal component analysis (PCA), as in Figure 2, made evident that neonatal and adult SSCs are different and localized in separated trees in the dendrogram or areas in the PCA.

The heat map analysis with an array of pluripotency and germ cell associated genes revealed that a cluster of various populations of neonatal SSCs was significantly different from the other groups, while adult SSCs from 7- and 12-week-old mice clustered in a separate tree.

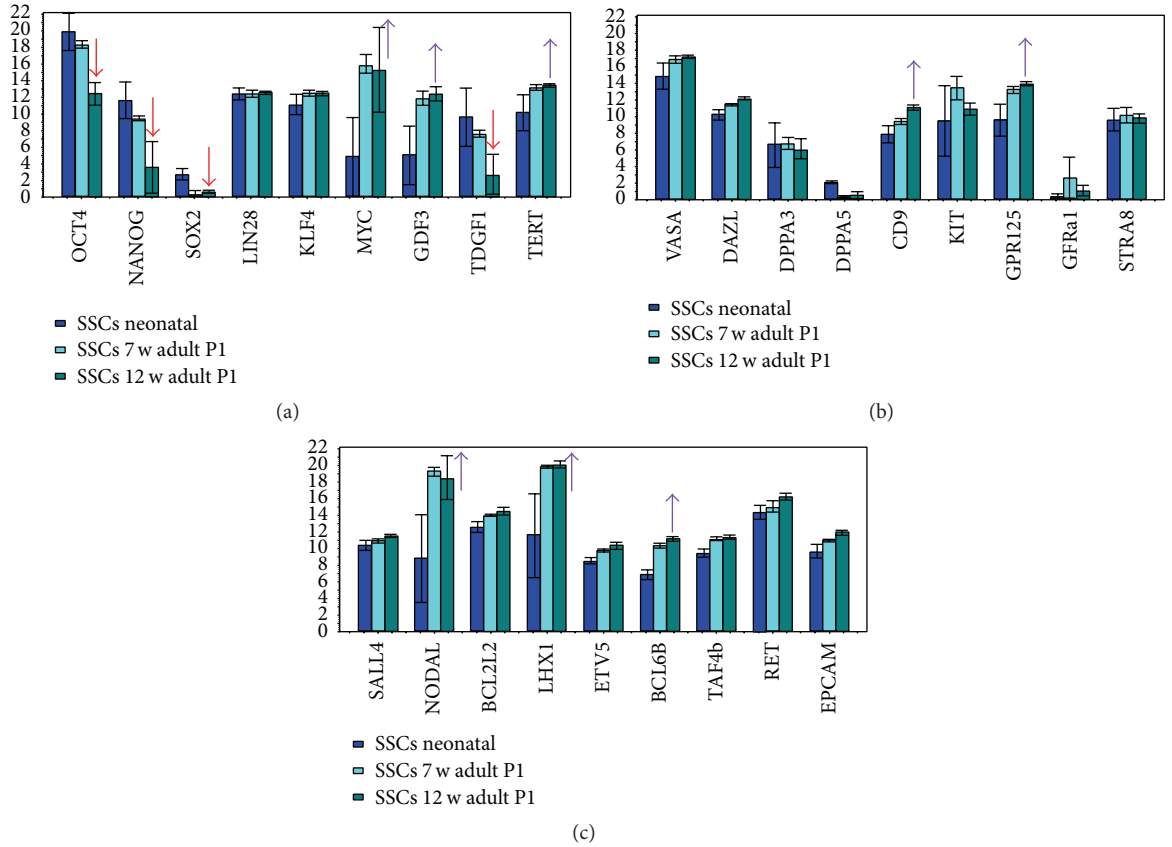

Figure 3: Bar plot showing expression of pluripotency and germ cell associated genes between neonatal SSCs (coloured dark blue), 7-week-old adult SSCs (coloured light blue), and 12-week-old adult SSCs (coloured green blue). Red arrows mark significantly downregulated genes and purple arrows mark upregulated genes in adult SSCs (more than 2-fold and $P < 0.05$). Note that the core pluripotency genes Oct4, Nanog, and Sox2 are downregulated in adult SSCs from 12-week-old mice.

The neonatal SSCs expressed a significantly higher level of the pluripotency *genes Oct4, NANOG, TDGF1*, and *Sox2* in comparison to adult SSCs (fold change > 2 and t-test $P < 0.05$) (Figures 2 and 3; Supplementary Table 1).

In contrast, several germ cell associated genes in the adult SSCs were expressed in descending order *MYC, NODAL, LHX1, GDF3, GPR125, BCL6B, TERT, CD9, ITGB1,VASA, TAF4b, EPCAM, BCL2L2, ETV5, DAZL, KLF4, RET*, and *THY1* and at a significantly higher level than in neonatal SSCs (fold change > 2 and t-test $P < 0.05$).

Not significantly regulated between neonate and adult SSCs were *GFRa1, KIT, STRA8, LIN28*, and *DPPA3* (fold change > 2 and t-test $P < 0.05$).

In a comparison between neonatal SSCs and SSCs obtained from 12-week-old mice, these differences became even more apparent (see Supplementary Tables). Moreover, comparing SSCs from 7-week-old and 12-week-old mice, the pluripotency genes are significantly higher expressed in SSCs obtained from 7-week-old mice.

As apparent in the bar plot (Figure 3), the core pluripotency genes Oct4, Nanog, and Sox2 were significantly downregulated in adult SSCs from 12-week-old mice, while the expression of germ cell genes was found more stable in the more developed and differentiated epithelium of spermatogenesis. In contrast to neonatal SSCs and those from 7-week-old mice, Oct4 was also insignificantly differentially expressed in 12-week-old mice in comparison to fibroblasts. This possibly indicates that an important prerequisite for a natural shift to pluripotency in male germ cells is lost during adolescence. The decline in the expression of pluripotency genes at the edge of adultness is demonstrated in aheat map and correlation analyses in Figure 4 as well. The expression levels of core pluripotency genes *Oct4, Nanog*, and *Sox2* decrease in SSCs with the age of the animal.

3.3. The Occurrence of Pluripotent ESC-Like Cells from Oct4 GFP Positive Cells Is Restricted to Neonatal up to 7-Week-Old Mice. As documented in Figures 5 and 6, ESC-like cells could only be generated from SSCs obtained from mice not older than 7 weeks, during a cultivation time of these SSCs between 46 days and 143 days. As shown in Figures 5(a) and 5(b), ESC-like colonies were observed in days 46, 48, 84, 91, 101, and 119 in neonatal SSCs and after 116 and 143 days in 7-week-old mice, counting from initiation of the culture (Figures 5 and 6). No ESC-like cells or colonies could be observed in the groups of SSCs obtained from 9–16-week-old and 23-24-week-old mice (Figures 5 and 6).

We observed no development of ESC-like colonies from the SSC cultures at all before 46 days and after 143 days.

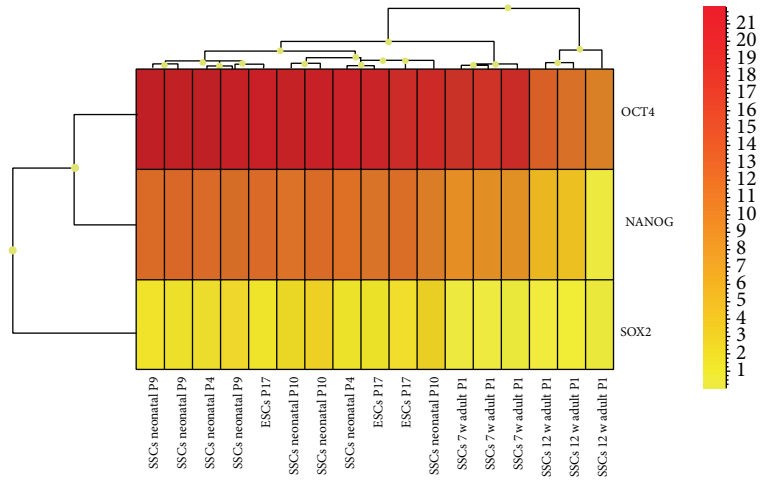

(a)

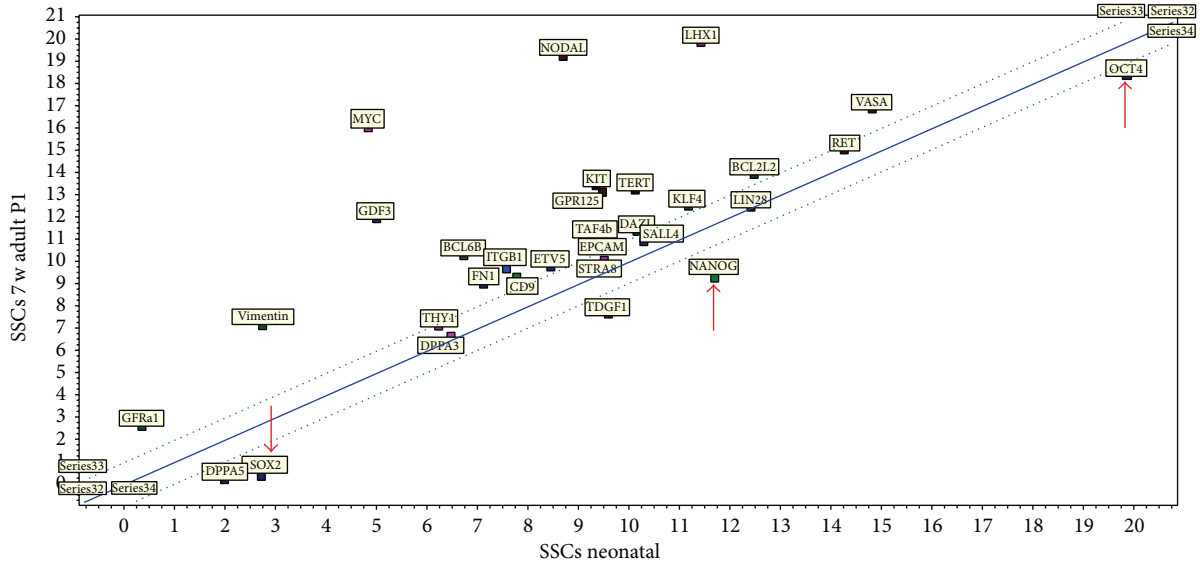

(b)

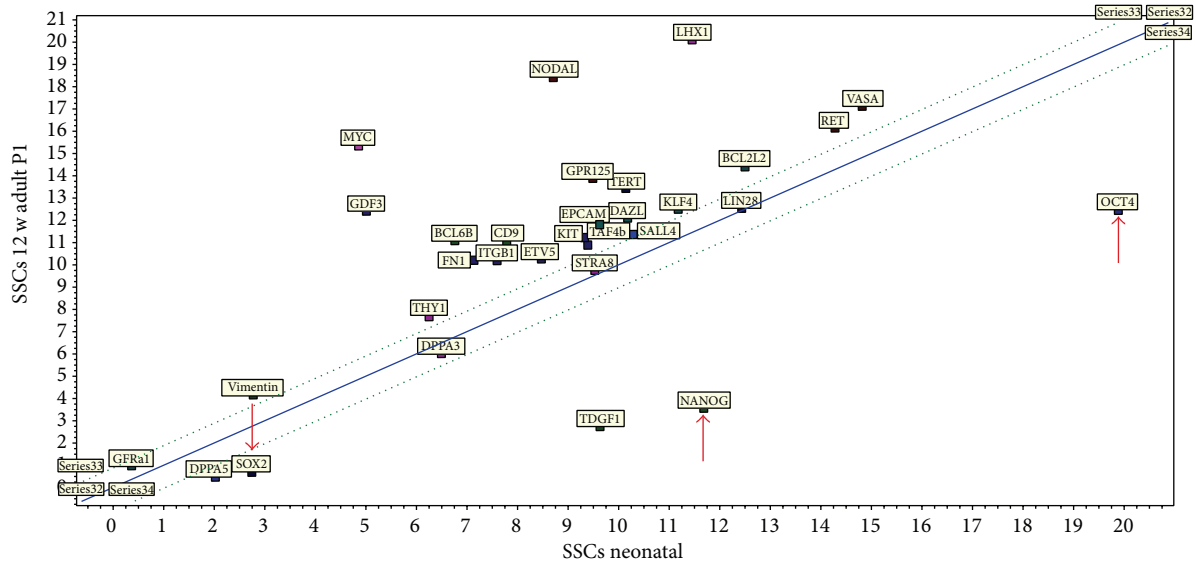

(c)

Figure 4: Continued.

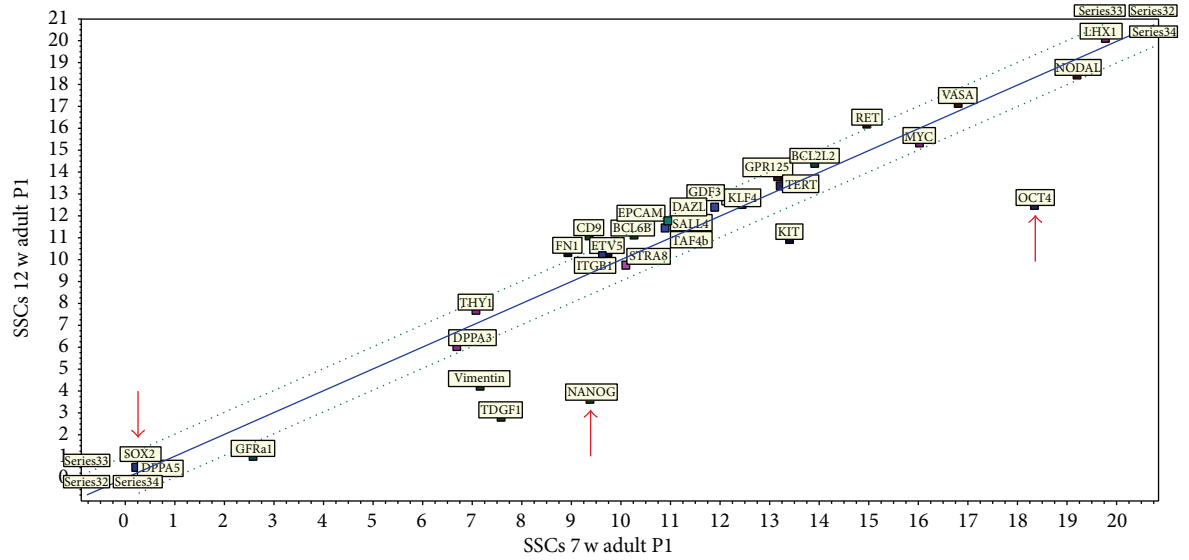

(d)

Figure 4: (a) Heat map and (b–d) correlation analyses reveal expression levels of core pluripotency genes Oct4, Nanog, and Sox2 decrease in SSCs with age of the animal. A decline in Oct4, Nanog, and Sox2 expression is clearly observable after 7 weeks of age and becomes even more evident after 12 weeks of age. Arrows in (b–d) mark the localization of Oct4, Nanog, and Sox2 in the correlations.

Neonatal	3–7 weeks old	9–16 weeks old	23-24 weeks old
$n = 4$	$n = 5$	$n = 4$	$n = 4$
ESC-like cells after 46–119 days	ESC-like cells after 116–143 days	No ESC-like cells up to 370 days	

(a)

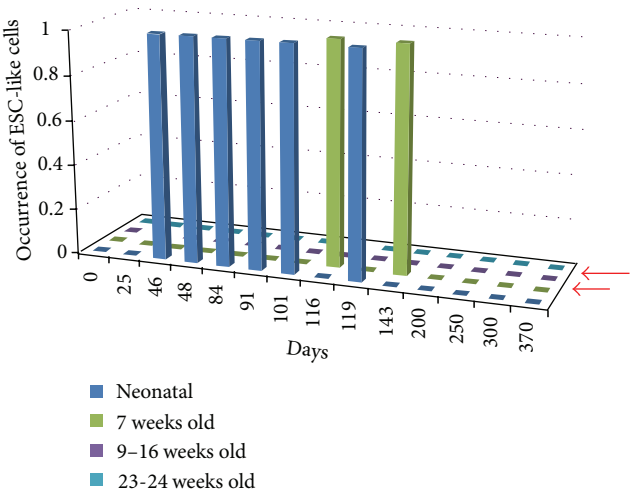

(b)

Figure 5: (a) Table and (b) graph demonstrate that ESC-like cells can only be obtained with SSCs obtained from mice until the age of 7 weeks. SSCs obtained from older adult animals are unable to show a shift to pluripotency (red arrows).

3.4. The ESC-Like Cells Are Fully Pluripotent, Form Teratoma, and Produce Chimera. ESC-like colonies had a packed spindle- to round-shaped morphology with smooth borders (Supplementary Figure 2A1). Moreover, they displayed a high intensity of the Oct4-GFP signal (Supplementary Figures 2A2, 2A3). The ESC-like cell lines were passaged 1 : 5–1 : 8 for more than 15 times following trypsin digestion, with an estimated doubling time of 48–72 h. They still expressed Oct4-GFP after long-term cultivation. The cells preserved their undifferentiated state in multiple passages. The established ESC-like cell lines were successfully expanded, cryopreserved, and thawed with no loss in proliferation or

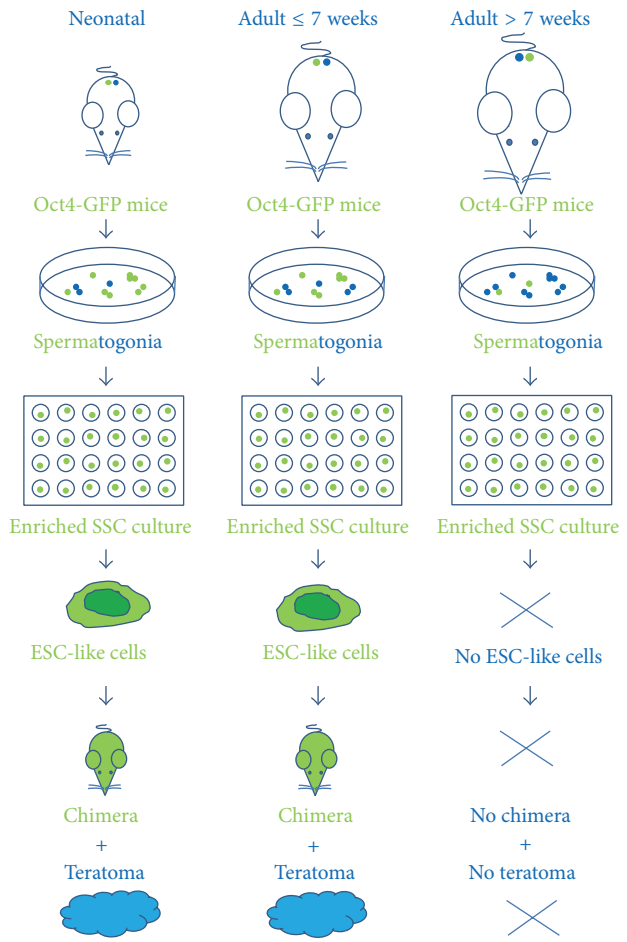

Figure 6: Schematic illustration pinpoints that occurrence of pluripotent ESC like cells from Oct4 GFP positive cells with the production of chimera and formation of teratoma is restricted to neonatal up to 7-week-old mice.

differentiation capacities. Figures 7 and 8 make evident the close similarity of the gene expression profiles of ESC-like cells and ESC with germ cell-enriched and pluripotency associated genes but show clear distinction to fibroblasts. Reading the dendrogram, PCA, and heat map, we observe the ESCs derivation from neonatal and 7-week-old mice and the ESCs intermingling in den trees und areas. Moreover, it becomes evident from the bar plots that all of the pluripotency genes were strongly expressed in ESC-like cells and ESCs (Figures 7 and 8; Supplementary Tables 1 and 2). *DPPA3, BCL2L2, SALL4*, and *Nanog* were upregulated in ESC-like cells in comparison to ESCs (fold change > 1.5 and t-test $P < 0.05$).

The ESC-like cell lines showed the ability to differentiate spontaneously *in vitro* into derivatives of all three germ layers by EB formation at day 10 and after plating (Supplementary Figure 4 and Supplementary Figure 5A). mRNA and protein expression of the lineage specific marker genes for ectoderm (*Nestin*, *Map2*, *Tuj1*, *NeuN*, *GFAP*, and *Pax6*) (Supplementary Figure 4), mesoderm (*Gata4*, *Brachyury*, *EPCAM1*, *Myf5*, *MyoD*, *Islet1*, *SM-actin*, and *FLK1*), and endoderm (*Afp* and *Keratin-18*) demonstrate this (Supplementary Figure 5A). Moreover, directed differentiation into cardiomyocytes showed 14 (±3) beating areas for each well of 6-well plate with 87 (±36) beating contractions per minute (Supplementary Figure 3C; Supplementary film). Also differentiated cardiomyocytes were analyzed by whole-cell current clamp for pacemaker activity. It was observed that beating cells have a rhythmic action potential generation over time, with a constant amplitude (Supplementary Figure 3C).

Thus, the expression of lineage specific marker genes, *Map2*, *Nestin*, *NeuN*, *Pax6, Tuj1*, and *GFAP*, demonstrated the directed differentiation into the neural cell phenotype (Supplementary Figure 4). We further examined the function of ESC-like cell-derived neuronal cells by patch clamp recordings (Supplementary Figure 3F). Upon a brief current pulse of 5 ms, all cells ($n = 6$) could fire an action potential. There were cells that would fire continuously (2 cells out of 6 cells recorded) and cells that would not fire (4 cells out of 6 cells recorded, data not shown). Interestingly, the recorded cells displayed a strong hypopolarizing current after action potential generation. Moreover, the resting membrane potential was variable between the cells.

We tested the capacity of the ESC-like cells to form a teratoma and to generate chimeric mice to further confirm their pluripotency. We subcutaneously transplanted 2×10^6 ESC-like cells into SCID mice. At four weeks after injection, ESC-like cells resulted in teratomas that contained all three germ layers (Figures 9(a)–9(d); Supplementary Figure 5B). Histological analyses showed the presence of neural structures and epidermis (as ectodermal derivatives), bone structure and adipose tissue (as mesodermal structures), and gut structure (as endodermal derivatives) in the teratoma sections (Figures 9(a)–9(d); Supplementary Figure 5B). To investigate chimera formation, ESC-like cells were transferred into blastocyst and chimeric mice were identified by coat color (Figures 9(e)–9(h)).

4. Discussion

SSCs are the only source of naturally occurring truly pluripotent stem cells in the organism after birth, which do not have to be artificially reprogrammed such as iPSCs. The molecular mechanisms underlying the natural shift from a unipotent to a completely pluripotent cell during the establishment of mouse ESC-like cells from SSCs are not completely understood until now. However, it appears that the age of animals, the mouse strain used, the culture conditions with growth factors involved, the cell density of SSCs during culture, the time period after initiation of culture, and the length of culture might all be key players in the transition process [5, 8–11].

In our work, we demonstrated the scarcity of the conversion of SSCs to ESC-like cells. Conversion occurred spontaneously from SSCs of neonate and up to 7-week-old mouse testis but not from older mice considered adult or even mature adult [12, 13]. This observation implies that the generation of ESC-like cells from SSCs coincides with the general development of the mouse up to an adolescent stage and thereafter ceases. Although mice are sexually mature by

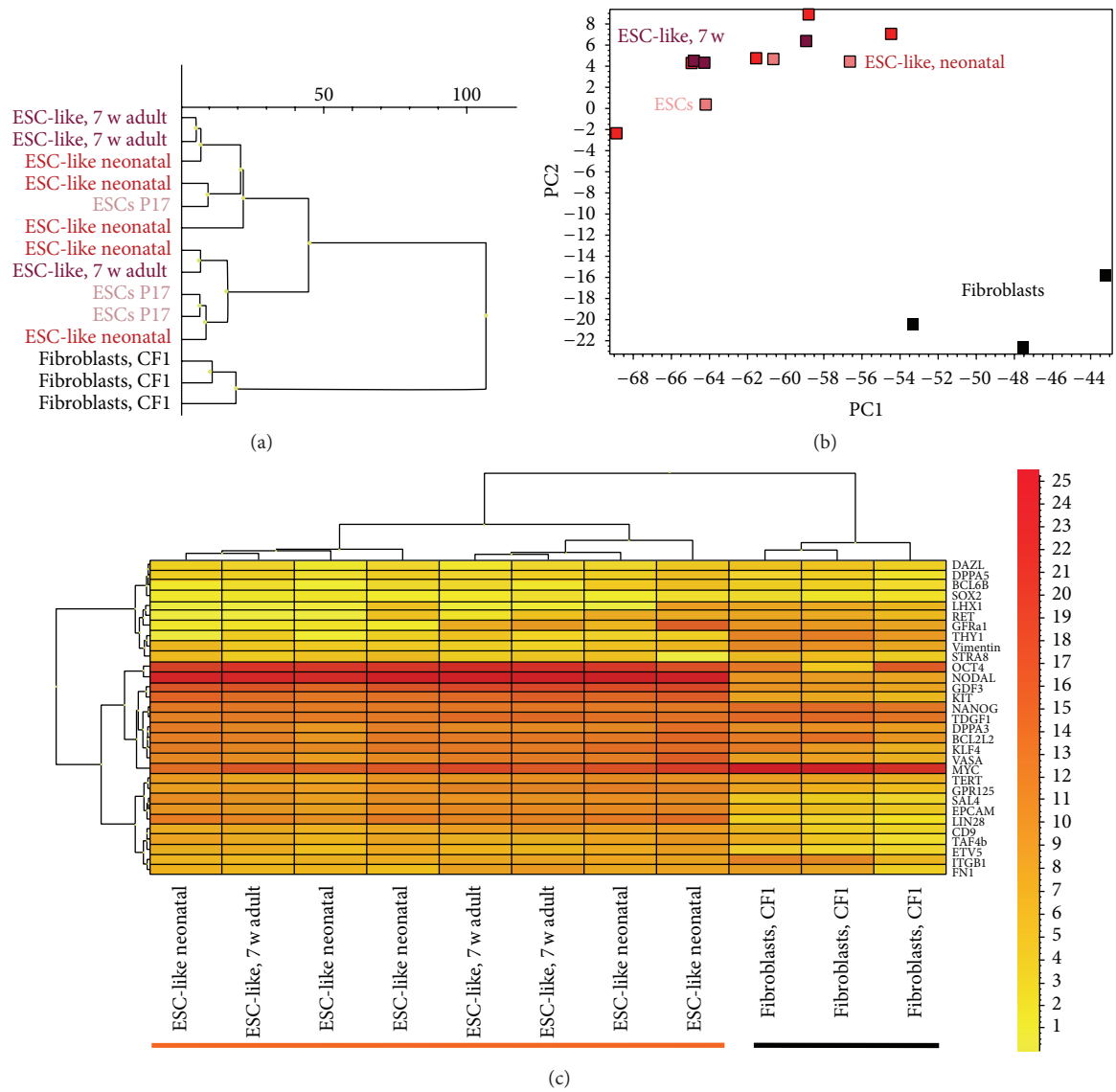

Figure 7: Similar gene expression profiles of ESC-like cells and mESCs with germ cell-enriched and pluripotency associated genes. (a) Dendrogram and (b) PCA clearly demonstrate that ESC-like cells and mESCs are similar to each other but distinct to fibroblasts which localize in separated trees or areas. (c) Heat map shows array of pluripotency and germ cell associated genes with a cluster of ESC-like cells and mESCs (both underlined with orange bar), while fibroblasts cluster in a separate tree (underlined with black bar).

35 days of age, relatively rapid maturational growth continues for most biological processes and cells. Tissues and organs continue to develop in the mouse until about three months of age [12, 13].

We observed that the amount of positive cells and signal density of Oct4-GFP in the seminiferous tubules of the neonate mouse testis was higher than in old mouse testis (after 7 weeks of age). Reduction of *Oct4, Nanog, Sox2*, and *TGFβ1* expression with aging may be related to a reduction of the undifferentiated SSC pool. These might include gonocytes and prespermatogonia in the testis of neonates and older animals. These observations might also indicate difficulties for the generation of ESC-like cells from older mice.

We also observed another limitation for appearance of ESC-like cells after initiation of culture that only occurred during a special time window (46 until 143 days) after initiation of SSCs cultures. Several reports concerning long-term cultivation for SSCs failed to describe this spontaneous shift of SSCs to pluripotent ESC-like cells [14, 15].

These results give the impression of a critical time window for the generation of pluripotent cells from SSCs and the impracticality of ESC-like cells being generated from continuous Oct4-GFP SSC culture. Kanatsu-Shinohara et al. also generated ESC-like cells during a time window about 4–7 weeks after initiation of culture in the neonate mouse SSCs [5]. To answer the question related to the origin of the SSC-ESC-like shift, different reporters including Stra8 [9], GPR125 [10], and Oct4 [7, 8] were employed for generation of ESC-like cells. Furthermore, Kanatsu-Shinohara et al. [16] analyzed the developmental fate of a single cell from

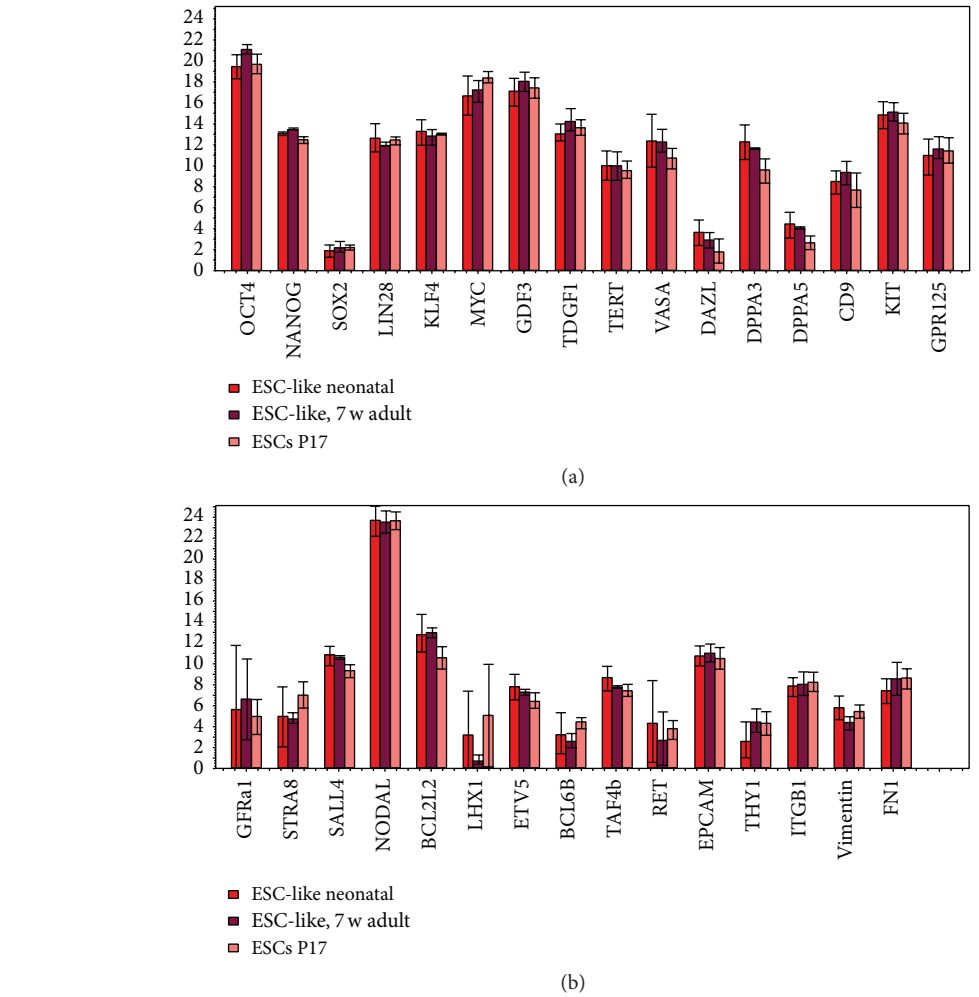

Figure 8: Bar plot showing expression of pluripotency and germ cell associated genes between ESC-like cells (coloured pink or dark red) and mESCs (coloured light red). Note that the core pluripotency genes Oct4, Nanog, and Sox2 are not differentially regulated between ESC-like cells and mESCs.

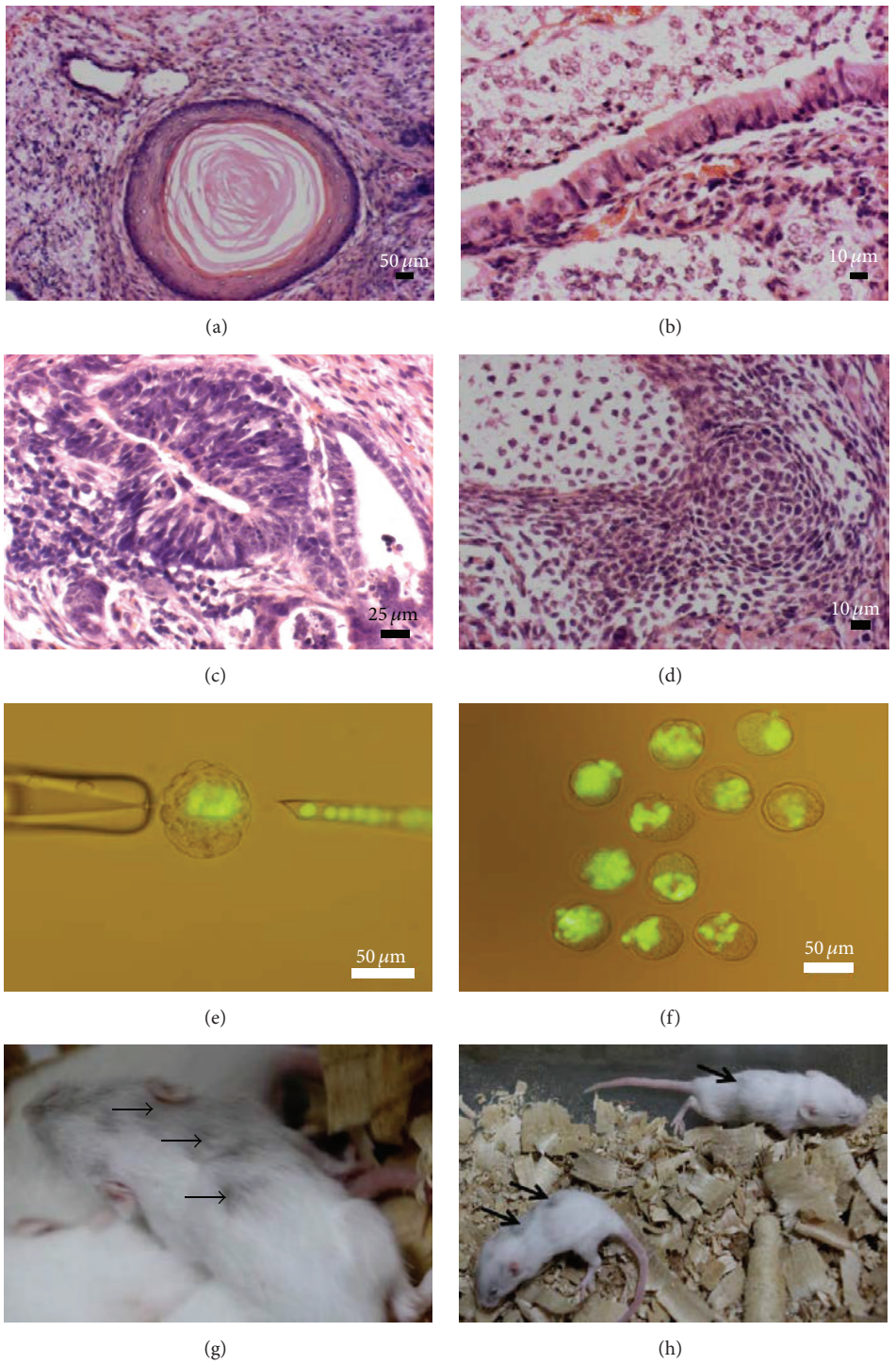

Figure 9: Pluripotency characterization of ESC-like cells with teratoma formation including tissue structures of all germ layers (a–d) and chimera formation (e–h). (a) Skin formation with keratinizing squamous epithelium, (b) respiratory epithelium with goblet cells, (c) neuronal rosette, and (d) primitive cartilage. (e, f) Blastocysts injected with GFP-marked ESC-like cells and chimera formation. Scale bars: (a), (e), and (f) 50 μm, (b) and (d) 10 μm, and (c) 25 μm.

a SSC culture that appeared during transfection experiments. But in all these experiments, the original cell source was heterogeneous, although the ESC-like cells were highly enriched.

Ko et al. [8] showed the induction of pluripotency from a SSC culture from Oct4 transgenic reporter mouse at postnatal day 35. They argued that this transition was mainly dependent on a distinct number of SSCs and on the length of culture

for reprogramming (2–4 weeks), while they did not really mention if reprogramming occurred in every stage of the SSC culture.

We demonstrated that the ESC-like cells are fully pluripotent, express pluripotency markers, have the potential for complex teratoma formation, and produce chimera in the recipient mouse similar to mouse ESCs. Moreover, they are highly capable of differentiating into neuronal and cardiomyocyte phenotypes after *in vitro* differentiation, which also has been shown by other groups [17, 18].

It would be of major interest to study factors, including small molecules, that could increase the probability and also the restricted time window of SSC to PSC conversion. Recently it has been shown that the addition of glycogen synthase kinase-3 inhibitors to the testis-derived SC cultures increases the likelihood for the occurrence of ESC-like cells from SSCs [11].

In the primary culture of isolated cells from Oct4 transgenic reporter mice, we observed that the Oct4-GFP signal was expressed at a moderate level in neonate up to a low level in older or adult SSCs. This expression was completely downregulated during short- and long-term SSC culture [19], and a high density signal only remerged after conversion to ESC-like cells.

mRNA expression profiling confirmed that the expression of germ cell specific genes increased with age and was therefore significantly higher in SSCs from 7- to 12-week-old mice compared with neonatal SSCs. In parallel, we observed that the expression of *Oct4a* and *Nanog*, *and Sox2* was significantly upregulated in neonatal SSCs and downregulated in the adult SSCs.

In PSCs, core transcriptional genes control the expression of different lineage specific genes and prevent pluripotent cells from differentiation [20]. It has been demonstrated that these genes as well as other genes associated with pluripotency are already expressed in neonatal SCCs although mostly to a lower extent [5]. Our analysis showed a crucial time window for a shift of SSCs to ESC-like cells derived from mouse SSCs which occurred with a downregulation of germ cell genes and upregulation of core pluripotency genes in the postnatal mouse until adolescence. The natural potential of mouse SSCs to convert into a fully pluripotent cell comparable to mouse ESCs is still not understood. Some controversial challenges for pluripotency and multipotency of ESC-like cells exist (especially in ESC-like cells which were generated from human testis) [6]. However, the natural shift from a unipotent cell involved in spermatogenesis to a versatile cell population, which is able to differentiate into germ cells and cells of all germ layers, offers an ethically unproblematic and nonartificial alternative for regenerative medicine. But there might be limitations, which could be related to the age of the donor and also to a special time window in which natural reprogramming of SSCs can be observed during culture.

This study has come to the conclusion that the natural reprogramming of unipotent SSCs into pluripotent cells cannot occur during adulthood and implies that this conversion is only observable until adolescence and during a special time window after initiation of culture.

Conflict of Interests

The authors declare that there is no conflict of interests regarding the publication of this paper.

Acknowledgments

The authors would like to convey thanks to all the colleagues who kindly helped them in this research: Steffen Albrecht, Gerald Bendner (Institute of Anatomy and Cell Biology, University of Heidelberg), and all other people and institutions supporting this research.

References

[1] M. J. Evans and M. H. Kaufman, "Establishment in culture of pluripotential cells from mouse embryos," *Nature*, vol. 292, no. 5819, pp. 154–156, 1981.

[2] J. A. Thomson, J. Itskovitz-Eldor, S. S. Shapiro et al., "Embryonic stem cell lines derived from human blastocysts," *Science*, vol. 282, no. 5391, pp. 1145–1147, 1998.

[3] K. Takahashi and S. Yamanaka, "Induction of pluripotent stem cells from mouse embryonic and adult fibroblast cultures by defined factors," *Cell*, vol. 126, no. 4, pp. 663–676, 2006.

[4] K. Takahashi, K. Tanabe, M. Ohnuki et al., "Induction of pluripotent stem cells from adult human fibroblasts by defined factors," *Cell*, vol. 131, no. 5, pp. 861–872, 2007.

[5] M. Kanatsu-Shinohara, K. Inoue, J. Lee et al., "Generation of pluripotent stem cells from neonatal mouse testis," *Cell*, vol. 119, no. 7, pp. 1001–1012, 2004.

[6] S. Conrad, M. Renninger, J. Hennenlotter et al., "Generation of pluripotent stem cells from adult human testis," *Nature*, vol. 456, no. 7220, pp. 344–349, 2008.

[7] K. Ko, N. Tapia, G. Wu et al., "Induction of pluripotency in adult unipotent germline stem cells," *Cell Stem Cell*, vol. 5, no. 1, pp. 87–96, 2009.

[8] K. Ko, M. J. Araúzo-Bravo, J. Kim, M. Stehling, and H. R. Schöler, "Conversion of adult mouse unipotent germline stem cells into pluripotent stem cells," *Nature Protocols*, vol. 5, no. 5, pp. 921–928, 2010.

[9] K. Guan, K. Nayernia, L. S. Maier et al., "Pluripotency of spermatogonial stem cells from adult mouse testis," *Nature*, vol. 440, no. 7088, pp. 1199–1203, 2006.

[10] M. Seandel, D. James, S. V. Shmelkov et al., "Generation of functional multipotent adult stem cells from GPR125+ germline progenitors," *Nature*, vol. 449, no. 7160, pp. 346–350, 2007.

[11] S.-F. Moraveji, F. Attari, A. Shahverdi et al., "Inhibition of glycogen synthase kinase-3 promotes efficient derivation of pluripotent stem cells from neonatal mouse testis," *Human Reproduction*, vol. 27, no. 8, pp. 2312–2324, 2012.

[12] K. Flurkey, J. Currer, and D. Harrison, "The mouse in aging research," in *The Mouse in Biomedical Research*, vol. 3, pp. 637–672, Academic Press, 2nd edition, 2007.

[13] B. L. Finlay and R. B. Darlington, "Linked regularities in the development and evolution of mammalian brains," *Science*, vol. 268, no. 5217, pp. 1578–1584, 1995.

[14] F.-J. Shen, C. Zhang, S.-X. Yang et al., "Long-term culture and identification of spermatogonial stem cells from BALB/c mice in vitro," *National Journal of Andrology*, vol. 14, no. 11, pp. 977–981, 2008.

[15] M. Kanatsu-Shinohara, N. Ogonuki, K. Inoue et al., "Long-term proliferation in culture and germline transmission of mouse male germline stem cells," *Biology of Reproduction*, vol. 69, no. 2, pp. 612–616, 2003.

[16] M. Kanatsu-Shinohara, J. Lee, K. Inoue et al., "Pluripotency of a single spermatogonial stem cell in mice," *Biology of Reproduction*, vol. 78, no. 4, pp. 681–687, 2008.

[17] K. Guan, S. Wagner, B. Unsöld et al., "Generation of functional cardiomyocytes from adult mouse spermatogonial stem cells," *Circulation Research*, vol. 100, no. 11, pp. 1615–1625, 2007.

[18] K. Guan, F. Wolf, A. Becker, W. Engel, K. Nayernia, and G. Hasenfuss, "Isolation and cultivation of stem cells from adult mouse testes," *Nature Protocols*, vol. 4, no. 2, pp. 143–154, 2009.

[19] F. Izadyar, F. Pau, J. Marh et al., "Generation of multipotent cell lines from a distinct population of male germ line stem cells," *Reproduction*, vol. 135, no. 6, pp. 771–784, 2008.

[20] L. A. Boyer, I. L. Tong, M. F. Cole et al., "Core transcriptional regulatory circuitry in human embryonic stem cells," *Cell*, vol. 122, no. 6, pp. 947–956, 2005.

Hindawi Publishing Corporation
Stem Cells International
Volume 2016, Article ID 3984937, 17 pages
http://dx.doi.org/10.1155/2016/3984937

Review Article

MicroRNAs: From Female Fertility, Germ Cells, and Stem Cells to Cancer in Humans

Irma Virant-Klun,[1] Anders Ståhlberg,[2] Mikael Kubista,[3,4] and Thomas Skutella[5]

[1]*Department of Obstetrics and Gynaecology, University Medical Center Ljubljana, SL-1000 Ljubljana, Slovenia*
[2]*Sahlgrenska Cancer Center, Department of Pathology, Institute of Biomedicine, University of Gothenburg, 40530 Gothenburg, Sweden*
[3]*TATAA Biocenter, 41103 Gothenburg, Sweden*
[4]*Institute of Biotechnology, Czech Academy of Sciences, 14220 Prague, Czech Republic*
[5]*Institute for Anatomy and Cell Biology, University of Heidelberg, 69120 Heidelberg, Germany*

Correspondence should be addressed to Irma Virant-Klun; irma.virant@kclj.si

Received 7 May 2015; Accepted 19 August 2015

Academic Editor: Gary E. Lyons

MicroRNAs are a family of naturally occurring small noncoding RNA molecules that play an important regulatory role in gene expression. They are suggested to regulate a large proportion of protein encoding genes by mediating the translational suppression and posttranscriptional control of gene expression. Recent findings show that microRNAs are emerging as important regulators of cellular differentiation and dedifferentiation, and are deeply involved in developmental processes including human preimplantation development. They keep a balance between pluripotency and differentiation in the embryo and embryonic stem cells. Moreover, it became evident that dysregulation of microRNA expression may play a fundamental role in progression and dissemination of different cancers including ovarian cancer. The interest is still increased by the discovery of exosomes, that is, cell-derived vesicles, which can carry different proteins but also microRNAs between different cells and are involved in cell-to-cell communication. MicroRNAs, together with exosomes, have a great potential to be used for prognosis, therapy, and biomarkers of different diseases including infertility. The aim of this review paper is to summarize the existent knowledge on microRNAs related to female fertility and cancer: from primordial germ cells and ovarian function, germinal stem cells, oocytes, and embryos to embryonic stem cells.

1. Introduction

It is estimated that only approximately 2% of the human genome represents the protein-coding region. More and more, it turns out that the key factor of this phenomenon may be microRNAs (miRNAs, miRs). It is known that miRNAs are a family of naturally occurring small noncoding RNA molecules of 19–24 nucleotides in length that play an important regulatory role in gene expression [1, 2]. They are thought to regulate a large proportion of protein-coding genes [3]. MiRNAs mediate the translational regulation and control gene expression posttranscriptionally by binding to a specific site at the 3′-UTR of target mRNA, which results in mRNA cleavage and translation repression. MiRNAs are transcribed by RNA polymerase II as part of polyadenylated primary transcripts (pri-miRNAs) that can be protein-coding or noncoding. The primary transcripts are then cleaved by the Drosha ribonuclease III enzyme that produce an approximately 70-nucleotide stem-loop precursor miRNA (pre-miRNA), which is further cleaved by the cytoplasmic Dicer ribonuclease (Dcr-1) to generate the mature miRNA and antisense miRNA star (miRNA*) products. Further, the mature miRNA is incorporated into RNA-induced silencing complex (RISC), which recognizes the target mRNAs through imperfect base pairing with the miRNA and mostly results in translational inhibition or destabilization of the target mRNA. In general, it has been estimated that about 30% or even more of human mRNAs are regulated by miRNAs [4]. Nearly 2865 mature miRNAs have been identified in the human genome until now, and it is believed

that these miRNAs may contribute to at least 60% of the human transcriptome. Recent scientific findings show that miRNAs are emerging as important regulators of cellular differentiation and dedifferentiation and are deeply involved in developmental processes. Moreover, it became evident that dysregulation of miRNA expression may play a fundamental role in progression and dissemination of different cancers. However, it is becoming clear that the activity of miRNAs is not always determined by their expression in cells. Their activity can be affected by RNA-binding proteins such as dead end (DND1), which inhibits the function of variety of miRNAs by blocking the access of target mRNAs [3]. Regarding all this new knowledge, miRNAs may play an important role in modulating gene expression during human preimplantation development from primordial germ cells to the embryo. The interest is still increased by discovery of exosomes, cell-derived vesicles, which are released from the cell when multivesicular bodies fuse with the plasma membrane or are released directly from the plasma membrane [5]. Exosomes can carry different proteins but also miRNAs and mRNAs [6] between different cells and are deeply involved in cell-to-cell communication. They can be found in almost all body fluids and also in media of cell cultures [7]. Exosomes have a great potential to be used for prognosis, therapy, and biomarkers of different diseases including infertility.

The analysis of small RNAs can now be performed by diverse techniques including cDNA cloning and sequencing, real-time PCR, microarrays, and RNA-sequencing. The RNA-seq massively improved and enabled the discovery of novel small RNAs, including miRNAs and sensitive quantitative small RNA expression analysis [8].

The aim of this review paper is to summarize the existent knowledge on miRNAs related to female fertility and cancer: from primordial germ cells and ovarian function, stem cells, oocytes, and embryos that lead to the birth of a new human being or else to aggressive cancers as something goes wrong on this long way. The data on humans reinforced some interesting findings in the animal models.

2. Primordial Germ Cells and Germ Cell Tumors

2.1. Primordial Germ Cells. The human preimplantation development may be supposed to begin with primordial germ cells (PGCs) which surprisingly arise outside the genital ridge region and can first be identified in the human embryo at about 3 weeks in the yolk sac epithelium near the base of developing allantois [9]. They are recognized by their distinctive morphology and alkaline phosphatase activity. The PGC population is expanded by mitosis and migrates by ameboid movement to the connective tissue of the hind gut and from there into the gut mesentery. About 30 days after fertilization, the majority of the PGCs pass into the region of the developing kidneys and then to adjacent gonadal primordial where they, based on chemotaxis, join the cells of the sex and medullary cords. It has been demonstrated that robust PGC migration is regulated by their miRNAs (e.g., miR-430) in the zebrafish model [10]. Throughout the PGC migration and early colonization, it is not possible to discriminate between female and male gonads and we talk about the indifferent gonads. In the human embryo, the PGC colonization is completed during the sixth week of gestation and after that time the female gonad, ovary, started to develop due to the lack of chromosome Y and the gene SRY, namely, and the PGCs start to develop into female gametes.

The germ cell development requires timely transition from PGCs self-renewal to meiotic differentiation, that is associated with several changes in gene expression, including downregulation of stem cell-associated genes, such as *OCT4* and *KIT*, and upregulation of genes related to germ cells and meiosis, such as *VASA*, *STRA8*, and *SYCP3*. It has already been evidenced that stem cell-expressed RNA-binding protein LIN28 is essential during normal germ cell development for PGC specification in mice. Recently, the expression of LIN28 was examined during normal germ cell development in the human fetal ovary, from the PGC stage, through meiosis and to the initiation of follicle formation [11]. It was found that LIN28 transcript levels were the highest when the fetal ovary contained only PGCs and decreased significantly with increasing time of gestation, concordant with the germ cell differentiation. In addition, immunohistochemistry revealed the expression of LIN28 protein to be germ cell-specific at all stages examined. All PGCs expressed LIN28, but at later gestation time the expression of this protein was restricted to a subpopulation of germ cells, which were demonstrated to be primordial and premeiotic germ cells based on immunofluorescent colocalization of proteins LIN28 and OCT4 and absence of meiosis marker SYCP3. Moreover, the expression of the LIN28 target precursor miRNA transcripts Let-7a/f/d and Let-7g was substantiated in the human fetal ovary, and that expression of these transcripts was the highest at the PGC stage, like for LIN28. The spatial and temporal restriction of LIN28 expression and coincident peaks of expression of LIN28 and target pri-miRNAs suggest important roles for this protein in the maintenance of the germline stem cell state and the regulation of miRNA activity in the developing human ovary. Beside this study, there is almost no data on miRNAs in human PGCs in literature and the main findings came from animal studies.

One of the most important roles of miRNAs in PGCs is targeting the epigenetics-related genes and DNA methylation process in developing gonads. In the mouse model, it has been found that miR-29b may play an important role in female gonadal development by targeting epigenetics-related genes such as *DNMT3A* and *DNMT3B* and thereby modulating methylation of genomic DNA in PGCs [12]. Similarly, it has been found in a chicken, where it has been confirmed that *DNMT3B* expression was reestablished in a female germ cell-specific manner, downregulation by four miRNAs: miR-15c, miR-29b, miR-383, and miR-222 [13]. Some other studies in the vertebrate species such as golden fish [14], zebrafish [15], medaka [16], frog [17], chicken [18], and fruit fly [19] revealed some other miRNAs that may be essential for development and maintenance of PGCs, as can be seen in Figure 1. The pattern of miRNA expression in PGCs seems to be species-specific although some miRNAs such as miR-29b and miR-430 overlap between different species. Some data show that a germline-specific RNA-binding protein DAZ-like (DAZL)

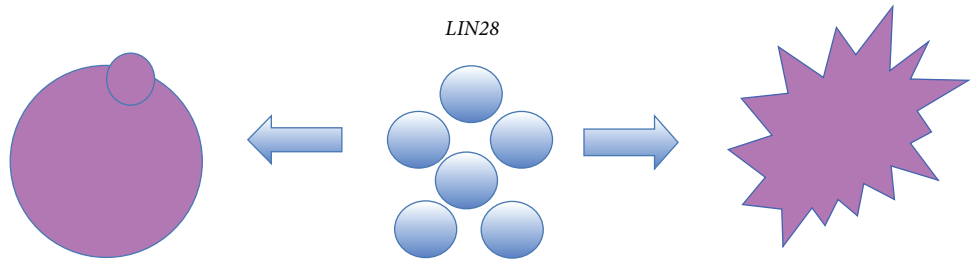

Mature oocytes	Primordial germ cells	Human germ cell tumors
Humans:	Humans:	Dysgerminoma (DS):
miR-10A, miR-100, miR-184, miR193a-5p, miR-297, miR-602, and miR-625	Let-7a/f/d, Let-7g Mouse: miR-29b Golden fish: miR-430 Zebrafish: miR-430 Frog: miR-427 Chicken: miR-15c, miR-29b, miR-181a*, miR-222, miR-302a, miR-383 miR-9c, and miR-969 Fruit fly: miR-969, miR-9c	miR-146b-5p, miR-155, and miR-182 Yolk sac tumor (YST): miR-122, miR-200b, miR-200c, miR-302a, miR-302c, miR-375, and miR-638 Immature teratoma (IT): no specific miRNAs reported All germ cell tumors: upregulated miR-371-373 and miR-302/367, downregulated Let-7

Figure 1: Most expressed miRNAs in primordial germ cells [10–19], germ cell tumors [24], and human oocytes [28, 29]. MiR-29b and miR-430 are overlapping between different vertebrate species. MiR302a, upregulated, and Let-7, downregulated, in germ cell tumors are overlapping with miRNAs identified in vertebrate PGCs. The expression of gene *LIN28* is essential during normal germ cell development for PGC specification. Tumor-suppressor Let-7 miRNA family is downregulated in malignant germ cell tumors because of abundant expression of the regulatory gene *LIN28*.

acts as an "anti-miRNA factor" during vertebrate germ cell development [15]. During zebrafish embryogenesis, miR-430 contributes to suppress NANOS1 and TDRD7 to primordial germ cells (PGCs) by mRNA deadenylation, mRNA degradation, and translational repression of NANOS1 and TDRD7 mRNAs in somatic cells. It was shown that DAZL can decrease the miR-430-mediated repression of TDRD7 mRNA by inducing poly(A) tail elongation (polyadenylation). These data indicated that DAZL acts as an "anti-miRNA factor" during vertebrate germ cell development. Interestingly, in the case of fruit flies, it was found that embryos derived from miR-969- and miR-9c-mutant mothers had reduced germ cell numbers and increased variance in the phenotype [19] thus indicating that miRNAs may be related to (in)fertility. In addition, it has been confirmed that Dicer1 (Dcr-1) and miRNAs are involved in maintenance and self-renewal of ovarian germinal stem cells in fruit fly ovaries [20–23].

2.2. Germ Cell Tumors. PGCs do not always further develop into female gametes but may form uncommon but aggressive and malignant germ cell tumors, which are mostly found in young women or adolescent girls and manifest as different types of malignancies: dysgerminoma (DS), yolk sac tumor (YST), and immature teratoma (IT) [24]. The origin of germ cell tumors traces back to PGCs in the embryo and reflects their specific characteristics such as totipotency and sensitivity to DNA damaging agents; therefore, germ cell tumors provide a useful model to study the gene regulation involved in oncogenesis [25]. Germ cell tumors show some similarities with pluripotent precursor PGCs and stem cells in terms of expression of genes/proteins related to pluripotency (e.g., NANOG, POU5F1, and SOX-2) and embryogenesis (e.g., GATA4, GATA6, and TFAP2C). The molecular characteristics are comparable to DS and testicular counterparts (KIT signaling pathway), while they are quite specific for YST (WNT/B-catenin and TGF-B/bone morphogenetic protein signaling pathways) [24].

The recent data show that dysregulation of miRNAs may be involved in the manifestation of germ cell tumors [24, 26, 27]. Different types of germ cell tumors may develop by different developmental processes involving insufficient sexual differentiation of PGCs and different irregular patterns of miRNA expression, as can be seen in Figure 1. Genomic and protein-coding transcriptomic data have suggested that

germ cell tumors (GCTs) in childhood are biologically distinct from those of adulthood. It has been shown that all malignant germ cell tumors overexpress the miR-371–373 and miR-302/367 clusters with increased serum levels, regardless of patient age, histological subtype, or anatomical site of tumor [26, 27]. The tumor-suppressor Let-7 miRNA family has also been shown to be universally downregulated in malignant germ cell tumors because of abundant expression of the regulatory gene *LIN28* and results in upregulation of oncogenes including *MYCN*, *AURKB*, and *LIN28* by itself.

Interestingly, some miRNAs such as miR-29b and miR-430 overlapped between different vertebrate species and some miRNAs upregulated (miR302a) or downregulated (Let-7) in germ cell tumors overlapped with miRNAs identified in vertebrate PGCs according to different studies, as can be seen in Figure 1. MiRNAs identified in PGCs and germ cell tumors differ from miRNAs that were found to be abundant in mature human oocytes [28, 29].

3. Ovary: Oocytes, Cumulus (Granulosa) Cells, and Follicular Fluid

3.1. Ovary. After migration and colonization, PGCs become oogonia in the forming fetal ovary. The oogonia proliferate extensively by mitotic divisions to up to 5–7 million cells in humans. Each oogonium inside the fetal ovary divides and enters into the initial stage of meiosis to become the primary oocyte. The diploid primary oocyte stopped at the first meiotic prophase stage. It has a nucleus called the germinal vesicle (GV); therefore, this stage refers to the GV-stage of maturity. GV oocytes are localized within the primordial follicles, where they are surrounded by flattened and condensed layer of surrounding granulosa cells. The data derived from the mouse model show that miRNA-376a regulates the primordial follicle assembly in the ovary by modulating the expression of proliferating cell nuclear antigen (*PCNA*) gene in mouse fetal and neonatal ovaries. MiR-376a negatively correlated with PCNA mRNA expression in fetal and neonatal mouse ovaries and directly bound to PCNA untranslated region [30], while there is no data available for humans at present.

By the end of the fetal period, all primary oocytes are formed and stopped at the first meiotic prophase stage. The primary oocytes are maintained for years, until puberty (menarche), when they finish the first meiotic division and divide into two daughter cells: a haploid secondary oocyte and an extruded polar body. During the reproductive period of life, in each menstrual cycle, only a few primary oocytes are recruited, and only one of them indeed matures and is ovulated to be fertilized. When the secondary oocyte enters the second meiotic division, it is not finished but arrested again and held at the metaphase II (MII) stage until fertilization. When the oocyte is fertilized, the process of meiosis is terminated and the second polar body is extruded. The MII-stage oocyte has the potential to be fertilized, while the immature GV-stage oocyte does not. During each menstrual cycle, only 15–20 early antral follicles/oocytes are recruited and only one dominant follicle, indeed, matures and is ovulated. The miRNAs are confirmed to be involved in follicular maturation. Three different miRNAs, miR-224, miR-378, and miR-383, have been found to be involved in the regulation of aromatase expression during follicle development. In addition, miR-21 proved to promote the follicular cell survival during ovulation. Proangiogenic miR-17-5p and let-7b were shown to be essential for normal development of the corpus luteum after ovulation [31]. The experimental data in a mouse model showed that ribonuclease III named Dicer1, essential for synthesis of mature functional miRNAs, is involved in the process of folliculogenesis [32]. Dicer1 protein was expressed in both oocytes and granulosa cells of follicles. The role of miRNAs in mouse ovarian development was explored by using Dicer1 conditional knockout (cKO) mouse in which Dicer1 was deleted specifically in granulosa cells. With Dicer1 deletion, miR-503, that is more abundant in a mouse ovary than in other tissues, was significantly downregulated. The increased pool of primordial follicles accelerated the early follicle recruitment and more degenerated follicles could be observed. The ovarian niche is extremely important for the growth and maturation of follicles/oocytes and irregularities may lead to infertility.

3.2. Oocyte-Cumulus Complex

3.2.1. Human Oocytes. Each oocyte develops and matures in the functional unit of the ovary, the follicle, surrounded and supported by granulosa and theca cells, which represent the important niche for oocyte growth and maturation. The communication between the oocyte and surrounding follicular cells is a prerequisite for normal growth and maturation of the oocyte resulting in fertilization and the development of an embryo. This oocyte-cumulus communication is still poorly understood and it is proposed that miRNAs may play an important role. There is little data on miRNAs in human oocytes because they do represent a scarce and sensitive biological material, which is mostly not available to researchers. Despite that, miRNAs have already been confirmed in human oocytes retrieved in the in vitro fertilization program in rare studies. In one study, the dynamic changes of miRNAs from GV- to MII-stages were analyzed [28] by miR-CURY LNA microarray platform and quantitative RT-PCR. Oocytes were divided into four groups, corresponding to GV oocytes, MI oocytes, MII oocytes in vitro matured at conventional FSH level (5.5 ng/mL), and MII oocytes matured in vitro at a high FSH level, 2,000 ng/mL, respectively. Altogether, 722 miRNAs were identified in oocytes. In mature MII-stage oocytes, four miRNAs were upregulated and eleven were downregulated in comparison to immature GV-stage oocytes, as can be seen in Figure 2. The RT-PCR analysis of miR-15a and miR-20a expression revealed the concordant dynamic changes of these two miRNAs during meiosis. Moreover, the high concentration of FSH in the in vitro maturation medium led to reverse effect on the expression of miR-15a and miR-20a, which confirmed the involvement of these two miRNAs in the oocyte maturation process influenced by FSH [28]. Another study illustrated that miR10A, miR100, and miR184 were abundant in human mature MII-stage oocytes and that they differed from the palette of miRNAs abundant in surrounding *cumulus oophorus*, a cluster of cells called cumulus cells

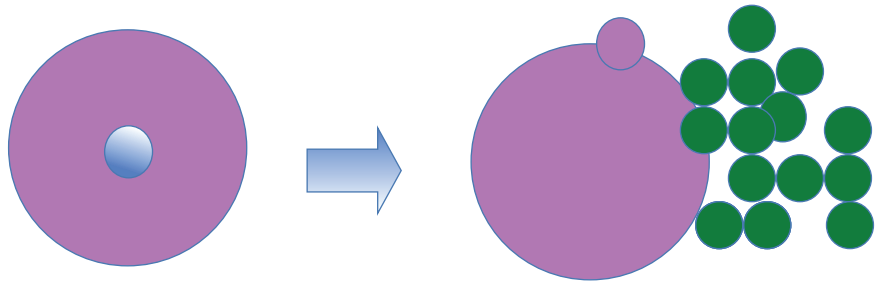

Immature (GV) oocyte

Mature MII oocyte

Upregulated:

miR-193a-5p, miR-297,

miR-625, and miR-602

Downregulated:

miR-888, miR-212,

miR-662, miR-299-5p, miR-339-5p,

miR-20a, miR-486-5p, miR-141,

miR-768-5p, miR-376a, miR-15a

Abundant:

miR10A, miR100, miR184

Mature (MII) oocytes with cumulus cells

Cumulus cells

Abundant:

miR-21, miR-29a, miR-30d,

miR-93*, miR125-a, miR-320a,

and Let-7*

Young, middle-aged women:

miR-425, miR-744, miR-146b, and Let-7d

Older women (>37 years):

miR-202, Let-7e

Steroidogenesis:

miR-133b, miR-513a-3p

Proliferation and apoptosis:

miR-15a, miR-188,

miR-10a, miR-105, and miR-182

Figure 2: Comparison of miRNAs in immature and mature human oocytes and surrounding cumulus cells according to female age, steroidogenesis, proliferation, and apoptosis [28, 29, 33, 40, 41, 45–47]. Legend: *miRNAs which are also abundant in the mouse cumulus cells.

surrounding the oocyte in the ovarian follicle (see Figure 2) [29].

The predicted target genes of the oocyte miRNAs were associated with the regulation of transcription and cell cycle, while genes targeted by cumulus cell miRNAs were involved in extracellular matrix and apoptosis. The comparison of predicted miRNA target genes and mRNA microarray data resulted in a list of several target genes that were differentially expressed in MII oocytes and cumulus cells, including *PTGS2*, *CTGF*, and *BMPR1B* that are important for cumulus-oocyte communication. Further functional analysis in primary granulosa cell cultures revealed that BCL2 and CYP19A1 mRNA levels were decreased when miR23a is overexpressed. These results suggested that miRNA could play an important role in the regulation of oocyte and cumulus cell cross talk [29]. Interestingly, some of miRNAs that were abundant in human cumulus cells such as miR-93 and Let-7 overlapped with those in mice [33].

Mammalian oocyte maturation is characterized by asymmetric cell division that results in a large oocyte and a small polar body in contrast to symmetric division in mitosis of somatic cells. The asymmetry results from oocyte polarization including spindle positioning, migration, and cortical reorganization, critical for fertilization and for early embryo development. The actin dynamics is involved in this process, and miRNAs are proposed to play an important regulatory role [34].

3.2.2. Animal Oocytes. Because human oocytes are a rare and difficult available research material, some confirmation and interesting findings came from animal experiments in other mammalian species, especially in mouse and bovine (see Supplementary Table 1 in Supplementary Material available online at http://dx.doi.org/10.1155/2016/3984937). Similar to human oocytes, 59 miRNAs were differently expressed in

immature and mature bovine oocytes [35]. Moreover, it was found that 47 and 51 of miRNAs were highly abundant in bovine GV and MII oocytes in comparison to the surrounding cumulus cells. Six miRNAs that were enriched in oocytes, namely, miR-96, miR-122, miR-146a, miR-146b-5p, miR-150, and miR-205, dramatically decreased during in vitro maturation [36]. Experiments with the bovine model showed that the expression of an oocyte-specific basic helix-loop-helix transcription factor FIGLA, essential for primordial follicle formation and expression of many genes required for fertilization and early embryonic survival, is regulated by miR-212 [37]. MiR-212 was expressed in oocytes and increased in early embryos. Using transient transfection and reporter assays, it turned out that miR-212 repressed the expression of FIGLA in bovine oocytes and embryos. Both LIN28a and LIN28b transcripts were abundant in mouse oocytes. In marked contrast to vertebrate PGCs, LIN28a and LIN28b were inactive during oocyte growth because their knockdown has no effect on Let-7a levels in intact germinal vesicle (GV) oocytes [38]. Furthermore, transgenic females were fertile and produced healthy offspring, and their overall breeding performance was comparable to that of wild-type mice. In spite of several miRNAs identified in mouse oocytes, some experimental data revealed that miRNA function may be globally suppressed in mouse oocytes and early embryos and that another type of small RNAs, small interfering RNAs (siRNAs), may play an important role [39]. It is known that the deletion of *Dgcr8,* also known as *Pasha* that is required for miRNA processing (binds to Drosha), specifically blocks the production of canonical miRNAs, while the deletion of *Dicer* blocks the production of both miRNAs and endo-siRNAs in cells. The conditional deletion of *Dicer* in mouse oocytes leads to severe defects in chromosomal alignment, spindle organization, and infertility. In contrast to *Dicer*, *Dgcr8*-deficient mouse oocytes matured normally and produced healthy offspring after fertilization. Their mRNA profiles were identical to oocytes of wild-type mice, while *Dicer*-null oocytes showed several misregulated transcripts. This phenomenon needs to be further elucidated in humans and other mammalian species.

3.3. Cumulus and Granulosa Cells. The data on human cumulus cells with predominating granulosa cells are much more abundant, because it is easier to retrieve the cumulus cells in the in vitro fertilization program than oocytes by themselves. The cumulus cells can be obtained mechanically (cutting) or by enzymatic (hyaluronidase) denudation of oocytes and are otherwise discarded in daily medical practice. Cumulus cells can be studied from various angles as they are related to oocyte maturation and quality. A large-scale profiling of EIF2C2- (protein argonaute-2-) bound miRNAs was performed in three human granulosa-derived cell lines (i.e., KGN, HSOGT, and GC1a) and in primary human granulosa cells using high-throughput sequencing [40]. Argonaute proteins with their argonaute-2 containing PIWI domain have a dominant effect on RNA interference. They interact with Dicer1 and participate in short-interfering-RNA-mediated gene silencing. MiR-21 accounted for more than 80% of EIF2C2-bound miRNAs thus suggesting that it was enriched in the RNA-induced silencing complex (RISC) and was important for human granulosa cells. The target of miR-21 in granulosa cells was COL4A1 mRNA that is related to a component of the basement membrane surrounding the granulosa cell layer and the granulosa-embedded extracellular structure.

3.3.1. Female Age. The increase in female age is the main factor reducing female fertility and the outcome of assisted conception. The mechanisms are still not well understood. It has been found that female aging alters the expression of variety of genes in human cumulus cells being essential for oocyte quality and potential targets of specific miRNAs previously identified in cumulus cells, such as miR-425, miR-744, miR-146b, and Let-7d for younger (<30 years) and middle-aged (31–34 years) women and miR-202 and Let-7e for elder (>37 years) women [41].

3.3.2. Follicle and Steroidogenesis. Some studies demonstrated that miRNA pattern is a dynamic feature in a follicle and may differ between different groups of follicular cells surrounding and supporting the oocyte. In more detail, there was a difference in the miRNA pattern between the *corona radiata*, the innermost layer of the *cumulus oophorus,* directly adjacent to the oocyte zona pellucida, and the rest of the cumulus cells [42]. A total of 785 and 799 miRNAs were identified in *corona radiata* and the rest of the cumulus cells. Seventy-two miRNAs were differently expressed between these two groups of cells. The bioinformatics analysis showed that these miRNAs were related to amino acid and energy metabolism. Another study determined the miRNA profile of two intrafollicular somatic cell types: mural (MGCs from the outer "wall" of the follicle) and cumulus (CGCs inner cells around the oocyte) granulosa cells from women undergoing controlled ovarian stimulation for in vitro fertilization [43]. Altogether, 936 annotated miRNAs and nine novel miRNAs were identified, and 90 of the annotated miRNAs were differentially expressed between MGCs and CGCs. The bioinformatic prediction revealed that different pathways, such as TGFβ, ErbB signaling, and heparan-sulfate biosynthesis, were targeted by miRNAs in both granulosa cell populations, while extracellular matrix remodeling, Wnt, and neurotrophin signaling pathways were enriched among miRNA targets in MGCs. Interestingly, two of the nine novel miRNAs identified were found to be of intronic origin: one from the aromatase and the other one from the FSH receptor gene; the latter miRNA was predicted to target the activin signaling pathway. These results suggest that posttranscriptional regulation of gene expression by miRNAs may play an important role in the modification of gonadotropin signaling [43]. This is in accordance with the general knowledge on granulosa cells. Within the follicle, the granulosa cells surrounding the oocyte are in intimate contact with it by gap and adhesion junctions and release several substances decisive for oocyte growth and maturation. Granulosa cells are also involved in the endocrine activity of follicle, steroidogenesis, by transforming the androgens (androstenedione) from theca cells into estrogens by aromatase activity. They possess FSH hormone receptors and the number of granulosa cells

increases directly in response to the increased levels of circulating gonadotropins or decreases in response to testosterone. They also produce some peptides involved in the regulation of ovarian hormone synthesis. Furthermore, the effect of transfection of cultured primary human ovarian granulosa cells with 80 different gene constructs encoding human pre-miRNAs on release of hormones, progesterone, testosterone, and estradiol, was evaluated by enzyme immunoassay [44]. In addition, two selected antisense constructs, blocking the corresponding miRNAs, were tested on progesterone release in granulosa cells. It has been shown that 36 out of 80 tested miRNA constructs resulted in inhibition of progesterone release and 10 miRNAs promoted progesterone release in human granulose cells. Fifty-seven miRNAs tested inhibited testosterone release, and only one miRNA enhanced testosterone output and 51 miRNAs suppressed estradiol release, while none of the miRNAs tested stimulated it. The authors suggested that miRNAs can control reproductive functions by enhanced or inhibited release of ovarian progestagen, androgen, and estrogen in human granulosa cells and suggested that such miRNA-mediated effects could be potentially used for the regulation of reproductive processes including fertility and for the treatment of reproductive and other steroid-dependent disorders of women [44]. The proof was given that miR-133b downregulates *FOXL2* expression by directly targeting the 3′UTR and inhibiting the FOXL2-mediated transcriptional repression of *StAR* and *CYP19A1* to promote estradiol production in the mouse granulosa cells [45].

It has also been found that miR-513a-3p is involved in the control of the luteinizing hormone/chorionic gonadotropin receptor (LHCGR) expression by an inversely regulated mechanism at the posttranscriptional level, essential for normal female reproductive function [46].

3.3.3. Proliferation and Apoptosis. One of the most important factors affecting the oocyte quality is apoptosis of granulosa cells surrounding the oocyte. The granulosa cell apoptosis can be related to impaired oocyte quality. To better elucidate the potential role of miRNAs in the regulation of proliferation and apoptosis in ovarian granulosa cells, the effect of transfection of cultured primary human granulosa cells with 80 different constructs encoding human pre-miRNAs on the expression of the proliferation marker, PCNA, and the apoptosis marker Bax was evaluated using immunocytochemistry [47]. The results showed that eleven out of 80 tested miRNA constructs resulted in stimulation, and 53 miRNAs resulted in inhibition of PCNA. Moreover, 11 out of the 80 miRNAs tested promoted accumulation of Bax, while 46 miRNAs caused a reduction in Bax in human granulosa cells. In the next step, two selected antisense constructs blocking the corresponding miRNAs miR-15a and miR-188 were used to evaluate their effects on the expression of PCNA. An antisense construct inhibiting miR-15a increased PCNA, while an antisense construct of miR-188 did not affect PCNA expression. Validation of effects of selected pre-miR-10a, miR-105, and miR-182 by using other markers of proliferation (cyclin B1) and apoptosis (TdT and caspase 3) confirmed the specific role of miRNAs in human granulosa cell proliferation and apoptosis [47].

3.4. Follicular Fluid and Plasma. It is of great advantage that miRNAs can be identified in body fluids such as follicular fluid retrieved in the in vitro fertilization program or in blood plasma. Follicular fluid is retrieved by ultrasound-guided aspiration of oocytes from follicles after controlled hormonal stimulation of ovaries for in vitro fertilization. When the oocytes are removed for in vitro fertilization, the follicular fluid is discarded in daily medical practice but can represent a perfect material to study the ovarian physiology and pathologies and the oocyte quality. It has been reported that miRNAs can readily be detected within membrane-enclosed vesicles of human follicular fluid. In a current research, 37 miRNAs were found to be upregulated in human follicular fluid in comparison to plasma in the same women [48]. It was evidenced that 32 of these miRNAs were carried by microvesicles, exosomes, that expressed the well-characterized exosomal markers such as CD63 and CD81. The authors suggested that these miRNAs identified in the follicular fluid are involved in the critically important pathways for follicle growth and oocyte maturation. Specifically, nine of these miRNAs are known to target and negatively regulate mRNAs expressed in the follicular microenvironment by encoding inhibitors of follicle maturation and meiosis resumption. It has been evidenced that increased female age affected the pattern of miRNAs in follicular fluid [49]. In the miRNA profile of the follicular fluid of younger (<31 years) and older (>38 years) women, there was a set of four differentially expressed miRNAs. The predicted targets of these miRNAs were genes involved in the heparan-sulfate biosynthesis, extracellular matrix-receptor interaction, carbohydrate digestion and absorption, p53 signaling, and cytokine-cytokine-receptor interaction. It needs to be exposed that several of these pathways are related to fertility, suggesting that this set of miRNAs and their targets need to be studied in relation to reproductive aging and assisted conception outcome.

Moreover, it has been found that ovarian pathologies such as polycystic ovary syndrome (PCOS) and premature ovarian failure (POF) or primary ovarian insufficiency affect the miRNA expression in follicular fluid and plasma.

3.4.1. Polycystic Ovary Syndrome. PCOS is a systematic disease represented by a set of symptoms due to hormone imbalance in women [50]. It is usually diagnosed by anovulation, high androgen levels, and several ovarian cysts detected by ultrasound. The typical symptoms include irregular or no menstrual periods, heavy periods, obesity, excess body and facial hair (hirsutism), acne, pelvic pain, low fertility and trouble getting pregnant, and patches of thick and darker skin. It can be related to the type 2 diabetes, obstructive sleep apnea, heart disease, mood disorders, and endometrial cancer. Moreover, PCOS is one of the most common endocrine disorders in women of reproductive age and causes low fertility. Microarray profiling of human follicular fluid revealed the expression of 235 miRNAs in human follicular fluid and 29 of them were differentially expressed between the PCOS and normal groups of women [51]. After PCR validation, 5 miRNAs showed significantly increased expression in the PCOS group of women (Figure 3). The potential target genes were related to insulin regulation and

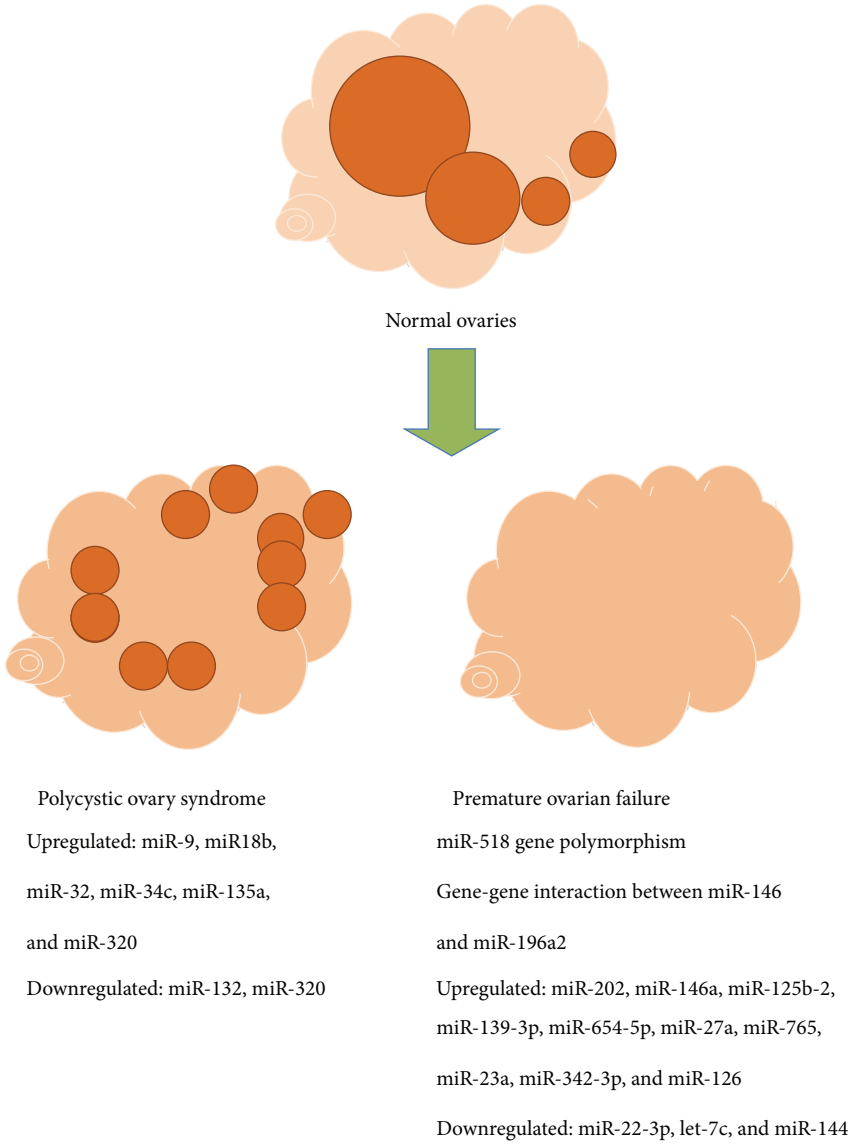

Figure 3: MiRNAs that were differently expressed in follicular fluid and plasma of women with polycystic ovary syndrome [51–54] and premature ovarian failure [55–60] in comparison to healthy women with normal ovaries.

inflammation. Moreover, the most highly expressed miRNA targeted genes were found to be associated with reproductive, endocrine, and metabolic processes. In another study, it has been found that two miRNAs, miR-132 and miR-320, were expressed at significantly lower levels in the follicular fluid of women with PCOS than in a group of healthy women, as can be seen in Figure 3. In addition, it has been evidenced that miR-132, miR-320, miR-520c-3p, miR-24, and miR-222 that are present in the follicular fluid regulate estradiol concentrations and miR-24, miR-193b, and miR-483-5p progesterone concentrations [52]. The authors concluded that there are several miRNAs in human follicular fluid and that some of them may play an important role in steroidogenesis and PCOS. Interestingly, the miR-320 was differently expressed in the follicular fluid of women with PCOS in still one study [53] and was along miR-383 upregulated in comparison with healthy (control) women. This study demonstrated that miR-320 regulates the proliferation and steroid production by targeting E2F1 and SF-1 in granulosa cells and is involved in the follicular development. The authors summarized that understanding the regulation of miRNA biogenesis and function in the follicular development in humans will potentiate the usefulness of miRNA in the treatment of some steroid-related disorders and female infertility. In comparison to healthy women, a total of 59 known miRNA were identified that were differentially expressed in cumulus granulosa cells of women with PCOS: 21 miRNAs were increased and 38 miRNAs decreased [54]. Several important processes could be targeted by these miRNAs, such as Notch signaling, regulation of hormones, and energy metabolism. Moreover, Notch3 and MAPK3, the members of Notch signaling and ERK-MAPK pathway, were found to be directly regulated by miR-483-5p.

3.4.2. Premature Ovarian Failure. Another indication of severe ovarian infertility is POF, which is defined as an ovarian disorder of multifactorial origin characterized by amenorrhea, hypergonadotropism (e.g., increased FSH levels), hypoestrogenism, and no follicles/oocytes to be fertilized in women under the age of 40 years [55]. The plasma samples are usually analyzed on miRNAs in patients with POF because they mostly do not have follicles. In one study, the microarray chip results demonstrated that 10 miRNAs were significantly upregulated and 2 miRNAs were downregulated in plasma of POF patients compared with normal women, as can be seen in Figure 3 [56]. Among miRNAs that were upregulated in plasma was miR23a, which has been confirmed to be of great importance in regulation of apoptosis in ovarian granulosa cells via decreasing X-linked inhibitor of apoptosis protein (XIAP) expression [57]. Further, miR-22-3p has been found to show a lower expression level in the plasma of women with POF and distinguish them from control subjects. In addition, it was negatively associated with serum FSH levels [58]. The target functions of miR-22-3p were apoptosis, endocytosis, and tumorigenesis. The authors suggested that decreased expression of miR-22-3p in plasma of POF patients reflects the diminished ovarian reserve as a consequence of the pathologic process of POF. Further, the current study provided the evidence to implicate miR-518 and TGFBR2 gene polymorphisms as novel susceptibility factors for POF, age at natural menopause, and early menopause risk [59]. Some findings suggest that putative gene-gene interaction between miR-146 and miR-196a2 may be involved in POF development [60]. It is very important to study the causes of diminished ovarian reserve. Actually, there are no relevant biomarkers available to estimate the ovarian reserve in (in)fertile women and to predict the assisted conception outcome. The existing ultrasound monitoring of ovaries and the determination of FSH and AMH hormone levels in serum have been proven to be insufficient and nonreliable. Therefore, some new biomarkers are needed.

4. Fertilization and Paternal Contribution to the Embryo

Fertilization is the fusion of gametes to initiate the development of a new individual organism and represent one of the main events in the human preimplantation development. Naturally, it occurs in the ampullary region of the oviduct but may also occur in vitro. During fertilization, sperm contribute some genetic and epigenetic factors that affect the early embryogenesis [61]. Epigenetic factors contributed by sperm include a functional centrosome, proper packaging of the chromatin with sperm-specific protamines, modifications of histones, and imprinting of genes. In addition, the fertilizing spermatozoon provides its own mRNAs and miRNAs, which may contribute to the embryonic transcriptome and regulate the embryonic gene expression. All these epigenetic factors may directly or indirectly affect the expression of genes in the developing embryo.

In general, spermatozoa are transcriptionally inactive, extremely specialized haploid cells with a head containing a compact nucleus and minimal cytoplasm. On the other hand, especially during recent years, it has been proven that sperm still contain a complex population of RNAs that comprises rRNA, mRNA, and both long and small noncoding RNAs. It was suggested that the intact mRNA sequences are enriched for genes associated with the infertility, fertilization, and early embryo development [8]. It has been demonstrated that mRNA is retained in sperm and increases after fertilization prior to zygotic genomic activation [62]. rRNA is the most enriched RNA population but highly fragmented thus ensuring the translationary inactivated state of the sperm cell.

Gradually, the overall functional significance of RNA in sperm is better recognized. Using the zona pellucida free hamster oocyte/human sperm penetration assay, it has been shown that sperm-specific transcripts, not present in the unfertilized oocyte, are transmitted to the oocyte upon fertilization [63]. Further, it has been demonstrated that injection of a sperm-borne transcript PLC-zeta, not present in the unfertilized oocyte, can be translated in the oocyte into a functional calcium oscillator and oocyte activator during fertilization [64]. The presence of noncoding RNAs in sperm also postulated potential roles in early postfertilization and embryonic development. These assumptions have been extended to the view that sperm-borne RNAs might have epigenetic effects on the phenotype of the developing organism. The region of mature sperm chromatin that harbors imprinted genes exhibits a dual nucleoprotamine/nucleohistone structure with DNase-sensitive regions that might be implicated in the establishment of efficient epigenetic information in the developing embryo [65, 66].

MiRNAs are the most characterized noncoding sperm RNAs. It has been suggested that miRNAs in sperm (Figure 4) might function in embryonic histone replacement [67] or transcriptionally balance the genome for early expression signaling or effect epigenetic modification [68] since nearly 10% of all small noncoding RNAs map to histone enriched TSS and promoter regions. MiR-34c is a highly abundant miRNA in humans [69]. It has been revealed that it is essential for early embryo development and required for the first cleavage division of the zygote in mice. Also miRNA precursors are present in human sperm, such as pri-miR-181, whose targets might have a function in early embryonic development and globally decrease at the 4–8-cell stage of human embryo development [8]. A specific target of pri-miRNA-181 is the embryonic stem cell pluripotency factor, termed coactivator-associated arginine methyltransferase I (CARM1). With the mouse model, it was demonstrated that miRNAs are present in mouse sperm structures that enter the oocyte at fertilization. The sperm contained a broad profile of miRNAs and a subset of potential mRNA targets, which were expressed in fertilizable metaphase II (MII) oocytes [70]. However, the levels of sperm-borne miRNAs were low in comparison to those of unfertilized MII oocytes, and fertilization did not alter the oocyte miRNA repertoire that included the most abundant sperm-borne miRNAs. In general, after fertilization, potential mechanisms and functions of sperm RNA could include translation of intact paternal mRNAs by the MII oocyte machinery, translational regulation by paternal miRNAs, activation of

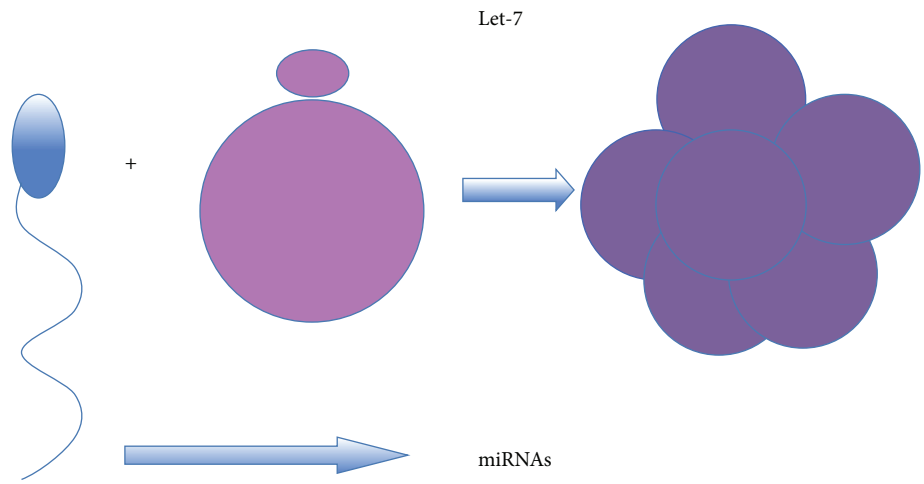

Sperm	Mature oocyte	Embryo
miR-34c pri-miR-181	Several miRNAs including miR-10A, miR-100, miR-184, miR193a-5p, miR-297, miR-602, and miR-625	(i) Euploid embryo: Upregulated: miR-372, miR-141, miR-27b, miR-339-3p, and miR-345 Downregulated: miR-191 (ii) Arrested embryo: Upregulated: miR-25, miR-302c, miR-196a2, and miR-181a (iii) Nonimplanted embryo: Upregulated: miR-191, miR-372, and miR-645

Figure 4: MiRNAs in human sperm, mature oocytes, and embryos, important for fertilization and embryo development [75–80]. Some miRNAs identified in sperm are contributed to the oocyte during the fertilization process and are involved in embryogenesis. Abundant maternal miRNAs of Let-7 family are involved in oocyte-to-embryo transition and are replaced by embryonic miRNAs, related to pluripotency.

paternal pri-miRNAs by maternal Dicer, and transcriptional regulation by paternal miRNAs. Noncoding RNAs have been postulated as epigenetic modifiers including histone modification and DNA methylation and playing a function in transgenerational epigenetic inheritance. The profiling of small RNAs by highly sensitive techniques, such as next generation sequencing and real-time PCR, might have some potential for the discovery of new fertility markers in human medicine [71]. The comparison of differential expressed small RNAs might lead to the discovery of new regulatory pathways underlying male infertility. The possibility that the profile of small noncoding RNA in sperm could be controlled by environmental factors, such as paternal stress exposure [72], early trauma [73], and pollution [74], also shed new light and

speculations on the determination of epigenetic traits to the next generation.

5. Embryo

The oocyte-to-embryo transition means the transformation of a highly differentiated oocyte into a totipotent zygote and pluripotent blastomeres of the preimplantation mammalian embryo. It includes the replacement of abundant maternal miRNAs that are enriched also in differentiated cells and exemplified by the Let-7 family, with embryonic miRNAs that are common in pluripotent stem cells (e.g., miR-290 family in the mouse) [38], as can be seen in Figure 4. The fertilization process is followed by the development of an embryo mainly developed on the basis of maternal mRNAs. The embryo starts to express its own genome at the stage of 4–8 cells before implantation. It develops through the morula stage with approximately 30 cells to the blastocyst stage with approximately 100 cells. The human embryo usually implants at the late morula or blastocyst stage. The role of miRNAs in early mammalian development, and particularly in the posttranscriptional regulation of maternal mRNAs, is still controversial. With the mouse model, it has been illustrated that the capacity to process the miRNAs diminishes after fertilization thus reducing the miRNA activity in the later stages of preimplantation development [75]. However, by analyzing the different precursor and mature forms of specific miRNAs that are abundant in the mouse blastocyst, such as miR-292-3p and miR-292-5p, it has been found that miRNA-duplexes and/or miRNAs bound to target mRNAs can appear and may serve as potential stock of miRNAs in the developing embryo. It has been suggested that such stockpile could directly provide functional and mature miRNAs in response to demand [75]. This phenomenon needs further research.

5.1. Genetic Status of Embryos. Human embryos have already been analyzed on miRNAs and it has been demonstrated that the miRNAs expression pattern depends on the chromosomal status (Figure 4). In one study, it has been found that the miRNA patterns of euploid embryos, normal for all chromosomes, differ from aneuploid embryos in humans [76]. The most highly expressed miRNA in euploid embryos was miR-372, as revealed by an array-based quantitative real-time polymerase chain reaction (qPCR). Several of the highly expressed miRNAs have shown to be critical to the maintenance of stem cell pluripotency and mammalian embryo development. There were some miRNAs, differently expressed between euploid and aneuploid embryos, such as miR-141, miR-27b, miR-339-3p, and miR-345 that were all upregulated in euploid embryos.

5.2. Embryo Development and Implantation. Surprisingly, it has been demonstrated that human embryos secrete miRNAs into culture media and that miRNAs may represent new biomarkers for embryo development and implantation [77, 78]. In human and bovine, differential miRNA gene expression was observed in (spent) media after culture of embryos that developed to the blastocyst stage and those that were arrested and failed to develop from the morula to the blastocyst stage. In spent media, miR-25, miR-302c, miR-196a2, and miR-181a expression were found to be higher in arrested embryos than in blastocysts [77], as can be seen in Figure 4.

The spent culture media from 55 single-embryo transfer cycles were tested for miRNA expression using an array-based quantitative real-time polymerase chain reaction analysis and the expression of the identified miRNA was correlated with pregnancy outcomes in these cycles [78]. Two miRNAs, miR-191 and miR-372, were expressed specifically in spent media after embryo culture. Interestingly, miRNAs were related to some bad condition: miR-191 was more highly concentrated in media from aneuploid embryos, and miR-191, miR-372, and miR-645 were more highly concentrated in media from failed in vitro fertilization cycles without pregnancy (Figure 4). In addition, miRNAs were found to be more highly concentrated in media after intracytoplasmic sperm injection (ICSI) and day-5 media samples when compared to media after classical in vitro fertilization with oocyte insemination (IVF) and day-4 samples, respectively [78]. Embryo implantation also depends on the endometrial receptivity. The repeated implantation failure (RIF) is one of the major problems encountered in the in vitro fertilization program. Thirteen miRNAs have been identified being different in RIF endometrial samples, compared to normal ones, and putatively regulate the expression of 3800 genes [79]. It was found that ten miRNAs were overexpressed in RIF endometrial samples, including miR-23b, miR-99a, and miR-145, whereas three were underexpressed. According to the miRNA-predicted targets, mRNA levels related to the cell adhesion molecules, Wnt signaling, and cell cycle pathways were lower in RIF-IVF patients. With the mouse model, it has been shown that a minimal uterine expression of miR-181 is essential for the onset of embryo implantation and that it is regulated by the leukemia inhibitory factor (LIF) [80].

5.3. Human Embryonic Stem Cells. Human embryonic stem cell (hESC) lines can be created from supernumerary embryos from the in vitro fertilization program. They can be retrieved by isolation and in vitro culture of blastocyst inner cell mass (ICM) which otherwise develops into embryonal tissues after implantation. The creation of hESC lines and their research has answered several important questions about pluripotency and stem cell self-renewal and differentiation. Moreover, several studies show that dysregulation of miRNA expression may play a fundamental role in progression and dissemination of different cancers.

5.3.1. Pluripotency. The miR-302/367 cluster represents the most abundant cluster of eight miRNAs that are specifically expressed in hESCs [81]. Functional studies identified important roles of miR-302/367 in regulation of pluripotency and differentiation of hESCs in vitro. Beside its role in TGF-β signaling, miR-302/367 also promotes the bone morphogenetic protein (BMP) signaling. Several studies [82–87] have shown that miRNAs are deeply involved in the balance between pluripotency and differentiation of hESCs by regulating the genes related to pluripotency, as can be seen in Table 1.

Table 1: MiRNAs regulating pluripotency and differentiation of hESCs.

Genes related to pluripotency						References
OCT4	*NANOG*	*SOX2*	*KLF4*	*LEFTY*	*NR2F2*	
Maintenance of pluripotency						
miR-203	miR-203					[82]
Regulation of stem cell renewal and differentiation						
	miR-200c					[83]
Delay of differentiation, balance between differentiation and pluripotency						
				miR-302s		[84]
Low in self-renewal and high during differentiation						
miR-145		miR-145	miR-145			[85]
Regulation of cell cycle genes in pluripotent stem cells						
miR-302a		miR-302a				[86]
Balance between pluripotency and differentiation, NR2F2 critical for neural gene activation						
miR-302					miR-302	[87]

5.3.2. Differentiation and Development of hESCs into All Three Germ Layers. Interestingly, there is a cluster of primate-specific miRNAs (ps-miRNAs), a set of 269 ps-miRNAs that are evolutionarily conserved and may contribute to the difference between high-level primates and nonprimate mammals or lower vertebrates [88]. They are enriched in chromosomes 19 and X and represented by the miR-548 family. Most ps-miRNAs were low expressed in adult tissues but were highly expressed in reproductive system and hESCs. The target genes were strongly associated with developmental processes and various cancers. It is suggested that ps-miRNAs may play critical roles in regulating of differentiation and growth during the early development and in maintaining the pluripotency of hESCs.

Several studies [89–93] proved that miRNAs are deeply involved in the differentiation of hESCs into different types of cells of all three germ layers (endoderm, mesoderm, and ectoderm), as can be seen in Table 2.

Some miRNAs are involved in maintaining the pluripotency of hESCs but direct their differentiation into a germ layer when they are upregulated [90].

All these recent findings are extremely important for the understanding of the early human development and the improvement of hESC differentiation protocols.

5.3.3. Cancer. If something goes wrong during the process of development and miRNAs are dysregulated, different types of cancers can occur. Oncogenic miRNAs are involved in manifestation of cancers, while another group of suppressive miRNAs is involved in the suppression of cancers [94]. A new mechanism of telomerase regulation by means of noncoding small RNAs has been revealed. It has been shown that miR-498 induced by vitamin D3 decreases the mRNA expression of human telomerase reverse transcriptase [95]. The levels of miR-498 expression are decreased in malignant human ovarian tumors as well as in human ovarian cancer cell lines.

The protein LIN28 is an evolutionarily conserved RNA-binding protein and is known to be a master regulator controlling the pluripotency of hESCs. Together with OCT4, SOX2, and NANOG, LIN28 can reprogram somatic cells and produce induced pluripotent stem cells (iPSCs). The expression of LIN28 is restricted to ESCs and developing tissues and is highly upregulated in human tumors. It functions as an oncogene promoting malignant transformation and tumor progression. It has been demonstrated that four miRNAs, let-7, miR-9, miR-30, and miR-125, directly repress the LIN28 expression in hESCs and cancer cells [96]. It has been suggested that global downregulation of these miRNAs may be one of the key mechanisms of LIN28 reactivation and manifestation of human cancers.

Dicer1, an endoribonuclease that is essential for the synthesis of miRNAs, also acts as a tumor suppressor. It has been demonstrated that inactivation of its RNase IIIB domain by mutation of D1709, a residue mutated in a subset of nonepithelial ovarian cancers, results in complete loss of 5p-derived mature miRNAs, including the tumor-suppressive let-7 family and the consequent progression of cancer [97].

5.4. Female (In)Fertility. Recently, the role of Dicer function in female reproductive tissues has begun to be elucidated by the use of knockout mouse models. As already mentioned, the ribonuclease III endonuclease, Dicer1 (also known as Dicer), is essential for the synthesis of miRNAs. Although it is generally established that miRNAs are expressed in the female reproductive tract, their functional role and effects on reproductive processes remain unknown. In an interesting study, the reproductive phenotype of mice with loxP insertions in the Dicer1 gene (Dicer1fl/fl) when crossed with mice expressing Cre-recombinase driven by the anti-müllerian hormone receptor 2 promoter (Amhr2Cre/+) was established for the first time [98]. Adult female Dicer1fl/fl;Amhr2Cre/+ mice displayed normal mating behavior but did not produce offspring after mating in experimental condition. Morphological and histological assessments of the reproductive tracts of mice showed that their uterus and oviducts were hypotrophic and highly disorganized. Natural mating of

Table 2: MiRNAs and their target genes related to differentiation of hESCs, development of *all three* germ layers *(endoderm, mesoderm, and ectoderm), and cancer*.

Development						References
Endoderm	Mesoderm	Cardiomyocytes	Neural lineage	Endothelial cells, angiogenesis	CANCER	
miR-302a (*OTX2*)						[89]
	miR-302/373 (*LEFTY*)					[90]
			miR-302 (*NR2F2, JMJD1C*)			[91]
		miR-1, miR-499				[92]
				miR-126, miR-210		[93]
					miR-498	[95]
					let-7, miR-9, miR-30, and miR-125	[96]
					let-7 family	[97]

Dicer1fl/fl;Amhr2Cre/+ females resulted in successful fertilization but the oviductal transport of embryos was disrupted, as evidenced by the failure of embryos to enter the uterus. These data implicated that Dicer1/miRNAs mediated posttranscriptional gene regulation in reproductive somatic tissues that is critical for female fertility. The loss of Dicer within the oocyte, the ovarian granulosa cells, the luteal tissue, the oviducts, and, potentially, also the uterus causes female infertility [99].

It has been shown that miR-290–295, a mammalian-specific cluster of miRNAs, plays a decisive role in embryonic development, as indicated by the partial lethality of mutant mouse embryos [100]. In surviving miR-290–295-deficient mouse embryos, only female fertility was compromised. It has been suggested that this fertility impairment arises from a defect in migrating PGCs and occurs equally in male and female mutant animals. However, male miR-290–295(−/−) mice were able to recover from this initial germ cell loss due to the extended proliferative lifespan of their germ cells and are fertile, while female miR-290–295(−/−) mice are unable to recover and are sterile because of premature ovarian failure.

6. Diagnostics and Treatment of Female Infertility: Prospects

The new knowledge and methodology on miRNAs may provide some new biomarkers of female infertility from different aspects: from ovarian physiology to the oocyte and embryo quality, embryo implantation potential, and endometrial receptivity. An important task remains to study the causes of diminished ovarian reserve because there are no relevant biomarkers available to estimate the ovarian reserve in (in)fertile women and to predict (or explain) the assisted conception outcome. miRNAs seem to be an extremely interesting tool to do that. Some of these miRNAs as well as the exosomes, vesicles transporting them, can be easily detectable in the bloodstream and could be used as reliable biomarkers of interest in infertility care. The data show that miRNAs can control reproductive functions by enhanced or inhibited release of ovarian progestagen, androgen, and estrogen in human granulosa cells and suggest that such miRNA-mediated effects could be potentially used for regulation of reproductive processes and for the treatment of reproductive and other steroid-dependent disorders in women with fertility problems.

At present, the oocytes and embryos retrieved in the in vitro fertilization program can be evaluated only by morphology or preimplantation genetic diagnostics after "aggressive" embryo biopsy. The secretion of miRNAs into the culture medium may represent an interesting noninvasive tool to evaluate the oocytes and embryos in the in vitro fertilization program. Moreover, the studies with animal models show that some suboptimal procedures, such as in vitro maturation of ovarian follicles, could be improved using miRNAs. It has been demonstrated that hCG supplementation and vitamin C status in the culture medium alter the miRNA expression profiles in oocytes and granulosa cells during in vitro growth of murine follicles [101]. Moreover, the transfection of murine granulosa cells with let-7c-, miR-27a-, and miR-322-inhibitor sequences increased the oocyte maturation rate by 1.5- to 2.0-fold in comparison with control during in vitro maturation of mouse follicles [102]. These findings suggest that sophisticated miRNA regulation in granulosa cells might improve oocyte maturation efficiency during ovarian follicle development in vitro. Last but not least, the new knowledge on miRNAs in hESCs leads to better understanding of the human development on the one hand and the manifestation of cancer on the other hand. This may result in optimized in vitro differentiation protocols and treatment of different cancers.

7. Conclusion

It may be concluded that miRNAs represent a great challenge in reproductive and regenerative medicine to understand the preimplantation development in humans including female reproductive tissues, PGCs, gametes, embryos, and embryonic stem cells better. The forthcoming new knowledge may provide new biomarkers and treatments of fertility disorders and degenerative diseases in the future.

Conflict of Interests

The authors declare that there is no financial or other conflict of interests related to this paper.

Acknowledgments

The authors would like to thank the staff of the Reproductive Unit, University Medical Centre Ljubljana, the Ministry of Youth, Education and Sports of the Czech Republic (RVO: 86652036, BIOCEV CZ.1.05/1.1.00/02.0109 from the ERDF), and Mrs. Ilse Christine Wagner, University of Heidelberg, for her corrections of the English language.

References

[1] V. Ambros, "The functions of animal microRNAs," *Nature*, vol. 431, no. 7006, pp. 350–355, 2004.

[2] D. P. Bartel, "microRNAs: genomics, biogenesis, mechanism, and function," *Cell*, vol. 116, no. 2, pp. 281–297, 2004.

[3] M. Kedde and R. Agami, "Interplay between microRNAs and RNA-binding proteins determines developmental processes," *Cell Cycle*, vol. 7, no. 7, pp. 899–903, 2008.

[4] B. P. Lewis, C. B. Burge, and D. P. Bartel, "Conserved seed pairing, often flanked by adenosines, indicates that thousands of human genes are microRNA targets," *Cell*, vol. 120, no. 1, pp. 15–20, 2005.

[5] A. M. Booth, Y. Fang, J. K. Fallon et al., "Exosomes and HIV Gag bud from endosome-like domains of the T cell plasma membrane," *The Journal of Cell Biology*, vol. 172, no. 6, pp. 923–935, 2006.

[6] H. Valadi, K. Ekström, A. Bossios, M. Sjöstrand, J. J. Lee, and J. O. Lötvall, "Exosome-mediated transfer of mRNAs and microRNAs is a novel mechanism of genetic exchange between cells," *Nature Cell Biology*, vol. 9, no. 6, pp. 654–659, 2007.

[7] E. van der Pol, A. N. Böing, P. Harrison, A. Sturk, and R. Nieuwland, "Classification, functions, and clinical relevance of extracellular vesicles," *Pharmacological Reviews*, vol. 64, no. 3, pp. 676–705, 2012.

[8] E. Sendler, G. D. Johnson, S. Mao et al., "Stability, delivery and functions of human sperm RNAs at fertilization," *Nucleic Acids Research*, vol. 41, no. 7, pp. 4104–4117, 2013.

[9] M. H. Johnson and B. J. Everitt, "Adult ovarian function," in *Essential Reproduction*, pp. 69–87, Blackwell Science, Oxford, UK, 5th edition, 2000.

[10] A. A. Staton, H. Knaut, and A. J. Giraldez, "miRNA regulation of Sdf1 chemokine signaling provides genetic robustness to germ cell migration," *Nature Genetics*, vol. 43, no. 3, pp. 204–211, 2011.

[11] A. J. Childs, H. L. Kinnell, J. He, and R. A. Anderson, "LIN28 is selectively expressed by primordial and pre-meiotic germ cells in the human fetal ovary," *Stem Cells and Development*, vol. 21, no. 13, pp. 2343–2349, 2012.

[12] S. Takada, E. Berezikov, Y. L. Choi, Y. Yamashita, and H. Mano, "Potential role of miR-29b in modulation of *Dnmt3a* and *Dnmt3b* expression in primordial germ cells of female mouse embryos," *RNA*, vol. 15, no. 8, pp. 1507–1514, 2009.

[13] D. Rengaraj, B. R. Lee, S. I. Lee, H. W. Seo, and J. Y. Han, "Expression patterns and miRNA regulation of DNA methyltransferases in chicken primordial germ cells," *PLoS ONE*, vol. 6, no. 5, Article ID e19524, 2011.

[14] J. Mei, H.-M. Yue, Z. Li et al., "C1q-like factor, a target of miR-430, regulates primordial germ cell development in early embryos of *Carassius auratus*," *International Journal of Biological Sciences*, vol. 10, no. 1, pp. 15–24, 2013.

[15] Y. Takeda, Y. Mishima, T. Fujiwara, H. Sakamoto, and K. Inoue, "DAZL relieves miRNA-mediated repression of germline mRNAs by controlling poly(A) tail length in zebrafish," *PLoS ONE*, vol. 4, no. 10, Article ID e7513, 2009.

[16] S. Tani, R. Kusakabe, K. Naruse, H. Sakamoto, and K. Inoue, "Genomic organization and embryonic expression of miR-430 in medaka (*Oryzias latipes*): insights into the post-transcriptional gene regulation in early development," *Gene*, vol. 457, no. 1-2, pp. 41–49, 2010, Erratum in *Gene*, vol. 475, no. 1-2, pp. 50–51, 2010.

[17] T. Yamaguchi, K. Kataoka, K. Watanabe, and H. Orii, "Restriction of the Xenopus DEADSouth mRNA to the primordial germ cells is ensured by multiple mechanisms," *Mechanisms of Development*, vol. 131, no. 1, pp. 15–23, 2014.

[18] S. I. Lee, B. R. Lee, Y. S. Hwang et al., "MicroRNA-mediated posttranscriptional regulation is required for maintaining undifferentiated properties of blastoderm and primordial germ cells in chickens," *Proceedings of the National Academy of Sciences of the United States of America*, vol. 108, no. 26, pp. 10426–10431, 2011.

[19] J. M. Kugler, Y. W. Chen, R. Weng, and S. M. Cohen, "Maternal loss of miRNAs leads to increased variance in primordial germ cell numbers in *Drosophila melanogaster*," *G3*, vol. 3, no. 9, pp. 1573–1576, 2013.

[20] Y. Li, J. Z. Maines, Ö. Y. Tastan, D. M. McKearin, and M. Buszczak, "Mei-P26 regulates the maintenance of ovarian germline stem cells by promoting BMP signaling," *Development*, vol. 139, no. 9, pp. 1547–1556, 2012.

[21] J. K. Park, X. Liu, T. J. Strauss, D. M. McKearin, and Q. Liu, "The miRNA pathway intrinsically controls self-renewal of *Drosophila* germline stem cells," *Current Biology*, vol. 17, no. 6, pp. 533–538, 2007.

[22] R. A. Neumüller, J. Betschinger, A. Fischer et al., "Mei-P26 regulates microRNAs and cell growth in the *Drosophila* ovarian stem cell lineage," *Nature*, vol. 454, no. 7201, pp. 241–245, 2008.

[23] Z. Jin and T. Xie, "Dcr-1 maintains *Drosophila* ovarian stem cells," *Current Biology*, vol. 17, no. 6, pp. 539–544, 2007.

[24] S. M. Kraggerud, C. E. Hoei-Hansen, S. Alagaratnam et al., "Molecular characteristics of malignant ovarian germ cell tumors and comparison with testicular counterparts: implications for pathogenesis," *Endocrine Reviews*, vol. 34, no. 3, pp. 339–376, 2013.

[25] R. Eini, L. C. Dorssers, and L. H. Looijenga, "Role of stem cell proteins and microRNAs in embryogenesis and germ cell cancer," *International Journal of Developmental Biology*, vol. 57, no. 2–4, pp. 319–332, 2013.

[26] M. J. Murray, J. C. Nicholson, and N. Coleman, "Biology of childhood germ cell tumours, focussing on the significance of microRNAs," *Andrology*, vol. 3, no. 1, pp. 129–139, 2015.

[27] R. D. Palmer, M. J. Murray, H. K. Saini et al., "Malignant germ cell tumors display common microRNA profiles resulting in global changes in expression of messenger RNA targets," *Cancer Research*, vol. 70, no. 7, pp. 2911–2923, 2010.

[28] Y.-W. Xu, B. Wang, C.-H. Ding, T. Li, F. Gu, and C. Zhou, "Differentially expressed micoRNAs in human oocytes," *Journal of Assisted Reproduction and Genetics*, vol. 28, no. 6, pp. 559–566, 2011.

[29] S. Assou, T. Al-Edani, D. Haouzi et al., "MicroRNAs: new candidates for the regulation of the human cumulus-oocyte complex," *Human Reproduction*, vol. 28, no. 11, pp. 3038–3049, 2013.

[30] H. Zhang, X. Jiang, Y. Zhang et al., "MicroRNA 376a regulates follicle assembly by targeting Pcna in fetal and neonatal mouse ovaries," *Reproduction*, vol. 148, no. 1, pp. 43–54, 2014.

[31] F. X. Donadeu, S. N. Schauer, and S. D. Sontakke, "Involvement of miRNAs in ovarian follicular and luteal development," *Journal of Endocrinology*, vol. 215, no. 3, pp. 323–334, 2012.

[32] L. Lei, S. Jin, G. Gonzalez, R. R. Behringer, and T. K. Woodruff, "The regulatory role of Dicer in folliculogenesis in mice," *Molecular and Cellular Endocrinology*, vol. 315, no. 1-2, pp. 63–73, 2010.

[33] S. M. Hawkins and M. M. Matzuk, "Oocyte-somatic cell communication and microRNA function in the ovary," *Annales d'Endocrinologie*, vol. 71, no. 3, pp. 144–148, 2010.

[34] S.-C. Sun and N.-H. Kim, "Molecular mechanisms of asymmetric division in oocytes," *Microscopy and Microanalysis*, vol. 19, no. 4, pp. 883–897, 2013.

[35] D. Tesfaye, D. Worku, F. Rings et al., "Identification and expression profiling of microRNAs during bovine oocyte maturation using heterologous approach," *Molecular Reproduction and Development*, vol. 76, no. 7, pp. 665–677, 2009.

[36] W. S. Abd El Naby, T. H. Hagos, M. M. Hossain et al., "Expression analysis of regulatory microRNAs in bovine cumulus oocyte complex and preimplantation embryos," *Zygote*, vol. 21, no. 1, pp. 31–51, 2013.

[37] S. K. Tripurani, G. Wee, K.-B. Lee, G. W. Smith, L. Wang, and J. Yao, "MicroRNA-212 post-transcriptionally regulates oocyte-specific basic-helix-loop-helix transcription factor, factor in the germline alpha (FIGLA), during bovine early embryogenesis," *PLoS ONE*, vol. 8, no. 9, Article ID e76114, 2013.

[38] M. Flemr, M. Moravec, V. Libova, R. Sedlacek, and P. Svoboda, "Lin28a is dormant, functional, and dispensable during mouse oocyte-to-embryo transition," *Biology of Reproduction*, vol. 90, no. 6, article 131, 2014.

[39] N. Suh, L. Baehner, F. Moltzahn et al., "MicroRNA function is globally suppressed in mouse oocytes and early embryos," *Current Biology*, vol. 20, no. 3, pp. 271–277, 2010.

[40] Y. Mase, O. Ishibashi, T. Ishikawa et al., "*MiR-21* is enriched in the RNA-induced silencing complex and targets *COL4A1* in human granulosa cell lines," *Reproductive Sciences*, vol. 19, no. 10, pp. 1030–1040, 2012.

[41] T. Al-Edani, S. Assou, A. Ferrières et al., "Female aging alters expression of human cumulus cells genes that are essential for oocyte quality," *BioMed Research International*, vol. 2014, Article ID 964614, 10 pages, 2014.

[42] X.-H. Tong, B. Xu, Y.-W. Zhang, Y.-S. Liu, and C.-H. Ma, "Research resources: comparative microRNA profiles in human corona radiata cells and cumulus oophorus cells detected by next-generation small RNA sequencing," *PLoS ONE*, vol. 9, no. 9, Article ID e106706, 2014.

[43] A. Velthut-Meikas, J. Simm, T. Tuuri, J. S. Tapanainen, M. Metsis, and A. Salumets, "Research resource: small RNA-seq of human granulosa cells reveals miRNAs in FSHR and aromatase genes," *Molecular Endocrinology*, vol. 27, no. 7, pp. 1128–1141, 2013.

[44] A. V. Sirotkin, D. Ovcharenko, R. Grossmann, M. Lauková, and M. Mlynček, "Identification of microRNAs controlling human ovarian cell steroidogenesis via a genome-scale screen," *Journal of Cellular Physiology*, vol. 219, no. 2, pp. 415–420, 2009.

[45] A. Dai, H. Sun, T. Fang et al., "MicroRNA-133b stimulates ovarian estradiol synthesis by targeting Foxl2," *FEBS Letters*, vol. 587, no. 15, pp. 2474–2482, 2013.

[46] B. Troppmann, N. Kossack, V. Nordhoff, A. N. Schüring, and J. Gromoll, "MicroRNA miR-513a-3p acts as a co-regulator of luteinizing hormone/chorionic gonadotropin receptor gene expression in human granulosa cells," *Molecular and Cellular Endocrinology*, vol. 390, no. 1-2, pp. 65–72, 2014.

[47] A. V. Sirotkin, M. Lauková, D. Ovcharenko, P. Brenaut, and M. Mlynček, "Identification of microRNAs controlling human ovarian cell proliferation and apoptosis," *Journal of Cellular Physiology*, vol. 223, no. 1, pp. 49–56, 2010.

[48] M. Santonocito, M. Vento, M. R. Guglielmino et al., "Molecular characterization of exosomes and their microRNA cargo in human follicular fluid: bioinformatic analysis reveals that exosomal microRNAs control pathways involved in follicular maturation," *Fertility and Sterility*, vol. 102, no. 6, pp. 1751–1761, 2014.

[49] A. Diez-Fraile, T. Lammens, K. Tilleman et al., "Age-associated differential microRNA levels in human follicular fluid reveal pathways potentially determining fertility and success of *in vitro* fertilization," *Human Fertility*, vol. 17, no. 2, pp. 90–98, 2014.

[50] L. C. Ecklund and R. S. Usadi, "Endocrine and reproductive effects of polycystic ovarian syndrome," *Obstetrics and Gynecology Clinics of North America*, vol. 42, no. 1, pp. 55–65, 2015.

[51] L. W. Roth, B. McCallie, R. Alvero, W. B. Schoolcraft, D. Minjarez, and M. G. Katz-Jaffe, "Altered microRNA and gene expression in the follicular fluid of women with polycystic ovary syndrome," *Journal of Assisted Reproduction and Genetics*, vol. 31, no. 3, pp. 355–362, 2014.

[52] Q. Sang, Z. Yao, H. Wang et al., "Identification of microRNAs in human follicular fluid: characterization of microRNAs that govern steroidogenesis in vitro and are associated with polycystic ovary syndrome in vivo," *Journal of Clinical Endocrinology and Metabolism*, vol. 98, no. 7, pp. 3068–3079, 2013.

[53] M. Yin, X. Wang, G. Yao et al., "Transactivation of microRNA-320 by microRNA-383 regulates granulosa cell functions by targeting E2F1 and SF-1 proteins," *The Journal of Biological Chemistry*, vol. 289, no. 26, pp. 18239–18257, 2014.

[54] B. Xu, Y. W. Zhang, X. H. Tong, and Y. S. Liu, "Characterization of microRNA profile in human cumulus granulosa cells: identification of microRNAs that regulate Notch signaling and are associated with PCOS," *Molecular and Cellular Endocrinology*, vol. 404, pp. 26–36, 2015.

[55] K. J. Woad, W. J. Watkins, D. Prendergast, and A. N. Shelling, "The genetic basis of premature ovarian failure," *Australian and New Zealand Journal of Obstetrics and Gynaecology*, vol. 46, no. 3, pp. 242–244, 2006.

[56] Y. Zhou, Y. Z. Zhu, S. H. Zhang, H. M. Wang, S. Y. Wang, and X. K. Yang, "MicroRNA expression profiles in premature ovarian

failure patients and its potential regulate functions," *Chinese Journal of Birth Health and Heredity*, vol. 19, pp. 20–22, 2011.

[57] X. Yang, Y. Zhou, S. Peng et al., "Differentially expressed plasma microRNAs in premature ovarian failure patients and the potential regulatory function of mir-23a in granulosa cell apoptosis," *Reproduction*, vol. 144, no. 2, pp. 235–244, 2012.

[58] Y. Dang, S. Zhao, Y. Qin, T. Han, W. Li, and Z.-J. Chen, "MicroRNA-22-3p is down-regulated in the plasma of Han Chinese patients with premature ovarian failure," *Fertility and Sterility*, vol. 103, no. 3, pp. 802–807.e1, 2015.

[59] X. Ma, Y. Chen, X. Zhao, J. Chen, C. Shen, and S. Yang, "Association study of TGFBR2 and miR-518 gene polymorphisms with age at natural menopause, premature ovarian failure, and early menopause among Chinese Han women," *Medicine*, vol. 93, no. 20, p. e93, 2014.

[60] H. Rah, Y. J. Jeon, S. H. Shim et al., "Association of miR-146a>G, miR-196a2T>C, and miR-499A>G polymorphisms with risk of premature ovarian failure in Korean women," *Reproductive Sciences*, vol. 20, no. 1, pp. 60–68, 2013.

[61] D. T. Carrell, "Contributions of spermatozoa to embryogenesis: assays to evaluate their genetic and epigenetic fitness," *Reproductive BioMedicine Online*, vol. 16, no. 4, pp. 474–484, 2008.

[62] R. Vassena, S. Boué, E. González-Roca et al., "Waves of early transcriptional activation and pluripotency program initiation during human preimplantation development," *Development*, vol. 138, no. 17, pp. 3699–3709, 2011.

[63] G. C. Ostermeier, D. Miller, J. D. Huntriss, M. P. Diamond, and S. A. Krawetz, "Reproductive biology: delivering spermatozoan RNA to the oocyte," *Nature*, vol. 429, no. 6988, p. 154, 2004.

[64] Y. Sone, M. Ito, H. Shirakawa et al., "Nuclear translocation of phospholipase C-zeta, an egg-activating factor, during early embryonic development," *Biochemical and Biophysical Research Communications*, vol. 330, no. 3, pp. 690–694, 2005.

[65] J. P. Dadoune, "Spermatozoal RNAs: what about their functions?" *Microscopy Research and Technique*, vol. 72, no. 8, pp. 536–551, 2009.

[66] M. Kumar, K. Kumar, S. Jain, T. Hassan, and R. Dada, "Novel insights into the genetic and epigenetic paternal contribution to the human embryo," *Clinics*, vol. 68, supplement 1, pp. 5–14, 2013.

[67] G. D. Johnson, C. Lalancette, A. K. Linnemann, F. Leduc, G. Boissonneault, and S. A. Krawetz, "The sperm nucleus: chromatin, RNA, and the nuclear matrix," *Reproduction*, vol. 141, no. 1, pp. 21–36, 2011.

[68] B. Khraiwesh, M. A. Arif, G. I. Seumel et al., "Transcriptional control of gene expression by microRNAs," *Cell*, vol. 140, no. 1, pp. 111–122, 2010.

[69] S. A. Krawetz, A. Kruger, C. Lalancette et al., "A survey of small RNAs in human sperm," *Human Reproduction*, vol. 26, no. 12, pp. 3401–3412, 2011.

[70] M. Amanai, M. Brahmajosyula, and A. C. Perry, "A restricted role for sperm-borne microRNAs in mammalian fertilization," *Biology of Reproduction*, vol. 75, no. 6, pp. 877–884, 2006.

[71] M. Abu-Halima, M. Hammadeh, C. Backes et al., "Panel of five microRNAs as potential biomarkers for the diagnosis and assessment of male infertility," *Fertility and Sterility*, vol. 102, no. 4, pp. 989.e1–997.e1, 2014.

[72] A. B. Rodgers, C. P. Morgan, S. L. Bronson, S. Revello, and T. L. Bale, "Paternal stress exposure alters sperm MicroRNA content and reprograms offspring HPA stress axis regulation," *Journal of Neuroscience*, vol. 33, no. 21, pp. 9003–9012, 2013.

[73] K. Gapp, A. Jawaid, P. Sarkies et al., "Implication of sperm RNAs in transgenerational inheritance of the effects of early trauma in mice," *Nature Neuroscience*, vol. 17, no. 5, pp. 667–669, 2014.

[74] Y. Li, M. Li, Y. Liu, G. Song, and N. Liu, "A microarray for microRNA profiling in spermatozoa from adult men living in an environmentally polluted site," *Bulletin of Environmental Contamination and Toxicology*, vol. 89, no. 6, pp. 1111–1114, 2012.

[75] J. García-López and J. del Mazo, "Expression dynamics of microRNA biogenesis during preimplantation mouse development," *Biochimica et Biophysica Acta*, vol. 1819, no. 8, pp. 847–854, 2012.

[76] E. M. Rosenbluth, D. N. Shelton, A. E. Sparks, E. Devor, L. Christenson, and B. J. Van Voorhis, "MicroRNA expression in the human blastocyst," *Fertility and Sterility*, vol. 99, no. 3, pp. 855–861, 2013.

[77] J. Kropp, S. M. Salih, and H. Khatib, "Expression of microRNAs in bovine and human pre-implantation embryo culture media," *Frontiers in Genetics*, vol. 5, article 91, 2014.

[78] E. M. Rosenbluth, D. N. Shelton, L. M. Wells, A. E. Sparks, and B. J. Van Voorhis, "Human embryos secrete microRNAs into culture media—a potential biomarker for implantation," *Fertility and Sterility*, vol. 101, no. 5, pp. 1493–1500, 2014.

[79] A. Revel, H. Achache, J. Stevens, Y. Smith, and R. Reich, "MicroRNAs are associated with human embryo implantation defects," *Human Reproduction*, vol. 26, no. 10, pp. 2830–2840, 2011.

[80] B. Chu, L. Zhong, S. Dou et al., "miRNA-181 regulates embryo implantation in mice through targeting leukemia inhibitory factor," *Journal of Molecular Cell Biology*, vol. 7, no. 1, pp. 12–22, 2015.

[81] I. Lipchina, Y. Elkabetz, M. Hafner et al., "Genome-wide identification of microRNA targets in human ES cells reveals a role for miR-302 in modulating BMP response," *Genes and Development*, vol. 25, no. 20, pp. 2173–2186, 2011.

[82] K. Kapinas, H. Kim, M. Mandeville et al., "microRNA-mediated survivin control of pluripotency," *Journal of Cellular Physiology*, vol. 230, no. 1, pp. 63–70, 2015.

[83] H.-N. Huang, S.-Y. Chen, S.-M. Hwang et al., "miR-200c and GATA binding protein 4 regulate human embryonic stem cell renewal and differentiation," *Stem Cell Research*, vol. 12, no. 2, pp. 338–353, 2014.

[84] A. Barroso-delJesus, G. Lucena-Aguilar, L. Sanchez, G. Ligero, I. Gutierrez-Aranda, and P. Menendez, "The nodal inhibitor Lefty is negatively modulated by the microRNA miR-302 in human embryonic stem cells," *The FASEB Journal*, vol. 25, no. 5, pp. 1497–1508, 2011.

[85] N. Xu, T. Papagiannakopoulos, G. Pan, J. A. Thomson, and K. S. Kosik, "MicroRNA-145 regulates OCT4, SOX2, and KLF4 and represses pluripotency in human embryonic stem cells," *Cell*, vol. 137, no. 4, pp. 647–658, 2009.

[86] D. A. Card, P. B. Hebbar, L. Li et al., "Oct4/Sox2-regulated miR-302 targets cyclin D1 in human embryonic stem cells," *Molecular and Cellular Biology*, vol. 28, no. 20, pp. 6426–6438, 2008.

[87] A. Rosa and A. H. Brivanlou, "A regulatory circuitry comprised of miR-302 and the transcription factors OCT4 and NR2F2 regulates human embryonic stem cell differentiation," *The EMBO Journal*, vol. 30, no. 2, pp. 237–248, 2011.

[88] S. Lin, W. K. Cheung, S. Chen et al., "Computational identification and characterization of primate-specific microRNAs in human genome," *Computational Biology and Chemistry*, vol. 34, no. 4, pp. 232–241, 2010.

[89] A. Hinton, S. E. Hunter, I. Afrikanova et al., "sRNA-seq analysis of human embryonic stem cells and definitive endoderm reveals differentially expressed microRNAs and novel IsomiRs with distinct targets," *Stem Cells*, vol. 32, no. 9, pp. 2360–2372, 2014.

[90] A. Rosa, M. D. Papaioannou, J. E. Krzyspiak, and A. H. Brivanlou, "MiR-373 is regulated by TGFβ signaling and promotes mesendoderm differentiation in human embryonic stem cells," *Developmental Biology*, vol. 391, no. 1, pp. 81–88, 2014.

[91] J. Wang, J. W. Park, H. Drissi, X. Wang, and R.-H. Xu, "Epigenetic regulation of miR-302 by JMJD1C inhibits neural differentiation of human embryonic stem cells," *The Journal of Biological Chemistry*, vol. 289, no. 4, pp. 2384–2395, 2014.

[92] J.-D. Fu, S. N. Rushing, D. K. Lieu et al., "Distinct roles of microRNA-1 and -499 in ventricular specification and functional maturation of human embryonic stem cell-derived cardiomyocytes," *PLoS ONE*, vol. 6, no. 11, Article ID e27417, 2011.

[93] N. M. Kane, M. Meloni, H. L. Spencer et al., "Derivation of endothelial cells from human embryonic stem cells by directed differentiation: analysis of microRNA and angiogenesis in vitro and in vivo," *Arteriosclerosis, Thrombosis, and Vascular Biology*, vol. 30, no. 7, pp. 1389–1397, 2010.

[94] S. Takasaki, "Roles of microRNAs in cancers and development," *Methods in Molecular Biology*, vol. 1218, pp. 375–413, 2015.

[95] R. Kasiappan, Z. Shen, A. K. Tse et al., "1,25-Dihydroxyvitamin D_3 suppresses telomerase expression and human cancer growth through microRNA-498," *The Journal of Biological Chemistry*, vol. 287, no. 49, pp. 41297–41309, 2012.

[96] X. Zhong, N. Li, S. Liang, Q. Huang, G. Coukos, and L. Zhang, "Identification of microRNAs regulating reprogramming factor LIN28 in embryonic stem cells and cancer cells," *Journal of Biological Chemistry*, vol. 285, no. 53, pp. 41961–41971, 2010.

[97] A. M. Gurtan, V. Lu, A. Bhutkar, and P. A. Sharp, "In vivo structure-function analysis of human Dicer reveals directional processing of precursor miRNAs," *RNA*, vol. 18, no. 6, pp. 1116–1122, 2012.

[98] X. Hong, L. J. Luense, L. K. McGinnis, W. B. Nothnick, and L. K. Christenson, "Dicer1 is essential for female fertility and normal development of the female reproductive system," *Endocrinology*, vol. 149, no. 12, pp. 6207–6212, 2008.

[99] L. J. Luense, M. Z. Carletti, and L. K. Christenson, "Role of Dicer in female fertility," *Trends in Endocrinology and Metabolism*, vol. 20, no. 6, pp. 265–272, 2009.

[100] L. A. Medeiros, L. M. Dennis, M. E. Gill et al., "Mir-290–295 deficiency in mice results in partially penetrant embryonic lethality and germ cell defects," *Proceedings of the National Academy of Sciences of the United States of America*, vol. 108, no. 34, pp. 14163–14168, 2011.

[101] Y. J. Kim, S. Y. Ku, Z. Rosenwaks et al., "MicroRNA expression profiles are altered by gonadotropins and vitamin C status during in vitro follicular growth," *Reproductive Sciences*, vol. 17, no. 12, pp. 1081–1089, 2010.

[102] Y. J. Kim, S. Y. Ku, Y. Y. Kim et al., "MicroRNAs transfected into granulosa cells may regulate oocyte meiotic competence during *in vitro* maturation of mouse follicles," *Human Reproduction*, vol. 28, no. 11, pp. 3050–3061, 2013.

Hindawi Publishing Corporation
Stem Cells International
Volume 2016, Article ID 8530207, 8 pages
http://dx.doi.org/10.1155/2016/8530207

Research Article

Effective Mobilization of Very Small Embryonic-Like Stem Cells and Hematopoietic Stem/Progenitor Cells but Not Endothelial Progenitor Cells by Follicle-Stimulating Hormone Therapy

Monika Zbucka-Kretowska,[1] Andrzej Eljaszewicz,[2] Danuta Lipinska,[2,3] Kamil Grubczak,[2] Malgorzata Rusak,[4] Grzegorz Mrugacz,[5] Milena Dabrowska,[4] Mariusz Z. Ratajczak,[6,7] and Marcin Moniuszko[2,8]

[1]*Department of Reproduction and Gynecological Endocrinology, Medical University of Bialystok, 15-276 Bialystok, Poland*
[2]*Department of Regenerative Medicine and Immune Regulation, Medical University of Bialystok, 15-269 Bialystok, Poland*
[3]*Department of Endocrinology, Diabetology and Internal Medicine, Medical University of Bialystok, 15-276 Bialystok, Poland*
[4]*Department of Hematological Diagnostics, Medical University of Bialystok, 15-276 Bialystok, Poland*
[5]*Center for Reproductive Medicine Bocian, 15-267 Bialystok, Poland*
[6]*Stem Cell Institute at James Graham Brown Cancer Center, University of Louisville, Louisville, KY 40202, USA*
[7]*Department of Regenerative Medicine, Medical University of Warsaw, 02-091 Warsaw, Poland*
[8]*Department of Allergology and Internal Medicine, Medical University of Bialystok, 15-276 Bialystok, Poland*

Correspondence should be addressed to Marcin Moniuszko; marcin.moniuszko@umb.edu.pl

Received 1 May 2015; Accepted 8 June 2015

Academic Editor: Irma Virant-Klun

Recently, murine hematopoietic progenitor stem cells (HSCs) and very small embryonic-like stem cells (VSELs) were demonstrated to express receptors for sex hormones including follicle-stimulating hormone (FSH). This raised the question of whether FSH therapy at clinically applied doses can mobilize stem/progenitor cells in humans. Here we assessed frequencies of VSELs (referred to as $Lin^-CD235a^-CD45^-CD133^+$ cells), HSPCs (referred to as $Lin^-CD235a^-CD45^+CD133^+$ cells), and endothelial progenitor cells (EPCs, identified as $CD34^+CD144^+$, $CD34^+CD133^+$, and $CD34^+CD309^+CD133^+$ cells) in fifteen female patients subjected to the FSH therapy. We demonstrated that FSH therapy resulted in statistically significant enhancement in peripheral blood (PB) number of both VSELs and HSPCs. In contrast, the pattern of responses of EPCs delineated by different cell phenotypes was not uniform and we did not observe any significant changes in EPC numbers following hormone therapy. Our data indicate that FSH therapy mobilizes VSELs and HSPCs into peripheral blood that on one hand supports their developmental origin from germ lineage, and on the other hand FSH can become a promising candidate tool for mobilizing HSCs and stem cells with VSEL phenotype in clinical settings.

1. Introduction

Maintenance of appropriate size and composition of both stem cell and progenitor cell pool is tightly regulated by continuous responding to surrounding and long-range orchestrating signals. Interestingly, sex hormones appeared lastly as important regulators of hematopoietic stem/progenitor cells (HSPCs) proliferation [1]. Recently, Nakada and colleagues revealed that hematopoietic stem cells (HSCs) expressed high levels of estrogen receptor and the administration of estradiol increased HSC cell division and self-renewal [2]. In support of this notion, murine HSPCs along with very small embryonic-like stem cells (VSELs) were also recently demonstrated to express receptors for pituitary-derived sex hormones, namely, follicle-stimulating hormone (FSH) and luteinizing hormone (LH) [3]. In concert with this finding, murine HSPCs and VSELs following either *in vitro* or *in vivo* FSH and LH stimulation presented with high proliferative

Table 1: The clinical and hormonal characteristics of female patients ($n = 15$) subjected to FSH stimulation.

Studied parameter	Mean	SD	Minimum	Maximum
Age (years)	32.9	3.9	27	39
Duration of stimulation (days)	8.8	1.1	8	11
Mean daily dose of FSH (IU)	194.4	43.8	120	262.5
Number of mature follicles after FSH stimulation	10.9	3.4	5	16
Estradiol at 7th day (pg/mL)	1153	405	540	1684
Progesterone at 7th day (ng/mL)	0.5	0.15	0.25	0.67
LH at 7th day (mIU/mL)	1.1	0.67	0.31	2.33
Estradiol at the last day (pg/mL)	2314	1367	1367	3294
Progesterone at the last day (ng/mL)	0.8	0.33	0.32	1.52
LH at the last day (mIU/mL)	1.7	0.85	0.72	2.97

response as evidenced by BrdU incorporation. In the light of above mentioned observations, it is tempting to hypothesize the existence of developmental link between HSCs and VSELs and primordial germ cells (PGCs) that are naturally responsive to sex hormones [4, 5].

To date, however, it remained unknown whether the fact that stem cells are susceptible to signaling mediated by sex hormones can be used for mobilization of these cells in clinical settings. Moreover, based on the currently available scarce data, it is difficult to speculate if therapies using sex hormones will affect only fate of primordial stem cells and HSCs or rather would exert their actions toward all progenitor cell populations. Therefore, in the current study, we wished to investigate the effects of FSH therapy at clinically applied doses on mobilization of HSCs and VSELs as well as populations of endothelial progenitor cells (EPCs). In this study, EPCs were chosen as an example of easily identifiable, highly differentiated, and relatively numerous progenitor cell populations that account for endothelial repair and thus largely contribute to maintenance of appropriate vasculature [6–8]. On the other hand, quantification of decreased numbers of EPCs was found to improve prognostication of cardiovascular diseases (CVD) [9–11]. Thus, the search for therapeutic approaches aimed at efficient mobilization of functional EPCs is continuously warranted.

Here we tested in human model the actions of widely accepted regimens of FSH treatment with regard to three stem/progenitor cell subsets at different developmental hierarchy and differentiation level, namely, VSELs, HSCs, and EPCs. Moreover, given the previous reports indicating the crucial role of stroma derived factor-1 (SDF-1) for mobilization of stem cells [12–14], we set out to analyze whether any actions of clinically applied gonadotropins could affect not only stem cells and progenitor cells but also mediators regulating their migratory pathways.

2. Material and Methods

2.1. Patients and FSH Stimulation. For the purpose of the study we recruited fifteen women aged 32.9 ± 3.9 years (range: 27–39 years) who were prepared for *in vitro* fertilization and underwent controlled FSH ovarian stimulation. FSH stimulation has been initiated on 3rd day of menstrual cycle and FSH dose was adjusted based on patient age, ovarian reserve, and previous response to FSH stimulation (if performed). Only two patients received stimulation based on combination of FSH and LH. EDTA-anticoagulated peripheral blood was collected twice: before FSH ovarian stimulation (or in five cases within first days of such stimulation) and at the end of FSH stimulation (days 7–11). Mean daily dose of FSH (either Gonal F, Merck Serono, or Puregon, Schering, or, in two patients, Menopur, Ferring) was 194.4 IU. Detailed characteristics of hormonal status of analyzed patients are presented in Table 1.

All patients' samples were collected upon the approval of Ethics Committee of the Medical University of Bialystok.

2.2. Extracellular Staining and Flow Cytometry. 170 μL of fresh EDTA-anticoagulated whole blood was stained with the set of murine anti-human monoclonal antibodies described in detail in Table 2. Samples were incubated for 30 min at room temperature in the dark. Thereafter, 2 mL of FACS lysing solution (BD) was added, followed by 15 min incubation in the dark. Cells were washed twice with cold PBS (phosphate-buffered saline) and fixed with CellFix (BD Biosciences). Appropriate fluorescence-minus-one (FMO) controls were used for setting compensation and for assuring correct gating. The gating strategy for HSCs and VSELs is shown in Figure 1, while gating strategy for identifying $CD34^+$ cells and EPCs is presented in Figure 2. Samples were acquired using FACSCalibur flow cytometer (BD Biosciences). Obtained data were analyzed using FlowJo version 7.6.5 software (Tree Star).

2.3. Enzyme-Linked Immunosorbent Assays. SDF-1 plasma levels were quantified by means of commercially available enzyme-linked immunosorbent assays (ELISA, DuoSet, R&D). Samples were directly assayed according to manufacturer's instructions. The protein levels in the specimens were calculated from a reference curve generated by using reference standards. The detection range of used ELISA set was

Table 2: Detailed characteristics of monoclonal antibodies used in the study.

Name	Clone	Isotype	Format	Additional information	Manufacturer
Mouse anti-human anti-CD34	8G12	IgG1	FITC	This antibody binds to 105–120 kDa single-chain transmembrane glycoprotein, IVD	Becton Dickinson
Anti-human lineage cocktail 2 (lin 2)			FITC		Becton Dickinson
Mouse anti-human anti-CD3	SK7	IgG1		This antibody binds to epsilon chain of the CD3 antigen, IVD	
Mouse anti-human anti-CD19	SJ25C1	IgG1		This antibody recognizes a 90 kDa antigen, IVD	
Mouse anti-human anti-CD20	L27	IgG1		This antibody binds to phosphoprotein with a molecular weight of 35 or 37 kilodaltons (kDa), depending on the degree of phosphorylation, IVD	
Mouse anti-human anti-CD14	$M_{\varphi}P9$	IgG2b		This antibody reacts with a 53–55 kDa glycosylphosphatidylinositol- (GPI-) anchored and single chain glycoprotein, IVD	
Mouse anti-human anti-CD56	NCAM16.2	IgG2b		This antibody recognizes a heavily glycosylated 140 kDa isoform of NCAM, a member of the immunoglobulin (Ig) superfamily, IVD	
Mouse anti-human anti-CD235a	GA-R2	IgG2b	FITC	This antibody binds to glycophorin A, a sialoglycoprotein present on human red blood cells (RBC) and erythroid precursor cells	Becton Dickinson
Mouse anti-human anti-CD45	HI30	IgG1	PE	This antibody binds to 190, 190, 205, and 220 kDa protein isoforms, RUO	Becton Dickinson
Mouse anti-human anti-CD144	55-7H1	IgG1	PE	This antibody reacts with calcium-independent epitope on cadherin 5, RUO	Becton Dickinson
Mouse anti-human anti-CD309	89106	IgG1	PE	This antibody reacts with CD309 (vascular endothelial growth factor receptor-2 (VEGFR-2))	Becton Dickinson
Mouse anti-human anti-CD133	AC133	IgG1	APC	This antibody reacts with epitope 1 of CD133, RUO	Miltenyi Biotec

IVD: this clone is used for *in vitro* diagnostics; RUO: suitable for research use only.

between 7,81 and 500 pg/mL. The samples were analyzed with automated light absorbance reader (LEDETEC 96 system). Results were calculated by MicroWin 2000 software.

2.4. Statistics. Statistical analysis was carried out using GraphPad Prism 6 (GraphPad software). Wilcoxon test was used. The differences were considered statistically significant at $p < 0.05$. The results are presented as medians (interquartile range).

3. Results

First, we analyzed the effects of FSH administration on the frequencies of circulating HSCs (Figure 3(a)). We found that FSH treatment resulted in statistically significant increase in $Lin^{-}CD133^{+}CD45^{+}$ HSC numbers ((from 125.5 (66–133.5) to 175.5 (83.5–428.8) cells per 170 μL of whole blood), $p = 0.0303$). Similarly, FSH treatment led to significant enhancement of $Lin^{-}CD133^{+}CD45^{-}$ VSEL levels (Figure 3(b)). Following FSH therapy, VSEL numbers increased from 4 cells (3–11,5) to 34 cells (16,5–57) per 170 μL of whole blood ($p = 0.0057$).

Next, we set out to investigate the influence of FSH administration on the frequencies of entire population of $CD34^{+}$ cells and the population of EPCs delineated by such phenotypes as $CD34^{+}CD144^{+}$, $CD34^{+}CD133^{+}$, and $CD34^{+}CD133^{+}CD309^{+}$ cells. Notably, we did not observe any significant changes in the numbers of single $CD34^{+}$ cells following FSH administration (Figure 4(a)). Similarly, we did not demonstrate any significant changes in numbers of EPCs identified as $CD34^{+}CD144^{+}$ cells (Figure 4(b)), $CD34^{+}CD133^{+}$ cells (Figure 4(c)), and $CD34^{+}CD133^{+}CD309^{+}$ cells (Figure 4(d)).

Finally, we wished to investigate whether FSH administration affected serum levels of SDF-1, one of crucial mobilizing factors for VSELs and HSCs (Figure 5). However, we did not find any significant change in SDF-1 concentrations upon completion of FSH administration ($p > 0.05$).

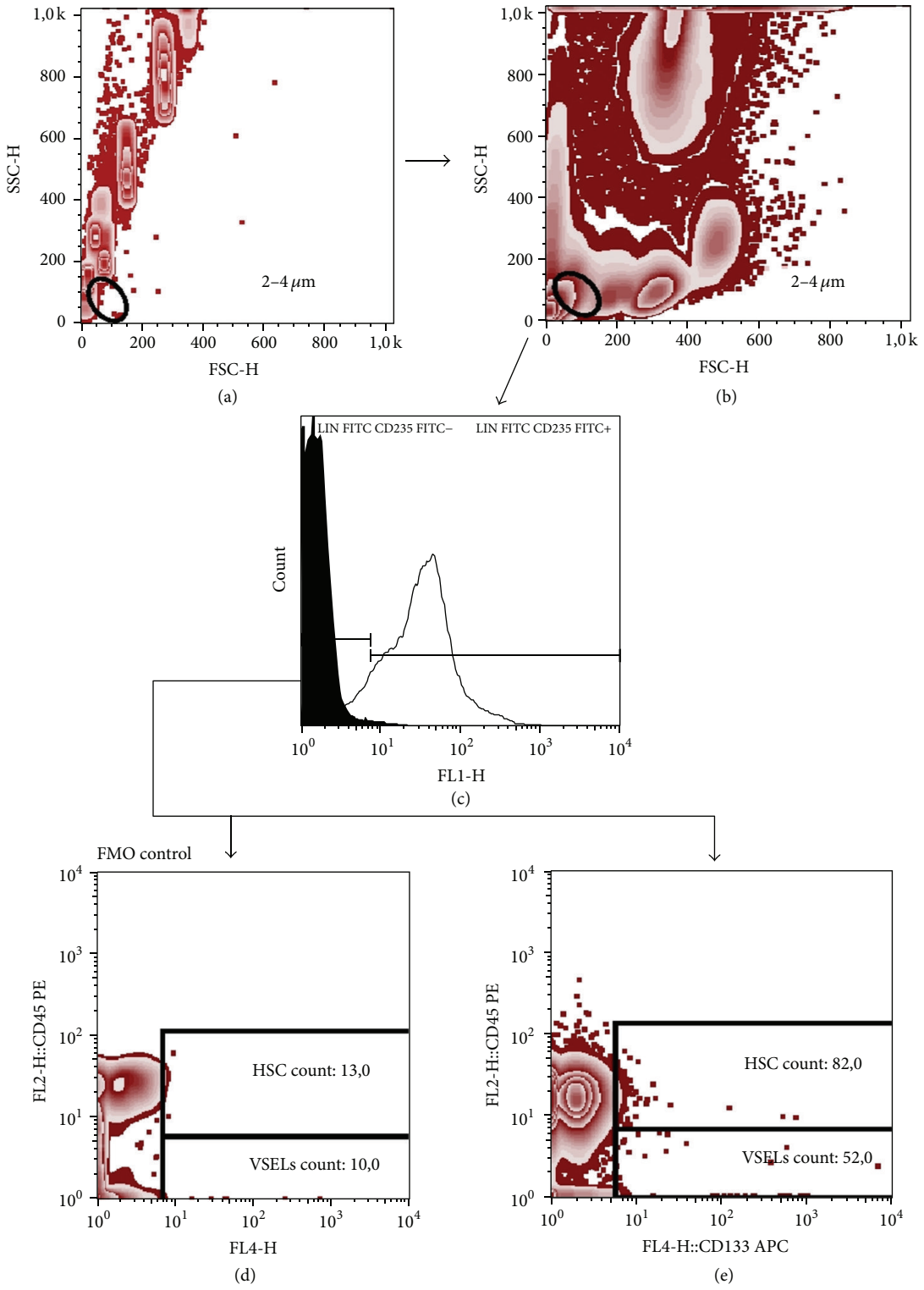

Figure 1: Representative FACS plots demonstrating gating strategy for HSC and VSELs. First, 2–4 μm size events were gated based on a forward and side scatter (FSC/SSC) dot plot (a). Then the 2–4 μm gate was visualized on sample data using a FSC/SSC dot plot (b). Next, 2–4 μm events were displayed on histogram plot (black peak, FMO control; grey peak identifies positive staining) and $Lin^-CD235a^-$ events were gated (c). Finally, FMO control was used to set the HSC and VSELs gate and exclude the background noise (d). Next, HSCs were defined as $Lin^-CD235a^-CD45^+CD133^+$ cells (upper gate) and VSELs were referred to as $Lin^-CD235a^-CD45^-CD133^+$ cells (e).

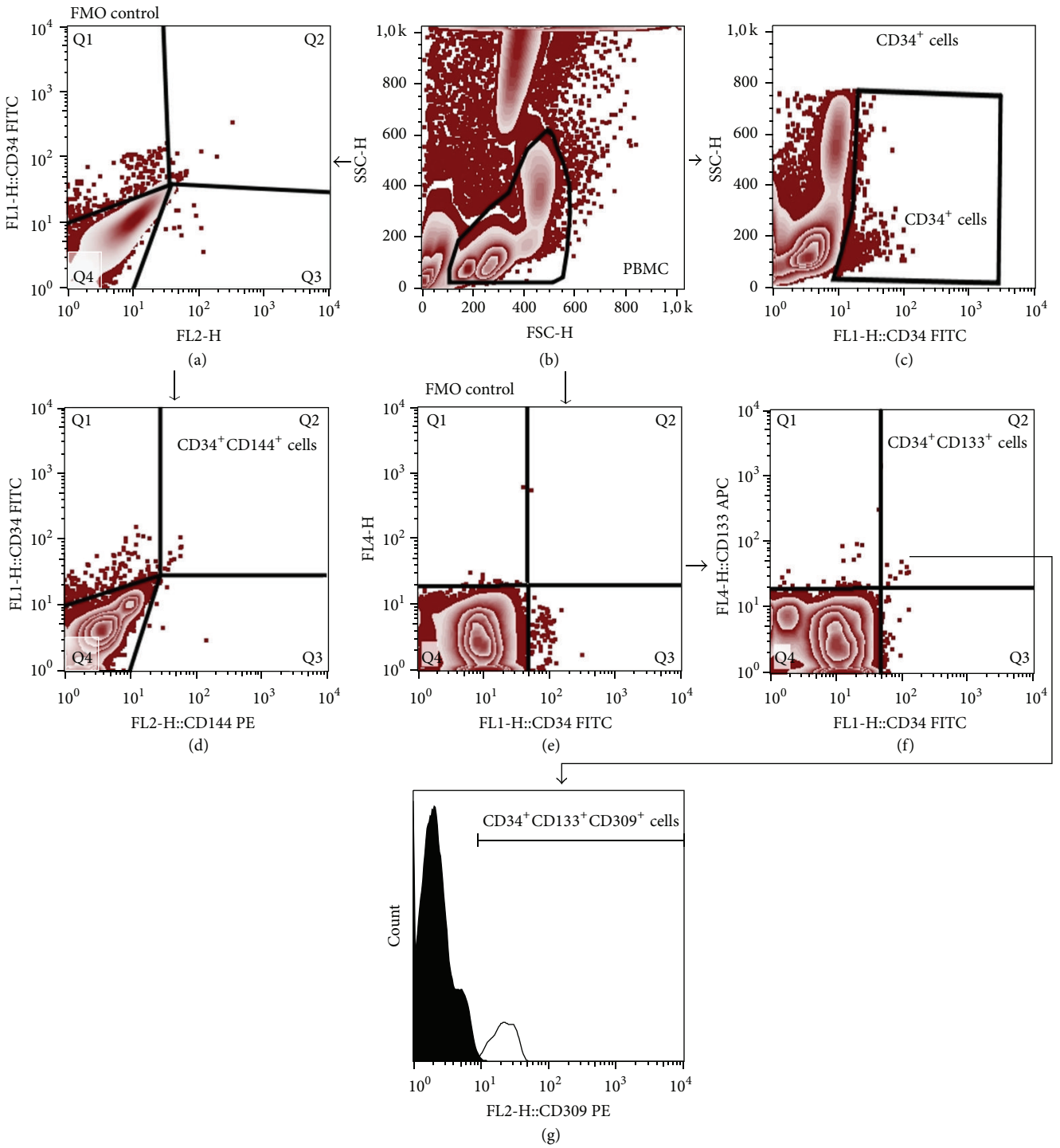

FIGURE 2: Representative FACS plots demonstrating the gating strategy for $CD34^+$ cells and EPCs. PBMCs were gated based on forward and side scatter (FSC/SSC) plot (b). $CD34^+$ cells were gated on CD34/SSC plot (c). $CD34^+CD144^+$ cells (upper right quadrant, Q2) were gated based on CD34/CD144 dot plot (d). FMO control was used to set the gates (a). In order to determine $CD34^+CD144^+CD309^+$ cell numbers, the PBMC events were displayed on the basis of FMO control sample (e) and gates were set to exclude the random noise. Next, the gates were visualized on CD34/CD133 plot (f) and $CD34^+CD133^+$ cells were gated (upper right quadrant, Q2). Finally, $CD34^+CD133^+CD309^+$ cells subsets were gated on histogram plot (g) (black peak, control; grey peak, positive staining).

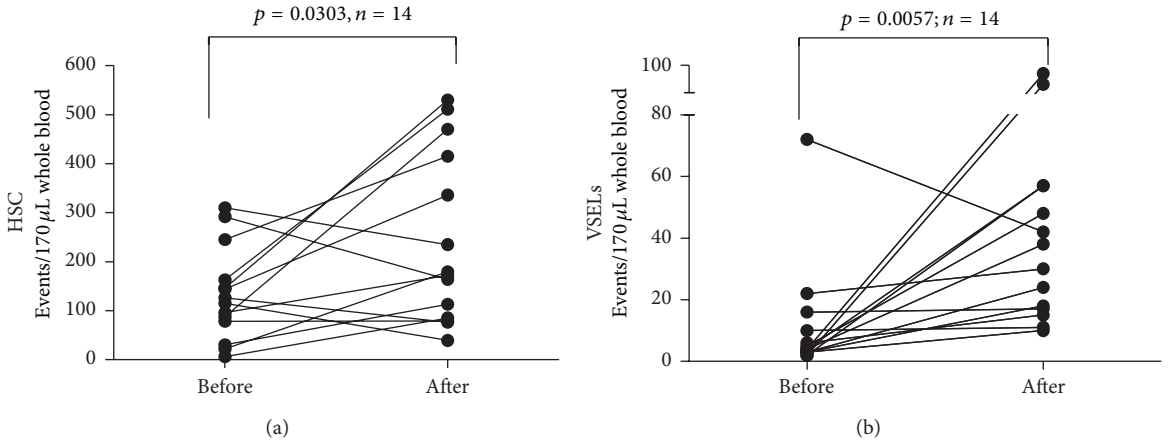

Figure 3: Summary of analyses of time-course changes of the numbers of HSCs (a) and VSELs (b) during FSH therapy.

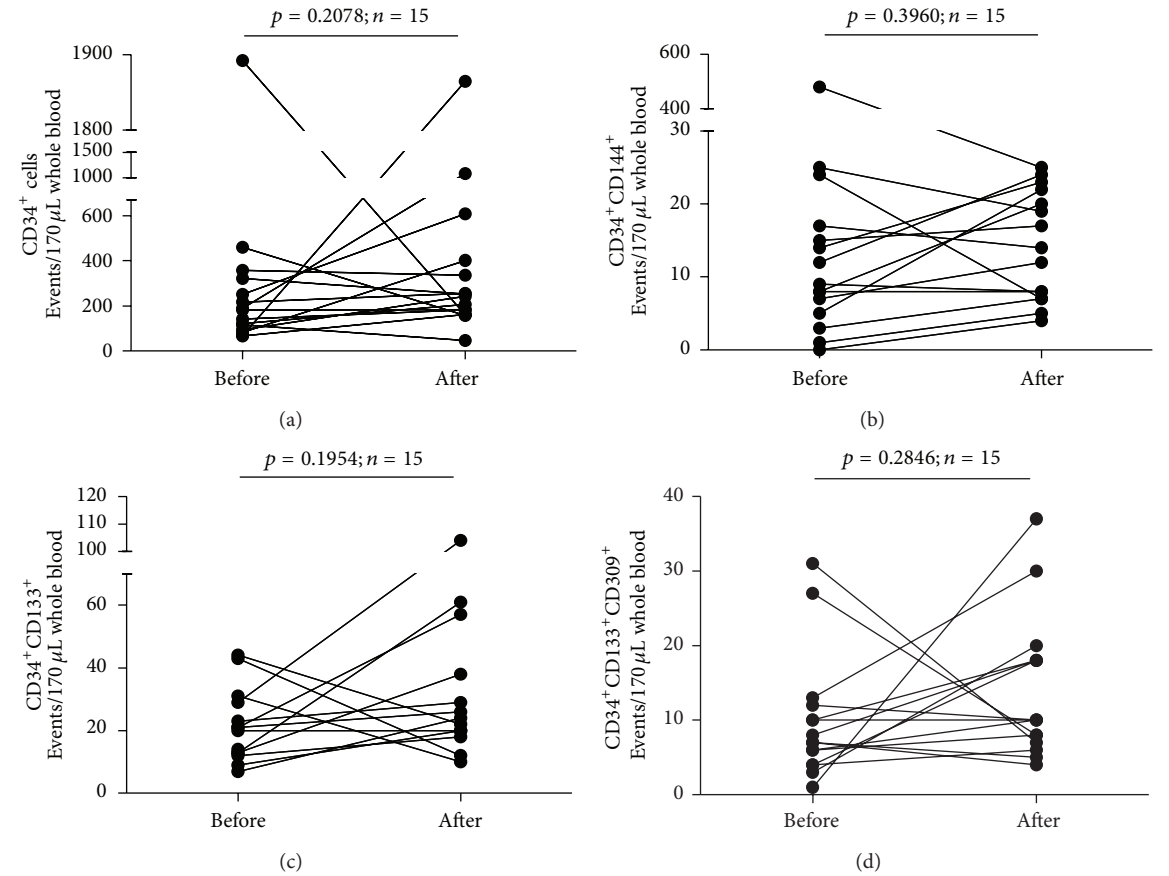

Figure 4: Summary of analyses of time-course changes of the numbers of $CD34^+$ cells (a), $CD34^+CD144^+$cells (b), $CD34^+CD133^+$ cells (c), and $CD34^+CD133^+CD309^+$ cells (d) in the course of FSH therapy.

4. Discussion

Here we demonstrated that administration of pituitary-derived sex hormones at clinically applied doses allowed for efficient mobilization of frequencies of VSELs and HSCs but not endothelial progenitor cells. These findings build a platform for developing novel sex-hormone- based therapeutic strategies aimed at enhancement of either VSELs or HSCs numbers in conditions that would require efficient mobilization of these cells subsets.

Notably, it was shown that the links between gonadotropin hormones and stem cells may extend far beyond the effects exerted on VSELs and HSCs. Tadokoro and colleagues showed that FSH was one of crucial regulators

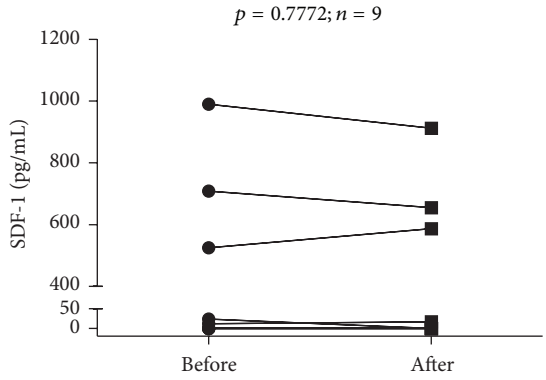

Figure 5: Time-course analysis of individual changes in serum levels of SDF-1 in the course of FSH therapy.

of germinal stem cell (GSC) fate [15]. FSH regulated homeostatic control of glial cell line-derived neurotrophic factor (GDNF) which in turn accelerated proliferation of GSCs. These findings indicated that regulation of GCS population size is regulated by the GDNF/FSH pathway. It remains to be established whether effects of FSH treatment on VSELs and HSCs were related to actions mediated by GDNF. Recently, in concert with this notion, Tourkova and colleagues demonstrated that mesenchymal stem cells (MSC) expressing FSH-R responded with adhesion and proliferation following addition of FSH [16]. Moreover, short-term treatment by FSH at doses comparable to those observed in menopause augmented MSC proliferation by affecting signaling associated with Erk1/2 phosphorylation.

It remains elusive whether mobilizing effects of FSH/LH therapy on VSELs and HSCs in female patients were related to their direct effects on bone marrow-derived stem cells or rather on mobilization of stem cells localized in ovaries. On the other hand, both possibilities do not have to be mutually exclusive. Previously, it was demonstrated that stem cells found in ovaries have the phenotype of VSELs and they can give rise to more differentiated ovarian GCS [17, 18]. This was confirmed by later studies by Parte and colleagues who demonstrated that VSELs and GSCs were present in ovary surface epithelium (OSE) [19]. In this study, FSH treatment resulted in prominent proliferation of stem cell-harboring OSE and release of functional stem cells from ovaries. Moreover, Patel and colleagues found that FSH treatment resulted in increased clonal expansion of ovary-associated stem cells (both VSELs and ovarian GCSs), while FSH receptors were expressed only on ovarian stem cells but not on ovarian epithelial cells [20]. Similarly, Sriraman and colleagues showed that PMSG (FSH analog) increased VSELs numbers in chemoablated female mice [21]. Nevertheless, the question of how effects of gonadotropin hormones on stem cell population size are related to ovaries would require enrollment of male patients subjected to therapy with FSH and/or LH, the condition that due to ethical reasons certainly could not be achieved in the settings of the current study.

Notably, in our study, we did not demonstrate any significant effects of gonadotropin therapy on the levels of EPCs. In concert with this notion, in a representative group of patients with inflammatory bowel disease, Garolla and colleagues did not find relationships between levels of FSH or LH and numbers of EPCs [22]. In some contrast, however, reduced numbers of EPCs were found in hypogonadotropic hypogonadal male patients presenting with low levels of FSH and LH [23]. Interestingly, receptor for FSH is expressed by the endothelium of blood vessels in the majority of metastatic tumors [24]. Therefore, despite lack of significant effects of gonadotropin therapy on numbers of circulating EPCs analyzed in the current study, the subject of mutual relationships among EPCs, endothelial cells, and pituitary-derived sex hormones certainly deserves further investigation.

Our findings also bring about an interesting perspective for understanding relationships between stem and progenitor cells and elevated levels of FSH and LH that are detected at elderly age. In the light of our data, it is tempting to hypothesize that enhanced FSH and LH levels in elderly individuals could represent the mechanism of enhancing otherwise diminished hematopoiesis and decreased stem cell numbers. Similarly, this observation was previously documented in mouse model, wherein the numbers of VSELs were shown to be highest in young subjects and decreased with age [25].

Given these data, FSH and LH therapy could become an attractive and easily available tool enabling mobilization of stem cells in regenerative medicine. However, given the broad spectrum of the effects exerted by sex hormones, the safety of such approach would need to be examined in further clinical studies performed in different groups of patients including males. One has to keep in mind that FSH and LH were found to be involved in the growth of certain tumors. As an example, Ji and colleagues found significantly higher levels of mRNA encoding receptor for FSH (FSHR) in invasive ovarian tumors compared to low malignant tumors and normal OSE [26]. Similarly, it was reported that overexpression of FSHR in OSE cells led to an increase in expression of proteins involved in ovarian cancer development such as EGFR, c-myc, and HER2/neu. Thus any therapeutic strategies aimed at enhancement of the size of stem/progenitor cell pool by the use of gonadotropin-based therapies would need to be carefully investigated in terms of clinical safety.

Altogether, our data support recent findings on the role of FSH in the biology of VSELs and HSCs that were reported by our group in mouse model [4]. Thus, these data support a concept of a developmental link between germ line, VSELs, and hematopoiesis [4, 5]. Finally, we demonstrated here for the first time that mobilization of stem cells with VSELs phenotype and HSPCs can be achieved by the use of widely available therapeutic regimens based on pituitary-derived sex hormones.

Conflict of Interests

The University of Louisville is the owner of patents on VSELs and some areas of VSEL technology, which are licensed to Neostem Inc., New York. None of the authors have any stock in Neostem Inc., New York, or any other biotechnological stem cell company.

Authors' Contribution

Monika Zbucka-Kretowska, Andrzej Eljaszewicz, and Danuta Lipinska equally contributed to the work.

Acknowledgments

The study was supported by funds of Leading National Research Center (KNOW) of Medical University of Bialystok. The authors wish to thank students of Scientific Society of Medical University of Bialystok for help in delivering blood samples.

References

[1] D. Gancz and L. Gilboa, "Hormonal control of stem cell systems," *Annual Review of Cell and Developmental Biology*, vol. 29, pp. 137–162, 2013.

[2] D. Nakada, H. Oguro, B. P. Levi et al., "Oestrogen increases haematopoietic stem-cell self-renewal in females and during pregnancy," *Nature*, vol. 505, no. 7484, pp. 555–558, 2014.

[3] K. Mierzejewska, S. Borkowska, E. Suszynska et al., "Hematopoietic stem/progenitor cells express several functional sex hormone receptors—novel evidence for a potential developmental link between hematopoiesis and primordial germ cells," *Stem Cells and Development*, vol. 24, no. 8, pp. 927–937, 2015.

[4] M. Z. Ratajczak, K. Marycz, A. Poniewierska-Baran, K. Fiedorowicz, M. Zbucka-Kretowska, and M. Moniuszko, "Very small embryonic-like stem cells as a novel developmental concept and the hierarchy of the stem cell compartment," *Advances in Medical Sciences*, vol. 59, no. 2, pp. 273–280, 2014.

[5] M. L. Scaldaferri, F. G. Klinger, D. Farini et al., "Hematopoietic activity in putative mouse primordial germ cell populations," *Mechanisms of Development*, vol. 136, pp. 53–63, 2015.

[6] M. Rusak, U. Radzikowska, B. Glowinska-Olszewska et al., "Endothelial progenitor cell levels in juvenile idiopathic arthritis patients; effects of anti-inflammatory therapies," *Pediatric Rheumatology*, vol. 13, no. 1, article 6, 2015.

[7] A. Y. Khakoo and T. Finkel, "Endothelial progenitor cells," *Annual Review of Medicine*, vol. 56, pp. 79–101, 2005.

[8] S. M. Goerke, J. Obermeyer, J. Plaha, G. B. Stark, and G. Finkenzeller, "Endothelial progenitor cells from peripheral blood support bone regeneration by provoking an angiogenic response," *Microvascular Research*, vol. 98, pp. 40–47, 2015.

[9] B. Głowińska-Olszewska, M. Moniuszko, A. Hryniewicz et al., "Relationship between circulating endothelial progenitor cells and endothelial dysfunction in children with type 1 diabetes: a novel paradigm of early atherosclerosis in high-risk young patients," *European Journal of Endocrinology*, vol. 168, no. 2, pp. 153–161, 2013.

[10] J. R. Lavoie and D. J. Stewart, "Genetically modified endothelial progenitor cells in the therapy of cardiovascular disease and pulmonary hypertension," *Current Vascular Pharmacology*, vol. 10, no. 3, pp. 289–299, 2012.

[11] S. Sen, S. P. McDonald, P. T. H. Coates, and C. S. Bonder, "Endothelial progenitor cells: novel biomarker and promising cell therapy for cardiovascular disease," *Clinical Science*, vol. 120, no. 7, pp. 263–283, 2011.

[12] M. Z. Ratajczak, C. H. Kim, A. Abdel-Latif et al., "A novel perspective on stem cell homing and mobilization: review on bioactive lipids as potent chemoattractants and cationic peptides as underappreciated modulators of responsiveness to SDF-1 gradients," *Leukemia*, vol. 26, no. 1, pp. 63–72, 2012.

[13] M. Kucia, R. Reca, K. Miekus et al., "Trafficking of normal stem cells and metastasis of cancer stem cells involve similar mechanisms: pivotal role of the SDF-1-CXCR4 axis," *Stem Cells*, vol. 23, no. 7, pp. 879–894, 2005.

[14] M. Kucia, J. Ratajczak, R. Reca, A. Janowska-Wieczorek, and M. Z. Ratajczak, "Tissue-specific muscle, neural and liver stem/progenitor cells reside in the bone marrow, respond to an SDF-1 gradient and are mobilized into peripheral blood during stress and tissue injury," *Blood Cells, Molecules, and Diseases*, vol. 32, no. 1, pp. 52–57, 2004.

[15] Y. Tadokoro, K. Yomogida, H. Ohta, A. Tohda, and Y. Nishimune, "Homeostatic regulation of germinal stem cell proliferation by the GDNF/FSH pathway," *Mechanisms of Development*, vol. 113, no. 1, pp. 29–39, 2002.

[16] I. L. Tourkova, M. R. Witt, L. Li et al., "Follicle stimulating hormone receptor in mesenchymal stem cells integrates effects of glycoprotein reproductive hormones," *Annals of the New York Academy of Sciences*, vol. 1335, no. 1, pp. 100–109, 2015.

[17] S. Parte, D. Bhartiya, J. Telang et al., "Detection, characterization, and spontaneous differentiation in vitro of very small embryonic-like putative stem cells in adult mammalian ovary," *Stem Cells and Development*, vol. 20, no. 8, pp. 1451–1464, 2011.

[18] I. Virant-Klun, N. Zech, P. Rozman et al., "Putative stem cells with an embryonic character isolated from the ovarian surface epithelium of women with no naturally present follicles and oocytes," *Differentiation*, vol. 76, no. 8, pp. 843–856, 2008.

[19] S. Parte, D. Bhartiya, D. D. Manjramkar, A. Chauhan, and A. Joshi, "Stimulation of ovarian stem cells by follicle stimulating hormone and basic fibroblast growth factor during cortical tissue culture," *Journal of Ovarian Research*, vol. 6, article 20, 2013.

[20] H. Patel, D. Bhartiya, S. Parte, P. Gunjal, S. Yedurkar, and M. Bhatt, "Follicle stimulating hormone modulates ovarian stem cells through alternately spliced receptor variant FSH-R3," *Journal of Ovarian Research*, vol. 6, article 52, 2013.

[21] K. Sriraman, D. Bhartiya, S. Anand, and S. Bhutda, "Mouse ovarian very small embryonic-like stem cells resist chemotherapy and retain ability to initiate oocyte-specific differentiation," *Reproductive Sciences*, 2015.

[22] A. Garolla, R. D'Incà, D. Checchin et al., "Reduced endothelial progenitor cell number and function in inflammatory bowel disease: a possible link to the pathogenesis," *American Journal of Gastroenterology*, vol. 104, no. 10, pp. 2500–2507, 2009.

[23] C. Foresta, L. de Toni, R. Selice, A. Garolla, and A. di Mambro, "Increased osteocalcin-positive endothelial progenitor cells in hypogonadal male patients," *Journal of Endocrinological Investigation*, vol. 33, no. 7, pp. 439–442, 2010.

[24] A. Siraj, V. Desestret, M. Antoine et al., "Expression of follicle-stimulating hormone receptor by the vascular endothelium in tumor metastases," *BMC Cancer*, vol. 13, article 246, 2013.

[25] M. Kucia, R. Reca, F. R. Campbell et al., "A population of very small embryonic-like (VSEL) $CXCR4^+SSEA\text{-}1^+Oct\text{-}4^+$ stem cells identified in adult bone marrow," *Leukemia*, vol. 20, no. 5, pp. 857–869, 2006.

[26] Q. Ji, P. I. Liu, P. K. Chen, and C. Aoyama, "Follicle stimulating hormone-induced growth promotion and gene expression profiles on ovarian surface epithelial cells," *International Journal of Cancer*, vol. 112, no. 5, pp. 803–814, 2004.

Hindawi Publishing Corporation
Stem Cells International
Volume 2016, Article ID 1741072, 8 pages
http://dx.doi.org/10.1155/2016/1741072

Review Article

Primordial Germ Cells: Current Knowledge and Perspectives

Aleksandar Nikolic,[1] Vladislav Volarevic,[1] Lyle Armstrong,[2] Majlinda Lako,[2] and Miodrag Stojkovic[1,3]

[1]*Center for Molecular Medicine and Stem Cell Research, Faculty of Medical Sciences, University of Kragujevac, 69 Svetozara Markovica Street, 34000 Kragujevac, Serbia*
[2]*Institute of Genetic Medicine, Newcastle University, The International Centre for Life, Central Parkway, Newcastle upon Tyne NE1 3BZ, UK*
[3]*Spebo Medical, Norvezanska 16, 16 000 Leskovac, Serbia*

Correspondence should be addressed to Miodrag Stojkovic; mstojkovic@spebo.co.rs

Received 15 April 2015; Accepted 17 May 2015

Academic Editor: Irma Virant-Klun

Infertility is a condition that occurs very frequently and understanding what defines normal fertility is crucial to helping patients. Causes of infertility are numerous and the treatment often does not lead to desired pregnancy especially when there is a lack of functional gametes. In humans, the primordial germ cell (PGC) is the primary undifferentiated stem cell type that will differentiate towards gametes: spermatozoa or oocytes. With the development of stem cell biology and differentiation protocols, PGC can be obtained from pluripotent stem cells providing a new therapeutic possibility to treat infertile couples. Recent studies demonstrated that viable mouse pups could be obtained from *in vitro* differentiated stem cells suggesting that translation of these results to human is closer. Therefore, the aim of this review is to summarize current knowledge about PGC indicating the perspective of their use in both research and medical application for the treatment of infertility.

1. Introduction

Today, in the second decade of this millennium, infertility remains a global condition with a high prevalence of occurrence [1, 2]. Boivin et al. [3] revealed that the rate of 12-month prevalence ranges from 3.5% to 16.7% in more developed and from 6.9% to 9.3% in less-developed countries, with an average prevalence of 9%. The diagnosis of infertility may become a cause of life crisis in many couples, so it is necessary to develop mechanisms to overcome temporary or permanent loss of fertility and the possibility to have a biological child [1]. For infertile couples that are unable to have a child by other treatments, artificial reproductive technique (ART) and the possibility to derive gametes from stem cells offer potential reproductive strategies to individuals who are infertile due to injuries, exposure to toxicants, or immune-suppressive treatments and suffer from gonadal insufficiency due to premature ovarian failure or azoospermia, reproductive aging, and idiopathic cases of poor gamete quality [4, 5].

In most multicellular organisms, germ cells are the origin of new organisms that provide the inheritance of the genetic and epigenetic information in the following generations [6]. The germ cell lineage is the source of totipotency, providing the creation of new organisms [7]. In the 19th century, August Weismann published the hypothesis according to which the presence of preformed germ cell determinants (germplasm) are inherited only through the germ cells ensuring the totipotency and continuity of the germ line [8]. This has been demonstrated in invertebrates and lower vertebrates, where the germplasm is required for germ cell formation, while in mammals, this process involves epigenetic mechanisms and not preformation. That regulated event, in which some environmental influences play a crucial role, and totipotency is maintained through the germ line, allowing further development in the following generation.

Germ cells undergo two significantly different developmental phases [9]. The first phase occurs during early embryogenesis, when primordial germ cells (PGCs) are formed and

actively migrate to the gonadal ridge [10, 11]. In the second phase, the germ cells receive appropriate signals from their environment and initiate one of two distinct programs of controlled cell division, meiosis, and differentiation-oogenesis or spermatogenesis, to form gametes. The molecular basis of both processes and early germ cell development is very well understood in two species, *Drosophila* and *Caenorhabditis elegans*, where systematic genetic reviews have identified many of the genes required in this process [12–15]. PGCs in humans have not been intensely investigated because of the technical and ethical obstacles to obtaining such cells from early embryos [16]. The greater part of our knowledge of mammalian PGC specification has been obtained from studies using early mouse embryos, in which the germ cell fate is induced in pluripotent proximal epiblast cells soon after implantation in the uterine wall [17].

In this review we summarize current knowledge about mammalian PGC and indicate the perspective of their use in research and to generate mature gametes that could be used in treatment of human infertility.

2. Origin and Development of Primordial Germ Cells

In mammals, the origin of the germ cell lineage in embryogenesis was initially unclear due to the absence of the characteristic germplasm present in the egg as seen in other organisms such as *X. laevis* and *D. melanogaster* [17]. PGCs were first identified in mammals by Chiquoine in 1954 [18]. He found a population of germ cell lineage cells capable of generating both, oocytes and spermatozoa at the base of the emerging allantois at E7.25 in the endoderm of the yolk sac of mouse embryos, immediately below the primitive streak, identified by high alkaline phosphatase (AP) activity. While ethical constraints limit our knowledge of the specification of human PGC, it is clear that common signaling pathways operate across mammals and possibly all vertebrates [19]. Based upon staining of AP different studies have suggested diverse sites of origin for the PGC including the posterior primitive streak (reviewed in [20]). The founder population of germ cells is few in number and deeply which causes major difficulties in studying the genetic basis for the specification of the germ cell lineage [8]. Germ cells, soon after their lineage restriction, acquire morphology which would reflect underlying unique molecular features. Saitou et al. have established a system to identify key factors that determine germ cell fate in mouse and to understand the distinctive features that the germ cells acquire at the molecular levels [21]. They dissected out an embryonic region with around 300 cells that contained the founder germ cells at E7.5 (EB stage) and dissociated it into single cells. These cells are morphologically similar but fall into two classes distinguishable by differential expression of two germ cell-specific genes, *Stella* and *Fragilis* [8]. The cluster of 300 cells demonstrates universal expression of *Fragilis* but *Stella* expression is restricted to a subset of cells within the centre of the cluster. Therefore, both genes appear to have major roles in germ cell development and their ability to differentiate [21]. *Stella* is the first gene to be expressed in the population of cells considered to be lineage restricted germ cells [8] that also show high expression of tissue nonspecific AP (*Tnap*), a gene for AP activity of PGC [22].

Migrating germ cells continue to show strong and specific expression of *Stella* but exhibit strong repression of all the homeobox genes examined (*Hoxb1*, *Hoxa1*, *Evx1*, and *Lim1*), despite high levels of expression of these genes in the neighbouring somatic cells [8]. Since the role of homeobox genes is to specify the regional identity of cells along the body axis or induce differentiation of cells towards specific somatic cell lineages, this suggests that the founder germ cells acquire the ability to avoid somatic specification by preventing or suppressing homeobox gene expression. This could be one of the key features that mammalian germ cells possess that allows them to maintain or regain totipotency and differ from other surrounding cells in the niche. This concept is supported by continued expression of *Oct4* and other pluripotency genes in germ cells [23].

In mouse, the specification of germline begins around E6.25 in the proximal epiblast in a small population of cells identified by expression of *Blimp1* (B-lymphocyte-induced maturation protein 1)/*Prdm1* (Pr domain containing protein 1) [24] and *Prdm14* [25]. Interestingly, Blimp1 and Prdm14 have distinct binding patterns relative to promoters [26] and Blimp1 has a dominant role for PGC specification. Blimp1 is important for the repression of almost all the genes normally downregulated in PGC with respect to their somatic neighbours, as well as for the restoration of pluripotency and epigenetic reprogramming. Conversely, Prdm14 regulates the restoration of pluripotency and epigenetic reprogramming independently from Blimp1 and defines a novel genetic pathway with strict specificity to the germ cell lineage [27]. Expression of these two factors starts independently in a small number of cells of the proximal posterior epiblast at the beginning of the early-streak stage [28]. These cells increase in number and form PGC with AP activity and *Stella* (also known as *Dppa3* or *Pgc7*) expression [21, 29]. PGCs in the mouse are induced during gastrulation by bone morphogenetic protein (BMP) signaling and as yet unidentified signal(s) from the extraembryonic ectoderm and visceral endoderm to underlying pluripotent epiblast cells at E6.5 [30]. This induction results in *Blimp1*/*Prdm1* mediated transcriptional regulation of epiblast cells which promotes the expression of PGC-specific genes, such as *Stella*, and represses the expression of somatic cell genes such as members of the *Hox* gene family [24, 31]. It is still unknown whether the Smads activate *Blimp1* and *Prdm14* transcription directly or indirectly [7]. Determination of the element(s) responsible for *Blimp1* expression in the epiblast in response to BMP4 and examination of whether or not the Smads directly bind to and control Blimp1 will be crucial to provide a definitive answer to this question. Induction of PGC seems to require BMP4 or BMP8b alone or in combination indicating that signalling for various BMPs occurs through separate receptors. In mice, a number of other factors which have been implicated in specification and maintenance of PGC occur at around E6.25, marked by the sequential expression of two transcription factors *Blimp1*/*Prdm1* and *Prdm14* in response to BMPs [32]. *Blimp1*, *Prdm14*, and *Stella*-positive PGC integrate key events to repress a somatic mesodermal differentiation program in

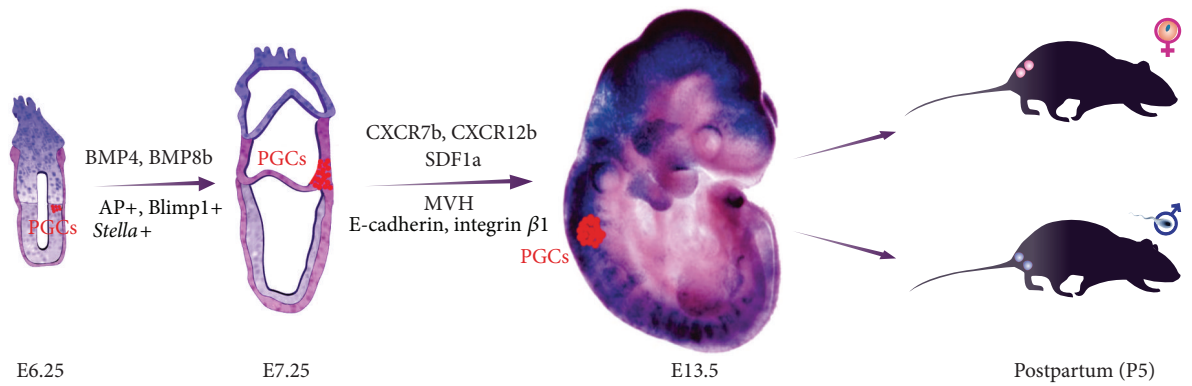

Figure 1: Time schedule and signals involved in the regulation of primordial germ cells (PGCs) migration and colonization in mice.

PGC [7]. WNT signalling is also essential for the PGC fate, possible through posttranscriptional interaction with suggesting that the WNT signaling may act posttranscriptionally on BMP signalling components [7]. WNT signaling can stabilize Smad1 by inhibiting GSK3-mediated phosphorylation of its linker region thereby preventing its degradation [33] but the tyrosine-kinase receptor c-kit and its ligand, stem cell factor, are essential for the maintenance of PGC in both sexes [19].

3. Migration of Primordial Germ Cells

In contrast to *D. melanogaster* and zebrafish, little is known about PGC migration and initiation of that process in mice [33]. Soon after specification, the cells begin to exhibit polarized morphology and cytoplasmic extensions and initiate migration through the primitive streak into the adjacent posterior embryonic endoderm, extraembryonic endoderm, and allantois [20]. The first step in mouse PGC migration is the movement of cells from the posterior primitive streak to the endoderm at E7.5. Between E8.5 and E13.5, the *Tnap* positive PGCs proliferate and migrate via the hindgut endoderm and mesentery followed by bilateral migration to the genital ridges, after which they can enter into meiosis in the female or mitotic arrest in the male and initiate differentiation into either oocytes or spermatozoa [16, 34]. During migration, the PGC population doubling time is fairly uniform at about 16 hours between 8.5 and 13.5 days. E13.5 mouse embryos should have about 24000 PGCs in their genital ridges [35]. In this migratory phase, PGCs undergo extensive genome reprogramming and alteration of epigenetic information, such as DNA methylation and histone modification patterns, and the erasure of gene imprinting that may be essential for restoring totipotency to the germ cell lineage [16].

Currently, there is no evidence for sex-specific differences during PGC migration in any organism. A subset of germ cells in the gonad acquires the ability to function as germline stem cells, which undergo meiosis to produce sperm and eggs and promote the next generation of embryonic development and PGC migration. Vasa protein is an essential component of germplasm and represents a poorly understood complex of RNA and proteins that is required for germ cell determination. Null mutation leads to sterility in female mice resulting from severe defects in oogenesis [10]. In humans, *VASA* expression begins at the end of the migratory phase of PGC development [9]. Tilgner et al. generated and characterized human embryonic stem cell (hESC) lines with a construct in which expression of the pEGFP-1 gene was driven by a DNA sequence representing the *VASA* reporter [36]. They demonstrated that hESC could be used as a development model system for PGC specification under *in vitro* conditions. Also, they were able to establish a small number of the presumed female PGCs isolated on the basis of *VASA* promoter driven GFP fluorescence. These results and the fact that specific expression of *Vasa* in the germ cell lineage during colonization of the gonadal ridge suggest that Vasa is required to maintain the functionality of germ cells. For instance, male mice homozygous for a targeted mutation of the mouse *Vasa* ortholog *Mvh* are sterile and exhibit severe defects in spermatogenesis while homozygous females are fertile [37, 38]. Other signals (Figure 1) involved in the regulation of PGC migration and colonization are the adhesion molecule *E-cadherin* [39] and extracellular matrix molecule integrin β1 [40, 41]. Unfortunately, the precise function of these factors and signalling pathways remain to be explained.

Migratory PGCs maintain a genomic program associated with pluripotency. They express core pluripotency genes (*Oct4*, *Nanog*, and *Sox2*) and are able to form teratomas after injection into postnatal mouse testes [6, 42, 43]. Besides these, migratory PGCs express stage-specific embryonic antigen 1 (SSEA1) [16]. Upon arrival in the gonad, germ cell-specific RNA binding protein DAZL (deleted in azoospermia-like) is essential for developing PGC [44]. Many studies revealed that the DAZL functions as a translational enhancer [45–47]. Knockout for target mRNA binding partners of DAZL (Mvh, Scp3, and Tex19.1) resulted in severe phenotypic changes [48–50] suggesting that DAZL may have additional roles during the PGC stage of mammalian gametogenesis. DAZL is also a gatekeeper of apoptosis in PGC and regulates the expression of key Caspases acting as an elegant fail-safe mechanism that prevents stray PGC from forming teratomas and eliminating aberrant PGC [51]. In the absence of DAZL, the germ cells fail

Table 1: Summarized genes that participate into PGC development.

Full name	Alternate names	Time of expression	Location of coded protein	References
Tissue nonspecific AP (Tnap)		E7.25-14	At the cell surface, linked to the cell membrane via a phosphatidylinositol glycan linkage	[22]
Stella	*Developmental pluripotency-associated 3 or Dppa3* or *Pgc7*	E7.5	Protein that may shuttle between the nucleus and cytoplasm	[8, 21]
Fragilis		E7.5	Transmembrane protein	[8, 21]
B-lymphocyte-induced maturation protein 1 (*Blimp1*)	Pr domain containing protein 1 (*Prdm1*)	E6.25	Cytoplasmic transcriptional repressor	[24]
Prdm14	Pr domain containing protein 14	E6.25	Transcriptional regulator	[25]
Mouse *Vasa* ortholog (*Mvh*)		E13.5(10.5) end of the migratory phase of PGC development	Cytoplasm	[9]
Deleted in azoospermia-like (DAZL)		E12.5(11.5)	Cytoplasmic protein	[44–52]

to develop beyond the PGC stage as shown by continued expression of pluripotency markers. These findings suggest that DAZL is a "licensing factor" required for sexual differentiation of PGC [52]. Genes that participate in PGC development are summarized in Table 1.

Postmigration PGCs, marked by the expression of several RNA binding proteins such as MVH, DAZL, and NANOS3, undergo sexual dimorphic development [46–53]. In mice, female germ cells quickly initiate meiosis and arrest at meiosis I stage, while male ones mitotically divide for several rounds and then enter a quiescent stage when they are known as gonocytes. Specifically, the PGCs upregulate a set of genes that enable them to undergo sexual differentiation and gametogenesis while suppressing their pluripotency program [54]. In the female XX embryo, the PGCs continue to proliferate and subsequently enter into the prophase I of meiotic divisions [35]. Hereafter, they are arrested at the diplotene stage of prophase I of meiosis. After birth, the gonocytes are surrounded by cells from the cortical interstitial layer and become primary oocytes in primordial follicles, thereby ending precursor proliferative potential and arresting their development process until puberty. After puberty, hormonal stimulation during ovulation causes the maturation and release of oocytes from the ovary into the oviduct followed by completion of the first meiotic division with concomitant extrusion of the first polar body. Upon fertilization with a haploid spermatozoon, the oocyte completes the second meiotic division and extrudes the second polar body [6, 55, 56].

In contrast to those in the female, XY PGCs enter into mitotic arrest upon entry into the genital ridges and stay quiescent in the G_0/G_1 phase of the cell cycle for the remaining embryonic period as a prospermatogonium, while retaining a proliferative precursor potential [57]. Around day 5 postpartum, many of prospermatogonia resume active proliferation, while some migrate to the basement membrane of the seminiferous tubule and form tight junctions with Sertoli cells thereby forming spermatogonial stem cells (SSC) incorporated into their appropriate niche. Thus, compared with the very limited size of the oocyte pools, the spermatozoa can be obtained from differentiation of SSC. In culture, germline stem cells bearing the abilities for long-term proliferation and for spermatogenesis upon transplantation into testes are established in the presence of GDNF (glial cell-derived neurotrophic factor), most readily from neonatal testes [6, 55, 56].

4. Derivation of PGC from Pluripotent Cells

PGC can be isolated from whole mouse embryos at E6.0 in serum- and feeder-free conditions in suspension [7]. Under such conditions leukaemia inhibitory factor has an activity to suppress the induction of goosecoid, a marker for the mesendoderm, which suggests that *Blimp1* expression in the serum-free medium might reflect a differentiation of epiblast cells into a mesendodermal lineage. The data indicate that essentially all epiblast cells at E6.0, if separated from visceral endoderm a source for inhibitory signals, are able to express *Blimp1* in response to BMP4 alone (Figure 1). Until now, evidence has been provided that isolated epiblasts can be induced to form *Blimp1*, *Prdm14*, and AP-positive PGC-like cells after 36 hours in a serum-free culture with BMP4 [58].

Meanwhile differentiation of hESC to PGC has substantial potential as a method to examine the mechanisms of normal and abnormal development of human germline. To derive larger numbers of human PGCs from hESC Tilgner et al. [16] have developed an *in vitro* growth system that demonstrates the usefulness of SSEA1 to enrich a population of putative PGC. The SSEA1-positive cells share many characteristics with *ex vivo* PGC, such as the expression of key genes (*VASA*, *OCT4*, and *STELLA*), but their cell-cycle status differs

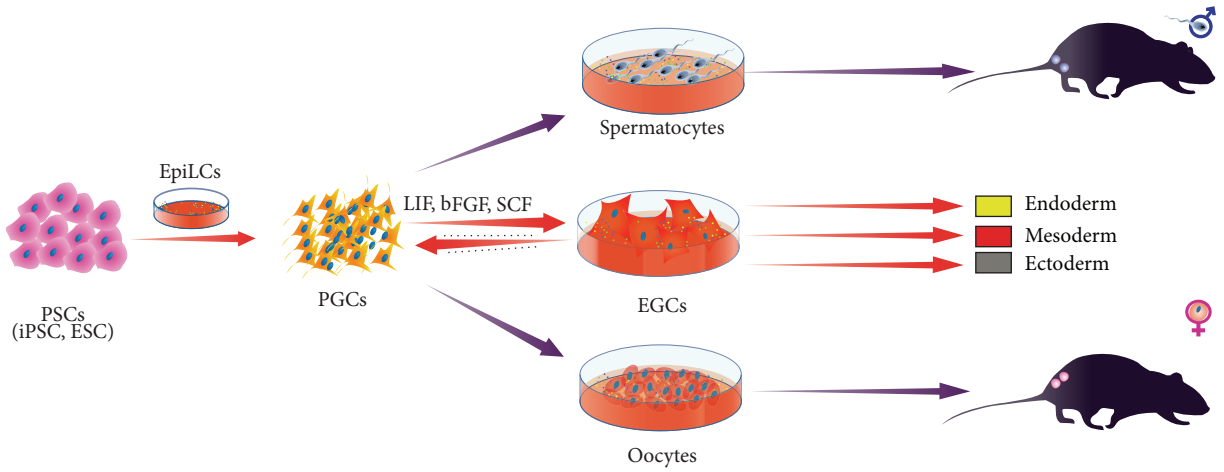

Figure 2: Making gametes from pluripotent stem cells (PSC). Primordial germ cells (PGCs), embryonic germ cells (EGCs).

from previous observations in embryonic mice, indicating that PGCs from E9.0 were largely arrested in G2/M, while the SSEA1-positive population is largely in S-phase, which suggests that the majority of the cells may still be in their mitotic expansion phase. Therefore, targeted differentiation of human pluripotent stem cells (PSC) offers an excellent opportunity to investigate the mechanisms involved in maturation of PGC. However, the limited number of publications indicates that the derivation of germ cells from PSC is still an immature technology [59–61]. The first reported study of induction of mouse germ cells from PSC was study by Hübner et al. [60] but Hayashi et al. [62] were the first to describe the high efficiency two-step procedure to obtain PGC-like cells (PGCLC) from mouse ESC and iPSC. In this procedure, ESC and iPSC were first induced into epiblast-like cells that were subsequently induced to PGCLC [62] and later ESC could be differentiated towards germ cells [63]. Chuma et al. [42] transplanted PGC in testis and obtained mature sperm whereas Matoba and Ogura [64] reported that PGCs isolated from E12.5 male foetus under the kidney capsule yield spermatids (Figure 2). The milestone of these studies is the birth of healthy offspring. Similar to Matoba and Ogura Hashimoto et al. [65] reported that PGCs isolated from female foetus when transplanted under the ovarian bursa or kidney capsule result in functional oocytes. Therefore, we are a step closer to obtaining human gametes from *in vitro* produced PGC using ESC or iPSC [62, 66, 67] but in human some obstacles remain: (i) how to make the PGC to convert to mature oocyte without transplantation and (ii) how to repeat the mouse work in humans to produce PGC for infertility treatment. Nevertheless, the advantage of using hESC and patient-specific iPSC is the possibility to decipher the mechanisms involved in differentiation and maturation of human gametes with the aim of completely translating gene expression profiling of these cells. This can be confirmed by previous publication [68] with clear evidence that the *SOX17* is the key regulator of human PGC fate. The study revealed that the *Blimp1* is downstream of *SOX17* and represses endodermal and other somatic genes during specification of human PGC, which was unexpected since *Sox17* does not have role in specification of mouse PGC. Once we have in our hands the protocol to drive differentiation of human iPSC towards functional gametes we will be able to produce patient-specific oocytes and spermatozoa under controlled *in vitro* conditions.

5. Conclusion

The possibility of generating mature gametes from PGC represents an area of investigation that provides more insight into signalling pathways of gametogenesis and reproductive dysfunction in humans. Very recent progress in work with targeted differentiation of iPSC offers tailor-made/personalized iPSC therapies also for the treatments of azoospermia in males or primary ovarian insufficiency in females [69–73]. However, problems in derivation of sperm cells and oocytes under *in vitro* conditions in human remain: the differentiation of germ cells is dependent on the somatic environment rather than the sex chromosome content of the germ cell. Therefore, the demonstration of gametogenesis from cultures of differentiating mouse ESC and iPSC suggests that "artificial" human gametes may also be obtained in this way, and the live birth of mouse pups suggests that the human cells may also be functional, although the successful demonstration of human gamete formation in this way is still awaited, but already followed by numerous ethical discussions. Nevertheless, obtaining of human viable spermatozoa and oocytes under *in vitro* conditions would for sure open in reproductive medicine new horizons to a new form of infertility treatment.

Conflict of Interests

The authors declare that there is no conflict of interests regarding the publication of this paper.

Acknowledgments

This study was supported by Serbian Ministry of Science (Grants ON175069, ON175103, and ON 175061). The authors

appreciate and acknowledge the generous assistance of Jasmin Nurkovic and Dzenan Hajrovic who contributed to the creation of figures in this paper.

References

[1] L. Bahamondes and M. Y. Makuch, "Infertility care and the introduction of new reproductive technologies in poor resource settings," *Reproductive Biology and Endocrinology*, vol. 12, no. 1, article 87, 2014.

[2] M. C. Inhrorn and P. Patrizio, "Infertility around the globe: new thinking on gender, reproductive technologies and global movements in the 21st century," *Human Reproduction Update*, 2015.

[3] J. Boivin, L. Bunting, J. A. Collins, and K. G. Nygren, "International estimates of infertility prevalence and treatment-seeking: potential need and demand for infertility medical care," *Human Reproduction*, vol. 22, no. 6, pp. 1506–1512, 2007.

[4] D. Bhartiya, I. Hinduja, H. Patel, and R. Bhilawadikar, "Making gametes from pluripotent stem cells—a promising role for very small embryonic-like stem cells," *Reproductive Biology and Endocrinology*, vol. 12, article 114, 2014.

[5] N. E. Skakkebæk, E. Rajpert-De Meyts, and K. M. Main, "Testicular dysgenesis syndrome: an increasingly common developmental disorder with environmental aspects," *Human Reproduction*, vol. 16, no. 5, pp. 972–978, 2001.

[6] M. Saitou and M. Yamaji, "Primordial germ cells in mice," *Cold Spring Harbor Perspectives in Biology*, vol. 4, no. 11, 2012.

[7] Y. Ohinata, H. Ohta, M. Shigeta, K. Yamanaka, T. Wakayama, and M. Saitou, "A signaling principle for the specification of the germ cell lineage in mice," *Cell*, vol. 137, no. 3, pp. 571–584, 2009.

[8] M. Saitou, B. Payer, U. C. Lange, S. Erhardt, S. C. Barton, and M. A. Surani, "Specification of germ cell fate in mice," *Philosophical Transactions of the Royal Society B: Biological Sciences*, vol. 358, no. 1436, pp. 1363–1370, 2003.

[9] D. H. Castrillon, B. J. Quade, T. Y. Wang, C. Quigley, and C. P. Crum, "The human VASA gene is specifically expressed in the germ cell lineage," *Proceedings of the National Academy of Sciences of the United States of America*, vol. 97, no. 17, pp. 9585–9590, 2000.

[10] E. E. Saffman and P. Lasko, "Germline development in vertebrates and invertebrates," *Cellular and Molecular Life Sciences*, vol. 55, no. 8-9, pp. 1141–1163, 1999.

[11] M. Gomperts, M. Garcia-Castro, C. Wylie, and J. Heasman, "Interactions between primordial germ cells play a role in their migration in mouse embryos," *Development*, vol. 120, no. 1, pp. 135–141, 1994.

[12] G. Seydoux and M. A. Dunn, "Transcriptionally repressed germ cells lack a subpopulation of phosphorylated RNA polymerase II in early embryos of *Caenorhabditis elegans* and *Drosophila melanogaster*," *Development*, vol. 124, no. 11, pp. 2191–2201, 1997.

[13] R. E. Boswell and A. P. Mahowald, "*tudor*, a gene required for assembly of the germ plasma in *Drosophila melanogaster*," *Cell*, vol. 43, no. 1, pp. 97–104, 1985.

[14] E. E. Capowski, P. Martin, C. Garvin, and S. Strome, "Identification of grandchildless loci whose products are required for normal germ-line development in the nematode *Caenorhabditis elegans*," *Genetics*, vol. 129, no. 4, pp. 1061–1072, 1991.

[15] L. B. Christerson and D. M. McKearin, "orb is required for anteroposterior and dorsoventral patterning during *Drosophila oogenesis*," *Genes and Development*, vol. 8, no. 5, pp. 614–628, 1994.

[16] K. Tilgner, S. P. Atkinson, A. Golebiewska, M. Stojković, M. Lako, and L. Armstrong, "Isolation of primordial germ cells from differentiating human embryonic stem cells," *Stem Cells*, vol. 26, no. 12, pp. 3075–3085, 2008.

[17] M. Ginsburg, M. H. L. Snow, and A. McLaren, "Primordial germ cells in the mouse embryo during gastrulation," *Development*, vol. 110, no. 2, pp. 521–528, 1990.

[18] A. D. Chiquoine, "The identification, origin, and migration of the primordial germ cells in the mouse embryo," *The Anatomical Record*, vol. 118, no. 2, pp. 135–146, 1954.

[19] H. Moore, R. Udayashankar, and B. Aflatoonian, "Stem cells for reproductive medicine," *Molecular and Cellular Endocrinology*, vol. 288, no. 1-2, pp. 104–110, 2008.

[20] R. Anderson, T. K. Copeland, H. Schöler, J. Heasman, and C. Wylie, "The onset of germ cell migration in the mouse embryo," *Mechanisms of Development*, vol. 91, no. 1-2, pp. 61–68, 2000.

[21] M. Saitou, S. C. Barton, and M. A. Surani, "A molecular programme for the specification of germ cell fate in mice," *Nature*, vol. 418, no. 6895, pp. 293–300, 2002.

[22] G. R. MacGregor, B. P. Zambrowicz, and P. Soriano, "Tissue non-specific alkaline phosphatase is expressed in both embryonic and extraembryonic lineages during mouse embryogenesis but is not required for migration of primordial germ cells," *Development*, vol. 121, no. 5, pp. 1487–1496, 1995.

[23] Y. I. I. Yeom, G. Fuhrmann, C. E. Ovitt et al., "Germline regulatory element of Oct-4 specific for the totipotent cycle of embryonal cells," *Development*, vol. 122, no. 3, pp. 881–894, 1996.

[24] Y. Ohinata, B. Payer, D. O'Carroll et al., "Blimp1 is a critical determinant of the germ cell lineage in mice," *Nature*, vol. 436, no. 7048, pp. 207–213, 2005.

[25] M. Yamaji, Y. Seki, K. Kurimoto et al., "Critical function of Prdm14 for the establishment of the germ cell lineage in mice," *Nature Genetics*, vol. 40, no. 8, pp. 1016–1022, 2008.

[26] U. Günesdogan, E. Magnúsdóttir, and M. A. Surani, "Primoridal germ cell specification: a context-dependent cellular differentiation event," *Philosophical Transactions of the Royal Society B: Biological Sciences*, vol. 369, no. 1657, 2013.

[27] K. Kurimoto, Y. Yabuta, Y. Ohinata, M. Shigeta, K. Yamanaka, and M. Saitou, "Complex genome-wide transcription dynamics orchestrated by Blimp1 for the specification of the germ cell lineage in mice," *Genes and Development*, vol. 22, no. 12, pp. 1617–1635, 2008.

[28] Y. Yabuta, K. Kurimoto, Y. Ohinata, Y. Seki, and M. Saitou, "Gene expression dynamics during germline specification in mice identified by quantitative single-cell gene expression profiling," *Biology of Reproduction*, vol. 75, no. 5, pp. 705–716, 2006.

[29] M. Sato, T. Kimura, K. Kurokawa et al., "Identification of PGC7, a new gene expressed specifically in preimplantation embryos and germ cells," *Mechanisms of Development*, vol. 113, no. 1, pp. 91–94, 2002.

[30] Y. Saga, "Mouse germ cell development during embryogenesis," *Current Opinion in Genetics and Development*, vol. 18, no. 4, pp. 337–341, 2008.

[31] M. Saitou, B. Payer, D. O'Carroll, Y. Ohinata, and M. A. Surani, "Blimp1 and the emergence of the germ line during development in the mouse," *Cell Cycle*, vol. 4, no. 12, pp. 1736–1740, 2005.

[32] M. Saitou, "Germ cell specification in mice," *Current Opinion in Genetics and Development*, vol. 19, no. 4, pp. 386–395, 2009.

[33] L. C. Fuentealba, E. Eivers, A. Ikeda et al., "Integrating patterning signals: Wnt/GSK3 regulates the duration of the BMP/Smad1 signal," *Cell*, vol. 131, no. 5, pp. 980–993, 2007.

[34] K. A. Molyneaux, J. Stallock, K. Schaible, and C. Wylie, "Time-lapse analysis of living mouse germ cell migration," *Developmental Biology*, vol. 240, no. 2, pp. 488–498, 2001.

[35] P. P. L. Tam and M. H. L. Snow, "Proliferation and migration of primordial germ cells during compensatory growth in mouse embryos," *Journal of Embryology and Experimental Morphology*, vol. 64, pp. 133–147, 1981.

[36] K. Tilgner, S. P. Atkinson, S. Yung et al., "Expression of GFP under the control of the RNA helicase VASA permits fluorescence-activated cell sorting isolation of human primordial germ cells," *Stem Cells*, vol. 28, no. 1, pp. 84–92, 2010.

[37] D. B. Menke, J. Koubova, and D. C. Page, "Sexual differentiation of germ cells in XX mouse gonads occurs in an anterior-to-posterior wave," *Developmental Biology*, vol. 262, no. 2, pp. 303–312, 2003.

[38] P. F. Lasko and M. Ashburner, "Posterior localization of vasa protein correlates with, but is not sufficient for, pole cell development," *Genes and Development*, vol. 4, no. 6, pp. 905–921, 1990.

[39] M. R. Bendel-Stenzel, M. Gomperts, R. Anderson, J. Heasman, and C. Wylie, "The role of cadherins during primordial germ cell migration and early gonad formation in the mouse," *Mechanisms of Development*, vol. 91, no. 1-2, pp. 143–152, 2000.

[40] R. Anderson, R. Fässler, E. Georges-Labouesse et al., "Mouse primordial germ cells lacking β1 integrins enter the germline but fail to migrate normally to the gonads," *Development*, vol. 126, no. 8, pp. 1655–1664, 1999.

[41] S.-R. Chen, Q.-S. Zheng, Y. Zhang, F. Gao, and Y.-X. Liu, "Disruption of genital ridge development causes aberrant primordial germ cell proliferation but does not affect their directional migration," *BMC Biology*, vol. 11, article 22, 2013.

[42] S. Chuma, M. Kanatsu-Shinohara, K. Inoue et al., "Spermatogenesis from epiblast and primordial germ cells following transplantation into postnatal mouse testis," *Development*, vol. 132, no. 1, pp. 117–122, 2005.

[43] K. Hayashi, S. M. C. D. S. Lopes, and M. A. Surani, "Germ cell specification in mice," *Science*, vol. 316, no. 5823, pp. 394–396, 2007.

[44] Y. Lin and D. C. Page, "Dazl deficiency leads to embryonic arrest of germ cell development in XY C57BL/6 mice," *Developmental Biology*, vol. 288, no. 2, pp. 309–316, 2005.

[45] N. Reynolds, B. Collier, V. Bingham, N. K. Gray, and H. J. Cooke, "Translation of the synaptonemal complex component Sycp3 is enhanced in vivo by the germ cell specific regulator Dazl," *RNA*, vol. 13, no. 7, pp. 974–981, 2007.

[46] N. Reynolds, B. Collier, K. Maratou et al., "Dazl binds *in vivo* to specific transcripts and can regulate the pre-meiotic translation of Mvh in germ cells," *Human Molecular Genetics*, vol. 14, no. 24, pp. 3899–3909, 2005.

[47] M. Zeng, Y. Lu, X. Liao et al., "DAZL binds to 3′UTR of Tex19.1 mRNAs and regulates Tex19.1 expression," *Molecular Biology Reports*, vol. 36, no. 8, pp. 2399–2403, 2009.

[48] M. Ruggiu, R. Speed, M. Taggart et al., "The mouse *Dazla* gene encodes a cytoplasmic protein essential for gametogenesis," *Nature*, vol. 389, no. 6646, pp. 73–77, 1997.

[49] S. Tsui, T. Dai, S. T. Warren, E. C. Salido, and P. H. Yen, "Association of the mouse infertility factor DAZL1 with actively translating polyribosomes," *Biology of Reproduction*, vol. 62, no. 6, pp. 1655–1660, 2000.

[50] H. J. Cooke, M. Lee, S. Kerr, and M. Ruggiu, "A murine homologue of the human DAZ gene is autosomal and expressed only in male and female gonads," *Human Molecular Genetics*, vol. 5, no. 4, pp. 513–516, 1996.

[51] H. Chen, M. Welling, D. Bloch et al., "DAZL limits pluripotency, differentiation, and apoptosis in developing primordial germ cells," *Stem Cell Reports*, vol. 3, no. 5, pp. 892–904, 2014.

[52] M. E. Gill, Y.-C. Hu, Y. Lin, and D. C. Page, "Licensing of gametogenesis, dependent on RNA binding protein DAZL, as a gateway to sexual differentiation of fetal germ cells," *Proceedings of the National Academy of Sciences of the United States of America*, vol. 108, no. 18, pp. 7443–7448, 2011.

[53] A. McLaren, "Primordial germ cells in the mouse," *Developmental Biology*, vol. 262, no. 1, pp. 1–15, 2003.

[54] Y. C. Hu, P. K. Nicholls, Y. Q. Soh et al., "Licensing of primordial germ cells for gametogenesis depends on genital ridge signaling," *PLoS Genetics*, vol. 11, no. 3, Article ID e1005019, 2015.

[55] B. Aflatoonian and H. D. Moore, "Germ cells from mouse and human embryonic stem cells," *Reproduction*, vol. 132, no. 5, pp. 699–707, 2006.

[56] R. L. Brinster, "Germline stem cell transplantation and transgenesis," *Science*, vol. 296, no. 5576, pp. 2174–2176, 2002.

[57] A. McLaren, "Mammalian germ cells: birth, sex, and immortality," *Cell Structure and Function*, vol. 26, no. 3, pp. 119–122, 2001.

[58] K. A. Lawson, N. R. Dunn, B. A. J. Roelen et al., "Bmp4 is required for the generation of primordial germ cells in the mouse embryo," *Genes & Development*, vol. 13, no. 4, pp. 424–436, 1999.

[59] P. P. L. Tam and D. A. F. Loebel, "Gene function in mouse embryogenesis: get set for gastrulation," *Nature Reviews Genetics*, vol. 8, no. 5, pp. 368–381, 2007.

[60] K. Hübner, G. Fuhrmann, L. K. Christenson et al., "Derivation of oocytes from mouse embryonic stem cells," *Science*, vol. 300, no. 5623, pp. 1251–1256, 2003.

[61] Y. Li, X. Wang, X. Feng et al., "Generation of male germ cells from mouse induced pluripotent stem cells *in vitro*," *Stem Cell Research*, vol. 12, no. 2, pp. 517–530, 2014.

[62] K. Hayashi, H. Ohta, K. Kurimoto, S. Aramaki, and M. Saitou, "Reconstitution of the mouse germ cell specification pathway in culture by pluripotent stem cells," *Cell*, vol. 146, no. 4, pp. 519–532, 2011.

[63] W. Wei, T. Qing, X. Ye et al., "Primordial germ cell specification from embryonic stem cells," *PLoS ONE*, vol. 3, no. 12, Article ID e4013, 2008.

[64] S. Matoba and A. Ogura, "Generation of functional oocytes and spermatids from fetal primordial germ cells after ectopic transplantation in adult mice," *Biology of Reproduction*, vol. 84, no. 4, pp. 631–638, 2011.

[65] K. Hashimoto, M. Noguchi, and N. Nakatsuji, "Mouse offspring derived from fetal ovaries or reaggregates which were cultured and transplanted into adult females," *Development Growth and Differentiation*, vol. 34, no. 2, pp. 233–238, 1992.

[66] K. Hayashi, S. Ogushi, K. Kurimoto, S. Shimamoto, H. Ohta, and M. Saitou, "Offspring from oocytes derived from in vitro primordial germ cell-like cells in mice," *Science*, vol. 338, no. 6109, pp. 971–975, 2012.

[67] K. Hayashi and M. Saitou, "Generation of eggs from mouse embryonic stem cells and induced pluripotent stem cells," *Nature Protocols*, vol. 8, no. 8, pp. 1513–1524, 2013.

[68] N. Irie, L. Weinberger, W. W. Tang et al., "SOX17 is a critical specifier of human primordial germ cell fate," *Cell*, vol. 160, no. 1-2, pp. 253–268, 2015.

[69] C. Ramathal, J. Durruthy-Durruthy, M. Sukhwani et al., "Fate of iPSCs derived from azoospermic and fertile men following Xenotransplantation to murine seminiferous tubules," *Cell Reports*, vol. 7, no. 4, pp. 1284–1297, 2014.

[70] L. Leng, Y. Tan, F. Gong et al., "Differentiation of primordial germ cells from induced pluripotent stem cells of primary ovarian insufficiency," *Human Reproduction*, vol. 30, no. 3, pp. 737–748, 2015.

[71] H. Cai, X. Xia, L. Wang et al., "In vitro and in vivo differentiation of induced pluripotent stem cells into male germ cells," *Biochemical and Biophysical Research Communications*, vol. 433, no. 3, pp. 286–291, 2013.

[72] K. Okita, T. Ichisaka, and S. Yamanaka, "Generation of germline-competent induced pluripotent stem cells," *Nature*, vol. 448, no. 7151, pp. 313–317, 2007.

[73] M. Imamura, T. Aoi, A. Tokumasu et al., "Induction of primordial germ cells from mouse induced pluripotent stem cells derived from adult hepatocytes," *Molecular Reproduction and Development*, vol. 77, no. 9, pp. 802–811, 2010.

Hindawi Publishing Corporation
Stem Cells International
Volume 2016, Article ID 5756901, 10 pages
http://dx.doi.org/10.1155/2016/5756901

Research Article

Endurance Exercise Mobilizes Developmentally Early Stem Cells into Peripheral Blood and Increases Their Number in Bone Marrow: Implications for Tissue Regeneration

Krzysztof Marycz,[1,2] Katarzyna Mierzejewska,[3] Agnieszka Śmieszek,[1,2] Ewa Suszynska,[3] Iwona Malicka,[4] Magda Kucia,[3,5] and Mariusz Z. Ratajczak[3,5]

[1]*Faculty of Biology, University of Environmental and Life Sciences, 50-375 Wroclaw, Poland*
[2]*Wroclaw Research Center EIT+, 54-066 Wroclaw, Poland*
[3]*Department of Regenerative Medicine, Medical University of Warsaw, 02-091 Warsaw, Poland*
[4]*Department of Physiotherapy, University School of Physical Education, 51-617 Wroclaw, Poland*
[5]*Stem Cell Biology Program, James Graham Brown Cancer Center, Louisville, KY 40202, USA*

Correspondence should be addressed to Krzysztof Marycz; krzysztofmarycz@interia.pl
and Mariusz Z. Ratajczak; mariusz.ratajczak@louisville.edu

Received 18 February 2015; Accepted 26 March 2015

Academic Editor: Irma Virant-Klun

Endurance exercise has been reported to increase the number of circulating hematopoietic stem/progenitor cells (HSPCs) in peripheral blood (PB) as well as in bone marrow (BM). We therefore became interested in whether endurance exercise has the same effect on very small embryonic-like stem cells (VSELs), which have been described as a population of developmentally early stem cells residing in BM. Mice were run daily for 1 hour on a treadmill for periods of 5 days or 5 weeks. Human volunteers had trained in long-distance running for one year, six times per week. FACS-based analyses and RT-PCR of murine and human VSELs and HSPCs from collected bone marrow and peripheral blood were performed. We observed that endurance exercise increased the number of VSELs circulating in PB and residing in BM. In parallel, we observed an increase in the number of HSPCs. These observations were subsequently confirmed in young athletes, who showed an increase in circulating VSELs and HSPCs after intensive running exercise. We provide for the first time evidence that endurance exercise may have beneficial effects on the expansion of developmentally early stem cells. We hypothesize that these circulating stem cells are involved in repairing minor exercise-related tissue and organ injuries.

1. Introduction

Bone marrow (BM) contains a variety of stem cells, including hematopoietic stem/progenitor cells (HSPCs), endothelial progenitor cells (EPCs), mesenchymal stem cells (MSCs), and the dormant population of stem cells from early embryonic development that have been named very small embryonic-like stem cells (VSELs) [1–3]. It has been shown that BM-derived stem cells, especially HSPCs, circulate in peripheral blood (PB) at a very low level under steady-state conditions [4]. This circulation allows the pool of stem cells maintained in BM to be spread to bones located in distant parts of the body. Another important suggested purpose of this circulation is that various types of such circulating stem cells play a role in "patrolling" peripheral tissues to prevent infections and tissue damage [5].

Evidence has also accumulated that HSPCs and EPCs expand in bone marrow (BM) in response to endurance exercise and are subsequently mobilized into peripheral blood (PB) [6–9]. Therefore, we became interested in whether the pool of BM-residing VSELs would respond in a similar way as HSPCs to endurance exercise. These cells, as demonstrated in several reports, have the ability to differentiate into cells from all three germ layers [10] and play an important role in tissue and organ rejuvenation [11], and their number positively correlates with life span in experimental animals [12].

Egress of stem cells from the BM is triggered by activation of the complement cascade, which releases important active cleavage fragments, such as the C5 component C5a, that induce granulocytes and monocytes in BM to release proteolytic enzymes that attenuate stem cell retention signals in BM niches and permeabilize the BM–PB barrier, thus facilitating the egress of stem cells [13]. The major chemoattractant for stem cells in PB is sphingosine-1-phosphate (S1P), and, in the process of mobilization, certain other factors are also involved, including α-chemokine stromal-derived factor 1 (SDF-1) [14]. It has also been proposed that mobilization of particular types of stem cells may be modulated by stem cell type-specific factors, such as vascular endothelial growth factor (VEGF), which is involved in mobilization of EPCs [15]. Our recent research demonstrated that mobilization of stem cells not only is triggered by but also correlates with activation of the complement cascade, and its activation can be easily measured in PB using commercially available ELISA assays to detect, for example, the C5b-C9 membrane attack complex (MAC) [16].

Our data confirm that HSPCs are released from BM into PB in response to physical exercise and demonstrate for the first time that, in parallel, VSELs are also mobilized. Importantly, we demonstrate a positive effect of exercise on expansion of this primitive pool of stem cells in BM. Since these small cells may differentiate into several types of cells across the three germ layers, their increase may explain, in a novel way, the positive effect of regular exercise on tissue and organ rejuvenation. Of note, a similar positive effect on this pool of cells by caloric restriction has recently been demonstrated [17]. Therefore, VSELs may be able to reconcile reported observations of a positive effect of both exercise and caloric restriction on life quality and extension of life span. However, we are aware that more direct data are necessary to fully support this novel concept.

2. Materials and Methods

2.1. Animal Care and Use. Conducted studies were approved by the II Local Ethical Committee, Environmental and Life Science University, and adhered to American College of Sports Medicine (ACSM) animal care standards.

2.2. Experimental Animals. The experiments were performed on 90 4-week-old C57BL/6 mice. Sedentary control (SED) and exercise-trained (EX) C57Bl/6 mice were housed three per cage in an ultraclean facility on ventilated racks and were provided food and water *ad libitum* during the experiment period. The animals were purchased from the Animal Laboratory House, Wroclaw Medical School, and housed in the Animal Experimental Laboratory (Wroclaw Medical School, Norwida 34, Poland). Mice were maintained on a 12 h light-dark cycle at 22 ± 0.2°C.

2.2.1. Mice Endurance Exercise on Treadmill. The animals used in this study were divided into two groups: sedentary control animals, which did not undergo physical activity ($n = 6$), and animals undergoing physical activity ($n = 6$). Animals were exercise-trained ($n = 6$) on an Exer 3/6 Treadmill (Columbus Instruments, Columbus, OH, USA) 3 d/wk (Monday, Wednesday, and Friday) for 5 wk. The mice were accustomed to the treadmill a week before training. For the 5 wk training period, mice were subjected to a progressive exercise protocol, with the training portion of the protocol beginning at 14 m/min for 45 min (wk 1) and increasing to 24 m/min for 45 min (wk 5). The training portion of the protocol was always preceded by a 10 min warm-up at 10 m/min and followed by a 5 min cool-down at 10 m/min as described previously [8]. SED mice ($n = 6$) were exposed to the treadmill and were given similar inducements on the same days as EX mice but were not subjected to training. The training intensity corresponded to 70–75% of $VO_{2\,max}$ (murine maximal oxygen uptake). Electrical stimulation was not used to encourage the animals to run.

2.2.2. Mice Exercise on Rotating Wheels. Twelve 4-week-old C57BL/6 mice were accustomed for 7 days to the presence of a rotating wheel and were subsequently subjected to controlled 45-minute exercise on rotating wheels. Standard mouse exercise wheels were attached directly to the side wall of the cages, and each wheel had a magnet directly attached. Prior to commencement of the running trial, the mice in the EX group were placed in a cage containing an exercise wheel and kept there for 7 days.

2.2.3. Human Volunteers. Twelve healthy volunteers, with a mean age of 24 ± 1 years (20–28 years old), mean body weight of 85.0 ± 3.2 kg (68.0–93.5 kg), and mean $VO_{2\,max}$ of 49.4 ± 1.6 mL kg^{-1} min^{-1} (43.3–55.1 mL, kg^{-1}, min^{-1}) were recruited to take part in the experiment. All individuals were divided into two groups: sedentary ($n = 6$) and physically active students ($n = 6$). The volunteers recruited to the sedentary group were students at Wroclaw Medical School and were not engaged in regular training. Physically active students were recruited from Wroclaw Sport Club (WKS Slask) and had trained in long-distance running for one year, with endurance training performed six times per week during the year. The regular training sessions consisted of endurance running at a distance of 9-10 km/day with a speed of 0.2 km/min, which is equivalent to ~65% of $VO_{2\,max}$. The peripheral blood from physically active students was collected 30 min after the last training session in the Faculty of Pharmacy, Medical University in Wroclaw. Following routine medical screening, subjects were advised of the purpose of the study and associated risks, and all provided written informed consent. The experimental protocol was approved by the Local Ethical Committee at Wroclaw Medical School.

2.2.4. FACS-Based Analysis of VSELs and HSPCs from Murine BM and PB. Total nucleated cells (TNCs), which were obtained from BM and PB, were subsequently stained for CD45, hematopoietic lineage markers (Lin), and Sca-1 antigen for 30 min in medium containing 2% fetal bovine serum. The following anti-mouse antibodies (BD Pharmingen) were used for staining: rat anti-CD45 (allophycocyanin/Cy7, clone 30F11), anti-CD45R/B220 (PE, clone RA-6B2), anti-Gr-1 (PE, clone RB6-8 C5), anti-T-cell receptor-$\alpha\beta$ (PE, clone H57-5970),

anti-T-cell receptor-$\gamma\delta$ (PE, clone GL3), anti-CD11b (PE, clone M1/70), anti-Ter119 (PE, clone TER-119), and anti-Ly-6A/E (also known as Sca-1, biotin, clone E13-161.7, with streptavidin conjugated to PE–Cy5). Cells were then washed, resuspended in RPMI medium with 2% fetal bovine serum, and sorted with an Influx cell sorter (BD, CA, USA). Two populations were analyzed: $Lin^-Sca\text{-}1^+CD45^-$ (VSELs) and $Lin^-Sca\text{-}1^+CD45^+$ (HSPCs) [18].

2.2.5. FACS-Based Analysis of VSELs and HSPCs from Human PB. Whole human PB was lysed in BD lysing buffer (BD Biosciences, USA) for 15 min at room temperature and washed twice in phosphate-buffered saline (PBS). A single-cell suspension was stained for lineage markers (CD2 clone RPA-2.10, CD3 clone UCHT1, CD14 clone M5E2, CD66b clone G10F5, CD24 clone ML5, CD56 clone NCAM16.2, CD16 clone 3G8, CD19 clone HIB19, and CD235a clone GA-R2) conjugated with fluorescein isothiocyanate (FITC), CD45 (clone HI30) conjugated with phycoerythrin (PE), and a combination of CD133 (CD133/1) conjugated with APC, CD34 (clone 581) conjugated with PB, CD31 (clone WM59) (APC-Cy7), and CD51 (clone 23C6 RUO) conjugated with PE-Cy7 for 30 min on ice. After washing, VSELs ($CD45^-Lin^-CD133^+$ and $CD45^-Lin^-CD34^+$ cells), HSPCs ($CD45^+Lin^-CD133^+$ and $CD45^+Lin^-CD34^+$ cells), EPCs ($CD34^+CD133^+KDR^+$), and MSCs ($CD45^-Lin^-CD31^-$ $CD51^+$) were analyzed by fluorescence-activated cell sorting (FACS, Navios, Beckman Coulter, USA). At least 10^6 events were acquired and analyzed using Kaluza software.

2.2.6. Real-Time Quantitative Reverse Transcription PCR (RQ-PCR). Total RNA was isolated from cells harvested from BM and PB from experimental and control mice by employing the RNeasy Kit (Qiagen, Valencia, CA). The RNA was reverse-transcribed with MultiScribe reverse transcriptase and oligo-dT primers (Applied Biosystems, Foster City, CA). Quantitative assessment of mRNA levels was performed by real-time reverse transcriptase polymerase chain reaction (RT-PCR) on an ABI 7500 Fast instrument employing Power SyBR Green PCR Master Mix reagent. Real-time conditions were as follows: 95°C (15 sec) followed by 40 cycles at 95°C (15 sec) and 60°C (1 min). According to melting point analysis, only one PCR product was amplified under these conditions. The relative quantity of target, normalized to the endogenous control β-2 microglobulin gene and relative to a calibrator, is expressed as fold change ($2^{-\Delta\Delta Ct}$), where ΔCt = (Ct of target gene) − (Ct of the endogenous control gene, β-2 microglobulin) and $\Delta\Delta Ct$ = (ΔCt of target gene) − (ΔCt of calibrator for the target gene). The following primer pairs were used: β2-microglobin, 5′-CAT ACG CCT GCA GAG TTA AGC A-3′ (forward) and 5′-GAT CAC ATG TCT CGA TCC CAG TAG-3′ (reverse); Oct-4, 5′-TTC TCA ATG CTA GTT CGC TTT CTC T-3′ (forward) and 5′-ACC TTC AGG AGA TAT GCA AAT CG-3′ (reverse); Sox2, 5′-GCG GAG TGG AAA CTT TTG TCC-3′ (forward) and 5′-GGG AAG CGT GTA CTT ATC CTT CT-3′ (reverse); Rex1, 5′-AGA TGG CTT CCC TGA CGG ATA-3′ (forward) and 5′-CCT CCA AGC TTT CGA AGG ATT T-3′ (reverse).

2.2.7. In Vitro Clonogenic Assays of Murine HSPCs. The growth of murine HSPCs isolated from BM and PB was evaluated by an *in vitro* clonogenic assay, as described previously [17]. Briefly, 2×10^5 BM-derived and 4×10^5 PB-derived cells were resuspended in 0.4 mL of RPMI-1640 medium and mixed with 1.8 mL of MethoCult HCC-4230 methylcellulose medium (StemCell Technologies Inc., Canada), supplemented with L-glutamine and antibiotics. Specific murine recombinant growth factors (all from R&D Systems, USA) were added. To stimulate granulocyte-macrophage colony-forming units (CFU-GM), IL-3 (20 U/mL), SCF (10 ng/mL), and GM-CSF (5 ng/mL) were used. EPO (5 U/mL), SCF (10 ng/mL), and IL-3 (20 U/mL) were used to stimulate erythrocyte burst-forming units (BFU-E). The colonies were counted under an inverted microscope after 7–10 days of culture. Each clonogenic assay was performed in quadruplicate.

2.2.8. ELISA to Detect Murine MAC, SDF-1, and VEGF. Fifty microliters of PB was taken from the vena cava of the six C57BL/6 mice and collected into Microvette EDTA-coated tubes (Sarstedt Inc., Newton, NC). The concentration of C5b-C9 (MAC) was measured by employing the commercially available, highly sensitive enzyme-linked immunosorbent assay (ELISA) kit K-ASSAY (Kamiya Biomedical Company, Seattle, WA, USA), according to the manufacturer's protocol. The concentrations of SDF-1 and VEGF were measured by employing the commercially available, highly sensitive enzyme-linked immunosorbent assay (ELISA) (R&D Systems, Europe Ltd.).

2.2.9. ELISA to Detect Human Oct-4, Sox2, and Nanog. Fifty microliters of PB was taken from the vena cava of the six C57BL/6 mice and collected into Microvette EDTA-coated tubes (Sarstedt Inc., Newton, NC). The concentrations of Oct-4, Sox2, and Nanog were measured by employing the commercially available, highly sensitive enzyme-linked immunosorbent assay (ELISA) (MyBioSource), according to the manufacturer's protocol. Results were calculated and presented as percentage fold difference.

2.2.10. Statistical Analysis. All data were analyzed using Microsoft Excel 2007 and Statistica version 7.1 software. Most results are presented as mean ± standard error of the mean. The Mann-Whitney U and Student's t-tests were used, and statistical significance was defined as $P < 0.05$.

3. Results

3.1. Short Exercise on Rotating Wheels Mobilizes VSELs into Peripheral Blood. It has been demonstrated that physical activity mobilizes HSPCs, both in mice and humans [6–9]. To address the effect of short periods of physical activity on the mobilization of VSELs, we exercised normal mice for 45 minutes on a standard rotating wheel, and immediately afterwards mice were evaluated for the numbers of VSELs and HSPCs circulating in peripheral blood (PB, Figures 1(a) and 1(b)) and activation of the complement cascade (Figure 1(c)), which, as we demonstrated previously, is crucial for egress of stem cells from the bone marrow (BM) microenvironment

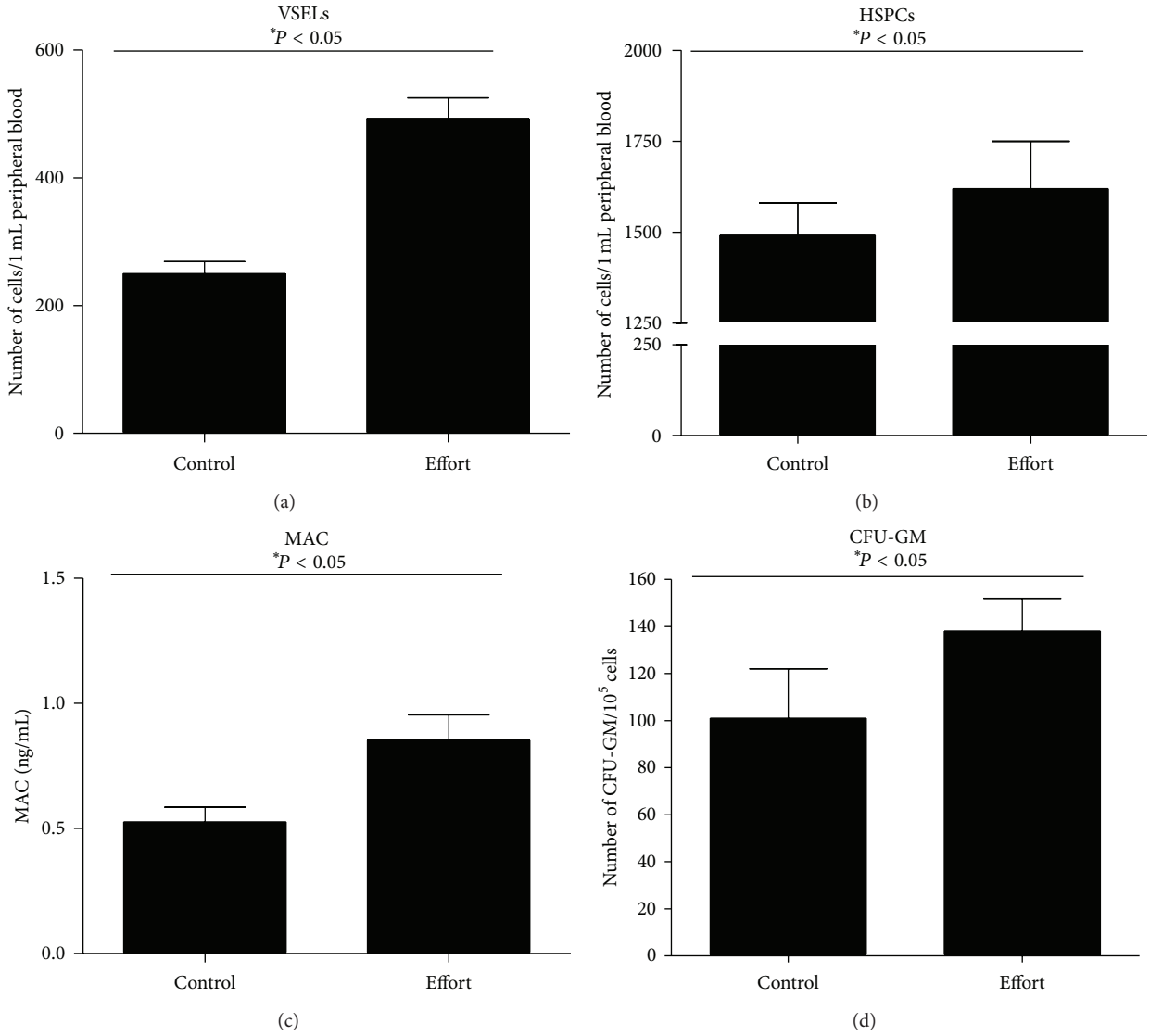

Figure 1: Effect of short (45 min) exercise on a rotating wheel on stem cell mobilization in mice. (a, b) The number of VSELs (a) and HSPCs (b) circulating in PB after 45 min of exercise on a rotating wheel (effort) compared with nonexercising mice (control). (c) Activation of the complement cascade in PB after 45 min of exercise on a rotating wheel (effort) compared with nonexercising mice (control) measured by C5b-C9 (MAC) ELISA. (d) The increase in the number of clonogenic progenitors circulating in PB after 45 min of exercise on rotating wheels (effort) compared with nonexercising mice (control) ($n = 6$ mice/group).

into PB [13–15]. We observed a significant ~2x increase in the numbers of VSELs (Figure 1(a)), increased numbers of HSPCs (Figure 1(b)), and increased numbers of clonogenic CFU-GM circulating in PB (Figure 1(d)). The increases in number of these circulating cells correlated with activation of the complement cascade, as evidenced by an increase in C5bC9 (also known as the membrane attack complex (MAC)) measured in PB plasma by ELISA (Figure 1(c)).

3.2. Prolonged Endurance Exercise on a Treadmill Increases the Number of VSELs Circulating in PB as well as Residing in BM. Subsequently, we performed an endurance exercise experiment in which mice were subjected to forced running on a treadmill for 5 days or 5 weeks. Figure 2(a) shows that forced exercise for 5 consecutive days or 5 weeks significantly enhanced the number of VSELs both circulating in PB (left panel) and residing in BM (right panel). This increase in the number of VSELs circulating in PB correlated with an increase in expression of mRNA for VSEL markers such as Oct-4, Sox2, and Nanog [11, 12] in PB mononuclear cells (Figure 2(b)). Again, mobilization of VSELs correlated with an increase in activation of the complement cascade (Figure 2(c)). A representative FACS analysis of VSELs circulating in PB in control mice as well as mice that had exercised for 5 days or 5 weeks is shown in *Supplemental Digital Content* available online at http://dx.doi.org/10.1155/2016/5756901.

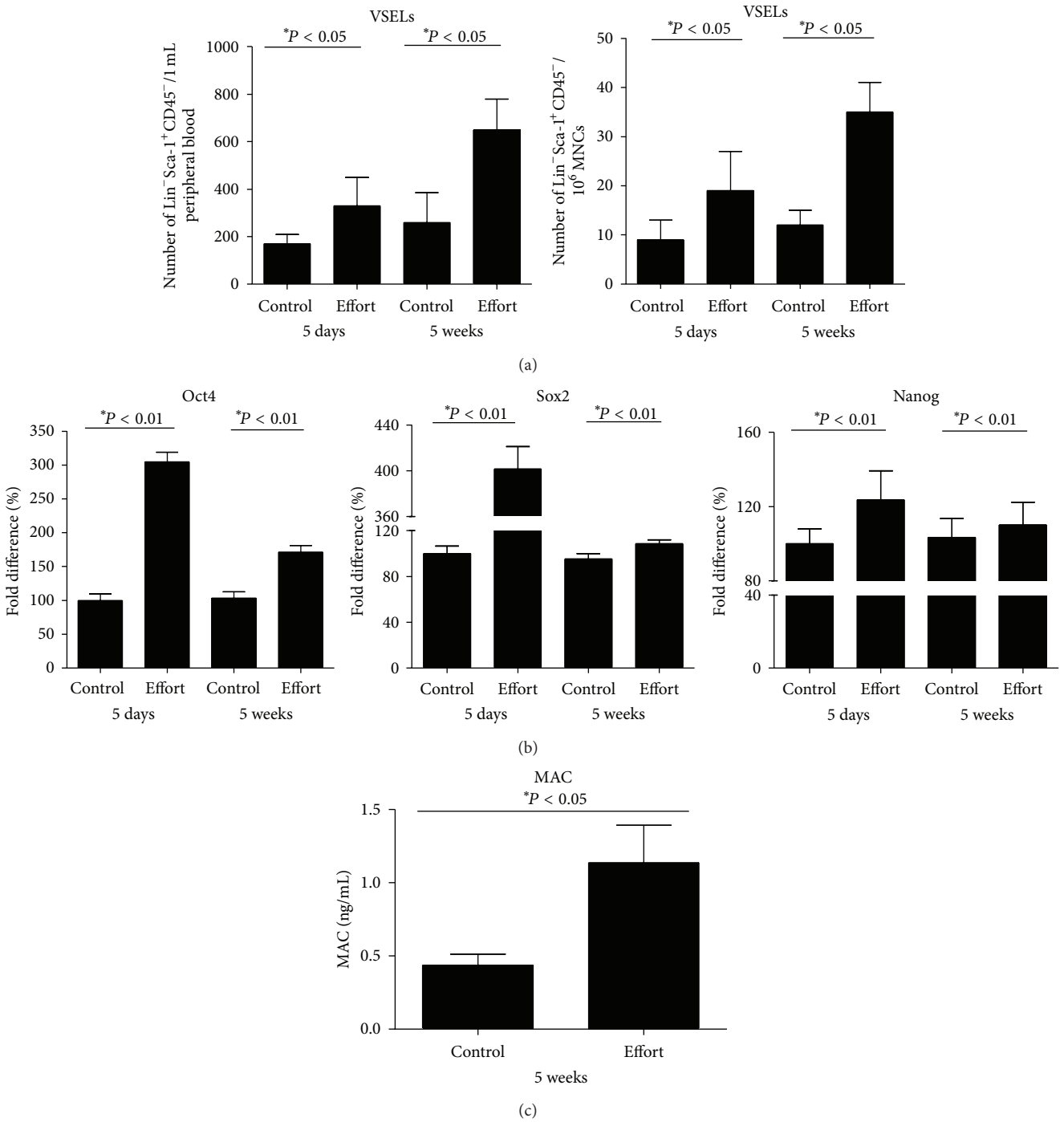

Figure 2: Effect of 5 days or 5 weeks of exercise on a treadmill on the number of VSELs in PB and BM. (a) The number of VSELs circulating in PB (left panel) and BM (right panel) after 5 days or 5 weeks of exercise on a treadmill (effort) compared with nonexercising mice (control). (b) Quantitative real-time PCR changes in expression of Oct4, Sox2, and Nanog in PB mononuclear cells after 5 days or 5 weeks of exercise on a treadmill (effort) compared with nonexercising mice (control), whose expression level was defined as 100%. (c) Activation of the complement cascade in PB measured by C5b-C9 (MAC) ELISA after 5-week exercise on a treadmill (effort) compared with nonexercising mice (control) (n = 6 mice/group).

Interestingly, these changes in the numbers of VSELs and HSPCs did not correlate with the plasma levels of SDF-1 or VEGF. In fact, we did not observe significant changes in the levels of these factors in PB between control and exercising mice (data not shown), which indicates, along with our previous observations in other models of stem cell mobilization, that if the complement cascade is activated and stem cells are released from their niches in BM due to

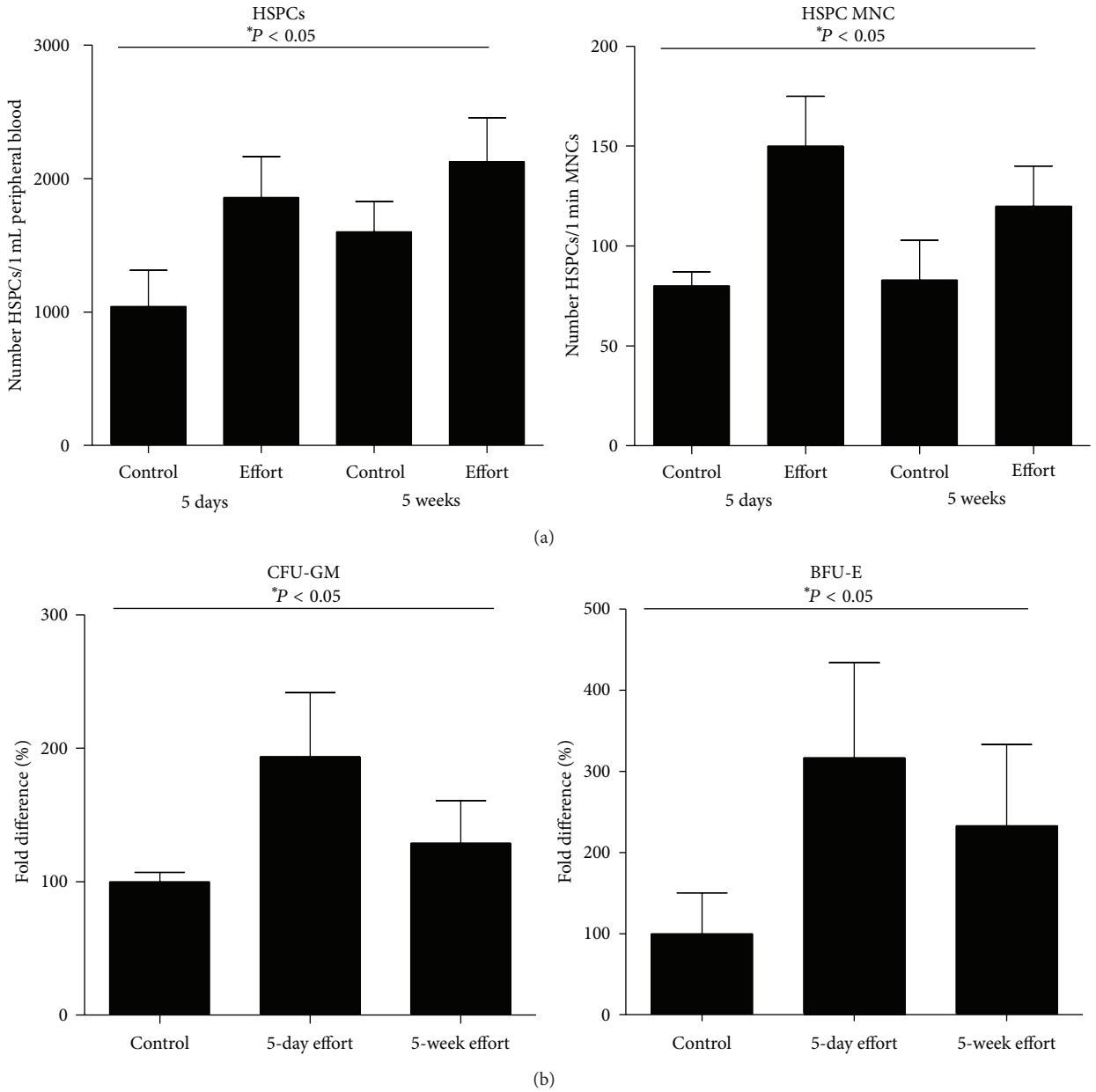

Figure 3: Effect of 5 days or 5 weeks of exercise on a treadmill on the number of HSPCs in PB and BM. (a) The number of HSPCs circulating in PB (left panel) and BM (right panel) after 5 days or 5 weeks of exercise on a treadmill (effort) compared with nonexercising mice (control). (b) The increase in the number of clonogenic progenitors (CFU-GM, left panel, and BFU-E, right panel) in BM after 5 days or 5 weeks of exercise on a treadmill (effort) compared with nonexercising mice (control) ($n = 6$ mice/group).

a proteolytic microenvironment, the plasma level of S1P is sufficiently high to induce egress of stem cells from BM into PB [14].

At the same time, we observed the predicted increase in HSPCs (Figure 3(a)), both circulating in PB (left panel) and residing in BM (right panel). An increase in the numbers of HSPCs in BM correlated with increases in the numbers of clonogenic CFU-GM and BFU-E progenitors (Figure 3(b)).

3.3. Increases in VSELs Circulating in PB after Running Exercise in Young Athletes. The effect of running exercise on increasing the numbers of HSPCs circulating in PB has already been demonstrated in humans [8]. In this study, encouraged by our murine data, we enumerated the number of small $CD34^+Lin^-CD45^-$ and $CD133^+Lin^-CD45^-$ cells circulating in PB (Figure 4(a)) that correspond to the VSEL population (left panels) in sedentary and physically active students, and, in parallel, we enumerated the number of $CD34^+Lin^-CD45^+$ and $CD133^+Lin^-CD45^+$ cells that correspond to HSPCs (right panels). Figure 4(a) shows an increase in the numbers of these cells circulating in PB in physically active subjects after running effort (90–120 min of

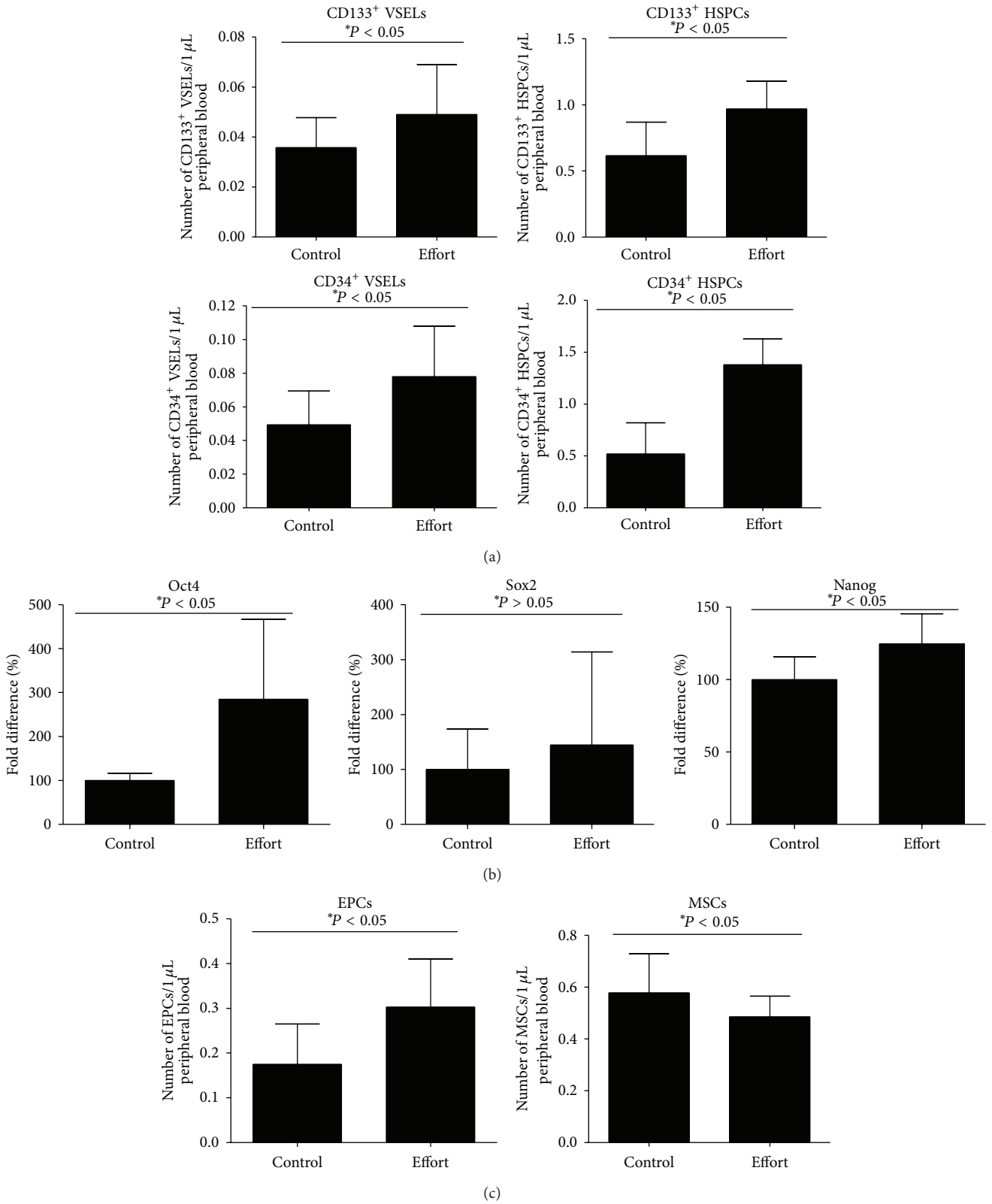

Figure 4: Effect of exercise on stem cell mobilization in healthy young volunteers. (a) The number of $CD133^+$ and $CD34^+$ VSELs (left) and $CD133^+$ and $CD34^+$ HSPCs (right) circulating in PB in young athletes after not exercising (control) or after running exercise (effort). (b) Quantitative real-time PCR changes in expression of Oct4, Sox2, and Nanog in PB mononuclear cells after running exercise (effort) compared with nonexercising subjects (control). Changes are shown compared with values detected in control volunteers (defined as 100%). (c) The number of EPCs (left panel) and MSCs (right panel) circulating in PB in young athletes after not exercising (control) or after running exercise (effort) ($n = 6$ volunteers/group).

training session corresponding to 65% of training consisting of VO_{2peak} at the distance of 8 km). An increase in the number of VSELs circulating in PB has been subsequently confirmed by ELISA to detect Oct-4, Sox2, and Nanog proteins (Figure 4(b)). We also observed a small increase in the number of EPCs but not MSCs circulating in PB (Figure 4(c)).

4. Discussion

The salient observation of this work is the positive effect of exercise on mobilization into PB and expansion in BM of VSELs. Since these small developmentally early cells may differentiate into several types of cells across all three germ layers and play a role in regeneration [10–12, 18], this observation may explain, in a novel way, the positive effect of regular exercise on tissue and organ rejuvenation.

In addition to VSELs, we have confirmed that physical activity also mobilizes HSPCs into PB. In support of this observation, there are several reports in the literature demonstrating that physical exercise mobilizes both HSPCs and EPCs into PB [6, 8, 9]. The efficacy of the mobilization may vary, depending on the intensity of the exercise protocols employed in human or animal subjects and the time of sample collection of PB or BM after exercise for enumeration of the stem cells. In our experiments, we evaluated the effect of exercise on the release of VSELs and HSPCs from BM immediately after a short, intensive run on rotating wheels or after repeated daily running exercise on a treadmill for 5 days or 5 weeks. We also evaluated the mobilization of VSELs and HSPCs in healthy young athletes after a 10 km run. It is most likely that stem cells mobilized during strenuous exercise act as "circulating paramedics," with a role in repairing microscopic damage in skeletal muscles as well as in other tissues. An important role in this phenomenon may be played by VSELs, which, in appropriate *in vivo* models, are reportedly able to differentiate into cells for different tissues, including mesenchymal precursors, lung alveolar epithelium, gametes, and endothelial cells [19–22]. *In vitro* research proved that not only does an enabling environment improve releasing and increasing cells' proliferation but both mechanical and physical stress, as well changed conditions (i.e., different culture surfaces), are associated with mechanisms controlling cellular functions. These findings provide evidence that endurance training may play modulating role in regulation of cellular functions and VSELs releasing [23–25]. This ability corresponds with several observations in which VSELs are released into PB in clinical situations of organ or tissue damage, such as heart infarct [26], stroke [27], skin burns [28], and neural tissue toxic damage [29], and the extent of their mobilization into PB may even have some prognostic value [26–28]. Our data presented herein show for the first time that not only are VSELs released from BM into PB in response to physical exercise but there is also a positive effect of exercise on the expansion of this primitive pool of stem cells in BM.

We also observed that endurance exercise increases the number of HSPCs in BM, corroborating reports from other investigators [7, 9]. Specifically, mice trained on a treadmill at progressive speeds over a 10-week period displayed increased medullary and mobilized HSPC content from 50 to 800%, depending on the HSPC type, and marrow cavity fat was reduced by 78% [6]. Interestingly, as has been demonstrated in another paper from this group, exercise promoted BM cell survival, and exercise training increased survival of recipient mice after BM transplantation with increased total blood cell reconstitution [30]. Based on this finding, endurance training has a positive prohematopoietic effect, both directly on HSPCs and on accessory cells in the BM microenvironment (e.g., stroma and osteoblasts) that provide niches for these cells [4]. Interestingly, in addition to HSPCs, it has been reported that physical activity also has a positive effect on neurogenesis in the adult and aging brain [31, 32]. Thus, physical activity has a positive effect on several types of tissue-committed stem cells in various organs, such as skeletal muscle satellite stem cells [31, 33], HSPCs [9], and neural progenitors, and several factors triggered by exercise, such as insulin-like growth factor 1, VEGF, platelet-derived growth factor, hepatocyte growth factor, and hormones such as androgens, mediate this effect [31]. On the other hand, it is very likely that other non-peptide-based regulators of cell growth, such as bioactive phosphosphingolipids and alarmines released from hypoxic tissues, may play an important role as well [31].

Mobilization into PB and expansion in BM of VSELs, which may differentiate into several types of cells across the three germ layers [10, 11, 19–22] and express several genes characteristic of early development stem cells (Oct-4, Sox-2, and Nanog), may explain, in a novel way, the positive effect of regular exercise on tissue and organ rejuvenation. Of note, there is a similar positive effect on this pool of stem cells by caloric restriction, as we demonstrated recently [16]. Therefore, VSELs may reconcile all observations reported so far of a positive effect of both exercise and caloric restriction on life quality and the extension of life span [12]. However, we are aware that more direct data are necessary to fully support this novel concept.

Mobilization of both HSPCs and VSELs correlated in our studies with activation of the complement cascade. This again confirms the pivotal role of this cascade, which is also seen as a response to infection or tissue and organ damage in triggering the mobilization process after strenuous exercise [13]. Since the complement cascade has robust cross-talk with two other evolutionarily ancient proteolytic cascades—the coagulation and fibrinolytic cascades [34]—further studies are needed to assess the role of the products of activation of these cascades on mobilization of stem cells in response to endurance exercise.

We conclude that physical activity may have a positive effect on improving life quality by directly affecting the pool of the most primitive stem cells residing in adult tissues. Future studies will be important to address the question of whether a combination of physical activity with caloric restriction and some pharmacological drugs, such as metformin, which is currently employed to increase life span, have a synergistic effect on VSELs and tissue and organ rejuvenation. These observations will be crucial for the development and optimization of novel treatment strategies

aimed at prolonging human life span, and physical activity is an important part of this.

Conflict of Interests

The authors declare that there is no conflict of interests regarding the publication of this paper.

Acknowledgments

This work was supported by NIH Grants 2R01 DK074720 and R01HL112788, the Stella and Henry Endowment, and Maestro Grant 2011/02/A/NZ4/00035 to Mariusz Z. Ratajczak. This work was supported by Wroclaw Research Centre EIT+ under Project "Biotechnologies and Advanced Medical Technologies," BioMed (POIG.01.01.02-02-003/08) financed from the European Regional Development Fund (Operational Programmed 10 Innovative Economy, 1.1.2.) to Krzysztof Marycz. The authors acknowledge the Leading National Research Centre "KNOW" (Krajowy Naukowy Ośrodek Wiodący) for covering the publication fee.

References

[1] H. Bonig and T. Papayannopoulou, "Hematopoietic stem cell mobilization: updated conceptual renditions," *Leukemia*, vol. 27, no. 1, pp. 24–31, 2013.

[2] M. Z. Ratajczak, T. Jadczyk, D. Pędziwiatr, and W. Wojakowski, "New advances in stem cell research: practical implications for regenerative medicine," *Polskie Archiwum Medycyny Wewnętrznej*, vol. 124, pp. 417–426, 2014.

[3] M. Z. Ratajczak, K. Marycz, A. Poniewierska-Baran, K. Fiedorowicz, M. Zbucka-Kretowska, and M. Moniuszko, "Very small embryonic-like stem cells as a novel developmental concept and the hierarchy of the stem cell compartment," *Advances in Medical Sciences*, vol. 59, no. 2, pp. 273–280, 2014.

[4] T. Lapidot and O. Kollet, "The brain-bone-blood triad: traffic lights for stem-cell homing and mobilization," *Hematology/the Education Program of the American Society of Hematology*, vol. 2010, pp. 1–6, 2010.

[5] S. Massberg, P. Schaerli, I. Knezevic-Maramica et al., "Immunosurveillance by hematopoietic progenitor cells trafficking through blood, lymph, and peripheral tissues," *Cell*, vol. 131, no. 5, pp. 994–1008, 2007.

[6] J. M. Baker, M. de Lisio, and G. Parise, "Endurance exercise training promotes medullary hematopoiesis," *The FASEB Journal*, vol. 25, no. 12, pp. 4348–4357, 2011.

[7] M. de Lisio and G. Parise, "Characterization of the effects of exercise training on hematopoietic stem cell quantity and function," *Journal of Applied Physiology*, vol. 113, no. 10, pp. 1576–1584, 2012.

[8] J. M. Kroepfl, K. Pekovits, I. Stelzer et al., "Exercise increases the frequency of circulating hematopoietic progenitor cells, but reduces hematopoietic colony-forming capacity," *Stem Cells and Development*, vol. 21, no. 16, pp. 2915–2925, 2012.

[9] K. A. Volaklis, S. P. Tokmakidis, and M. Halle, "Acute and chronic effects of exercise on circulating endothelial progenitor cells in healthy and diseased patients," *Clinical Research in Cardiology*, vol. 102, no. 4, pp. 249–257, 2013.

[10] A. M. Havens, H. Sun, Y. Shiozawa et al., "Human and murine very small embryonic-like cells represent multipotent tissue progenitors, in vitro and in vivo," *Stem Cells and Development*, vol. 23, no. 7, pp. 689–701, 2014.

[11] M. Kucia, M. Wysoczynski, J. Ratajczak, and M. Z. Ratajczak, "Identification of very small embryonic like (VSEL) stem cells in bone marrow," *Cell and Tissue Research*, vol. 331, no. 1, pp. 125–134, 2008.

[12] M. Z. Ratajczak, D.-M. Shin, R. Liu et al., "Very Small Embryonic/Epiblast-Like stem cells (VSELs) and their potential role in aging and organ rejuvenation—an update and comparison to other primitive small stem cells isolated from adult tissues," *Aging*, vol. 4, no. 4, pp. 235–246, 2012.

[13] H. M. Lee, W. Wu, M. Wysoczynski et al., "Impaired mobilization of hematopoietic stem/progenitor cells in C5-deficient mice supports the pivotal involvement of innate immunity in this process and reveals novel promobilization effects of granulocytes," *Leukemia*, vol. 23, no. 11, pp. 2052–2062, 2009.

[14] M. Z. Ratajczak, H. Lee, M. Wysoczynski et al., "Novel insight into stem cell mobilization-plasma sphingosine-1-phosphate is a major chemoattractant that directs the egress of hematopoietic stem progenitor cells from the bone marrow and its level in peripheral blood increases during mobilization due to activation of complement cascade/membrane attack complex," *Leukemia*, vol. 24, no. 5, pp. 976–985, 2010.

[15] S. Rafii, B. Heissig, and K. Hattori, "Efficient mobilization and recruitment of marrow-derived endothelial and hematopoietic stem cells by adenoviral vectors expressing angiogenic factors," *Gene Therapy*, vol. 9, no. 10, pp. 631–641, 2002.

[16] M. Wysoczynski, J. Ratajczak, D. Pedziwiatr, G. Rokosh, R. Bolli, and M. Z. Ratajczak, "Identification of heme oxygenase 1 (HO-1) as a novel negative regulator of mobilization of hematopoietic stem/progenitor cells," *Stem Cell Reviews and Reports*, vol. 11, no. 1, pp. 110–118, 2015.

[17] K. Grymula, K. Piotrowska, S. Słuczanowska-Głąbowska et al., "Positive effects of prolonged caloric restriction on the population of very small embryonic-like stem cells—hematopoietic and ovarian implications," *Journal of Ovarian Research*, vol. 7, no. 1, article 68, 2014.

[18] M. Suszynska, E. K. Zuba-Surma, M. Maj et al., "The proper criteria for identification and sorting of very small embryonic-like stem cells, and some nomenclature issues," *Stem Cells and Development*, vol. 23, no. 7, pp. 702–713, 2014.

[19] S. H. Kassmer, H. Jin, P.-X. Zhang et al., "Very small embryonic-like stem cells from the murine bone marrow differentiate into epithelial cells of the lung," *Stem Cells*, vol. 31, no. 12, pp. 2759–2766, 2013.

[20] S. H. Kassmer, E. M. Bruscia, P. X. Zhang, and D. S. Krause, "Nonhematopoietic cells are the primary source of bone marrow-derived lung epithelial cells," *Stem Cells*, vol. 30, no. 3, pp. 491–499, 2012.

[21] I. Virant-Klun, N. Zech, P. Rožman et al., "Putative stem cells with an embryonic character isolated from the ovarian surface epithelium of women with no naturally present follicles and oocytes," *Differentiation*, vol. 76, no. 8, pp. 843–856, 2008.

[22] D. Bhartiya, S. Kasiviswananthan, and A. Shaikh, "Cellular origin of testis-derived pluripotent stem cells: a case for very small embryonic-like stem cells," *Stem Cells and Development*, vol. 21, no. 5, pp. 670–674, 2012.

[23] M. Maredziak, K. Marycz, A. Śmieszek, D. Lewandowski, and N. Y. Toker, "The influence of static magnetic fields on canine and equine mesenchymal stem cells derived from adipose

tissue," *In Vitro Cellular & Developmental Biology: Animal*, vol. 50, no. 6, pp. 562–571, 2014.

[24] A. Donesz-Sikorska, K. Marycz, A. Śmieszek, J. Grzesiak, K. Kaliński, and J. Krzak-Roś, "Biologically active oxide coatings, produced by the sol-gel method on steel implant," *Przemysł Chemiczny*, vol. 92, no. 6, pp. 1110–1116, 2013.

[25] K. Marycz, J. Krzak-Roś, A. Śmieszek, J. Grzesiak, and A. Donesz-Sikorska, "Effect of oxide materials synthesized with sol–gel method on adhesion of mesenchymal stem cells," *Przemysl Chemiczny*, vol. 92, no. 6, pp. 1000–1003, 2013.

[26] W. Wojakowski, M. Tendera, M. Kucia et al., "Mobilization of bone marrow-derived Oct-4+ SSEA-4+ very small embryonic-like stem cells in patients with acute myocardial infarction," *Journal of the American College of Cardiology*, vol. 53, no. 1, pp. 1–9, 2009.

[27] E. Paczkowska, M. Kucia, D. Koziarska et al., "Clinical evidence that very small embryonic-like stem cells are mobilized into peripheral blood in patients after stroke," *Stroke*, vol. 40, no. 4, pp. 1237–1244, 2009.

[28] J. Drukała, E. Paczkowska, M. Kucia et al., "Stem cells, including a population of very small embryonic-like stem cells, are mobilized into peripheral blood in patients after skin burn injury," *Stem Cell Reviews and Reports*, vol. 8, no. 1, pp. 184–194, 2012.

[29] K. Grymula, M. Tarnowski, K. Piotrowska et al., "Evidence that the population of quiescent bone marrow-residing very small embryonic/epiblast-like stem cells (VSELs) expands in response to neurotoxic treatment," *Journal of Cellular and Molecular Medicine*, vol. 18, no. 9, pp. 1797–1806, 2014.

[30] M. de Lisio, J. M. Baker, and G. Parise, "Exercise promotes bone marrow cell survival and recipient reconstitution post-bone marrow transplantation, which is associated with increased survival," *Experimental Hematology*, vol. 41, no. 2, pp. 143–154, 2013.

[31] F. MacAluso and K. H. Myburgh, "Current evidence that exercise can increase the number of adult stem cells," *Journal of Muscle Research and Cell Motility*, vol. 33, no. 3-4, pp. 187–198, 2012.

[32] K. Fabel, S. A. Wolf, D. Ehninger, H. Babu, P. Leal-Galicia, and G. Kempermann, "Additive effects of physical exercise and environmental enrichment on adult hippocampal neurogenesis in mice," *Frontiers in Neuroscience*, vol. 3, article 50, 2009.

[33] T. Snijders, L. B. Verdijk, J. S. Smeets et al., "The skeletal muscle satellite cell response to a single bout of resistance-type exercise is delayed with aging in men," *Age*, vol. 36, no. 4, p. 9699, 2014.

[34] S. Borkowska, M. Suszynska, K. Mierzejewska et al., "Novel evidence that crosstalk between the complement, coagulation and fibrinolysis proteolytic cascades is involved in mobilization of hematopoietic stem/progenitor cells (HSPCs)," *Leukemia*, vol. 28, pp. 2148–2154, 2014.

Hindawi Publishing Corporation
Stem Cells International
Volume 2016, Article ID 5096596, 13 pages
http://dx.doi.org/10.1155/2016/5096596

Review Article

Novel Action of FSH on Stem Cells in Adult Mammalian Ovary Induces Postnatal Oogenesis and Primordial Follicle Assembly

Deepa Bhartiya,[1] Seema Parte,[1] Hiren Patel,[1] Kalpana Sriraman,[1] Kusum Zaveri,[2] and Indira Hinduja[2]

[1] *Stem Cell Biology Department, National Institute for Research in Reproductive Health, JM Street, Parel, Mumbai 400 012, India*
[2] *PD Hinduja Hospital, Veer Savarkar Marg, Mahim, Mumbai 400016, India*

Correspondence should be addressed to Deepa Bhartiya; deepa.bhartiya@yahoo.in

Received 4 May 2015; Accepted 8 June 2015

Academic Editor: Mariusz Z. Ratajczak

Adult mammalian ovary has been under the scanner for more than a decade now since it was proposed to harbor stem cells that undergo postnatal oogenesis during reproductive period like spermatogenesis in testis. Stem cells are located in the ovary surface epithelium and exist in adult and menopausal ovary as well as in ovary with premature failure. Stem cells comprise two distinct populations including spherical, very small embryonic-like stem cells (VSELs which express nuclear OCT-4 and other pluripotent and primordial germ cells specific markers) and slightly bigger ovarian germ stem cells (OGSCs with cytoplasmic OCT-4 which are equivalent to spermatogonial stem cells in the testes). These stem cells have the ability to spontaneously differentiate into oocyte-like structures *in vitro* and on exposure to a younger healthy niche. Bone marrow may be an alternative source of these stem cells. The stem cells express FSHR and respond to FSH by undergoing self-renewal, clonal expansion, and initiating neo-oogenesis and primordial follicle assembly. VSELs are relatively quiescent and were recently reported to survive chemotherapy and initiate oogenesis in mice when exposed to FSH. This emerging understanding and further research in the field will help evolving novel strategies to manage ovarian pathologies and also towards oncofertility.

1. Introduction

The central dogma of reproductive biology that ovary has fixed number of follicles at birth or shortly afterwards was first put forth by Heinrich Waldeyer, a German anatomist-embryologist in 1870. It stated that a woman is born with a finite and nonrenewing pool of germ cells whose numbers decline progressively with age, affecting ovarian function and sudden demise of follicles with age results in menopause. Besides the fixed number of follicles in the ovary, it is also a well-established fact that ovarian function is modulated by pituitary gonadotropins follicle stimulating hormone (FSH) and luteinizing hormone (LH). FSH acts on growing follicles through its receptors (FSHR) located on the granulosa cells and initial follicle growth particularly in women is gonadotropin independent [1]. LH is responsible for ovulation and synthesis of steroid hormones.

The concept of biological clock of ovary and that a female is born with a fixed number of follicles was challenged in 2004 by Professor Tilly and his group who rekindled the very essence of the topic of postnatal oogenesis and presented evidence that the rate of loss of oocytes in mice ovary due to atresia and ovulation were indeed counterbalanced by a mechanism which maintains a constant count of immature oocytes [2]. These observations favored the concept of ovarian stem cells and postnatal oogenesis and several groups were drawn into this area of research.

First major step was to prove the presence of stem cells in the ovary and their characterization, followed by how they function under normal conditions leading to postnatal oogenesis, and how they result in various pathologies like ovarian failure, menopause, and cancer. Also, it became pertinent to study whether stem cells present in the adult ovary could be manipulated to regain ovarian function under

certain specific conditions, for example, after oncotherapy in cancer survivors. Postnatal follicular regeneration in mouse ovary [3] and ovary surface epithelium (OSE) as a source of germ cells during fetal stage ovary was reported in the past [4, 5]. It was also proposed that OSE is the active site of origin for neoplasms and almost 90% of ovarian cancers arise from the OSE [6]. Various other methods like label retaining cells, Hoechst dye-excluding side population confirmed the presence of stem/ progenitor cells [7–9] and a novel population of stem-like cells coexpressing Lin28 and Oct-4 in epithelial ovarian cancers have been reported [10]. Flesken-Nikitin et al. [11] showed the presence of stem cells in the OSE in the hilum region as the niche for ovarian cancer cells.

Present review provides a brief overview of our current understanding on ovarian stem cells, their origin and characterization, and how they are implicated in postnatal oogenesis along with an interesting advance from the authors' laboratory that they express follicle stimulating hormone receptors (FSHR) and are modulated by FSH to undergo self-renewal, clonal expansion to form germ cell nests, proliferation, differentiation, and primordial follicle (PF) assembly in adult ovary. It also touches upon subtle technical issues that should be kept in mind to arrive at a consensus on existence of stem cells in adult mammalian ovary.

2. Stem Cells, Progenitors, and Germ Cell Nests in Adult Mammalian Ovary

Ovary is a dynamic organ lined by a single layer of cuboidal surface epithelial cells also called germinal epithelium which is relatively less differentiated and uncommitted and express epithelial and mesenchymal markers under normal conditions. OSE is involved in follicular rupture, release of the mature oocyte, subsequent ovarian remodeling, and repair of follicle walls and hence becomes a discontinuous layer in case of anovulatory cycles anovulatory cycles, polycystic ovarian syndrome and during menopause and in sclerotic ovaries [6]. First proof for the presence of ovarian stem cells in OSE was given by Tilly's group [2] when they showed MVH and BrdU coexpressing cells in the OSE along with meiotic markers (Scp3, Spo11, and Dmc1) and that on grafting wild type ovary in GFP mice led to formation of follicles with GFP oocyte enclosed by wild-type granulosa cells. Thereafter various research groups became involved and investigated ovarian stem cells with the help of varying approaches like immunomagnetic antibody and flow cytometry based cell sorting strategies (MACS and FACS), *in vitro* culture and differentiation of ovarian stem cells, genetic lineage tracing, and transplantation experiments, suggesting that the follicle pool is not a static but indeed a dynamic population of differentiating and regressing structure in adult mice and human ovary. Main highlights of various studies that were undertaken to show the presence of stem cells in adult ovaries have been compiled in Table 1 [13–35].

As evident, Tilly's and Bukovsky's groups were the first to report stem cells in adult mammalian OSE. Bukovsky's group reported spontaneous differentiation of oocyte-like structures *in vitro* from OSE cells for the first time and both the groups reported beneficial effect of bone marrow cells on ovarian function. Tilly's and Virant-Klun's groups detected stem cells in menopausal and POF women. The former group could restore ovarian function by providing a young niche in mice while the latter group demonstrated spontaneous differentiation of human OSE cells to oocyte-like structures *in vitro*. Using a handful of characteristic markers (meiotic and germ cells, PGCs, and primordial oocyte specific), Tilly's group has been successful to demonstrate PF assembly in cortical tissue slices *in vitro* [21]. Virant-Klun's group has extensively characterized the ovarian stem cells and reported the presence of spherical, very small 4 μm cells which express pluripotent and PGC specific markers [36]. Johnson et al. [18] also detected PGCs (Stella, Fragilis, and Nobox) and germ cells (Oct4, Mvh, and Dazl) specific transcripts in bone marrow.

Our group initially obtained institutional ethical approval to use human ovarian cortical tissue to establish methods to cryopreserve PF for cancer patients. But few samples analyzed by us revealed nil follicles/germ cells in the ovarian tissue. Then with technical help from Professor Bukovsky, we initially reported that adult rabbit, sheep, monkey, and human OSE harbored stem cells and for the first time demonstrated that there existed two distinct populations of stem cells in OSE including (i) spherical cells which were smaller than RBCs in agreement with Virant-Klun's observations and (ii) a slightly bigger population of "progenitors." Immunolocalization studies showed that the smaller cells were pluripotent and expressed nuclear OCT-4, whereas the bigger ones expressed cytoplasmic OCT-4 (Figure 1). A careful survey of literature showed that Professor Ratajczak's group had reported similar cells termed very small embryonic-like stem cells (VSELs) in various adult tissues [37]. Thus we realized that the smaller cells with nuclear OCT-4 were the VSELs and when they entered differentiation, nuclear OCT-4 was no longer required, shifted to cytoplasm, and eventually degraded as cells became more committed. The cells with cytoplasmic OCT-4 were termed ovarian germ stem cells (OGSCs) and appear to be similar to the oogonial stem cells (OSCs) reported by Tilly's group. We have reported similar VSELs in adult mammalian testes [38] as well and the OGSCs (OSCs) are equivalent to SSCs in the testes [12, 39, 40].

A careful examination of scraped OSE cells shows the presence of VSELs, OGSCs, and also occasional germ cell nests (GCN) which are formed by rapid, clonal expansion with incomplete cytokinesis of OGSCs. The detailed protocols to study these cells (VSELs, OGSCs, and GCN) by mechanical scraping of bigger sized mammalian ovaries and after enzymatic digestion of mouse OSE were recently described by us [12]. These cell types can also be successfully scraped from a sheep ovary fixed overnight in neutral buffered formalin (Figure 1(a)). Presence of germ cell markers in bone marrow and expression of PGC markers on these stem cells hints to the presence of a common population of VSELs in bone marrow/peripheral blood and ovary as suggested by Ratajczak's group [41].

Presence of stem cells and GCN in adult ovary contradicts the report by Lei and Spradling [42] and technical reasons resulting in the discrepancy have been discussed [34].

Table 1

Group	Year	Studies conducted	References
Jonathan L. Tilly	2004	They challenged the central dogma of fixed number of follicles. Cells in ovary surface epithelium expressed SCP3, MVH-BrdU. Bone marrow and peripheral blood were shown as a source of germ cells. Germ line markers were found in the bone marrow.	Johnson et al. [2]
	2005	Bone marrow and peripheral blood transplantation restored oocyte production in chemoablated (and also after total body irradiation) wild-type and mutant mice. Bone marrow transplantation in chemoablated ovaries resulted in formation of oocytes, but surprisingly from the endogenous cells.	Johnson et al. [18]
	2007	Aged mouse ovaries harbor stem cells expressing Stra8 and Dazl but no oocytes. These stem cells retain the ability to undergo neo-oogenesis when grafted in young wild type mice.	Lee et al. [19]
	2009	Germ line stem cells were isolated from adult mouse ovary and human cortical tissue by FACS using DDX4 as a marker. These cells could be expanded for months *in vitro* and spontaneously differentiated into 35–50 μm oocytes. Human cells from reproductive age group were tagged with GFP and injected into human cortical tissue and resulted in GFP positive oocytes in immunodeficient mice.	Niikura et al. [20]
	2012	They described and validated FACS based protocol to isolate rare mitotically active germline stem cells from adult mouse ovaries and human ovarian cortical tissue, which upon further passage could give rise to 35–50-μm oocytes *in vitro* validated by various methods, as well as generated oocytes *in vivo* upon xenotransplantation into immunodeficient female mice.	White et al. [21]
	2013	Gene expression profiles of Ddx4 sorted OSCs and cultured OSCs, ESCs, PGCs, and SSCs were compared. OSCs expressed germline markers but distinct signatures as compared to that of PGCs and SSCs. *In vitro* culture of OSCs triggered pluripotency gene expression similar to PGCs	Imudia et al. [22]
	2013	Bone morphogenetic protein 4 promotes mammalian oogonial stem cell differentiation and results in increased expression of meiosis specific markers (Stra8, Msx1, and Msx2) via Smad 1/5/8 activation	Park et al. [23]
Antonin Bukovsky	2004	Mesenchymal cells in tunica albuginea are bipotent progenitors which can differentiate into both granulosa and germ cells. They studied adult human ovarian tissue and concluded that granulosa cells originate in the OSE by epithelial-mesenchymal transition.	Bukovsky et al. [24]
	2005	Cultured adult human OSE cells in medium without phenol red led to development of granulosa-like cells and epithelial and neural and mesenchymal type cells. When OSE cells were cultured in the presence of phenol red medium, it resulted in the formation of >180 μm oocyte-like structures which exhibited germinal vesicle breakdown, polar body, and surface expression of zona pellucida proteins.	Bukovsky et al. [25]
	2008	Described neo-oogenesis and follicular assembly in adult ovary. Observed expression of meiotic entry synaptonemal complex protein 3 (SCP3)—a marker for meiosis in OSE.	Bukovsky et al. [26]
	2012	Follicular renewal in rodents is initiated by bone marrow derived cells related to the immune system, which interact with OSE cells in normal adult rats or medullary sex cord cells in adult neonatally estrogenized rats lacking OSE.	Bukovsky and Caudle [27]

Table 1: Continued.

Group	Year	Studies conducted	References
Irma Virant-Klun	2008	OSE cells from 20 postmenopausal and 5 women with premature ovarian failure were used to isolate putative stem cells. Small round cells with a bubble-like structure, 2 to 4 μm in size, were detected which expressed pluripotent markers SSEA4, Oct-4, Nanog, Sox-2, and c-kit.	Virant-Klun et al. [28]
	2009	Ovarian tissue from postmenopausal women was cultured to study oogenesis *in vitro*. Small round cells with a bubble-like structure and with a diameter from 2 to 4 μm were isolated from OSE. They expressed pluripotent markers including SSEA-4, Oct-4, Nanog, Sox-2, and c-kit. These cells on culture proliferated and formed embryoid body-like structures but did not form teratoma in SCID mice. Cells grew in size and reached a diameter of approximately 95 μm and expressed Oct-4, c-kit, VASA, and ZP2. Few expressed a zona pellucida-like structure, germinal vesicle, and polar body-like structures. Parthenote embryos were also observed which expressed Oct-4, Sox-2, and Nanog and were normal for chromosomes X, 13, 16, 18, 21, and 22.	Virant-Klun et al. [29]
	2011	Small, round SOX-2 positive stem cells were detected in the OSE of women with premature ovarian failure and high FSH and LH. On culture with follicular fluid to provide ovarian niche, primitive oocyte-like structures and cell clusters were observed which were alkaline phosphatase positive and expressed pluripotent markers SOX-2 and SSEA-4. Single oocyte-like cells expressed genes *OCT-4A, SOX-2, NANOG, NANOS, STELLA, CD9, LIN28, KLF4, GDF3,* and *MYC*, characteristic for pluripotent stem cells.	Virant-Klun et al. [30]
	2013	Small putative SSEA-4 positive stem cells up to 4 μm in size were isolated by FACS and MACS from cultures of human cortical tissue. They expressed pluripotent markers but were relatively low compared to hES cells. In addition, they expressed genes of primordial germ cell lineages VASA, PRDM1, PRDM14, and DPPA3.	Virant-Klun et al. [31, 32]
	2013	Ovarian cell cultures could be established from cortical biopsies and the cells expressed pluripotent markers (alkaline phosphatase, SSEA-4, OCT-4, SOX-2, NANOG, LIN28, and STELLA), germinal lineage (DDX4/VASA) and multipotency (M-CAM/CD146, Thy-1/CD90, and STRO-1). These cells were SSEA-4 positive, spherical in shape, and small up to 4 μm in size. These cells could be differentiated into 3 germ layers but did not form teratoma in immunodeficient mice.	Stimpfel et al. [33]

Table 1: Continued.

Group	Year	Studies conducted	References
Deepa Bhartiya	2011	Two distinct populations of stem cells were detected in OSE isolated from adult rabbit, monkey, sheep, and human ovaries. Spherical cells with high N/C ratio were smaller than RBCs in size and expressed nuclear OCT-4 and SSEA-4 and the bigger cell population expressed cytoplasmic OCT-4 and minimal SSEA-4. Oct-4, Oct-4A, Nanog, Sox-2, TERT, and Stat-3 were detected in human and sheep OSE cells by RT-PCR. The stem cells underwent spontaneous differentiation into oocyte-like structures, parthenote-like structures, embryoid body-like structures, cells with neuronal-like phenotype, and embryonic stem cell-like colonies, whereas the epithelial cells transformed into mesenchymal phenotype by epithelial-mesenchymal transition. Oocyte-like structures expressed c-KIT, DAZL, GDF-9, VASA, and ZP4.	Parte et al. [13]
	2012	PMSG (5IU) was observed to exert direct proliferative effect on OSE and increased expression of FSHR and PCNA. OSE appeared multilayered at several positions and MVH positive germ cell nests and cohort of newly formed PF were visualized along with increased expression of Oct-4A, Nanog, Scp-3, Oct-4B, and Mvh. Study provided first evidence that stem cells activity in OSE and neo-oogenesis is modulated by FSH in adult mammalian ovaries. Similar findings were also observed in normal estrus cycle coinciding with the proestrus peak of FSH and numbers of cohorts along the surface of the ovary were increased after PMSG treatment.	Bhartiya et al. [15]
	2013	Effect of FSH and bFGF was studied on human and marmoset ovarian cortical tissues in organ culture format. Ovarian stem cells were found to be released on the culture inserts and retained the potential to spontaneously differentiate into oocyte-like structures in extended cultures. Both FSH and bFGF induced proliferation of OSE along with increased expression of gene transcripts specific for pluripotent stem cells (Oct-4A and Nanog) suggestive of VSELs and early germ cells (Oct-4, c-Kit, and Vasa) suggestive of OGSCs and follicular transition (oocyte-specific Gdf-9 and Lhx8, and granulosa cell specific Amh).	Parte et al. [17]
	2013	Effect of FSH was studied on sheep stem cells in OSE *in vitro*. FSH increased stem cells self-renewal and clonal expansion evident by the appearance of stem cell clusters. FSH receptors were expressed on ovarian stem cells whereas the epithelial cells were distinctly negative. An increase in R3 mRNA transcripts was noted after 3 hrs of FSH treatment and was reduced to basal levels by 15 hrs, whereas R1 transcript expression remained unaffected. FSHR and OCT4 were immunolocalized in nuclei of stem cells and showed nuclear or ooplasmic localization in oocytes of primordial follicles and in cytoplasm of granulosa cells in growing follicles. Thus FSH appears to modulate ovarian stem cells activity via FSH-R3 to undergo potential self-renewal, clonal expansion as "cysts," and differentiation into oocytes. OCT-4 and FSHR proteins (required initially to maintain pluripotent state of VSELs and for FSH action, respectively) gradually shift from nuclei to cytoplasm of developing oocytes and are later possibly removed by surrounding granulosa cells as the oocyte prepares itself for fertilization.	Patel et al. [14]
	2013	A genetic lineage tracing study which failed to detect stem cells and germ cell clusters in adult mouse ovary was challenged. Cysts were observed and confocal microscopy imaging confirmed cytoplasmic continuity amongst the cells comprising the cysts. Germ cell nests expressed PCNA and SSEA-4 suggestive of their germ cell characteristic and rapid mitotic division.	Bhartiya et al. [34]
	2014	Ovarian stem cells and germ cell clusters were enriched by immunomagnetic sorting using SSEA-4 and were further characterized. Differential expression of markers specific for pluripotent VSELs (nuclear OCT-4A, SSEA-4, and CD133), OGSCs (cytoplasmic OCT-4) primordial germ cells (FRAGILIS, STELLA, and VASA), and germ cells (DAZL, GDF-9, and SCP-3) were studied. Within one week of culture, stem cells became bigger in size, developed abundant cytoplasm, differentiated into germ cells, revealed presence of Balbiani body-like structure (mitochondrial cloud), and exhibited characteristic cytoplasmic streaming.	Parte et al. [35]
	2015	Study was undertaken to investigate stem cells in adult mouse ovary, the effect of chemotherapy on them, and their potential to differentiate into germ cells. VSELs in adult mouse ovary were SCA-1+/Lin−/CD45− and positive for nuclear OCT-4, Nanog, and SSEA-1. VSELs survived chemotherapy and OSE culture of chemoablated ovary OSE resulted in appearance of proliferating germ cell clusters and MVH and GDF9 positive oocyte-like structures spontaneously differentiated by day 6. FSH exerted a direct stimulatory action on the OSE and induced stem cell proliferation and differentiation into premeiotic germ cell clusters during intact chemoablated ovary culture. PMSG treatment to chemoablated mice resulted in self-renewal of VSELs (LIN−/CD45−/SCA1+) that were 0.02 ± 0.008% in normal ovary and 0.03 ± 0.017% in chemoablated ovary and PMSG treatment to chemoablated ovary increased VSELs to 0.08 ± 0.03%.	Sriraman et al. [16]

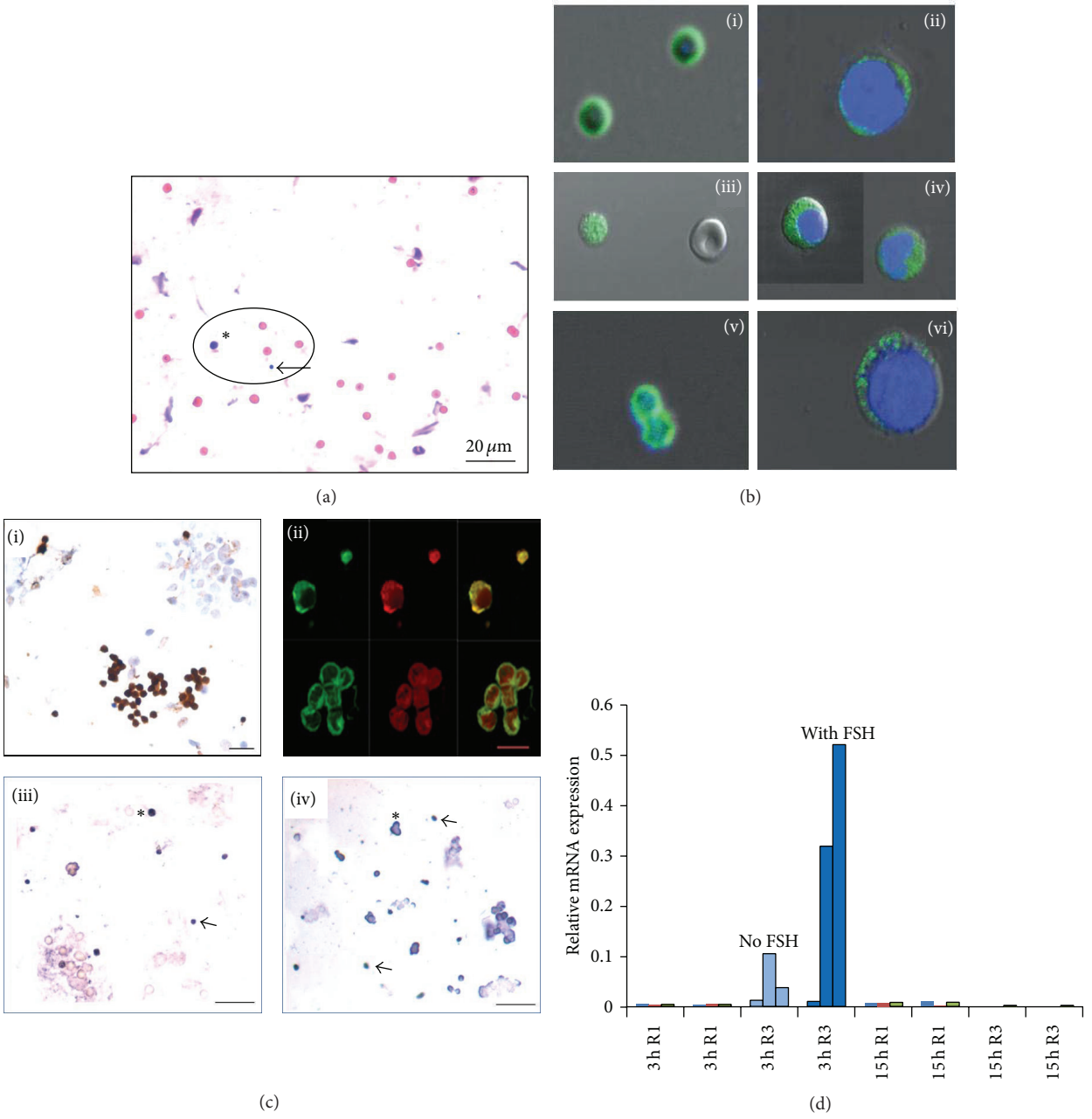

Figure 1: FSH-FSHR3-stem cell interaction in ovary surface epithelium. (a) H&E stained sheep OSE smear. Two distinct populations of stem cells (encircled) including VSELs (arrow) which are smaller than the red blood cells and slightly bigger OGSCs (asterix) are clearly visualized even after gently scraping sheep ovary fixed overnight in neutral buffered formalin. Red blood cells and epithelial cells are also clearly visualized [12]. (b) (i)–(vi) Characterization of ovarian stem cells using pluripotent OCT-4 and SSEA4 markers. Smaller VSELs express nuclear OCT-4 and cell surface SSEA4 whereas slightly bigger OGSCs express cytoplasmic OCT-4 and minimal SSEA4. Note the VSELs do not stain with DAPI [13]. (c) (i) Sheep OSE smear immunostained with FSHR antibody. Note epithelial cells are negative whereas the stem cells exhibit distinct positive stain. (ii) Confocal microcopy localization of FSHR on VSELs and OGSCs and on a germ cell nest. (iii)-(iv) *In situ* hybridization of FSHR on ovarian stem cells after FSH treatment using oligo probes specific for FSHR1 and FSHR3, respectively. Note active transcription of FSHR3 mRNA in the cytoplasm of stem cells after FSH treatment whereas FSHR1 is expressed in the stem cells and the expression is not affected by FSH treatment. (d) qRT-PCR analysis of FSHR1 and FSHR3 after 3 and 15 h of FSH treatment. Note that only FSHR3 levels are increased transiently after 3 and return to basal levels by 15 h. (c) and (d) Panels show earlier published from 3 different experiments represented individually by Patel et al. [14]. Please refer to the cited references for further details.

Similarly, we also explained as to why Byskov et al. [43] failed to detect stem cells and oogonia in adult human ovary [44]. Zhang and coworkers have published two papers [45, 46] wherein they contradict the presence of stem cells in adult ovary by using elegant lineage tracing studies. We had earlier discussed [34] technical issues related to use of MVH for lineage tracing studies by Zhang et al. [45]. Zhang et al. [46] did not acknowledge our comments, rather discussed the study by Lei and Spradling [42], and have performed further lineage tracing studies to generate evidence against presence of stem cells in adult ovary. But technology can never overtake biology and we have further discussed the study by Zhang et al. [46] in context of our work [16] below.

Yuan et al. [47] have also extensively studied stem cells in monkey ovary by different approaches like flow cytometry, immunolocalization, Western blot, and RT-PCR with completely negative results using testes and fetal ovary tissues as positive control. One thing that needs to be kept in mind is that the rate of turnover of stem cells in testis and fetal ovary is extremely high compared to production of 1-2 oocytes per cycle in adult ovary in women and monkeys and that absence of evidence is not evidence for absence. It is mentioned in the protocols followed in the study that ovarian filtrate was spun at 1200 rpm for further use. We know by our experience that ovarian VSELs and OGSCs do not pellet down when spun at a speed of 1200 rpm; rather we always isolate them by spinning at a speed of 1000 g. Using this speed we have successfully detected 3–5 μm sized VSELs in adult mouse and sheep ovary as LIN−/CD45−/SCA1+ in mice and as OCT4+ in sheep. We could detect 0.02 + 0.008% in normal mouse ovary as LIN−/CD45−/SCA1+ [16]. Similarly 1.26 ± 0.19% of (2–4 μm) and 6.86 ± 0.5% of (4–9 μm) cells expressing OCT-4 were detected in sheep OSE cell suspension [12]. Thus we need to sharpen the technology rather than doubt the biology. Moreover, if the study [47] used as mentioned, one out of every 20 sections (each 5 μm thick), it is very likely ovarian VSELs being 3–5 μm will inadvertently get missed. We still prefer to study ovarian stem cells in carefully scraped OSE cell smears rather than on sections and for flow cytometry/RNA extraction studies care is taken to spin the cells at 1000 g (rather than the standard 1200 rpm speed). Also extracting RNA from whole ovary, to detect few stem cells in OSE, may not be a good approach; rather RNA should be extracted from cortical tissue pieces or scraped OSE cells (various strategies to enrich stem cells).

3. Characterization of Ovarian Stem Cells

VSELs are considered to be the descendants of embryonic epiblast derived pluripotent primordial germ cells (PGCs) that, while migrating along the dorsal mesentery to the genital ridge, also gets deposited in various somatic tissues [41]. The VSELs detected in both adult ovaries and testes [36, 40, 48, 49] are probably the primordial germ cells that survive in adult gonads in few numbers. Similar concept that PGCs may survive in adult ovary was put forth by de Felici's group [50] and recently they supported Ratajczak's views that possibly there exists a mixing up of PGCs and hematopoietic precursors during early embryonic development [51]. Thus it was not at all surprising that both Virant-Klun and our group have reported that the VSELs in the adult ovary express both pluripotent and PGC specific markers (Table 1). Similar expression of markers was reported in pig ovary stem cells [52].

VSELs are distinctly spherical, with high nucleocytoplasmic ratio and nuclei stained dark with Hematoxylin and also do not stain easily with DAPI. DAPI is understood to preferentially stain heterochromatin [53, 54] and being pluripotent these cells are expected to have abundant euchromatin. Dark Hematoxylin stained nuclei is characteristic feature of a group of primitive spermatogonia in testis A_{dark} and we observe similar characteristic staining in primitive stem cells in ovary as well. Immunophenotyping studies on sheep OSE revealed the presence of two distinct populations of stem cells including 1.26 ± 0.19% of (2–4 μm) and 6.86 ± 0.5% of (4–9 μm) cells expressing OCT-4 [12]. Similarly, flow cytometry analysis shows that 0.02% + 0.01% cells are LIN−/CD45−/SCA1+ VSELs in normal mouse ovary [16].

However, presence of stem cells in adult mammalian ovary has not yet been well accepted; rather there are groups who have generated evidence against the presence of stem cells in adult ovary and have been also discussed above. This clearly shows that more research is required in the area. Above review of literature and Table 1 show that stem cells do exist in the OSE and it now becomes pertinent to understand how these stem cells function and contribute to postnatal oogenesis in normal adult ovaries. In the next section, various studies done in the authors' lab on how the ovarian stem cells are modulated by FSH are described.

4. Novel Action of FSH on Ovarian Stem Cells

The existing dogma in reproductive biology advocates that FSHR in the ovary are expressed exclusively on the granulosa cells and initial follicle growth is gonadotropin independent. Sairam's group has made seminal contributions and shown that sheep ovarian and testicular FSHR undergo alternative splicing resulting in 4 distinct isoforms of which FSHR1 and FSHR3 have biological functions [55]. Babu et al. [56] have reported FSHR isoforms in mouse ovary and their altered expression after PMSG treatment. Both FSHR1 and FSHR3 were detected by RT-PCR in normal ovary and FSHR3 expression was selectively increased after 24 and 48 h of PMSG treatment. Using a FSHR3 specific peptide IgG, Western blotting confirmed the presence and upregulation of FSHR3 in ovary after PMSG treatment. Sullivan et al. [57] have studied relative mRNA expression for alternately spliced FSHR transcripts (FSHR1, FSHR2, and FSHR3) and LHR in small, medium, and preovulatory sheep follicles and have found that FSHR3 is the predominant transcript by qRT-PCR studies and is expressed in higher levels compared to the canonical FSHR1 and that LHR are maximally expressed in the preovulatory follicles. We have found that ovarian stem cells are located in the ovary surface epithelium and express FSHR and that it is the alternatively spliced FSHR isoform FSHR3 which is actively transcribed on being stimulated by FSH and as a result the ovarian stem cells undergo

proliferation and clonal expansion to form germ cell nests (Figure 1) [14].

These results have relevance especially in light of the fact that no significant association has been observed between mutations or single nucleotide polymorphisms (SNPs) in the canonical FSHR1 with premature ovarian failure and infertility. We have discussed the possible role of FSH-FSHR3-stem cells interaction in the OSE resulting in ovarian cancers, POF, and menopause and how the reproductive biologists have been misled by screening for mutations in FSHR1 with a focus on exon 10 whereas FSHR3 may have a more significant role (has exon 11 and lacks exons 9 & 10) thus explaining the accumulated negative data on lack of mutations in FSHR in women with POF and cancer [58]. Various studies undertaken by us to decipher a novel role of FSH via FSHR3 in stimulating ovarian stem cells (in addition to its well-studied effect on follicular growth via FSHR located on the granulosa cells) resulting in postnatal oogenesis and follicle are listed below:

(1) In 2012, we reported [15] that PMSG (FSH analog) treatment to mice stimulates OSE and newer assembly of follicles was evident just below the OSE. PMSG treatment resulted in increased number of PF cohorts compared to normal ovary (Figures 2(A) and 2(B)). A subtle proliferation in OSE was also noted during the proestrus stage of estrus cycle in untreated normal ovary. PMSG treatment augmented this effect and it is crucial to mention here that PMSG shows this effect only when injected during carefully monitored proestrus stage of the estrus cycle.

(2) While studying effect of FSH and bFGF on human and marmoset ovarian cortical tissue culture, Parte et al. [17] reported a prominent effect of FSH on OSE (Figure 2(b), became hypertrophied and multilayered) in perimenopausal ovarian tissue and also showed that a large number of stem cells get shed onto the cell culture insert and retained the ability to spontaneously differentiate into oocyte-like structures. qRT-PCR on cortical tissue exposed to FSH and bFGF compared to untreated control showed increased expression of pluripotent (Oct-4A and Nanog), early germ cell (Oct-4, c-Kit, and Vasa), and PF growth initiation (oocyte specific Gdf-9, Lhx8, and granulosa cells specific Amh) markers. Results suggest that FSH exerts a direct action on the stem cells.

(3) Patel et al. [14] showed by immunolocalization studies presence of FSHR on the sheep ovarian stem cells whereas the epithelial cells were negative (Figure 1). Using specific oligo probes for *in situ* hybridization studies, they showed that both FSHR1 and FSHR3 mRNA were expressed in the stem cells but only FSHR3 mRNA was actively transcribed and expressed in the cytoplasm of stem cells after FSH treatment. These results were also confirmed by qRT-PCR studies for FSHR1 and FSHR3 transcripts. A prominent effect of FSH was observed on proliferation of stem cells and germ cell nest formation accompanied with upregulation of pluripotent markers Oct4A, Oct4, and Sox2. Thus a functional interaction of FSH-FSHR3-stem cells axis was deciphered for the first time in adult ovary.

(4) Ovarian stem cells (VSELs) survive chemotherapy in mice due to their quiescent nature and have the ability to initiate neo-oogenesis on stimulation with FSH. Flow cytometry data shows that LIN−/CD45−/SCA1+ VSELs in normal mouse ovary are 0.02% + 0.01% and after chemoablation are 0.03% + 0.017%. PMSG treatment to chemoablated ovary increased the numbers of VSELs to 0.08 + 0.03% [16].

(5) Also a prominent effect of FSH was observed on the OSE of chemoablated ovary after 7 days in culture (Figures 2(C) and 2(D)). BrdU positive cells in OSE were associated with the formation of germ cell clusters. Culture of OSE cells isolated from chemoablated ovary in the presence of FSH resulted in formation of germ cell nests that stained positive for PCNA and OCT-4 and oocyte-like structures *in vitro* that stained positive for MVH and GDF-9 [16].

These data generated by our group suggest a novel action of FSH on the stem cells located in the OSE and call for paradigm shift in the field of reproductive biology. A recent study describes presence of gonadotropin receptors on human bone marrow hematopoietic progenitors including VSELs [59] supporting a developmental link between hematopoiesis and the germline. It becomes extremely perplexing as to how does FSH act on the ovary when an infertility expert treats a woman in the clinic to collect eggs for assisted reproduction. Is FSH really only playing a survival role on ovarian follicles, preventing cell death of a cohort of eggs when they start growing or is it that FSH treatment exerts direct action on the ovarian stem cells and an altogether new cohort of follicles assembles and starts growing starting from the stem cells! We need better means to decipher these well kept secrets of Mother Nature on the surface of the ovary.

Initiation of maturation of the follicles from the primordial pool is a process that at least in humans is not dependent on gonadotropins. Although FSH is a primary factor controlling folliculogenesis, the "initial recruitment" of human PF is mainly controlled by factors produced in the ovaries [1]. In general FSH is secreted in high levels at mid cycle (preovulatory surge) but there is another smaller peak which occurs during late luteal phase and is termed the "intercycle peak" in humans or the "proestrus peak" (secondary surge) in rodents and is understood to be associated with recruitment of follicles for the next cycle. Rani and Moudgal [60] showed that rather than the "preovulatory" FSH peak, the "proestrus" peak affects follicular growth and blocks ovulation in the next cycle. It is probably this intercycle peak of FSH that triggers stem cell activity in the OSE, resulting in PF assembly [15, Figures 1-2] and these follicles then rapidly grow and mature. But more carefully planned studies need to be undertaken to generate more evidence to support this preliminary observation.

Lei and Spradling [42] failed to detect "germline cysts" by lineage tracing approach and thus concluded that adult

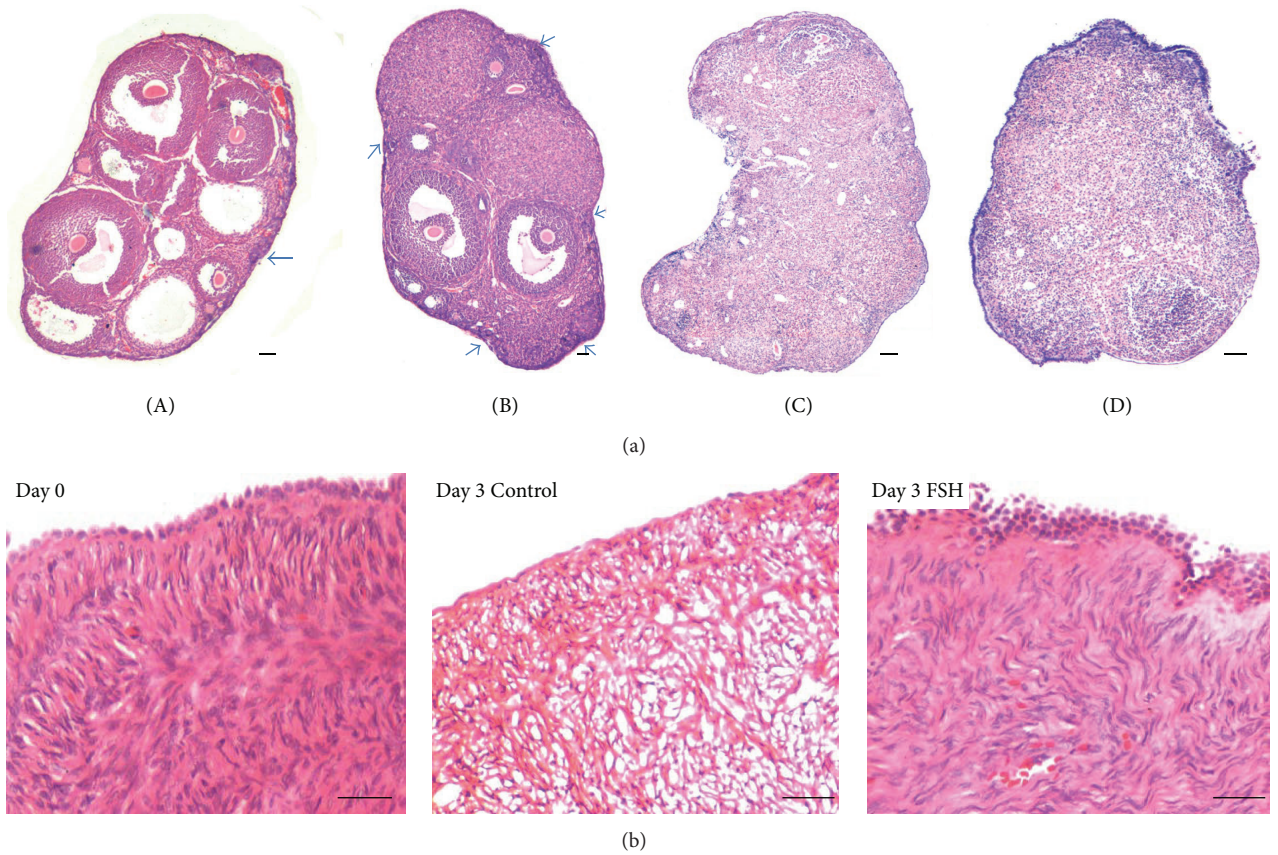

Figure 2: Novel action of FSH on adult mammalian ovary. (a) Effect of pregnant mare serum gonadotropin (PMSG) on intact and chemoablated mice ovaries. (A)-(B) PMSG treatment to intact ovaries results in increased cohorts of primordial follicles below the OSE compared to untreated control [15]. (C)-(D) Chemoablated mouse OSE also responds to PMSG treatment. Note overall thickening of OSE after PMSG treatment compared to untreated control. Chemoablated ovaries are otherwise devoid of follicles [16]. (b) Effect of FSH on human ovary surface epithelium cortical tissue *in vitro* [17]. H&E stained paraffin section on D0 at the start of culture exhibits a prominent OSE and the cortical tissue is almost degenerated by D3 in culture whereas FSH exerts a survival effect on the cortical tissue and note the hypertrophied nature of the OSE. Please refer to the cited references for further details.

mouse ovaries lack stem cells. They proposed that primordial follicle pool generated during fetal life is sufficient to sustain oogenesis and that there is no renewal of oocytes during adult life. We had discussed various reasons that could have led to their negative data [34] and also showed presence of "cyst" (germ cell nest) which expresses OCT-4 and SSEA4 in adult mouse OSE cell smears after PMSG treatment. Similar structures have also been characterized in human and sheep ovary [35]. Recently we published our protocols to isolate two populations of ovarian stem cells [12] and we found that it is the bigger OGSCs (equivalent to OSCs) that divide rapidly and form cysts with incomplete cytoplasmic division. Presence of cysts (germ cell nests) is considered to be a hallmark feature of stem cell activity in adult ovary [42].

Recently Zhang et al. [46] have provided compelling evidence against stem cell activity and postnatal oogenesis in adult mice using 3 genetically modified mouse models. Their experiments suggest that there is no generation of oocytes from stem cells in adult ovary and also no somatic cells get recruited to aid primordial follicle assembly with *de novo*-regenerated oocytes. In contrast to their study where genetic manipulations are done to answer a biological question, we used a more physiological approach to address the same question of postnatal oogenesis [16]. Firstly we characterized the stem cells in enzymatically separated OSE cells and used flow cytometry to study LIN−/CD45−/SCA+ VSELs in normal (0.02 + 0.01%) adult ovaries and chemoablated (0.03 + 0.017%) mouse ovary. The VSELs survive chemotherapy and 48 h of PMSG treatment to chemoablated ovary resulted in increase in their numbers (0.08 + 0.03%) accompanied by initiation of neo-oogenesis in the OSE layer. The process was modulated by FSH both in culture of mechanically isolated OSE cells and adult chemoablated intact ovary culture. Successful formation of germ cell nests was observed and the manuscript was accepted for publication after a very strict review process and only after we inserted images of 4 different germ co-expressing OCT-4, PCNA and DAPI to convince the reviewers.

Readers may wonder why we did not observe complete neo-oogenesis and follicle assembly from the stem cells in chemoablated ovary. The response is simple that chemotherapy affects the ovarian stem cell niche similar to the report in

testes [60]. Thus we saw self-renewal, clonal expansion, proliferation, and initial differentiation of stem cells into oocytes but the process of differentiation and PF assembly could not be completed because of the compromised niche. We recently achieved spectacular success of restoring spermatogenesis in chemoablated testis by providing a healthy niche by way of transplanting Sertoli or mesenchymal cells [61]. Transplanted cells act as a source of growth factors and cytokines essential for differentiation of surviving VSELs in chemoablated testes into sperm. Similar experiments could not be attempted in mice ovaries because of their small size which reduces further after chemotherapy. Here we encourage the readers to refer to the beneficial effects of mesenchymal cells (MSCs) transplantation to improve ovarian function reviewed recently [36]. It is intriguing that transplanting MSCs restores normal ovarian function/morphology (but do not themselves form oocytes) and rather endogenous oogenesis is restored (possibly from the VSELs that survive cytotoxic insult). Similarly, Tilly's group reported that transplanting bone marrow or peripheral blood cells in chemoablated ovary resulted in restoration of function and formation of oocytes from endogenous stem cells [18]. All this exciting data emerging from various laboratories suggests that a quiescent population of VSELs in adult mammalian ovary which survive oncotherapy should be appreciated and further exploited to restore ovarian function. VSELs may have a role in giving rise to PCOS was shown by our group [49], but needs to be investigated in details.

Zhang et al. [46] further state that rather than the ovarian stem cells, embryonic and induced pluripotent stem cells (iPS) have a promising future to generate oocytes for fertility treatment. Research efforts to make oocytes using mES cells are ongoing for last 30 years and recent efforts for using hES cells are ongoing for more than 15 years. Similarly iPS cells have also been used to make gametes *in vitro* but as concluded recently obtaining gametes from these stem cells remains a distant dream [62]. We recently discussed and compared the ovarian/testicular VSELs with ES/iPS cells and why VSELs (isolated from adult human, sheep, monkey, and rabbit OSE) and from chemoablated mice ovaries spontaneously differentiate into oocytes [16, 63]. Also for the first time, we succeeded to spontaneously differentiate testicular VSELs enriched from chemoablated mouse testis into sperm [64]. It is difficult to convert ES/iPS cells into PGCs as they have very distinct epigenetic status which cannot be replicated easily in a culture dish. On the other hand, VSELs are considered equivalent to PGCs and show excellent ability to differentiate into gametes.

5. Conclusions

To conclude, data emerging from various laboratories suggests the presence of stem cells in adult ovary surface epithelium. Our group has shown that stem cells in the OSE comprise smaller VSELs and slightly larger progenitors (OGCSs/OSCs) equivalent to SSCs in the testes. They have the ability to undergo postnatal oogenesis, differentiate into oocytes, and undergo PF assembly under the influence of FSH which acts through alternatively spliced FSHR3 isoform. This increasing understanding of ovarian stem cell biology led to initial success of restoration of function in chemoablated adult mice ovary. Further studies are warranted to confirm this amazing success achieved by our group and others in the field. A similar FSH-FSHR3-stem cell axis has recently been deciphered in mouse testis as well [65].

Abbreviations

ES cells: Embryonic stem cells
FSH: Follicle stimulating hormone
FSHR: FSH receptor
FSHR1: Canonical FSHR, acts via cAMP pathway
FSHR3: Alternately spliced FSHR transcript, acts via MAPK pathway
iPS: Induced pluripotent stem cells
MSCs: Mesenchymal stem cells
OGSCs: Ovarian germ stem cells
OSCs: Oogonial stem cells
OSE: Ovary surface epithelium
PCOS: Polycystic ovarian syndrome
PF: Primordial follicles
PGCs: Primordial germ cells
POF: Premature ovarian failure
SSCs: Spermatogonial stem cells
VSELs: Very small embryonic-like stem cells.

Disclosure

NIRRH Accession Number is REV/252/04-2015.

Conflict of Interests

Authors declare no conflict of interests.

Acknowledgments

Authors are thankful to Indian Council of Medical Research and Department of Science and Technology, Government of India, New Delhi, for financial support for studies to arrive at this understanding.

References

[1] I. E. Messinis, C. I. Messini, and K. Dafopoulos, "The role of gonadotropins in the follicular phase," *Annals of the New York Academy of Sciences*, vol. 1205, pp. 5–11, 2010.

[2] J. Johnson, J. Canning, T. Kaneko, J. K. Pru, and J. L. Tilly, "Germline stem cells and follicular renewal in the postnatal mammalian ovary," *Nature*, vol. 428, no. 6979, pp. 145–150, 2004.

[3] H. M. Kingery, "Oogenesis in the white mouse," *Journal of Morphology*, vol. 30, no. 1, pp. 261–315, 1917.

[4] C. S. Simkins, "Development of the human ovary from birth to sexual maturity," *The American Journal of Anatomy*, vol. 51, no. 2, pp. 465–505, 1932.

[5] P. M. Motta and S. Makabe, "Germ cells in the ovarian surface during fetal development in humans. A three dimensional microanatomical study by scanning and transmission electron

microscopy," *Journal of Submicroscopic Cytology*, vol. 18, no. 2, pp. 271–290, 1986.

[6] N. Auersperg, A. S. T. Wong, K.-C. Choi, S. K. Kang, and P. C. K. Leung, "Ovarian surface epithelium: biology, endocrinology, and pathology," *Endocrine Reviews*, vol. 22, no. 2, pp. 255–288, 2001.

[7] M. A. Goodell, K. Brose, G. Paradis, A. S. Conner, and R. C. Mulligan, "Isolation and functional properties of murine hematopoietic stem cells that are replicating in vivo," *The Journal of Experimental Medicine*, vol. 183, no. 4, pp. 1797–1806, 1996.

[8] J. W. Jonker, J. Freeman, E. Bolscher et al., "Contribution of the ABC transporters Bcrp1 and Mdr1a/1b to the side population phenotype in mammary gland and bone marrow of mice," *Stem Cells*, vol. 23, no. 8, pp. 1059–1065, 2005.

[9] P. P. Szotek, R. Pieretti-Vanmarcke, P. T. Masiakos et al., "Ovarian cancer side population defines cells with stem cell-like characteristics and Mullerian inhibiting substance responsiveness," *Proceedings of the National Academy of Sciences of the United States of America*, vol. 103, no. 30, pp. 11154–11159, 2006.

[10] S. Peng, N. J. Maihle, and Y. Huang, "Pluripotency factors Lin28 and Oct4 identify a sub-population of stem cell-like cells in ovarian cancer," *Oncogene*, vol. 29, no. 14, pp. 2153–2159, 2010.

[11] A. Flesken-Nikitin, C.-I. Hwang, C.-Y. Cheng, T. V. Michurina, G. Enikolopov, and A. Y. Nikitin, "Ovarian surface epithelium at the junction area contains a cancer-prone stem cell niche," *Nature*, vol. 495, no. 7440, pp. 241–245, 2013.

[12] S. Parte, H. Patel, K. Sriraman, and D. Bhartiya, "Isolation and characterization of stem cells in the adult mammalian ovary," *Methods in Molecular Biology*, vol. 1235, pp. 203–229, 2015.

[13] S. Parte, D. Bhartiya, J. Telang et al., "Detection, characterization, and spontaneous differentiation in vitro of very small embryonic-like putative stem cells in adult mammalian ovary," *Stem Cells and Development*, vol. 20, no. 8, pp. 1451–1464, 2011.

[14] H. Patel, D. Bhartiya, S. Parte, P. Gunjal, S. Yedurkar, and M. Bhatt, "Follicle stimulating hormone modulates ovarian stem cells through alternately spliced receptor variant FSH-R3," *Journal of Ovarian Research*, vol. 6, no. 1, article 52, 2013.

[15] D. Bhartiya, K. Sriraman, P. Gunjal, and H. Modak, "Gonadotropin treatment augments postnatal oogenesis and primordial follicle assembly in adult mouse ovaries?" *Journal of Ovarian Research*, vol. 5, article 32, 2012.

[16] K. Sriraman, D. Bhartiya, S. Anand, and S. Bhutda, "Mouse ovarian very small embryonic-like stem cells resist chemotherapy and retain ability to initiate oocyte-specific differentiation," *Reproductive Sciences*, 2015.

[17] S. Parte, D. Bhartiya, D. D. Manjramkar, A. Chauhan, and A. Joshi, "Stimulation of ovarian stem cells by follicle stimulating hormone and basic fibroblast growth factor during cortical tissue culture," *Journal of Ovarian Research*, vol. 6, article 20, 2013.

[18] J. Johnson, J. Bagley, M. Skaznik-Wikiel et al., "Oocyte generation in adult mammalian ovaries by putative germ cells in bone marrow and peripheral blood," *Cell*, vol. 122, no. 2, pp. 303–315, 2005.

[19] H.-J. Lee, K. Selesniemi, Y. Niikura et al., "Bone marrow transplantation generates immature oocytes and rescues long-term fertility in a preclinical mouse model of chemotherapy-induced premature ovarian failure," *Journal of Clinical Oncology*, vol. 25, no. 22, pp. 3198–3204, 2007.

[20] Y. Niikura, T. Niikura, and J. L. Tilly, "Aged mouse ovaries possess rare premeiotic germ cells that can generate oocytes following transplantation into a young host environment," *Aging*, vol. 1, no. 12, pp. 971–978, 2009.

[21] Y. A. R. White, D. C. Woods, Y. Takai, O. Ishihara, H. Seki, and J. L. Tilly, "Oocyte formation by mitotically active germ cells purified from ovaries of reproductive-age women," *Nature Medicine*, vol. 18, no. 3, pp. 413–421, 2012.

[22] A. N. Imudia, N. Wang, Y. Tanaka, Y. A. R. White, D. C. Woods, and J. L. Tilly, "Comparative gene expression profiling of adult mouse ovary-derived oogonial stem cells supports a distinct cellular identity," *Fertility and Sterility*, vol. 100, no. 5, pp. 1451.e2–1458.e2, 2013.

[23] E.-S. Park, D. C. Woods, and J. L. Tilly, "Bone morphogenetic protein 4 promotes mammalian oogonial stem cell differentiation via Smad1/5/8 signaling," *Fertility and Sterility*, vol. 100, no. 5, pp. 1468–1475, 2013.

[24] A. Bukovsky, M. R. Caudle, M. Svetlikova, and N. B. Upadhyaya, "Origin of germ cells and formation of new primary follicles in adult human ovaries," *Reproductive Biology and Endocrinology*, vol. 2, article 20, 2004.

[25] A. Bukovsky, M. Svetlikova, and M. R. Caudle, "Oogenesis in cultures derived from adult human ovaries," *Reproductive Biology and Endocrinology*, vol. 3, article 17, 2005.

[26] A. Bukovsky, M. R. Caudle, S. K. Gupta et al., "Mammalian neo-oogenesis and expression of meiosis-specific protein SCP3 in adult human and monkey ovaries," *Cell Cycle*, vol. 7, no. 5, pp. 683–686, 2008.

[27] A. Bukovsky and M. R. Caudle, "Immunoregulation of follicular renewal, selection, POF, and menopause in vivo, vs. neo-oogenesis in vitro, POF and ovarian infertility treatment, and a clinical trial," *Reproductive Biology and Endocrinology*, vol. 10, article 97, 2012.

[28] I. Virant-Klun, N. Zech, P. Rožman et al., "Putative stem cells with an embryonic character isolated from the ovarian surface epithelium of women with no naturally present follicles and oocytes," *Differentiation*, vol. 76, no. 8, pp. 843–856, 2008.

[29] I. Virant-Klun, P. Rožman, B. Cvjeticanin et al., "Parthenogenetic embryo-like structures in the human ovarian surface epithelium cell culture in postmenopausal women with no naturally present follicles and oocytes," *Stem Cells and Development*, vol. 18, no. 1, pp. 137–150, 2009.

[30] I. Virant-Klun, T. Skutella, M. Stimpfel, and J. Sinkovec, "Ovarian surface epithelium in patients with severe ovarian infertility: a potential source of cells expressing markers of pluripotent/multipotent stem cells," *Journal of Biomedicine and Biotechnology*, vol. 2011, Article ID 381928, 12 pages, 2011.

[31] I. Virant-Klun, T. Skutella, M. Hren et al., "Isolation of small ssea-4-positive putative stem cells from the ovarian surface epithelium of adult human ovaries by two different methods," *BioMed Research International*, vol. 2013, Article ID 690415, 15 pages, 2013.

[32] I. Virant-Klun, T. Skutella, M. Kubista, A. Vogler, J. Sinkovec, and H. Meden-Vrtovec, "Expression of pluripotency and oocyte-related genes in single putative stem cells from human adult ovarian surface epithelium cultured in vitro in the presence of follicular fluid," *BioMed Research International*, vol. 2013, Article ID 861460, 18 pages, 2013.

[33] M. Stimpfel, T. Skutella, B. Cvjeticanin et al., "Isolation, characterization and differentiation of cells expressing pluripotent/multipotent markers from adult human ovaries," *Cell and Tissue Research*, vol. 354, no. 2, pp. 593–607, 2013.

[34] D. Bhartiya, K. Sriraman, S. Parte, and H. Patel, "Ovarian stem cells: absence of evidence is not evidence of absence," *Journal of Ovarian Research*, vol. 6, no. 1, article 65, 2013.

[35] S. Parte, D. Bhartiya, H. Patel et al., "Dynamics associated with spontaneous differentiation of ovarian stem cells in vitro," *Journal of Ovarian Research*, vol. 7, no. 1, article 25, 2014.

[36] I. Virant-Klun, "Postnatal oogenesis in humans: a review of recent findings," *Stem Cells and Cloning*, vol. 8, pp. 49–60, 2015.

[37] E. K. Zuba-Surma, M. Kucia, A. Abdel-Latif et al., "Morphological characterization of very small embryonic-like stem cells (VSELs) by ImageStream system analysis," *Journal of Cellular and Molecular Medicine*, vol. 12, no. 1, pp. 292–303, 2008.

[38] D. Bhartiya, S. Kasiviswanathan, S. K. Unni et al., "Newer insights into premeiotic development of germ cells in adult human testis using Oct-4 as a stem cell marker," *Journal of Histochemistry & Cytochemistry*, vol. 58, no. 12, pp. 1093–1106, 2010.

[39] D. C. Woods and J. L. Tilly, "An evolutionary perspective on adult female germline stem cell function from flies to humans," *Seminars in Reproductive Medicine*, vol. 31, no. 1, pp. 24–32, 2013.

[40] I. Virant-Klun, M. Stimpfel, B. Cvjeticanin, E. Vrtacnik-Bokal, and T. Skutella, "Small SSEA-4-positive cells from human ovarian cell cultures: related to embryonic stem cells and germinal lineage?" *Journal of Ovarian Research*, vol. 6, no. 1, article 24, 2013.

[41] M. Z. Ratajczak, E. Zuba-Surma, W. Wojakowski et al., "Very small embryonic-like stem cells (VSELs) represent a real challenge in stem cell biology: recent pros and cons in the midst of a lively debate," *Leukemia*, vol. 28, no. 3, pp. 473–484, 2014.

[42] L. Lei and A. C. Spradling, "Female mice lack adult germline stem cells but sustain oogenesis using stable primordial follicles," *Proceedings of the National Academy of Sciences of the United States of America*, vol. 110, no. 21, pp. 8585–8590, 2013.

[43] A. G. Byskov, P. E. Høyer, C. Y. D. Andersen, S. G. Kristensen, A. Jespersen, and K. Møllgård, "No evidence for the presence of oogonia in the human ovary after their final clearance during the first two years of life," *Human Reproduction*, vol. 26, no. 8, pp. 2129–2139, 2011.

[44] D. Bhartiya, "The continued presence of stem cells and oogonia in the adult mammalian ovary," *Human Reproduction*, vol. 27, no. 3, article 938, 2012.

[45] H. Zhang, W. Zheng, Y. Shen, D. Adhikari, H. Ueno, and K. Liu, "Experimental evidence showing that no mitotically active female germline progenitors exist in postnatal mouse ovaries," *Proceedings of the National Academy of Sciences of the United States of America*, vol. 109, no. 31, pp. 12580–12585, 2012.

[46] H. Zhang, L. Liu, X. Li et al., "Life-long in vivo cell-lineage tracing shows that no oogenesis originates from putative germline stem cells in adult mice," *Proceedings of the National Academy of Sciences of the United States of America*, vol. 111, no. 50, pp. 17983–17988, 2014.

[47] J. Yuan, D. Zhang, L. Wang et al., "No evidence for neo-oogenesis may link to ovarian senescence in adult monkey," *Stem Cells*, vol. 31, no. 11, pp. 2538–2550, 2013.

[48] D. Bhartiya, S. Parte, H. Patel, S. Anand, K. Sriraman, and P. Gunjal, "Pluripotent very small embryonic-like stem cells in adult mammalian gonads," in *Adult Stem Cell Therapies: Alternatives to Plasticity*, M. Ratajczak, Ed., Stem Cell Biology and Regenerative Medicine, pp. 191–209, Springer, New York, NY, USA, 2014.

[49] D. Bhartiya, S. Unni, S. Parte, and S. Anand, "Very small embryonic-like stem cells: implications in reproductive biology," *BioMed Research International*, vol. 2013, Article ID 682326, 10 pages, 2013.

[50] M. de Felici, "Germ stem cells in the mammalian adult ovary: considerations by a fan of the primordial germ cells," *Molecular Human Reproduction*, vol. 16, no. 9, pp. 632–636, 2010.

[51] M. L. Scaldaferri, F. G. Klinger, D. Farini et al., "Hematopoietic activity in putative mouse primordial germ cell populations," *Mechanisms of Development*, vol. 136, pp. 53–63, 2015.

[52] H.-T. Bui, N. Van Thuan, D.-N. Kwon et al., "Identification and characterization of putative stem cells in the adult pig ovary," *Development*, vol. 141, no. 11, pp. 2235–2244, 2014.

[53] Z. Jasencakova, A. Meister, J. Walter, B. M. Turner, and I. Schubert, "Histone H4 acetylation of euchromatin and heterochromatin is cell cycle dependent and correlated with replication rather than with transcription," *The Plant Cell*, vol. 12, no. 11, pp. 2087–2100, 2000.

[54] T. E. Crowley, E. M. Kaine, M. Yoshida, A. Nandi, and D. J. Wolgemuth, "Reproductive cycle regulation of nuclear import, euchromatic localization, and association with components of pol II mediator of a mammalian double-bromodomain protein," *Molecular Endocrinology*, vol. 16, no. 8, pp. 1727–1737, 2002.

[55] M. R. Sairam and P. S. Babu, "The tale of follitropin receptor diversity: a recipe for fine tuning gonadal responses?" *Molecular and Cellular Endocrinology*, vol. 260–262, pp. 163–171, 2007.

[56] P. S. Babu, N. Danilovich, and M. R. Sairam, "Hormone-induced receptor gene splicing: enhanced expression of the growth factor type I follicle-stimulating hormone receptor motif in the developing mouse ovary as a new paradigm in growth regulation," *Endocrinology*, vol. 142, no. 1, pp. 381–389, 2001.

[57] R. R. Sullivan, B. R. Faris, D. Eborn, D. M. Grieger, A. G. Cino-Ozuna, and T. G. Rozell, "Follicular expression of follicle stimulating hormone receptor variants in the ewe," *Reproductive Biology and Endocrinology*, vol. 11, no. 1, article 113, 2013.

[58] D. Bhartiya and J. Singh, "FSH-FSHR3-stem cells in ovary surface epithelium: basis for adult ovarian biology, failure, aging, and cancer," *Reproduction*, vol. 149, no. 1, pp. R35–R48, 2015.

[59] K. Mierzejewska, S. Borkowska, E. Suszynska et al., "Hematopoietic stem/progenitor cells express several functional sex hormone receptors—novel evidence for a potential developmental link between hematopoiesis and primordial germ cells," *Stem Cells and Development*, vol. 24, no. 8, pp. 927–937, 2015.

[60] C. S. S. Rani and N. R. Moudgal, "Examination of the role of FSH in periovulatory events in the hamster," *Journal of Reproduction and Fertility*, vol. 50, no. 1, pp. 37–45, 1977.

[61] S. Anand, D. Bhartiya, K. Sriraman, H. Patel, and D. D. Manjramkar, "Very small embryonic-like stem cells survive and restore spermatogenesis after busulphan treatment in mouse testis," *Journal of Stem Cell Research and Therapy*, vol. 4, article 216, 2015.

[62] R. S. Legro and E. Y. Adashi, "Introduction: Germline stem cell therapy in humans: two are not enough," *Fertility and Sterility*, vol. 101, no. 1, pp. 1–2, 2014.

[63] D. Bhartiya, I. Hinduja, H. Patel, and R. Bhilawadikar, "Making gametes from pluripotent stem cells—a promising role for very small embryonic-like stem cells," *Reproductive Biology and Endocrinology*, vol. 12, no. 1, p. 114, 2014.

[64] S. Anand, H. Patel, and D. Bhartiya, "Chemoablated mouse seminiferous tubular cells enriched for very small embryonic-like stem cells undergo spontaneous spermatogenesis in vitro," *Reproductive Biology and Endocrinology*, vol. 13, no. 1, p. 33, 2015.

[65] H. Patel and D. Bhartiya, "Novel action of follicle stimulating hormone (FSH) on mouse testicular stem cells," *Andrology, Supplement*, abstract no. 63, p. 93, 2015.

Hindawi Publishing Corporation
Stem Cells International
Volume 2016, Article ID 1970843, 8 pages
http://dx.doi.org/10.1155/2016/1970843

Review Article

Parthenogenesis and Human Assisted Reproduction

Adriana Bos-Mikich,[1] Fabiana F. Bressan,[2] Rafael R. Ruggeri,[1] Yeda Watanabe,[3] and Flávio V. Meirelles[2]

[1]*Department of Morphological Sciences, ICBS, Federal University of Rio Grande do Sul, 90050-170 Porto Alegre, RS, Brazil*
[2]*Department of Veterinary Medicine, Faculty of Animal, Science and Food Engineering (FZEA), University of São Paulo (USP), 13635-000 Pirassununga, SP, Brazil*
[3]*WTA Fertilização In Vitro Ltda, 14140-000 Cravinhos, SP, Brazil*

Correspondence should be addressed to Adriana Bos-Mikich; adriana.bosmikich@gmail.com

Received 21 April 2015; Revised 20 June 2015; Accepted 24 June 2015

Academic Editor: Irma Virant-Klun

Parthenogenetic activation of human oocytes obtained from infertility treatments has gained new interest in recent years as an alternative approach to create embryos with no reproductive purpose for research in areas such as assisted reproduction technologies itself, somatic cell, and nuclear transfer experiments and for derivation of clinical grade pluripotent embryonic stem cells for regenerative medicine. Different activating methods have been tested on human and nonhuman oocytes, with varying degrees of success in terms of parthenote generation rates, embryo development stem cell derivation rates. Success in achieving a standardized artificial activation methodology for human oocytes and the subsequent potential therapeutic gain obtained from these embryos depends mainly on the availability of gametes donated from infertility treatments. This review will focus on the creation of parthenotes from clinically unusable oocytes for derivation and establishment of human parthenogenetic stem cell lines and their potential applications in regenerative medicine.

1. Introduction

Parthenogenesis is a reproduction strategy common in some jawed vertebrate species such as the whiptail lizard (*Aspidoscelis uniparens*) [1], in which no sperm is involved to trigger embryonic development from the oocyte and the female generates an offspring with no paternal inheritance. In mammals, parthenogenesis is not a natural form of reproduction, as the birth of an offspring is considered not possible. However, parthenogenetic activation of mammalian oocytes by artificial manipulation results in early embryonic development and in some instances fetal early development can be achieved (mouse forelimb stage E9.5) stage [2]. No further development is achieved due to the lack of expression of imprinted paternal genes necessary for the establishment of a functional placenta [3]. On the other hand, genetic modification technologies have made the creation and birth of fertile animals from mouse parthenogenetically activated oocytes possible [4].

Why then do we study parthenogenesis in the scope of assisted reproduction technologies (ART) if no human baby can be generated from this reproductive maneuver?

Renewed interest in parthenogenetic activation of mammalian oocytes has come about for scientific, medical, and economic reasons. First of all, experimental work involving parthenogenetic embryos circumvents the ethical and legal problems concerning the use of human embryos generated for reproductive purposes. Parthenotes may be employed in different research areas related to ART, studies on human pluripotent stem cells or basic science uncovering regulatory mechanisms that command human embryonic development and cloning experiments using somatic cell or nuclear transfer in mammalian oocytes.

Last but not least, the creation of clinical grade parthenogenetic human embryonic stem cell (hpESC) lines have the potential to benefit a considerable large number of patients, when used in cell therapies, with a reduced risk of transplant rejection. However, to this end, efforts should

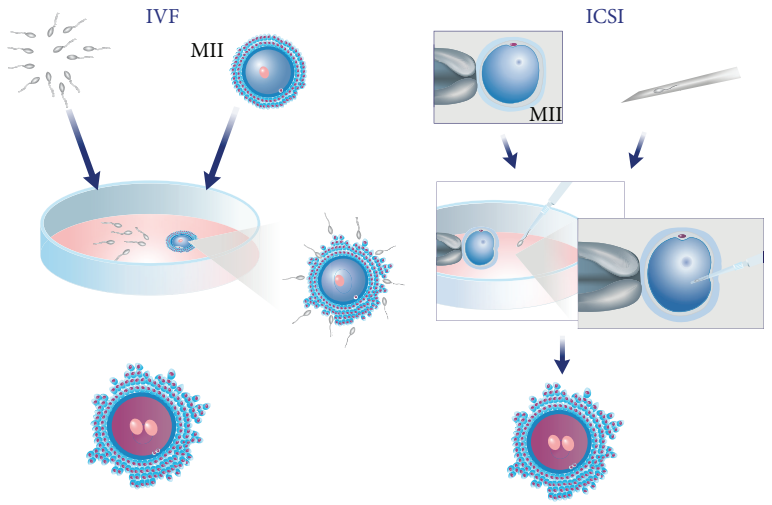

Figure 1: Oocyte insemination by *in vitro* fertilization (IVF) and intracytoplasmic sperm injection (ICSI) techniques.

be directed to clinicians to participate in research projects. The establishment of parthenogenetic clinical grade human embryonic stem cell lines for use in cell or tissue therapies will only be possible, if research laboratories obtain enough biological material from ART centers to evaluate activation strategies, derivation, and culture media adequate for future therapeutic use of phESC lines. Furthermore, well trained committed staff, with good practice and knowledge of basic embryology, is paramount for the conscious and successful use of spare oocytes and embryos obtained from assisted reproduction centers.

This review will explore techniques of parthenogenetic activation, derivation, and cell and tissue differentiation achieved in animal models, which reinforce the therapeutic potential of these pluripotent embryonic stem cells, despite concerns related to their putative genetic instability, an inherent feature due to their monoparental origin [4].

ART In Vitro Fertilization and Intracytoplasmic Sperm Injection Techniques. Among the several treatments regarded as ART, there are two insemination methods employed for the generation of human embryos in the laboratory, the *in vitro* fertilization (IVF) and the intracytoplasmic sperm injection (ICSI) (Figure 1).

When performing IVF, oocytes and sperm are mixed together and left to undergo the fertilization process in a culture system that mimics the fallopian tubes environment. Thus, IVF may be considered an assisted reproduction technology that mimics "natural" fertilization phenomena [5]. With IVF, the fertilizing spermatozoon will penetrate through the surrounding *cumulus* cells, interact with the *zona pellucida* proteins, and eventually attach and fuse with the oocyte plasma membrane.

ICSI was developed to overcome situations where sperm count, motility, or morphology is compromised. By using this insemination technology, the embryologist may choose the "best looking" spermatozoon to inseminate the oocyte, even if it is in very low numbers or presents limited motility in the ejaculate.

ICSI is performed with the aid of a pair of glass pipettes adjusted to an inverted microscope, where the embryologist holds the oocyte with one pipette and injects the chosen spermatozoon with the second pipette straight into the ooplasm.

2. Parthenogenetic Activation Methodologies

2.1. Biochemistry of Oocyte Activation. Arrested nonfertilized metaphase II (MII) oocytes will remain at this stage until a stimulus, which may come from the fertilizing spermatozoon or from an artificial agent (Figure 2), triggers intracytoplasmic Ca^{2+} rises and meiosis resumption. Intracellular Ca^{2+} oscillations will inhibit the action of the metaphase promoting factor (MPF) and the cytostatic factor (CSF) and lead to metaphase/anaphase transition, segregation of sister chromatids, and extrusion of second polar body. The importance of these Ca^{2+} transients for oocyte activation was shown by the prevention of the intracellular elevation of Ca^{2+} after sperm penetration by preloading the oocytes with the Ca^{2+} chelator BAPTA 1-AM [6]. In the absence of any intracellular Ca^{2+} increase, activation and subsequent embryo development failed to occur. In mammals, intracellular Ca^{2+} transients are triggered by a putative sperm factor, the testis specific phospholipase C-*zeta* (plc-*zeta*), or the newly described postacrosomal sheath WW domain-binding protein PAWP released by the sperm during the normal fertilization process [7]. Regardless of the exact nature of the sperm factor responsible for eliciting the Ca^{2+} oscillations, its presence is paramount for successful oocyte activation and embryonic development. The activating agents used for parthenogenetic activation may mimic the sperm bound stimuli to trigger Ca^{2+} release from the endoplasmic reticulum, exit from meiotic arrest, and start embryonic development.

2.2. Techniques of Parthenogenetic Activation. A wide range of artificial stimuli have been employed as agents to trigger the activation process in oocytes of several animal species.

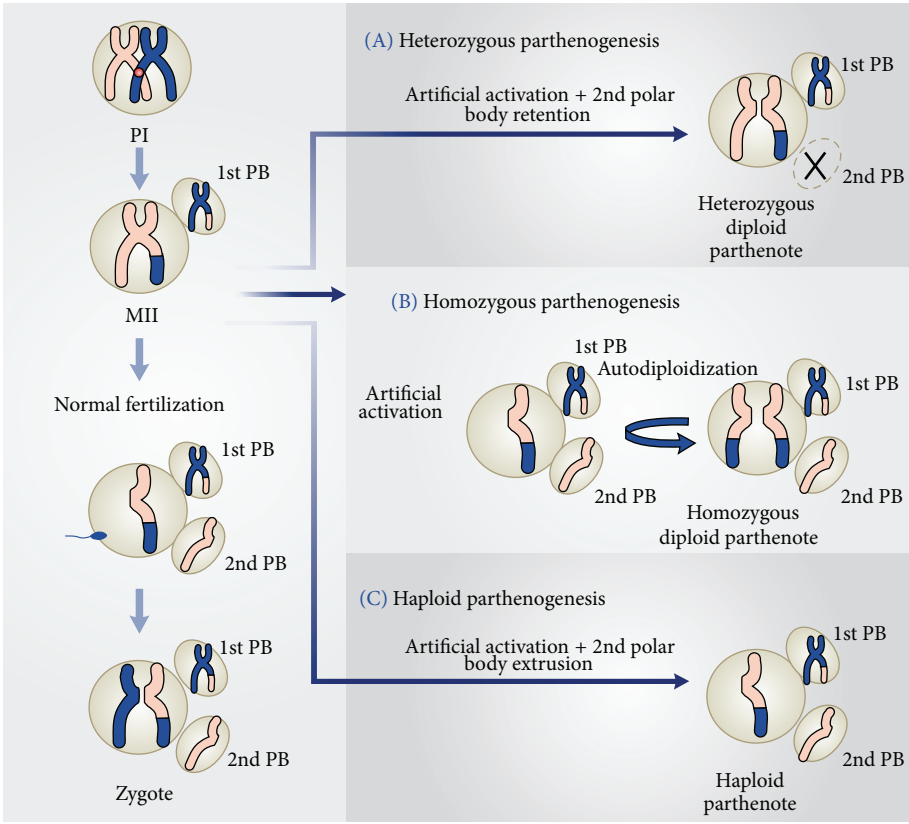

Figure 2: Meiosis and embryonic results after normal fertilization and different artificial activation protocols.

All the techniques which have been described for artificial activation can be divided into two major groups, depending on the nature of the activating stimulus, that is, chemical or physical agents. Except for Sr^{2+} [6], all other artificial agents that have been studied do not produce repetitive Ca^{2+} oscillations normally observed during fertilization. However, the single rise in intracellular Ca^{2+} that is produced by agents such as Ca^{2+} ionophore, ionomycin, or ethanol is adequate to trigger the meiotic resumption and cortical granule release. Specific oocyte activation protocols using strontium chloride ($SrCl_2$) to induce continuous Ca^{2+} oscillations during exit from second meiosis and first embryonic mitosis seem to have a role in long-term embryonic events, such as the number of cells in the inner cell mass (ICM) and trophectoderm of the resulting blastocyst [8].

Despite the fact that various methods have been investigated for parthenogenetically activating oocytes through intracytoplasmic Ca^{2+} elevations, it seems that there is not a single method that activates oocytes from every species studied. Thus, parthenogenetic activation strategies have presented varying degrees of success, regarding activation rates and subsequent embryonic development according to the protocol employed and the species.

Figure 2 shows how embryos are generated after fertilization of an MII oocyte and the three possible parthenotes that may result according to the activation protocol employed to stimulate exit from MII, in the absence of a fertilizing spermatozoon.

In the first instance (Figure 2(A)), treatment with an activating agent such as $SrCl_2$, ethanol, Ca^{2+} ionophore, or ionomycin is followed by another chemical, for instance, 6-DMAP (broad protein synthesis inhibitor) or cytochalasin B or D (inhibitors of actin filaments polymerization), which blocks second polar body (PB2) extrusion. Thus, the resulting parthenote is a "pseudodiploid" heterozygous embryo containing the two sister chromatids of each maternal chromosome present in the MII oocyte.

Alternative activation methodology may allow PB2 extrusion and the resulting parthenote containing a single copy of the sister chromatids undergoes spontaneous diploidization giving rise to a completely homozygous embryo (Figure 2(B)).

Last, the activating agent induces exit from MII and PB2 extrusion, without diploidization (Figure 2(C)). The result of this strategy is a haploid zygote, which develops into a haploid parthenote. However, in this instance, embryo development to the blastocyst stage is generally very low (Bos-Mikich, personal communication).

High oocyte activation and blastocyst formation rates were achieved, when mouse oocytes were exposed to Ca^{2+}-free medium supplemented with 10 mM $SrCl_2$ for 2 hours [6, 9]. However, similar success rates were not achieved

when the same protocol was employed to activate human and bovine oocytes [10].

On the other hand, bovine oocytes presented high activation rates and development to the blastocyst stage, when exposed to the Ca^{2+} salt ionomycin for 5 minutes, followed by 2 mM 6-dimethylaminopurine (6-DMAP) for 3.5 hours [11]. This last activating method has been employed to generate parthenogenetic bovine pluripotent embryonic stem cell, resulting in high rates of derivation and proliferation of primary embryonic stem cell colonies [12].

2.3. Activating Protocols for Fresh Human Oocytes. Human oocytes have been artificially activated mainly with the aim to generate blastocysts for the creation of parthenogenetic human embryonic stem cell (phESC) lines [13]. Notably, parthenogenetic embryo development and ESC derivation efficiencies are similar to those of sperm fertilized counterparts [14].

The first phESC lines were created using Ca^{2+} ionomycin together with 6-DMAP [15]. In that study, fresh oocytes were obtained from shared oocyte donation cycles and the activation procedure took place few hours (3-4 hours) after collection. Twenty-three blastocysts (50%) were generated, from which six phESC lines were established. Mai et al. [14] described an activation methodology that combines electrical and chemical stimuli using ionomycin and 6-DMAP, for the artificial activation of fresh oocytes. Despite the fact that their parthenogenetic blastocyst rate was lower (21%) than the previous report [15], the inner cell mass of three blastocysts was used for the successful derivation of two new parthenogenetic stem cell lines. Blastocyst formation rates also vary considerably in ART cycles, depending on several factors such as the age of the patient, ovarian stimulation protocol, and culture conditions, among others. Thus, it is not surprising that reports on developmental rates of human parthenogenetic embryos vary between studies, as the age of the donors and the stimulation protocols may differ considerably, affecting the final blastocyst rates and consequently their ICM quality.

2.4. Activation of Failure to Fertilize Human Oocytes. The detection of nonfertilized oocytes after insemination is not uncommon in ART treatments, both due to gamete immaturity and unknown factor that led to a failure to fertilize (FF). Most frequently, FF occurs after IVF. In this situation, the oocyte will remain arrested in MII. Rescue insemination by ICSI, few hours after detection of FF, has been proposed as a valid alternative to induce the creation of zygotes from the nonfertilized oocytes [16–19]. There is, however, the underlying risk of chromosome abnormalities in the resulting embryo, mainly because of oocyte aging from the collection time to the moment of reinsemination by ICSI, which may occur 30 hours (or more) after oocyte pick-up. Also, the resulting clinical gestation rates vary considerably from center to center, which hampers rescue insemination to be used as a routine procedure in infertility treatments.

On the other hand, it has been shown that unwanted, FF human oocytes retain their developmental potential and may generate viable blastocysts by exposure to ionomycin followed by 6-DMAP and a protein synthesis inhibitor, cyclohexamide [20]. The embryos presented a similar gene expression profiling and developmental potential as normally fertilized ones making the unwanted artificially activated oocytes an alternative route for the generation of human embryonic stem cell lines.

A recent study [21] compared the efficacy of $SrCl_2$ or Ca^{2+} ionophore on the activation rates of 3-day-old FF human oocytes and observed that the treatment with the ionophore was more efficient in activating aged unfertilized oocytes and embryo development to the blastocyst stage. However, these reports on the activation of FF oocytes do not reflect the real parthenogenetic embryonic development potential of the human oocyte as the studies mentioned earlier [11, 14, 15], because, in these last instances, there is a high probability that a paternal genome is present in the ooplasm, considering that IVF or ICSI was previously performed.

As an adjunct procedure in ART cycles, two intracellular Ca^{2+} releasing agents, $SrCl_2$, and ionomycin have been used aiming at activating oocytes during fertilization. In a series of nine cases of couples who have had total fertilization failure or very low fertilization rates in previous cycles, Kyono et al. [22] exposed oocytes soon after insemination by ICSI to chemical stimulation using $SrCl_2$. Fertilization rates increased from 21.7% in the previous cycles to 64.5% in the cycles using $SrCl_2$ artificial activation. Six pregnancies were established, four of which went to term. Five healthy children were born and their 1-year followup did not show any physical or neurological abnormality. In another study, the same group of authors employed the Ca^{2+} ionophore to activate zygotes generated by ICSI using globozoospermic sperm [23]. The alternative use of Ca^{2+} ionophore to activate the oocytes during fertilization and induce embryo development and gestation in cases of previous FF of human oocytes was also reported with relatively good success rates by other groups [24–27].

The exposure to $SrCl_2$ or Ca^{2+} ionophore may have induced the release and oscillations of intracellular Ca^{2+} needed for oocyte exit from the meiotic arrest and embryonic development [6, 9]. However, the putative epigenetic effects of this procedure demands caution and more research on the procedure. Also, the long-term followup of the children born by this methodology is necessary, before it can be considered as a routine methodology in human ART programs.

2.5. Oocyte Activation after In Vitro Maturation. In classical, stimulated ART cycles, immature germinal vesicle (GV) or metaphase I (MI) oocytes are commonly collected together with the mature MII. The immature oocytes may be submitted to *in vitro* maturation and ICSI to produce embryos for reproductive purposes. Resulting implantation and pregnancy rates are generally poor and there are controversies on whether to use these immature oocytes and embryos for reproductive purposes [28]. However, attempts to *in vitro* mature GV or MI oocytes obtained from stimulated ovaries may yield MII oocytes and potentially parthenotes, under suitable IVM conditions. Liu et al. [29] have shown that cryopreserved GV or MI oocytes collected from stimulated cycles yield good rates of high quality blastocysts, after insemination by ICSI and exposure to the activating agent

ethanol. Thus, immature oocytes collected from stimulated ovaries should not be neglected as an additional source of gametes for parthenogenetic activation. Research should focus on protocols devised specifically to improve their cytoplasmic and nuclear maturation to generate blastocysts with high quality ICMs.

On the other hand, IVM protocols to promote maturation of oocytes collected from unstimulated ovaries exist and they are employed in several fertility centers around the world, as an alternative to classical, stimulated cycles [30–32]. The present results show that implantation and gestation rates after IVM are close to those obtained in classical stimulated cycles. Thus, surplus immature oocytes obtained from IVM cycles or from oophorectomy, in patients who undergo sex reassignment surgery [33], for instance, may represent an important source of gametes for artificial parthenogenetic activation and blastocyst formation after exposure to adequate IVM conditions.

3. Genetic and Epigenetic Outcomes in Parthenogenetic Stem Cells

The uniparental origin of parthenogenetic SCs (pESCs) confers its great advantage of producing immunocompatible pESCs [34], an adequate alternative source of pluripotent SCs presenting the main features of biparental stem cells, for example, typical morphology, expression of the pluripotency markers, self-renewal, and cell fate determination [35]. Moreover, some lineages have been reported as homozygous for human leukocyte antigens and therefore may be useful for regenerative therapies for a large number of patients [36].

Many aspects related to the biology of these cell lines, however, still need to be elucidated. Probably one of the major concerns of using pESCs cell for regenerative medicine is the inability of parthenote mammal embryos to support full-term development. It is known already that the accurate establishment of epigenetic regulation and maintenance of genomic imprints during embryogenesis are essential for normal embryonic/placental development [37]. The genomic imprinting phenomenon is conserved amongst eutherian mammals [38, 39] and is believed to have an important role in the allocation of maternal resources to fetal growth [40, 41].

In parthenotes, the lack of sperm alleles leads to the transcription of both alleles of maternally expressed imprinted genes and the absence of paternally expressed imprinted genes, possibly causing the overexpression of imprinted genes often associated developmental abnormalities [42, 43]. Indeed, the importance of the parental origin of genes was demonstrated when Kono and collaborators [4] successfully produced viable parthenogenetic offspring in mice by correcting the imprinted genes Igf2/H19 dosage. Genetic manipulation of oocytes allowed authors to demonstrate the possibility of parthenote survival.

Although parthenogenetic embryos retain aberrant imprints and consequently cannot develop to term, established parthenogenetic ESCs were reported morphologically indistinguishable from ES derived from fertilized embryos and may also present normal gene expression or even correction genomic imprinting in chimeras, when pESCs were used in tissue contribution [44]. Hence, the possibility of using cells or tissues derived from parthenotes for therapeutic applications is still important and desired.

4. Parthenogenetic Stem Cells for Regenerative Medicine

Whereas bone marrow transplantation is an example of stem cell therapy that is in clinical use worldwide, the therapeutic use of pluripotent stem cells, such as human embryonic stem cells (hESCs) or phESCs, is still in its infancy. First clinical trials in the US using hESCs involved specific conditions such as macular degeneration [45]. The wider application of hESCs is limited due to their genetic background, which will most likely be divergent from a potential patient. phESCs may overcome this limitation presented by hESCs in autologous histocompatible transplantations, as they should be isogenic with the gamete donor. One particularly interesting characteristic of phESCs is the fact that they show frequent homozygosity in the major histocompatibility locus, which may allow efficient immune matching [46, 47]. Furthermore, detailed genetic analysis on five rhesus monkey pESC lines showed that high levels of heterozygosity are maintained at loci, which were polymorphic in the oocyte donors [36] (see Figure 2(B)). While no clinical trial has been reported so far, exciting findings on the potential therapeutic use in of pESCs have been reported in mice and primate experimental models. Espejel et al. [48] demonstrated that pESC differentiated into hepatocytes and provided normal liver function in adult mice with lethal liver failure due to deficiency of fumarylacetoacetate hydrolase (Fah). Also in mice, it has already been shown that pESC derivates supported long-term hematopoiesis [49] and integrated electrically into recipient myocardium, becoming functionally undistinguishable from the recipient cardiomyocytes [34]. Finally, primate pESCs that differentiated into dopamine neurons presented long-term survival after transplantation into brain (allograft), without any teratoma formation [50].

Taken together, these observations indicate that pESC lines have the potential to be used in regenerative medicine, not only for autologous transplantation into oocyte donors, but also for creation of a bank of histocompatible cell lines. However, the possibility of an interplay of epigenetic reprogramming on a monoparental background, together with the lack of paternal imprinted genes expression, cast caution on hpESCs therapeutic application. Thus, additional research is needed to ensure the safety of using parthenogenetically derived ESC lines in regenerative medicine.

4.1. Generation of Gametes from Stem Cells. Despite all the advances in infertility treatments since the birth of Louse Brown in 1978, one challenging situation that remains to be overcome by ART is the patients with complete absence of gametes or gonads, who cannot have their genetically related child. Presently, gamete donation is the available alternative for these patients to conceive their children. Unfortunately, a worldwide shortage of altruistic gamete donors has exposed

an increasing transaction of donor sperm and oocytes across borders [51]. This uncomfortable, sometimes ethically questionable, situation should be highly benefitted by advances on the generation of sperm and oocytes by manipulation of their progenitor cells or somatic cells [52].

Tesarik [53] proposed more than a decade ago the creation of haploid MII oocytes by introducing female somatic cell nuclei into enucleated MII oocytes. These gametes would undergo second polar body extrusion and haploidization *in vitro*, but fundamental limitations of chromosome segregation and imprinting relegated this methodology to the realm of the "fantastic" [54]. However, a recent report demonstrated that the use of a specific medium (4i) together with growth factors and Rho-kinase inhibitor for the culture of human embryonic stem cells and human induced pluripotent stem cells leads to the formation of embryo bodies, from which primordial germ-like cells were generated [55].

In another elegant study by Duggal et al. [56], the authors demonstrated that the synergism between inductive signals facilitates primordial germ cell, directed specification of embryonic stem cells followed by a premeiotic induction, in the presence of adequate IVM culture conditions.

These findings represent important steps towards the development of novel therapies in cases where patients are entirely devoid of viable gametes. Considering that *in vitro* differentiation of hpESCs has already provided completely different cell types [57, 58], the ability of these cells to generate primordial germ cells and mature oocytes may soon become a reality, which would represent an enormous gain in infertility treatments and related research areas.

5. Conclusion

It is clear from the information presented here that parthenogenetic activation of human oocytes rescued from infertility treatments results in embryos which are comparable to their biparental counterparts. The use of human parthenogenetic embryos as a source of cells for the generation of pluripotent stem cell lines is feasible and should be given more relevance in the present ESC research scenario. Considering the large number of oocytes discarded in infertility treatments [59], the *in vitro* differentiation of human parthenogenetically derived clinical grade stem cells shall produce a wide range of cell types, which will eventually have many clinical applications, including ART procedures.

Conflict of Interests

The authors declare that there is no conflict of interests regarding the publication of this paper.

Acknowledgments

The authors would like to thank Ms. Sandra Navarro Bresciani for the art work. This review was supported by CEPID-CTC from FAPESP 2013/08135-2.

References

[1] D. Crews, M. Grassman, and J. Lindzey, "Behavioral facilitation of reproduction in sexual and unisexual whiptail lizards," *Proceedings of the National Academy of Sciences of the United States of America*, vol. 83, no. 24, pp. 9547–9550, 1986.

[2] M. H. Kaufman, S. C. Barton, and M. A. H. Surani, "Normal postimplantation development of mouse parthenogenetic embryos to the forelimb bud stage," *Nature*, vol. 265, no. 5589, pp. 53–55, 1977.

[3] J. McGrath and D. Solter, "Completion of mouse embryogenesis requires both the maternal and paternal genomes," *Cell*, vol. 37, no. 1, pp. 179–183, 1984.

[4] T. Kono, Y. Obata, Q. Wu et al., "Birth of parthenogenetic mice that can develop to adulthood," *Nature*, vol. 428, no. 6985, pp. 860–864, 2004.

[5] S. D. Fleming, "IVF: the gold standard for assisted reproduction treatment," *Austin Journal of In Vitro Fertilization*, vol. 1, no. 2, pp. 1–2, 2014.

[6] D. Kline and J. T. Kline, "Repetitive calcium transients and the role of calcium in exocytosis and cell cycle activation in the mouse egg," *Developmental Biology*, vol. 149, no. 1, pp. 80–89, 1992.

[7] J. Kashir, M. Nomikos, K. Swann, and F. A. Lai, "PLCζ or PAWP: revisiting the putative mammalian sperm factor that triggers egg activation and embryogenesis," *Molecular Human Reproduction*, vol. 21, no. 5, pp. 383–388, 2015.

[8] A. Bos-Mikich, D. G. Whittingham, and K. T. Jones, "Meiotic and mitotic Ca^{2+} oscillations affect cell composition in resulting blastocysts," *Developmental Biology*, vol. 182, no. 1, pp. 172–179, 1997.

[9] A. Bos-Mikich, K. Swann, and D. G. Whittingham, "Calcium oscillations and protein synthesis inhibition synergistically activate mouse oocytes," *Molecular Reproduction and Development*, vol. 41, no. 1, pp. 84–90, 1995.

[10] A. Bos-Mikich, R. Ruggeri, J. L. Rodrigues, N. P. Oliveira, M. Croco, and P. H. Prak, "Employment oocyte disposal as a source of blastocysts parthenotes to generate stem cell lines with clinical grade human embryonic," *Jornal Brasileiro de Reprodução Assistida*, vol. 15, no. 3, pp. 38–40, 2011.

[11] R. R. Ruggeri, Y. Watanabe, F. Meirelles, F. F. Bressan, N. Frantz, and A. Bos-Mikich, "The use of parthenotegenetic and IVF bovine blastocysts as a model for the creation of human embryonic stem cells under defined conditions," *Journal of Assisted Reproduction and Genetics*, vol. 29, no. 10, pp. 1039–1043, 2012.

[12] R. R. Ruggeri, F. F. Bressan, N. M. Siqueira et al., "Derivation and culture of putative parthenogenetic embryonic stem cells in new gelatin substrates modified with galactomannan," *Macromolecular Research*, vol. 22, no. 10, pp. 1053–1058, 2014.

[13] T. A. L. Brevini and F. Gandolfi, "Parthenotes as a source of embryonic stem cells," *Cell Proliferation*, vol. 41, supplement 1, pp. 20–30, 2008.

[14] Q. Mai, Y. Yu, T. Li et al., "Derivation of human embryonic stem cell lines from parthenogenetic blastocysts," *Cell Research*, vol. 17, no. 12, pp. 1008–1019, 2007.

[15] E. S. Revazova, N. A. Turovets, O. D. Kochetkova et al., "Patient-specific stem cell lines derived from human parthenogenetic blastocysts," *Cloning and Stem Cells*, vol. 9, no. 3, pp. 432–449, 2007.

[16] K. S. Park, H. B. Song, and S. S. Chun, "Late fertilization of unfertilized human oocytes in in vitro fertilization and intracytoplasmic sperm injection cycles: conventional insemination versus ICSI," *Journal of Assisted Reproduction and Genetics*, vol. 17, no. 8, pp. 419–424, 2000.

[17] W. Kuczyski, M. Dhont, C. Grygoruk, P. Pietrewicz, S. Redzko, and M. Szamatowicz, "Rescue ICSI of unfertilized oocytes after IVF," *Human Reproduction*, vol. 17, no. 9, pp. 2423–2427, 2002.

[18] E. Lombardi, M. Tiverón, R. Inza, A. Valcárcel, E. Young, and C. Bisioli, "Live birth and normal 1-year follow-up of a baby born after transfer of cryopreserved embryos from rescue intracytoplasmic sperm injection of 1-day-old oocytes," *Fertility and Sterility*, vol. 80, no. 3, pp. 646–648, 2003.

[19] Z. O. Amarin, B. R. Obeidat, A. A. Rouzi, M. F. Jallad, and Y. S. Khader, "Intracytoplasmic sperm injection after total conventional in-vitro fertilization failure," *Saudi Medical Journal*, vol. 26, no. 3, pp. 411–415, 2005.

[20] S. F. Sneddon, P. A. Desousa, R. E. Arnesen, B. A. Lieberman, S. J. Kimber, and D. R. Brison, "Gene expression analysis of a new source of human oocytes and embryos for research and human embryonic stem cell derivation," *Fertility and Sterility*, vol. 95, no. 4, pp. 1410–1415, 2011.

[21] Y. Liu, X.-J. Han, M.-H. Liu et al., "Three-day-old human unfertilized oocytes after in vitro fertilization/intracytoplasmic sperm injection can be activated by calcium ionophore A23187 or strontium chloride and develop to blastocysts," *Cellular Reprogramming*, vol. 16, no. 4, pp. 276–280, 2014.

[22] K. Kyono, S. Kumagai, C. Nishinaka et al., "Birth and follow-up of babies born following ICSI using SrCl2 oocyte activation," *Reproductive BioMedicine Online*, vol. 17, no. 1, pp. 53–58, 2008.

[23] K. Kyono, Y. Nakajo, C. Nishinaka et al., "A birth from the transfer of a single vitrified-warmed blastocyst using intracytoplasmic sperm injection with calcium activation in a globozoospermic patient," *Fertility and Sterility*, vol. 91, no. 3, pp. e7–e11, 2009.

[24] Y. Murase, Y. Araki, S. Mizuno et al., "Pregnancy following chemical activation of oocytes in a couple with repeated failure of fertilization using ICSI: case report," *Human Reproduction*, vol. 19, no. 7, pp. 1604–1607, 2004.

[25] J. Pinto and J. H. Check, "Correction of failed fertilization despite intracytoplasmic sperm injection with oligoasthenoteratozoospermia but with acrosomes present by oocyte activation with calcium ionophore—case report," *Clinical and Experimental Obstetrics & Gynecology*, vol. 35, no. 4, pp. 252–254, 2008.

[26] E. Borges Jr., D. P. D. A. F. Braga, T. C. de Sousa Bonetti, A. Iaconelli Jr., and J. G. Franco Jr., "Artificial oocyte activation using calcium ionophore in ICSI cycles with spermatozoa from different sources," *Reproductive BioMedicine Online*, vol. 18, no. 1, pp. 45–52, 2009.

[27] J. H. Check, D. Summers-Chase, R. Cohen, and D. Brasile, "Artificial oocyte activation with calcium ionophore allowed fertilization and pregnancy in a couple with long-term unexplained infertility where the female partner had diminished EGG reserve and failure to fertilize oocytes despite intracytoplasmic sperm injection," *Clinical and Experimental Obstetrics & Gynecology*, vol. 37, no. 4, pp. 263–265, 2010.

[28] Y. Shu, J. Gebhardt, J. Watt, J. Lyon, D. Dasig, and B. Behr, "Fertilization, embryo development, and clinical outcome of immature oocytes from stimulated intracytoplasmic sperm injection cycles," *Fertility and Sterility*, vol. 87, no. 5, pp. 1022–1027, 2007.

[29] Y. Liu, Y. X. Cao, Z. G. Zhang, and Q. Xing, "Artificial oocyte activation and human failed-matured oocyte vitrification followed by in vitro maturation," *Zygote*, vol. 21, no. 1, pp. 71–76, 2013.

[30] A. Trounson, C. Wood, and A. Kausche, "In vitro maturation and the fertilization and developmental competence of oocytes recovered from untreated polycystic ovarian patients," *Fertility and Sterility*, vol. 62, no. 2, pp. 353–362, 1994.

[31] N. Frantz, A. Bos-Mikich, G. Frantz, M. Höher, and M. Ferreira, "Pregnancy after in vitro maturation of oocytes collected without hormonal stimulation in a patient with polycystic ovaries," *Jornal Brasileiro de Reprodução Assistida*, vol. 12, no. 1, pp. 45–47, 2008.

[32] T. Strowitzki, "In vitro maturation (IVM) of human oocytes," *Archives of Gynecology and Obstetrics*, vol. 288, no. 5, pp. 971–975, 2013.

[33] P. Imesch, D. Scheiner, M. Xie et al., "Developmental potential of human oocytes matured *in vitro* followed by vitrification and activation," *Journal of Ovarian Research*, vol. 6, no. 1, article 30, 2013.

[34] M. Didié, P. Christalla, M. Rubart et al., "Parthenogenetic stem cells for tissue-engineered heart repair," *The Journal of Clinical Investigation*, vol. 123, no. 3, pp. 1285–1298, 2013.

[35] T. A. L. Brevini, G. Pennarossa, M. de eguileor et al., "Parthenogenetic cell lines: an unstable equilibrium between pluripotency and malignant transformation," *Current Pharmaceutical Biotechnology*, vol. 12, no. 2, pp. 206–212, 2011.

[36] V. Dighe, L. Clepper, D. Pedersen et al., "Heterozygous embryonic stem cell lines derived from nonhuman primate parthenotes," *Stem Cells*, vol. 26, no. 3, pp. 756–766, 2008.

[37] F. F. Bressan, T. H. C. De Bem, F. Perecin et al., "Unearthing the roles of imprinted genes in the placenta," *Placenta*, vol. 30, no. 10, pp. 823–834, 2009.

[38] W. Dean and A. Ferguson-Smith, "Genomic imprinting: mother maintains methylation marks," *Current Biology*, vol. 11, no. 13, pp. R527–R530, 2001.

[39] A. Wagschal and R. Feil, "Genomic imprinting in the placenta," *Cytogenetic and Genome Research*, vol. 113, no. 1–4, pp. 90–98, 2006.

[40] W. Reik, M. Constância, A. Fowden et al., "Regulation of supply and demand for maternal nutrients in mammals by imprinted genes," *The Journal of Physiology*, vol. 547, no. 1, pp. 35–44, 2003.

[41] M. Constância, E. Angiolini, I. Sandovici et al., "Adaptation of nutrient supply to fetal demand in the mouse involves interaction between the Igf2 gene and placental transporter systems," *Proceedings of the National Academy of Sciences of the United States of America*, vol. 102, no. 52, pp. 19219–19224, 2005.

[42] H. Sritanaudomchai, H. Ma, L. Clepper et al., "Discovery of a novel imprinted gene by transcriptional analysis of parthenogenetic embryonic stem cells," *Human Reproduction*, vol. 25, no. 8, pp. 1927–1941, 2010.

[43] B. Daughtry and S. Mitalipov, "Concise review: parthenote stem cells for regenerative medicine: genetic, epigenetic, and developmental features," *Stem Cells Translational Medicine*, vol. 3, no. 3, pp. 290–298, 2014.

[44] T. Horii, M. Kimura, S. Morita, Y. Nagao, and I. Hatada, "Loss of genomic imprinting in mouse parthenogenetic embryonic stem cells," *Stem Cells*, vol. 26, no. 1, pp. 79–88, 2008.

[45] S. D. Schwartz, J.-P. Hubschman, G. Heilwell et al., "Embryonic stem cell trials for macular degeneration: a preliminary report," *The Lancet*, vol. 379, no. 9817, pp. 713–720, 2012.

[46] K. Kim, P. Lerou, A. Yabuuchi et al., "Histocompatible embryonic stem cells by parthenogenesis," *Science*, vol. 315, no. 5811, pp. 482–486, 2007.

[47] E. S. Revazova, N. A. Turovets, O. D. Kochetkova et al., "HLA homozygous stem cell lines derived from human parthenogenetic blastocysts," *Cloning and Stem Cells*, vol. 10, no. 1, pp. 11–24, 2008.

[48] S. Espejel, S. Eckardt, J. Harbell, G. R. Roll, K. J. Mclaughlin, and H. Willenbring, "Brief report: parthenogenetic embryonic stem cells are an effective cell source for therapeutic liver repopulation," *Stem Cells*, vol. 32, no. 7, pp. 1983–1988, 2014.

[49] S. Eckardt, N. A. Leu, H. L. Bradley, H. Kato, K. D. Bunting, and K. J. McLaughlin, "Hematopoietic reconstitution with androgenetic and gynogenetic stem cells," *Genes & Development*, vol. 21, no. 4, pp. 409–419, 2007.

[50] R. Sánchez-Pernaute, L. Studer, D. Ferrari et al., "Long-term survival of dopamine neurons derived from parthenogenetic primate embryonic stem cells (Cyno-1) after transplantation," *Stem Cells*, vol. 23, no. 7, pp. 914–922, 2005.

[51] B. C. Heng, "Legal and ethical issues in the international transaction of donor sperm and eggs," *Journal of Assisted Reproduction and Genetics*, vol. 24, no. 4, pp. 107–109, 2007.

[52] S. Hendriks, E. A. F. Dancet, A. M. M. van Pelt, G. Hamer, and S. Repping, "Artificial gametes: a systematic review of biological progress towards clinical application," *Human Reproduction Update*, vol. 21, no. 3, pp. 285–296, 2015.

[53] J. Tesarik, "Reproductive semi-cloning respecting biparental embryo origin: embryos from syngamy between a gamete and a haploidized somatic cell," *Human Reproduction*, vol. 17, no. 8, pp. 1933–1937, 2002.

[54] H. Tateno, K. E. Latham, and R. Yanagimachi, "Reproductive semi-cloning respecting biparental origin: a biologically unsound principle," *Human Reproduction*, vol. 18, no. 3, pp. 472–473, 2003.

[55] N. Irie, W. W. C. Tang, and M. A. Surani, "Germ cell specification and pluripotency in mammals: a perspective from early embryogenesis," *Reproductive Medicine & Biology*, vol. 13, no. 4, pp. 203–215, 2014.

[56] G. Duggal, B. Heindryckx, S. Warrier et al., "Exogenous supplementation of Activin A enhances germ cell differentiation of human embryonic stem cells," *Molecular Human Reproduction*, vol. 21, no. 5, pp. 410–423, 2015.

[57] R. Gonzalez, I. Garitaonandia, T. Abramihina et al., "Deriving dopaminergic neurons for clinical use: a practical approach," *Scientific Reports*, vol. 3, pp. 1463–1467, 2013.

[58] D. Paull, V. Emmanuele, K. A. Weiss et al., "Nuclear genome transfer in human oocytes eliminates mitochondrial DNA variants," *Nature*, vol. 493, no. 7434, pp. 632–637, 2013.

[59] K. E. Vrana, J. D. Hipp, A. M. Goss et al., "Nonhuman primate parthenogenetic stem cells," *Proceedings of the National Academy of Sciences of the United States of America*, vol. 100, no. 1, pp. 11911–11916, 2003.

Hindawi Publishing Corporation
Stem Cells International
Volume 2016, Article ID 2749461, 10 pages
http://dx.doi.org/10.1155/2016/2749461

Research Article

Improvement in Isolation and Identification of Mouse Oogonial Stem Cells

Zhiyong Lu,[1,2] Meng Wu,[1] Jinjin Zhang,[1] Jiaqiang Xiong,[1] Jing Cheng,[1] Wei Shen,[1] Aiyue Luo,[1] Li Fang,[1] and Shixuan Wang[1]

[1]*Department of Obstetrics and Gynecology, Tongji Hospital, Tongji Medical College, Huazhong University of Science and Technology, 1095 Jiefang Road, Wuhan, Hubei 430030, China*
[2]*Hubei Key Laboratory of Embryonic Stem Cell Research, Tai-He Hospital, Hubei University of Medicine, Shiyan, Hubei, China*

Correspondence should be addressed to Shixuan Wang; sxwang2012@hotmail.com

Received 13 April 2015; Revised 19 June 2015; Accepted 22 June 2015

Academic Editor: Irma Virant-Klun

Female germline stem cells (FGSCs) or oogonial stem cells (OSCs) have the capacity to generate newborn oocytes and thus open a new door to fight ovarian aging and female infertility. However, the production and identification of OSCs are difficult for investigators. Rare amount of these cells in the ovary results in the failure of the acquisition of OSCs. Furthermore, the oocyte formation by OSCs in vivo was usually confirmed using tissue sections by immunofluorescence or immunohistochemistry in previous studies. STO or MEF feeder cells are derived from mouse, not human. In our study, we modified the protocol. The cells were digested from ovaries and cultured for 2-3 days and then were purified by magnetic-activated cell sorting (MACS). The ovaries and fetus of mice injected with EGFP-positive OSCs were prepared and put on the slides to directly visualize oocyte and progeny formation under microscope. Additionally, the human umbilical cord mesenchymal stem cells (hUC-MSCs) were also used as feeder cells to support the proliferation of OSCs. The results showed that all the modified procedures can significantly improve and facilitate the generation and characterization of OSCs, and hUC-MSCs as feeder will be useful for isolation and proliferation of human OSCs avoiding contamination from mouse.

1. Introduction

Ovarian aging is characteristic of progressive decline of follicle reservoir, and thus women suffer aging-related health problem and psychological stress. Since 2004, the research of stem cells related with female germ cell commitment emerged, gradually increased, and became a hot spot [1–8]. Female germline stem cells (FGSCs) or oogonial stem cells (OSCs), first reported by Wu group and subsequently by Tilly group [9, 10], demonstrated the existence of a population of germline stem cells in postmammalian ovaries [11]. However, after the onset of isolation and identification of FGSCs/OSCs, the controversy against these observations continues to exist [12–15]. Perhaps this is firstly because no enough comprehensive evidence, especially regenerated oocytes or follicles in vivo from FGSCs/OSCs, was obtained to testify prior observations and challenge traditional paradigm and secondly because generation and characterization of FGSCs/OSCs-related complication hampered the new researchers into this field. For instance, only rare cells were acquired in the process of two-step enzymatic digestion of ovaries from mice, resulting in even minimal cells after magnetic-activated cell sorting (MACS) or fluorescence-activated cell sorting (FACS), which means that it is extremely hard to successfully establish oogonial stem cell lines. In addition, it is comparably difficult for newcomers to perform the experiments on the observation of differentiation into oocytes or progenies. Thus, we attempted to make some modification to facilitate these experiments [9, 10, 16, 17]. So the aim of our study is to facilitate the derivation and identification of OSCs, overcoming the difficulties on the way to obtain the OSC lines and to attract more researchers into the field. Only if more researchers work in this field and publish more comprehensive studies about OSCs, we can determine

the true nature of the OSCs to conclude the debate. Initially, we performed the MACS for cell suspension of ovarian tissue 2-3 days after culture of total population of dispersed cells from the digested ovaries; thus, there were more cells and more viable cells for sorting based on antibodies. In addition, 2-3-day culture after digestion can avoid further damage in the process of MACS and restore the viability of cells to some extent. Secondly, identifying the differentiation capacity of OSCs through immunofluorescence or immunohistology on consecutive sections greatly decreases the possibility and increases the difficulty to find the positive oocytes or follicles originating from EGFP-expressing OSCs. Therefore, we developed a novel method to directly visualize the fluorescence from EGFP-expressing oocytes or follicles under microscope. Briefly, the ovaries injected with EGFP-expressing OSCs were dissected; then, these ovaries were mechanically or enzymatically dispersed to release oocytes or follicles which were harvested together with remaining tissues to be visualized on the slides with a cover glass under fluorescence microscopy. Next, we found that the fetus at E12.0 can be visualized under fluorescence microscopy to verify if EGFP-positive mice are generated. This helps the investigators to obtain the outcomes of differentiation as fast as possible and does not need any expensive instruments like live imaging system. Finally, the human umbilical cord mesenchymal stem cells (hUC-MSCs) were employed to support the growth of OSCs, which aim to establish human OSC lines without any contamination from mouse. In brief, using these modifications, the isolation and identification can be easily finished, and the improvement will facilitate and prompt future researches on the oogonial stem cells.

2. Materials and Methods

2.1. Animals. Six-week-old C57BL/6 mice used in this study were purchased from the Center of Medical Experimental Animals of Hubei Province (Wuhan, China) and the Center of Experimental Animals of Chinese Academy of Medical Science (Beijing, China). All procedures involving animals were approved by the Animal Care and Use Committee of Tongji Medical College and were conducted in accordance with the National Research Council Guide for Care and Use of Laboratory Animals.

2.2. Isolation and Culture of OSCs. OSCs were isolated from 6-week-old mice using the methods described previously [9, 10, 16, 17]. Briefly, the ovaries from female mice were dissected and minced into slurry in the collagenase/Dnase I solution (Worthington, USA) and then incubated at 37°C for 20 minutes which was repeated once or followed by trypsin treatment for 5–10 min and finally the trypsin was neutralized by 10% fetal bovine serum (FBS). After centrifugation of suspension and removal of supernatant, the pellet was placed onto 6-well plate without STO feeder layer. Two or three days later, the cells were trypsinized and purified by MACS using Fragilis antibody and goat anti-rabbit IgG microbeads [18]. The sorted cells were cultured onto feeder cells with the medium which consisted of minimum essential medium α medium (MEM-α) (32561-102, Invitrogen), 10% FBS (06902, Stemcell), 1 mM sodium pyruvate (P2256-25, Sigma), 1 mM nonessential amino acids (11140-050, Gibco), 0.1 mM β-mercaptoethanol (ES-007-E, Millipore), 1000 units/mL LIF (ESG1106, Millipore), 1 ng/mL bFGF (13256-029, Gibco), 10 ng/mL EGF (PHG0311L, Gibco), 20 ng/mL human GDNF (212-GD-010, R&D), 1×-concentrated N2-supplement (AR009, R&D), and 1×-concentrated penicillin-streptomycin. Subculture of oogonial stem cells (OSCs) was performed according to reports published previously.

2.3. Culture and Preparation of STO Cell Line and hUC-MSCs. The OSCs were plated onto mitotically inactivated STO cell feeders from ATCC. STO cells were cultured in Dulbecco's modified Eagle's medium (DMEM) with high glucose (Life Technologies), supplemented with 1 mM nonessential amino acids (11140-050, Gibco), 2 mM glutamine, 30 mg/L penicillin, 75 mg/L streptomycin, and 10% FBS (Invitrogen), which was described in previous reports. To prepare STO cell feeder, the STO cells were first treated with mitomycin C (10 μg/mL, Sigma) for 2-3 hours and then washed with PBS and plated on 24-well plate.

Human umbilical cord mesenchymal stem cells (hUC-MSCs) were donated from Hubei Key Laboratory of Embryonic Stem Cell Research in Taihe hospital, and the medium preparation and cell culture were performed as described by them [19]. To prepare hUC-MSCs cell feeder, like STO cells, the hUC-MSCs of passages 3–5 were treated with mitomycin (10 μg/mL, Sigma) for 3 hours, washed, and plated on 24-well plate.

2.4. Immunofluorescence. OSCs were fixed with 4% paraformaldehyde for 15 min at room temperature and then incubated in blocking solution (10% normal goat serum in PBS) for 1 h at room temperature. Following the incubation at 37°C for 1 h with primary antibodies (rabbit polyclonal anti-MVH (1 : 200 dilution, ab13840, Abcam), rabbit polyclonal anti-Fragilis (1 : 500 dilution, ab15592, Abcam)), OSCs were incubated with FITC conjugated secondary antibody (goat anti-rabbit IgG, 1 : 1000 dilution) and then were stained by DAPI for 15 min.

2.5. Reverse Transcription-Polymerase Chain Reaction. Total RNA was extracted with RNAiso reagent (Takara, China) according to the manufacturer's instructions. Approximately 2 μg of RNA was treated by Dnase I to remove trace amounts of DNA contamination; then, the RNA was used to synthesize cDNA using transcriptor reverse transcriptase (transcriptor cDNA first strand synthesis kit, Roche) following the manufacturer's manual. Finally, the cDNA was performed for PCR amplification and the primers are listed in Table 1 with reference to other reports [9, 10].

2.6. Karyotype Analysis of OSCs. After 3 days of OSC passage, the cells were treated with OSC medium supplemented with 80 ng/mL colchicine for 3 h and were then hypotonically treated with 40 mM KCl for 30 min. Following the fixation

Table 1: Details regarding PCR primers used in RT-PCR for mouse ovary and OSCs.

Gene	Accession number	Product size (bp)	Primer sequence (5′-3′)
Gdf9	NM_008110	709	F: TGCCTCCTTCCCTCATCTTG R: CACTTCCCCCGCTCACACAG
Nobox	NM_130869	379	F: CCCTTCAGTCACAGTTTCCGT R: GTCTCTACTCTAGTGCCTTCG
Zp3	NM_011776	183	F: CCGAGCTGTGCAATTCCCAGA R: AACCCTCTGAGCCAAGGGTGA
Fragilis	NM_012013	151	F: GTTATCACCATTGTTAGTGTCATC R: AATGAGTGTTACACCTGCGTG
MVH	NM_010029	216	F: ACCCAGTTTGGTCATTCAGTTCG R: TTGTTCCTTTGATGGCATTCCTG
Prdm1	NM_007548	149	F: ACAGAATGGCAAGATCAAGTATGA R: GGTGGGCGAGCTGAGTAAAA
Tert	NM_009354	120	F: GCTTCCCTTTGACCAGCGTGTTA R: GCCTTTAGTGTCATTCCTGGATTCTT
Dazl	NM_010021	358	F: GTTAGGATGGATGAAACCGAAAT R: ATGCCTGAACATACTGAGTGATA
Gapdh	NM_008084	458	F: GTCCCGTAGACAAAATGGTGA R: TGCATTGCTGACAATCTTGAG

in methanol-acetic acid (3 : 1) for 1 h, the slides were stained with Giemsa buffer and observed under the microscope.

2.7. Self-Inactivation of Lentivectors in OSCs. To observe whether transduced OSCs were unable to produce infectious lentiviral particles, the infected OSCs with EGFP expression were seeded on 6-well plates and cultured to confluency without changing the medium. The supernatant was then collected and filtered through a 0.45 μm pore-sized polyethersulfone membrane, and 1 or 2 mL was incubated with wild-type OSCs without EGFP expression. Then, the EGFP expression of wild-type cells was observed.

2.8. Alkaline Phosphatase Staining. Alkaline phosphatase activity was assayed by AP detection kit (1101-050, SiDanSai, Shanghai, China) according to the manufacturer's instructions. Briefly, the cells cultured on the plates were fixed with 4% paraformaldehyde for 1-2 minutes and washed by PBS twice and then incubated by TBST solution. Finally, the AP staining solution was prepared with solutions A, B, and C according to instructions and then was added to the cells for 15 minutes. The cells were then observed under microscope.

2.9. OSCs Infection with Lentivirus Vector and Transplantation into Recipient Mice. The lentivirus vector expressing EGFP and its packaged virus particles were purchased from Genechem company (Shanghai, China). The established OSCs were infected according to the company's manual. At least 1 week after infection, the OSCs were trypsinized into cell suspension and about 1×10^4 cells were injected into each ovary of the recipient mice using Nanofil syringe (World Precision Instruments, USA) according to the protocol described previously [9, 16].

2.10. Southern Blotting. DNA probe for southern blotting was synthesized by PCR amplification from plasmid DNA carrying EGFP gene as template using the specific primers: 5′-ATGGTGAGCAAGGGCGAGG-3′ and 5′-CGTCCTCGATGTTGTGG-3′. The 523 bp amplification products were electrophoresed and purified. Digoxigenin labeling was done by using the DIG high prime DNA labeling and detection starter kit I (Roche). Genomic DNA was extracted from the tails of the progenies digested with PstI and the digested DNA samples of 25–30 μg were electrophoresed in 0.8% agarose gels. Plasmid DNA was used as positive control. The separated DNA fragments were transferred to 0.45 μm nylon membranes and fixed by UV cross-linking; then hybridization and stringency washes were carried out. Finally, the detection was performed using anti-Anti-Digoxigenin Alkaline phosphatase (AP) and its substrate with the above DIG detection kit (Roche) following the manufacturer's manual.

3. Results

3.1. Isolation and Long-Term Culture of OSCs. According to improved MACS method by Zou et al., we employed Fragilis as the marker for selection of OSCs [18]. If the dissected ovaries are enzymatically treated and MACS is promptly performed, the purification will likely fail considering that the harvested cells from digested ovaries are in considerably small amount and suffer further damage of their viability due to the two-step preparation including digestion and MACS. So, we cultured the digested cells from 6 ovaries for 2-3 days during which the total number of cells increased to 0.5–1 $\times 10^5$; then, these cells were used for MACS by antibody of Fragilis and finally 2–5 $\times 10^4$ cells (about 5%) flushed "positive cells" (including contaminated false-positive cells)

were obtained from the total cells. Then, these rare cells were cultured on the STO feeders for about 5–7 days in 24-well plates, and until the cells grew to confluence, they were prepared into cell suspension by trypsin and passaged onto a new 24-well plate with STO feeders. Usually after in vitro culture and proliferation for about 1 month, these purified putative OSCs can be established. The morphology of our established OSCs was the same as previous reports, which represented as ovoid and clustered cells with a large ratio of nuclear plasma (Figure 1(a)). After the OSCs were established in vitro for over 1 month, these cells were cultured in the absence of feeder cells, just like the report by Tilly et al. [10, 16].

3.2. Identification of OSCs for Gene Expression, Immunofluorescence, AP Staining, and Karyotyping. After the OSCs were established, these cells were subsequently identified for gene expression profile which displayed the cells having the characteristics of female germ cells, not oocytes (Figure 1(b)). The specific genes for oocytes including Gdf9, Nobox, and Zp3 showed that Gdf9 and Zp3 were weak positive to OSCs, which suggested that during the culture some OSCs have differentiated. The genes for germ cells including Fragilis, MVH, Prdm1, and Tert were positive to OSCs. To extend mRNAs analyses of MVH and Fragilis, which are classic primitive germline markers, proteins coded by both genes were detected and found to exhibit a pattern of membrane or plasma subcellular localization (Figure 1(c)), which agrees with previous reports. These OSCs showed positive staining for Alkaline phosphatase (AP) as compared to strong staining of mouse embryonic stem cells (mESCs) (Figure 1(d)). Finally, we performed karyotyping of the OSCs and the results displayed the normal karyotype in about 62% (Figures 1(e) and 1(f)).

3.3. Differentiation of OSCs into Oocytes, Follicles, and Progeny Formation. To confirm the oogenic capacity of these putative OSCs, they were stably transfected with a lentivirus EGFP-expressing vector (Figure 2(a)). Due to the concern about the remaining lentivirus particles in the OSCs which can contaminate the endogenous oocyte or follicle population in the ovary, we cultured these EGFP-OSCs and passaged them for at least 1 week to avoid the risk of contamination after successful transfection (most of cells expressed EGFP (Figure 2(b)), hereafter called EGFP-OSCs). At the same time, we conducted self-inactivation of EGFP-OSCs to verify whether these cells can still generate lentivirus particles and the results showed that no EGFP signals were detected in wild-type OSCs suggesting EGFP-OSCs did not generate virus particles. In addition, although most of the OSCs expressed EGFP after transfection, there was still a small amount of OSCs without EGFP expression. Subsequently, approximately 1×10^4 infected EGFP-OSCs were injected into the ovaries of recipient female mice pretreated with cyclophosphamide and busulphan or into the ovaries of wild-type mice. We collected ovaries for retrieval of oocytes and follicles at least 12 days after injection to detect the presence of EGFP-positive oocytes or follicles. These ovaries were slightly dissected and dispersed by needle and then put on the slides with coverslip and were directly visualized under fluorescence microscope. We successfully found some EGFP-expressing oocytes in the ovaries (Figure 2(c)). To our surprise, these EGFP-expressing oocytes were similar with primitive immature oocytes and mature oocytes or follicles were hardly detected by fluorescence. This is likely because EGFP expression was silent in the process of oocyte development in spite of the integration of EGFP gene into genomes of oocytes from OSCs and also because of the very weak signal in matured oocytes due to the pUbi promoter. Subsequently, the recipient female mice were mated with wild-type male mice, and at E12.0 fetuses were collected and placed onto the slides to observe the fluorescence under microscope. We easily found EGFP-positive as well as EGFP-negative samples mainly because fetuses at this stage were thoroughly transparent (Figures 2(d) and 2(e)); so we only need general microscope to distinguish the fetus integrated with EGFP. Finally, the progenies were obtained from the mated recipients which had a rate of 6–9 offspring per pregnant mouse. The genome DNA from the fetus and offspring, together with wild-type mice as negative control was extracted and PCR was performed to screen whether the exogenous EGFP gene was integrated into genome. The results showed that both the samples from fetus and offspring were EGFP-positive; however, the controls were all negative (Figures 3(a)–3(c)). Subsequently, the PCR products from the positive samples were extracted and sequenced, confirming the successful EGFP integration (data not shown). The southern blot analysis was performed to further confirm the integration of EGFP and showed five positive and one negative sample (Figure 3(d)). As shown in the southern blot, lanes 2 and 5 displayed fewer number of integration sites than lanes 1, 3, and 4, which suggested there were two types of transgenic structure in F1 offspring. To sum up, the results suggested that our established OSCs possess the capacity of differentiation into oocytes, ultimately resulting in the generation of progenies.

3.4. Comparison between STO and hUC-MSCs as Feeder Cells. To evaluate whether hUC-MSCs can serve as feeder cells, established OSCs were placed on respective STO and hUC-MSCs. After they proliferated at confluence at passage 2, they were harvested and RNA was extracted for reversed transcriptional PCR (RT-PCR) to examine their expression profiles. OSCs cultured on hUC-MSCs showed the nest-like colony morphology that was distinct from that cultured on STO (Figure 4(a)). However, OSCs on hUC-MSCs still retained germline expression pattern similar to OSCs on STO (Figure 4(b)), which showed that hUC-MSCs could be used as feeder layer for OSCs, especially for human OSCs, so that we can obtain human OSCs free of any mouse cellular contamination in the future.

4. Discussion

The presence and validation of FGSCs or OSCs are of significance for reproductive biology; therefore, some researchers

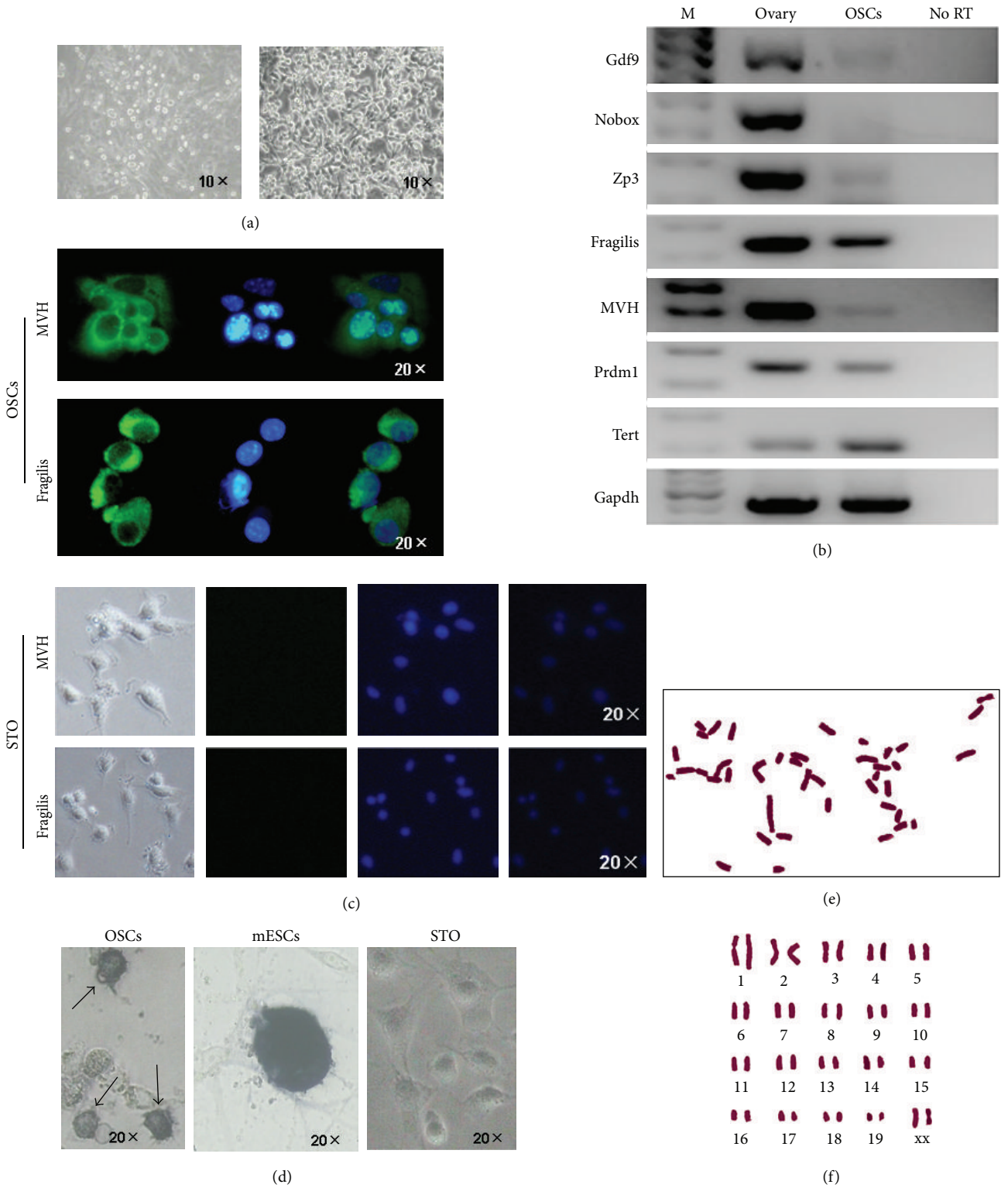

Figure 1: Morphology and characteristics of the established OSCs. (a) Overview of the OSCs immediately after MACS (left) and the established OSCs (right) which formed the typical structure of cell clusters. (b) Reverse transcriptional PCR analysis for expression profile of OSCs and ovarian tissues as the positive control. There were two set of genes: one for oocytes including Gdf9, Nobox, and Zp3 and another one for germ cells including Fragilis, MVH, Prdm1, and Tert, displaying that OSCs are characteristic of germ cells. No RT, PCR of RNA sample without reverse transcription. (c) Immunofluorescence for MVH and Fragilis in established OSCs and STO as negative control. Green, MVH, and Fragilis immunofluorescence; Blue, DAPI. At the bottom are the images (bright field, Green, DAPI, and merge) of STO from left to right. (d) Alkaline phosphatase staining for established OSCs, mESCs, and STO showed that OSCs (arrows) were positive, whereas mESCs were strongly positive. mESCs, mouse embryonic stem cells. (e-f) Cytogenetic analysis for established OSCs showed normal karyotype.

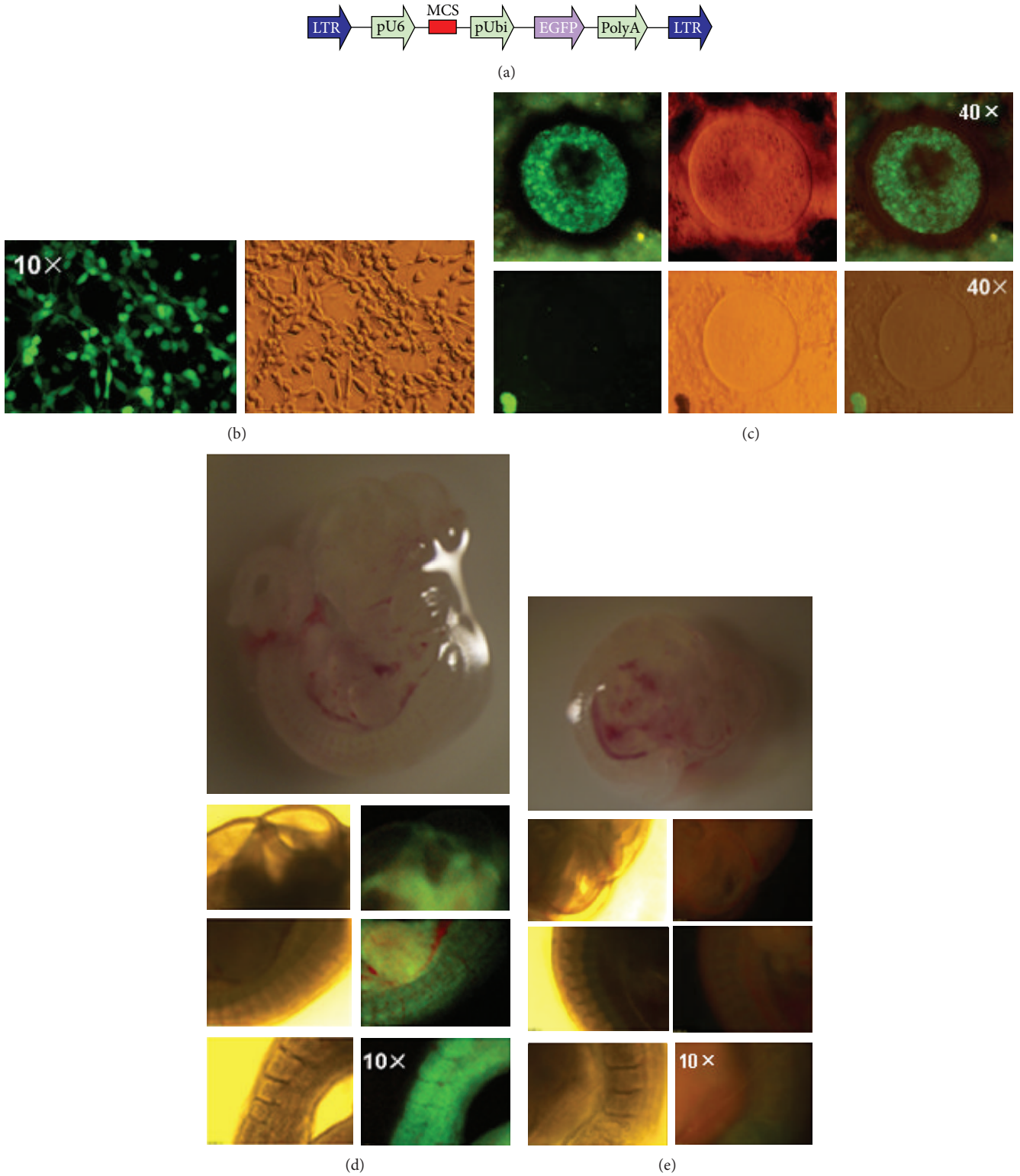

Figure 2: Transfection of OSCs and transplantation into ovaries of recipient mice. (a) Schematic diagram for the lentivirus vector with EGFP. LTR, long terminal repeat; pUbi, ubiquitin promoter. (b) Immunofluorescence-based analysis (right) and bright field view (left) of OSCs transfected with EGFP vector. (c) The ovaries from the recipient were dissected 12 days after injection with EGFP-expressing OSCs and the oocytes within these ovaries were visualized under fluorescence microscope. EGFP-positive oocyte (above) displayed fluorescence and the negative one (below) showed no fluorescence. (d, e) The fetuses from the mated recipients were obtained and observed under fluorescence microscope under the same exposure time. (d) On the top is the overview of the EGFP-positive fetus under stereoscope and at the bottom are the images from the head, body, and tail section showing fluorescence. (e) On the top is the EGFP-negative fetus under stereoscope and at the bottom are the images showing no signal in three sections under fluorescence microscope.

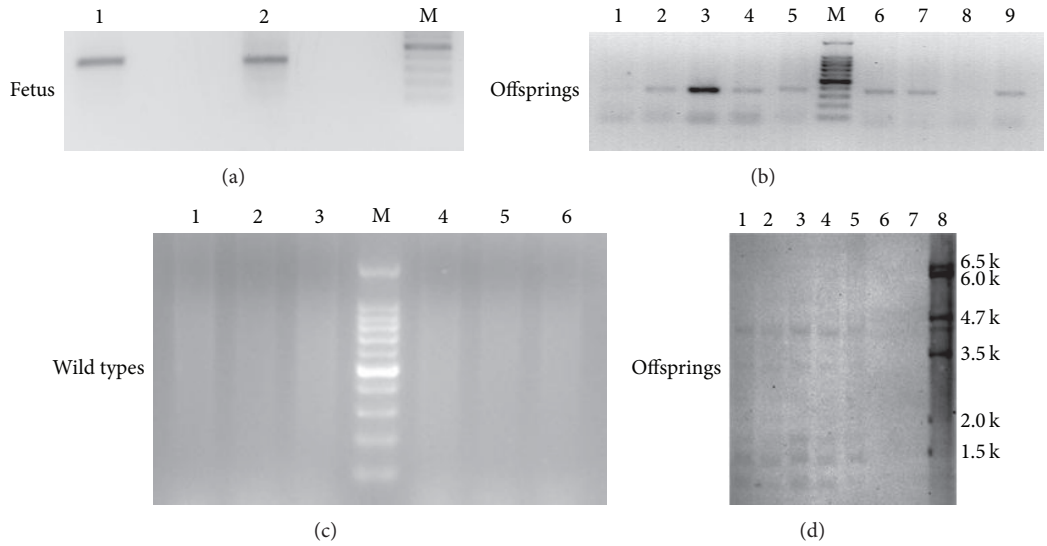

Figure 3: PCR for detection of EGFP gene integrated into the genomes of fetus and offspring. (a–c) Examples of PCR analysis of fetus, offspring and the wild types for detection of EGFP integrated into recipient genomes. There were positive outcomes of 366 bp PCR product in both fetus (a) and offspring (b), but no positive band was found in the wild types (c) which served as the negative control. (d) Southern blot analysis of tail DNA from six offspring, produced from the same recipient mouse and one wild type using a 523-bp PCR product from the control plasmid with primers for EGFP gene as a probe, showing five positive and one negative. Genomic DNA was digested with PstI. Size markers are indicated in the right of southern blot. Lanes 1–6, transgenic mice; lane 7, WT mouse; and lane 8, the control plasmid.

paid attention to whether or not oogenesis occurs from these stem cells in vivo in the adult mammalian ovary [12–15]. In return, supporters of OSCs also criticized their investigations by showing that various adult body organs possess two types of stem cells including active and also dormant stem cells [16, 20–23], which may suggest in vivo OSCs can represent the dormant state as well, resulting in no oogenesis. In addition, other types of germ stem cell in adult ovary have been reported which suggests the existence of niche for germ stem cell in ovary [24–29]. Factually, identification and isolation of FGSCs/OSCs clearly demonstrated their existence although the in vivo counterpart of OSCs showed no direct evidence for active differentiation into newborn follicles after birth. Practically, we could call this state of in vivo OSCs "silence" or "mitotically active state" rather than deny the existence of these cells [11]. Also, in vitro cultured OSCs have been a great tool to researchers; for instance, the OSCs were used for attempts in in vitro differentiation into oocytes [30], in generation of transgenic animals [31, 32], and in cell therapy [33]. Therefore, the isolation and related researches of OSCs should be prompted which will ultimately settle the controversy on this issue.

The reason for selection of 2-3 days after culture of dispersed ovarian tissues is that this period of time can enable the cells to not only restore its viability from the damage of prior treatment but also reach the optimum amount of cells for MACS. In addition, within 2-3 days, the cells can also retain the initial state to the maximal extent as in vivo. Alternatively, selective adhesion method can be chosen to remove large amount of granulosa cells and stromal cells, and this method can enable dispersed cells to proliferate for even longer time because the period of selective adhesion is usually about 7 days, and ultimately more putative OSCs can be obtained after MACS sorting.

The capacity of differentiation into oocytes and progeny is most relevant to the OSCs. However, previous studies observed and evaluated the oocytes and follicles formation all through consecutive sections and subsequent staining such as immunofluorescence. Although these methods effectively helped the investigators to reach their goals, yet it is not a unique choice compared with the method employed in our studies. It is more optimal if the EGFP fluorescence signal can be directly visualized under general fluorescence microscope. In our experiments, we indeed found some EGFP-expression oocytes; however, only few oocytes displayed the fluorescence signal. It is known that pUbi promoter drives weak expression of the downstream gene and that the expression of exogenous gene such as EGFP is complicated by the integrated location in the genome. If the CMV or other optimal promoters are to be used in this study, the EGFP expression can be easily detected and perhaps be observed in the majority of follicles in ovaries. Since the outcome from this method has some limitation, we should optimize the method to easily detect the EGFP-positive oocytes or follicles. In addition, due to the concern about the possible contamination from the virus particles generated from the transduced OSCs, we performed the test to verify whether these cells produced particles [34] and the results showed that the EGFP-positive oocytes detected cannot be false-positive because no fluorescence was observed by the wild-type cells as control. Finally, considering

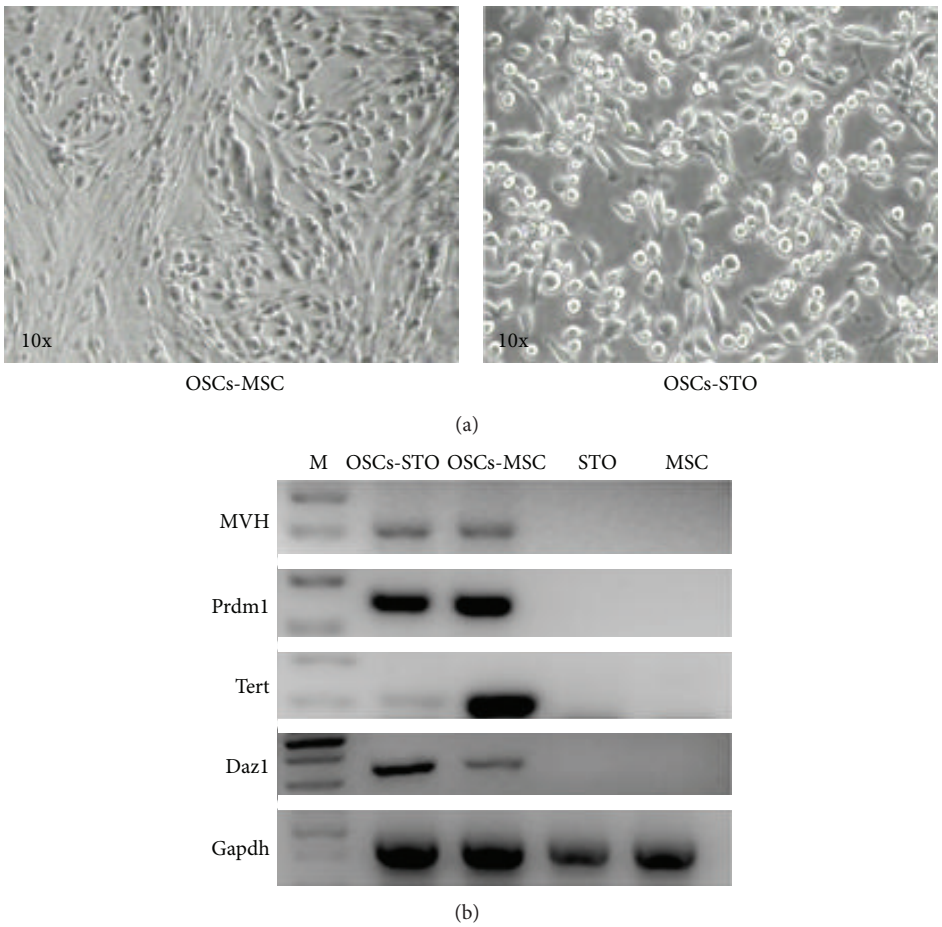

Figure 4: Comparison of STO and hUC-MSCs as feeder cells. (a) Morphological overview showed that OSCs cultured on the hUC-MSCs represented nest-like colonies (left), as compared to the typical cluster-like structures on STO (right). (b) RT-PCR analysis for gene expression profiles of OSCs cultured on STO and hUC-MSCs. The results displayed that, compared to STO feeder, OSCs on hUC-MSCs still retained the germ cell markers. STO and MSC, the negative controls for RT-PCR.

that we did not purify the transduced OSCs by FACS, the EGFP-OSCs invariantly included some untransduced OSCs whose oocytes could not express EGFP.

Likewise, the fetuses at E12.0 were selected to examine if EGFP-expressing progeny was produced because they are transparent and can be easily visualized under general fluorescence microscope. Indeed, to some extent, visualization of EGFP was more easy and more sensitive under fluorescence microscope than live imaging system. Moreover, this method is more convenient and can provide investigators with more confidence to perform their identification tests. However, the limitation from the weak promoter influenced the observation; thus, based on our experience, the fetus for fluorescence screening should be earlier than E12.0 because the size of fetus more than E12.0 usually becomes larger and therefore hardly transparent. In addition, EGFP expression is much complicated in transgenic animals resulting in no EGFP expression in some organs of offspring; however, all the organs of the fetus can be easily screened and thus do not suffer due to the limitation. Additionally, the fetuses were subsequently used for PCR screening. The results were consistent with the observation under fluorescence microscope. We also used the genome DNA extracted from the positive fetus for southern blot analysis in another study and found that it is as feasible as tail DNA from the offspring. In contrast to the PCR, southern blot analysis can supply detailed information about the genetic structure of the transgenic alteration, for example, transgene copy number and the number of integration sites within the genome. As shown in Figure 3(d), we found that multiple insertions occurred in offspring which suggested the successful integration of EGFP gene.

In summary, we demonstrated the modifications on the MACS selection and identification of mouse OSCs, including presort culturing for 2-3 days, and the direct visualization of EGFP-positive oocytes and fetus. In addition, hUC-MSCs as the feeder layer will be useful to the clinical application for human OSCs as well. Although there are restrictions in our study, the outcome of this study may facilitate the research

on the OSCs and attract more researchers into this field to make novel investigations to settle the remaining debate about OSCs.

Conflict of Interests

The authors declare that there is no conflict of interests regarding the publication of this paper.

Acknowledgments

This work was supported by grants from the National Natural Science Foundation of China (nos. 81300453, 81370469), Program of International Science and technology Cooperation of China (no. 2013DFA31400), and Hubei Provincial Department of Education (B2013111).

References

[1] J. Johnson, J. Canning, T. Kaneko, J. K. Pru, and J. L. Tilly, "Germline stem cells and follicular renewal in the postnatal mammalian ovary," *Nature*, vol. 428, no. 6979, pp. 145–150, 2004.

[2] J. Johnson, J. Bagley, M. Skaznik-Wikiel et al., "Oocyte generation in adult mammalian ovaries by putative germ cells in bone marrow and peripheral blood," *Cell*, vol. 122, no. 2, pp. 303–315, 2005.

[3] A. Bukovsky, M. Svetlikova, and M. R. Caudle, "Oogenesis in cultures derived from adult human ovaries," *Reproductive Biology and Endocrinology*, vol. 3, article 17, 2005.

[4] I. Virant-Klun, N. Zech, P. Rzŏman et al., "Putative stem cells with an embryonic character isolated from the ovarian surface epithelium of women with no naturally present follicles and oocytes," *Differentiation*, vol. 76, no. 8, pp. 843–856, 2008.

[5] I. Virant-Klun, P. Rožman, B. Cvjeticanin et al., "Parthenogenetic embryo-like structures in the human ovarian surface epithelium cell culture in postmenopausal women with no naturally present follicles and oocytes," *Stem Cells and Development*, vol. 18, no. 1, pp. 137–150, 2009.

[6] I. Virant-Klun, T. Skutella, M. Stimpfel, and J. Sinkovec, "Ovarian surface epithelium in patients with severe ovarian infertility: a potential source of cells expressing markers of pluripotent/multipotent stem cells," *Journal of Biomedicine and Biotechnology*, vol. 2011, Article ID 381928, 12 pages, 2011.

[7] A. Bukovsky, "Ovarian stem cell niche and follicular renewal in mammals," *The Anatomical Record*, vol. 294, no. 8, pp. 1284–1306, 2011.

[8] S. Parte, D. Bhartiya, J. Telang et al., "Detection, characterization, and spontaneous differentiation in vitro of very small embryonic-like putative stem cells in adult mammalian ovary," *Stem Cells and Development*, vol. 20, no. 8, pp. 1451–1464, 2011.

[9] K. Zou, Z. Yuan, Z. Yang et al., "Production of offspring from a germline stem cell line derived from neonatal ovaries," *Nature Cell Biology*, vol. 11, no. 5, pp. 631–636, 2009.

[10] Y. A. R. White, D. C. Woods, Y. Takai, O. Ishihara, H. Seki, and J. L. Tilly, "Oocyte formation by mitotically active germ cells purified from ovaries of reproductive-age women," *Nature Medicine*, vol. 18, no. 3, pp. 413–421, 2012.

[11] K. Hummitzsch, R. A. Anderson, D. Wilhelm et al., "Stem cells, progenitor cells, and lineage decisions in the ovary," *Endocrine Reviews*, vol. 36, no. 1, pp. 65–91, 2015.

[12] L. Lei and A. C. Spradling, "Female mice lack adult germline stem cells but sustain oogenesis using stable primordial follicles," *Proceedings of the National Academy of Sciences of the United States of America*, vol. 110, no. 21, pp. 8585–8590, 2013.

[13] H. Zhang, W. Zheng, Y. Shen, D. Adhikari, H. Ueno, and K. Liu, "Experimental evidence showing that no mitotically active female germline progenitors exist in postnatal mouse ovaries," *Proceedings of the National Academy of Sciences of the United States of America*, vol. 109, no. 31, pp. 12580–12585, 2012.

[14] H. Zhang, L. Liu, X. Li et al., "Life-long in vivo cell-lineage tracing shows that no oogenesis originates from putative germline stem cells in adult mice," *Proceedings of the National Academy of Sciences of the United States of America*, vol. 111, no. 50, pp. 17983–17988, 2014.

[15] J. Yuan, D. Zhang, L. Wang et al., "No evidence for neo-oogenesis may link to ovarian senescence in adult monkey," *Stem Cells*, vol. 31, no. 11, pp. 2538–2550, 2013.

[16] D. C. Woods and J. L. Tilly, "Isolation, characterization and propagation of mitotically active germ cells from adult mouse and human ovaries," *Nature Protocols*, vol. 8, no. 5, pp. 966–988, 2013.

[17] H. Wang, L. J. Shi, J. Xiang et al., "Isolation, culture and transplantation of female germline stem cells from neonatal and prepubertal mice," *Protocol Exchange*, 2013.

[18] K. Zou, L. Hou, K. Sun, W. Xie, and J. Wu, "Improved efficiency of female germline stem cell purification using fragilis-based magnetic bead sorting," *Stem Cells and Development*, vol. 20, no. 12, pp. 2197–2204, 2011.

[19] X. L. Wang, P. Hu, X. R. Guo et al., "Reprogramming human umbilical cord mesenchymal stromal cells to islet-like cells with the use of in vitro-synthesized pancreatic-duodenal homebox 1 messenger RNA," *Cytotherapy*, vol. 16, no. 11, pp. 1519–1527, 2014.

[20] D. Bhartiya, K. Sriraman, S. Parte, and H. Patel, "Ovarian stem cells: absence of evidence is not evidence of absence," *Journal of Ovarian Research*, vol. 6, no. 1, article 65, 2013.

[21] C. Aguilar-Gallardo, E. C. Rutledge, A. M. Martínez-Arroyo, J. J. Hidalgo, S. Domingo, and C. Simón, "Overcoming challenges of ovarian cancer stem cells: novel therapeutic approaches," *Stem Cell Reviews and Reports*, vol. 8, no. 3, pp. 994–1010, 2012.

[22] C. E. Dunlop, E. E. Telfer, and R. A. Anderson, "Ovarian stem cells—potential roles in infertility treatment and fertility preservation," *Maturitas*, vol. 76, no. 3, pp. 279–283, 2013.

[23] E.-S. Park and J. L. Tilly, "Use of DEAD-box Polypeptide-4 (DdX4) gene promoter-driven fluorescent reporter mice to identify mitotically active germ cells in post-natal mouse ovaries," *Molecular Human Reproduction*, vol. 21, no. 1, pp. 58–65, 2014.

[24] M. de Felici and F. Barrios, "Seeking the origin of female germline stem cells in the mammalian ovary," *Reproduction*, vol. 146, no. 4, pp. R125–R130, 2013.

[25] D.-M. Shin, M. Suszynska, K. Mierzejewska, J. Ratajczak, and M. Z. Ratajczak, "Very small embryonic-like stem-cell optimization of isolation protocols: an update of molecular signatures and a review of current in vivo applications," *Experimental & Molecular Medicine*, vol. 45, no. 11, article e56, pp. 125–130, 2013.

[26] S. Parte, D. Bhartiya, D. D. Manjramkar, A. Chauhan, and A. Joshi, "Stimulation of ovarian stem cells by follicle stimulating hormone and basic fibroblast growth factor during cortical tissue culture," *Journal of Ovarian Research*, vol. 6, no. 1, article 20, 2013.

[27] D. Bhartiya, S. Unni, S. Parte, and S. Anand, "Very small embryonic-like stem cells: Implications in reproductive biology," *BioMed Research International*, vol. 2013, Article ID 682326, 10 pages, 2013.

[28] I. Virant-Klun, T. Skutella, M. Hren et al., "Isolation of small SSEA-4-positive putative stem cells from the ovarian surface epithelium of adult human ovaries by two different methods," *BioMed Research International*, vol. 2013, Article ID 690415, 15 pages, 2013.

[29] I. Virant-Klun, T. Skutella, M. Kubista, A. Vogler, J. Sinkovec, and H. Meden-Vrtovec, "Expression of pluripotency and oocyte-related genes in single putative stem cells from human adult ovarian surface epithelium cultured in vitro in the presence of follicular fluid," *BioMed Research International*, vol. 2013, Article ID 861460, 18 pages, 2013.

[30] E.-S. Park, D. C. Woods, and J. L. Tilly, "Bone morphogenetic protein 4 promotes mammalian oogonial stem cell differentiation via Smad1/5/8 signaling," *Fertility and Sterility*, vol. 100, no. 5, pp. 1468.e2–1475.e2, 2013.

[31] L. Zhou, L. Wang, J. X. Kang et al., "Production of fat-1 transgenic rats using a post-natal female germline stem cell line," *Molecular Human Reproduction*, vol. 20, no. 3, pp. 271–281, 2014.

[32] Y. Zhang, Z. Yang, Y. Yang et al., "Production of transgenic mice by random recombination of targeted genes in female germline stem cells," *Journal of Molecular Cell Biology*, vol. 3, no. 2, pp. 132–141, 2011.

[33] P. Terraciano, T. Garcez, L. Ayres et al., "Cell therapy for chemically induced ovarian failure in mice," *Stem Cells International*, vol. 2014, Article ID 720753, 8 pages, 2014.

[34] D. M. Suter, L. Cartier, E. Bettiol et al., "Rapid generation of stable transgenic embryonic stem cell lines using modular lentivectors," *Stem Cells*, vol. 24, no. 3, pp. 615–623, 2006.

Hindawi Publishing Corporation
Stem Cells International
Volume 2016, Article ID 4148923, 14 pages
http://dx.doi.org/10.1155/2016/4148923

Research Article

The Paracrine Effect of Transplanted Human Amniotic Epithelial Cells on Ovarian Function Improvement in a Mouse Model of Chemotherapy-Induced Primary Ovarian Insufficiency

Xiaofen Yao, Yuna Guo, Qian Wang, Minhua Xu, Qiuwan Zhang, Ting Li, and Dongmei Lai

The Center of Research Laboratory and Department of Gynecology, The International Peace Maternity and Child Health Hospital, School of Medicine, Shanghai Jiaotong University, Shanghai 200030, China

Correspondence should be addressed to Dongmei Lai; laidongmei@hotmail.com

Received 13 February 2015; Accepted 30 March 2015

Academic Editor: Irma Virant-Klun

Human amnion epithelial cells (hAECs) transplantation via tail vein has been reported to rescue ovarian function in mice with chemotherapy-induced primary ovarian insufficiency (POI). To test whether intraperitoneally transplanted hAECs could induce therapeutic effect and to characterize the paracrine effect of transplanted hAECs, we utilized a chemotherapy induced mice model of POI and investigated the ability of hAECs and conditioned medium collected from cultured hAECs (hAECs-CM) to restore ovarian function. We found that transplantation of hAECs or hAECs-CM either 24 hours or 7 days after chemotherapy could increase follicle numbers and partly restore fertility. By PCR analysis of recipient mice ovaries, the presence of SRY gene was only detected in mice transplanted with male hAECs 24 hours following chemotherapy. Further, the gene expression level of VEGFR1 and VEGFR2 in the ovaries decreased, although VEGFA increased 2 weeks after chemotherapy. After treatment with hAECs or hAEC-CM, the expression of both VEGFR1 and VEGFR2 increased, consistent with the immunohistochemical analysis. In addition, both hAECs and hAECs-CM treatment enhanced angiogenesis in the ovaries. The results suggested that hAECs-CM, like hAECs, could partly restore ovarian function, and the therapeutic function of intraperitoneally transplanted hAECs was mainly induced by paracrine-mediated ovarian protection and angiogenesis.

1. Introduction

Primary ovarian insufficiency (POI), which used to be defined as premature ovarian failure or primary ovarian failure, is a subclass of ovarian dysfunction that has been caused by damage within the ovary [1]. POI is characterized by the triad of amenorrhoea, increased secretion of gonadotropins, and diminished production of estrogen under the age of 40 years. Chemotherapy for cancer has been suggested to be associated with POI. Ovarian tissue will often show follicle loss, cortical fibrosis, and vascular damage after chemotherapy by histologic examination [2–4]. Alkylating agents (such as cyclophosphamide) and busulfan appear to be high risk for inducing gonadotoxicity [5]. We used mice sterilized by intraperitoneal injection of busulphan and cyclophosphamide (Bu/Cy) to establish an infertile mice model [6].

Developed from the epiblast 8 days after fertilization and before gastrulation, human amniotic epithelial cells (hAECs) might maintain the plasticity of pregastrulation embryo cells. hAECs have been demonstrated to maintain the capability to differentiate into liver (endoderm), pancreas (endoderm), cardiomyocyte (mesoderm), and neural cells (ectoderm) *in vitro* [7]. Pluripotency, low immunogenicity, few ethical problems with usage, and nontumorigenicity make hAECs a useful source of stem cells for cell transplantation and regenerative medicine [8]. Transplanted hAECs have been shown to improve cardiac function in a rat model of myocardial infarction via injection of hAECs into the infarction area [9]. And intraperitoneal administration of hAECs into lung-injured mice decreased pulmonary fibrosis, reduced structural lung damage, and preserved lung function [10, 11]. Our previous study suggested that intravenously

injected hAECs could transdifferentiate into granulose cells and restore folliculogenesis in a POI mouse model [12]. However, it is not clear whether hAECs could restore ovarian function through paracrine effects.

Vascular endothelial growth factor A (VEGFA) plays an important role in the regulation of angiogenesis in the ovary [13]. Although VEGFA is most well known as an angiogenic factor, it is also involved in many key events in the course of an ovulatory cycle, including follicular growth, ovulation, and corpus luteum development [14]. *In vivo*, the number of primary and secondary follicles increased after injection of VEGF into rat ovaries [15]. In addition, both the antrum formation rate and the progression of meiosis to the MII stage were enhanced after adding VEGFA to the culture medium of caprine preantral follicles [16]. What is more, though inhibition of both VEGFR1 and VEGFR2 could reduce both vascular and follicle development, inhibition of VEGFR2 blocks follicle progression but does not necessarily disrupt vascular development in perinatal rat ovaries, which suggests that VEGFA and its receptors could potentially be involved in nonangiogenic and angiogenic mechanisms in the regulation of follicle development [17].

Herein we investigated if hAECs transplantation could restore Bu/Cy-damaged ovarian function by intraperitoneal administration and whether the therapeutic efficacy is mediated by the paracrine effect. We also detected the expression of VEGFA and its receptors in the mice ovaries induced by Bu/Cy administration and analyzed the effects of transplanted hAECs and factors secreted by hAECs on the ovarian angiogenesis.

2. Materials and Methods

2.1. Isolation and Culture of hAECs. Male hAECs were isolated and cultured as described previously [12]. In brief, discarded placentas from male fetus were obtained at term pregnancy during uncomplicated caesarean sections with written informed consent from woman who tested negative for HIV-I and hepatitis B and C. The indication for caesarean section is breech presentation, repeat operation, fetal distress, and twins. The institutional ethics committee approved the use of human amnions for this project.

After mechanically peeled from the chorionic portion of the placenta, the amniotic membrane, which looks like a translucent sheet, was placed in 250 mL flasks containing Dulbecco's modified eagle medium (DMEM)/F12. After cut with a razor to yield 0.5 to 1.0 cm^2 segments, the placental segments were digested with 0.25% trypsin/EDTA at 37°C for 45 min. Centrifuged at 250 ×g for 5 minutes at 25°C, the cells were resuspended with PBS after the supernatant was discarded. Then after being filtered through a 100 μm cell strainer, washed with PBS once, and resuspended, the resulting cell suspensions were seeded in a six-well plate in DMEM/F12 medium supplemented with 10% fetal bovine serum (FBS, Gibco, Grand Island, NY, USA), streptomycin (100 U/mL; Gibco), penicillin (100 U/mL; Gibco), and glutamine (0.3 mg/mL; Gibco) and incubated at 37°C 5% CO_2 in humidified air. Once hAECs reached 80 to 90% confluence, cells were ready for experiments.

2.2. Immunofluorescence Staining. hAECs were fixed with 4% paraformaldehyde for 20 minutes at room temperature and then washed twice (5 minutes each) with PBS. Cells were permeabilized with 0.1% Triton X-100 for 10 minutes at room temperature and then washed twice with 1 × PBS. Then cells were blocked with blocking solution for 30 minutes and incubated overnight at 4°C with anti-Cytokeratin 18 (mouse anti-human 1 : 200, Boster, Wuhan, China), anti-CD34 antibody (rabbit anti-human 1 : 100, Abcam, Cambridge, MA, USA), and anti-Vimentin (rabbit anti-human 1 : 100, Cell Signaling Technology, Danvers, MA, USA). Washed three times with PBS, the cells were probed with FITC-labeled IgG (1 : 200, Santa Cruz, CA, USA) or Rhodamine- (TRITC-) labeled IgG (1 : 100, Invitrogen, CA, USA). Fluorescence images were obtained with a Leica DMI3000 microscope (Heidelberg, Germany).

2.3. Preparation of Conditioned Medium (CM) from Cultured hAECs. The CM of hAECs was prepared according to a protocol described previously by Yang et al. [18], with minor modifications. Eighty percent of confluent hAECs were washed with PBS twice and then fed with serum-free medium for 24 hours. The medium was then collected and used for *in vivo* experiments. For each animal, we used CM generated by 4×10^6 hAECs. The CM was centrifuged at 300 g for 5 minutes and sterilized through a 220 nm filter. The collected CM was concentrated using Amicon Ultra-15 centrifugal filter units (3 kDa cut-off; Millipore).

2.4. Animals. Six-week-old female C57BL/6 wild-type mice were purchased from Shanghai SLAC Laboratory Animal Co., Ltd. All animals were maintained on 12-hour light/dark cycles with food and water available ad libitum. To establish the POI model of chemotherapy-induced ovarian damage, a total of 85 mice used as recipients were sterilized by one intraperitoneal (IP) injection of Bu/Cy (busulphan, 30 mg/kg, and cyclophosphamide, 120 mg/kg, both resuspended in DMSO) [6]. All procedures involving animals were approved by the Institutional Animal Care and Use Committee of Shanghai and were conducted in accordance with the National Research Council Guide for Care and Use of Laboratory Animals. After injection, Bu/Cy-treated and control animals were weighed twice a week at 9 a.m.

2.5. IP Injection of hAECs and hAECs-CM. The C57BL/6 wild-type mice were randomly divided into six groups. The normal control mice received no treatment ($n = 20$). In the Bu/Cy group, the mice were administered Bu/Cy only ($n = 15$). In the Bu/Cy + hAECs (24 h) group ($n = 20$), mice received Bu/Cy administration and then an IP transplantation of 4×10^6 hAECs in a volume of 0.2 mL PBS 24 h later. In the Bu/Cy + hAECs-CM (24 h) group ($n = 15$), mice received Bu/Cy administration and then an IP injection of 0.2 mL CM generated by 4×10^6 hAECs 24 h later. In the Bu/Cy + hAECs (7 d) group ($n = 20$), mice received

Table 1: Primers sequence for real-time PCR (hAECs).

Gene		Primer sequence $5' \rightarrow 3'$	Amplicon size (bp)
Oct4	Forward	GGCCCGAAAGAGAAAGCGAACC	224
	Reverse	ACCCAGCAGCCTCAAAATCCTCTC	
Nanog	Forward	TTCCTTCCTCCATGGATCTG	213
	Reverse	TCTGCTGGAGGCTGAGGTAT	
SOX2	Forward	GCCGAGTGGAAACTTTTGTC	264
	Reverse	GTTCATGTGCGCGTAACTGT	
E-cadherin	Forward	TGAGCTTGCGGAAGTCAGTT	219
	Reverse	ACCGTGAACGTGTAGCTCT	
N-cadherin	Forward	CGCCATCCGCTCCACTT	227
	Reverse	GGACTCGCACCAGGAGTAAT	
Vimentin	Forward	CTCTGGCACGTCTTGACCTT	231
	Reverse	ACCATTCTTCTGCCTCCTGC	
CK19	Forward	CCTACAGCTATCGCCAGTCG	243
	Reverse	TGGTTAGCTTCTCGTTGCCC	
Snail	Forward	CTCGGACCTTCTCCCGAATG	223
	Reverse	TCATCAAAGTCCTGTGGGGC	
Beta-actin	Forward	TCGCCTTTGCCGATCC	202
	Reverse	GAATCCTTCTGACCCATGCC	

Bu/Cy administration and then an IP transplantation of 4×10^6 hAECs 7 days later. In the Bu/Cy + hAECs-CM (7 d) group ($n = 15$), mice received Bu/Cy administration and then an IP injection of CM generated by 4×10^6 hAECs 7 days later. The administration of hAECs or hAECs-CM was repeated the following day. While five mice in each group were kept for mating experiments, the other mice were culled either 14 or 28 days following Bu/Cy administration or the second treatment. The bilateral ovaries were collected from each animal for analysis.

2.6. Mating Experiment. The control mice, Bu/Cy-treated only mice, and mice treated with Bu/Cy and then hAECs or hAECs-CM were housed with C57BL/6 male mice one month after chemotherapy. Adult males of proven fertility were housed with females at a ratio of 1 : 2. The number of litters per pregnancy was recorded.

2.7. Ovarian Follicle Counts and Morphologic Analysis. One month after treatment, the ovaries were collected and the follicles were detected and classified. The removed ovaries were fixed in 4% paraformaldehyde for at least 24 hours. After fixation, the ovaries were dehydrated, paraffin-embedded, serially sectioned at 5 μm, and mounted on glass microscope slides. Routine hematoxylin and eosin (H&E) staining was performed for histologic examination with light microscopy. Primordial, primary, secondary, and antral follicles were counted in every fifth section. Only follicles containing an oocyte were counted to avoid counting any follicle twice. Follicles were classified as follows: primordial follicle, oocyte surrounded by a single layer of squamous granulosa cells; primary follicle, intact enlarged oocyte with a visible nucleus and one layer of cuboidal granulosa cells; secondary follicle, more than one layer of cuboidal granulosa cells without antral space; antral follicles (including preovulatory follicles), emerging antral spaces [19].

2.8. Real-Time Quantitative PCR. The hAECs cells were collected when the cells reached 80 to 90% confluence. And ovarian samples were collected 2 weeks after last treatment. Then total RNA was isolated from the ovarian samples and 500 ng of total RNA from each sample was reverse transcribed using the primescript RT reagent kit (Takara Bio Inc., Shiga, Japan). Real-time PCR was performed on cDNA using SYBR Premix Ex Taq (Takara) on the Mastercycler ep realplex (Eppendorf, Hamburg, Germany). All reactions were carried out in triplicate, using a 25 μL volume. In brief, PCR amplification was carried out using an initial denaturation at 95°C for 5 min, followed by 40 cycles for 30 sec at 95°C, 30 sec at 60°C, and 30 sec at 72°C. A sample lacking template DNA was used as a negative control. The primers for the genes are provided in Tables 1 and 2.

2.9. Immunohistochemical Analysis. Ovaries from treated and control animals were fixed, dehydrated, vitrified, and embedded in paraffin. The ovarian sections (5 μm thick) were deparaffinized with xylene and hydrated using an ethanol gradient. The hydrated sections were washed in 3% hydrogen peroxide in methanol for 20 min at room temperature and blocked in PBS (Sigma) containing 3% BSA (Sigma) for 30 min. Sections were treated with primary antibodies including rabbit anti-CD34 antibody (1 : 200; Abcam, Cambridge, MA, USA), rabbit anti-VEGFA antibody (1 : 50; Abcam), rabbit anti-VEGFR1 antibody (1 : 200; Cell Signaling Technology, Danvers, MA, USA), or rabbit anti-VEGFR2 antibody (1 : 200; Abcam) for antibody detection

Table 2: Primers sequence for real-time PCR (mice ovaries).

Gene		Primer sequence 5′ → 3′	Amplicon size (bp)
VEGFA	Forward	GCAGCGACAAGGCAGACTAT	169
	Reverse	AACCTCCTCAAACCGTTGGC	
VEGFR1	Forward	TCAAGCTAGAGGTGTCCCCG	152
	Reverse	CTCGGCACCTATAGACACCC	
VEGFR2	Forward	GGCGGTGGTGACAGTATCTT	152
	Reverse	GAGGCGATGAATGGTGATCT	
Beta-actin	Forward	TGGCTCCTAGCACCATGAAG	193
	Reverse	AACGCAGCTCAGTAACAGTCC	

at 4°C overnight. After washing, slides were then incubated with HRP labeled anti-rabbit antibody (Peroxidase reaction kits, Vector Laboratories, Burlingame, CA, USA). Peroxidase substrate was developed by using a DAB (3,39-diaminobenzidine) substrate kit (Vector Laboratories). Slides were counterstained with hematoxylin QS (Vector Laboratories) and were dehydrated and mounted with VectaMount Permanent Mounting Medium (Vector Laboratories).

2.10. Determination of Microvessel Density (MVD). Angiogenesis was measured by MVD, which was assessed by light microscopic analysis (400×) for areas of the sections containing the most microvessels. Two independent researchers who were blinded to the experimental conditions were assigned to observe and calculate the MVD in five sections at ten sections intervals. Microvessel was defined as a brown-staining endothelial cell cluster with incomplete CD34+ endothelial cell–cell contact. The microvessel numbers from the five sections were counted and calculated for the mean number of microvessels per ovary [20]. Further, sections from five ovaries of each group were investigated for the average MVD.

2.11. PCR Analysis. To predict whether hAECs from male fetus placentas could migrate to the mouse ovaries, a multiplex PCR for amplification of the Y-specific *SRY* sequences was done as suggested by Tungwiwat et al. [21], with little modification. Ovarian DNA was extracted using the TIANamp Genomic DNA Kit (TIANGEN, China) with the protocol supplied by the manufacturer. The *SRY*-specific sequence was amplified firstly by PCR primer pair, Y1.5 (5′-CTAGACCGCAGAGGCGCCATC-3′) and Y1.6 (5′-TAGTACCCACGCCTGCTCCGG-3′). Using the first PCR product as a template, the SRY-specific sequence was amplified by another primer pair Y1.7 (5′-CATCCAGAGCGTCCCTGGCTT-3′) and Y1.8 (5′-CTTTCCACAGCCACATTTGTC-3′). Ten microliters of each product was analyzed on a 2% agarose gel electrophoresis and visualized under UV light after ethidium bromide staining. The nested Y-specific fragment *SRY* gene was 198 bp in length [21]. Identifications of the Y-specific sequences in hAECs from male and female fetus placentas were used as positive and negative controls. Ovarian DNA of female mice without hAECs injection was also used as template for negative control.

2.12. Data Analysis and Statistics. Data were expressed in each experimental group as mean ± SEM. Statistical significance was determined by statistical analysis software (GraphPad Prism, GraphPad Software Inc., USA) and evaluated with Student's *t*-test. Statistical significance was accorded when $P < 0.05$.

3. Results

3.1. Characterization of Isolated hAECs. Under light microscope, the hAECs formed confluent cobblestone-shaped monolayer epithelial cells (Figure 1(a)). To examine the stem cell specific genes and epithelial gene in hAECs, real-time PCR was done. Consistent with previous studies [7], we found that the isolated AE cells expressed *Oct-4, Nanog,* and *Sox2*, which are all involved in cellular pluripotency [22–24]. In addition, we detected the expression of epithelial (*Cytokeratin 19* (*CK19*) and *E-cadherin*) and mesenchymal (*N-cadherin, Vimentin,* and *Snail*) markers in cultured cells. As shown in Figure 1(c), both *E-cadherin* and *Cytokeratin 19* were highly expressed in cultured hAECs cells. Comparatively, mRNA expression of mesenchymal cell marker, including *N-cadherin* and *Vimentin,* was low and the expression of *Snail* gene was scarcely detected.

To further identify the purity of the freshly isolated hAECs, immunofluorescence staining was done. The cells were clarified with positive staining against Cytokeratin 18 and negative for CD34 and Vimentin (Figure 1(d)). Almost all freshly isolated hAECs were Cytokeratin positive. Simultaneously, no CD34 staining was observed, which indicated that the isolates are not contaminated with hematopoietic stem cells such as umbilical cord blood or embryonic fibroblasts. Meanwhile, absence of Vimentin suggested that the hAECs were not contaminated with mesenchymal cells from amniotic membrane.

3.2. Effect of hAECs and hAECs-CM Treatment after Bu/Cy Administration on Body Weight. To assess the effect of human hAECs and hAECs-CM on total body weight, wild-type female mice were sterilized by pretreatment with Bu/Cy and then intraperitoneally administrated with hAECs or hAECs-CM. Compared to normal control mice, administration of Bu/Cy resulted in a significant reduction in body weight over 7 days (18.72 ± 0.33 g versus 17.07 ± 0.26 g, $P < 0.01$, Figures 2(a) and 2(b)). No significant difference was observed

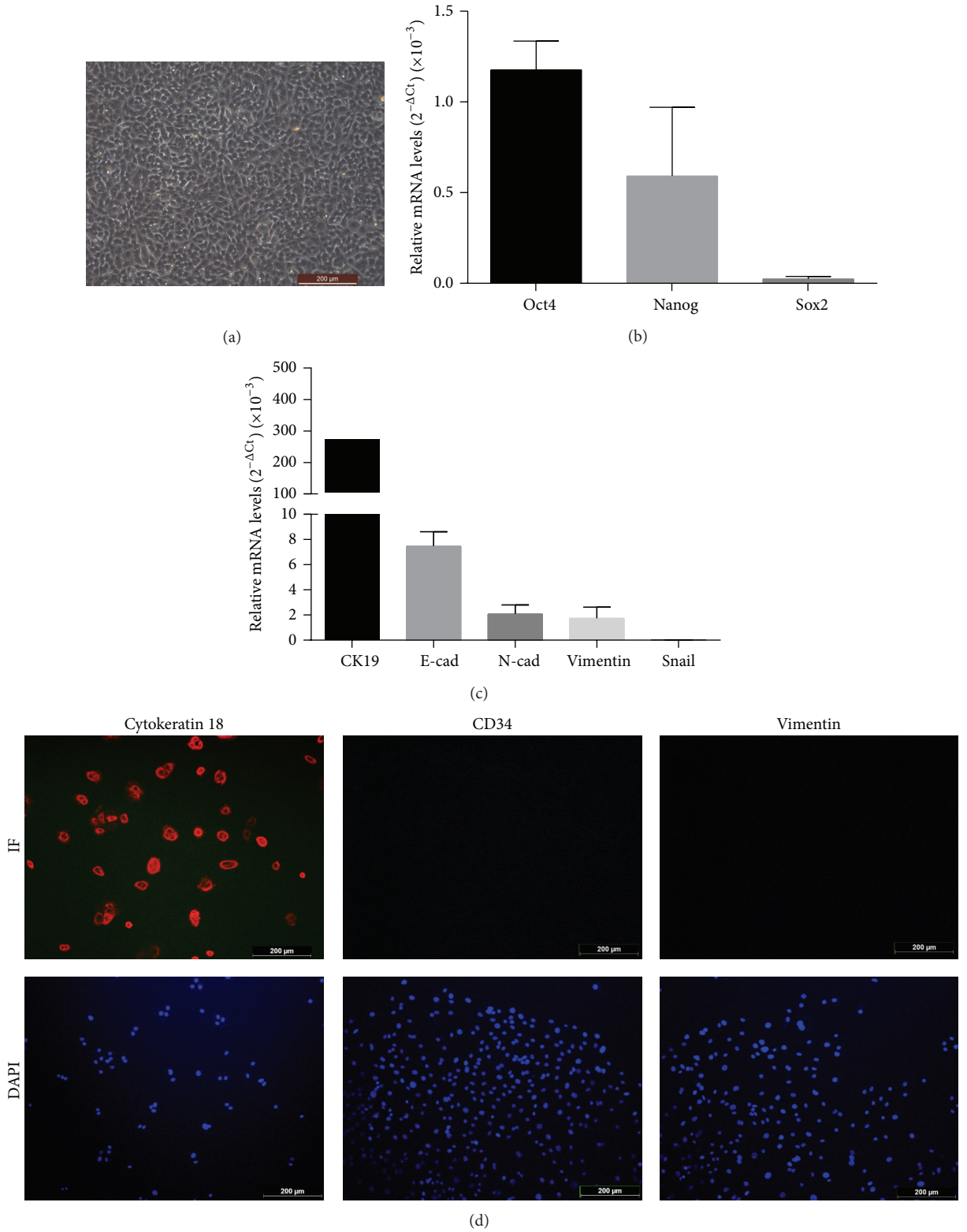

Figure 1: Identification and characterization of isolated hAECs. (a) The representative characteristics of hAECs under light microscope. (b) Expression of *Oct-4, Nanog,* and *Sox2* (relative to a beta-actin internal control) in cultured hAECs by real-time PCR analysis. The results presented were the average values from five different donors. (c) The analysis of epithelial and mesenchymal markers expression (relative to a beta-actin internal control) in isolated hAECs by real-time PCR. The results presented were the average values from five different donors. (d) Immunofluorescence detection of Cytokeratin 18, CD34, and Vimentin in cultured hAECs. Scale bar: 200 μm.

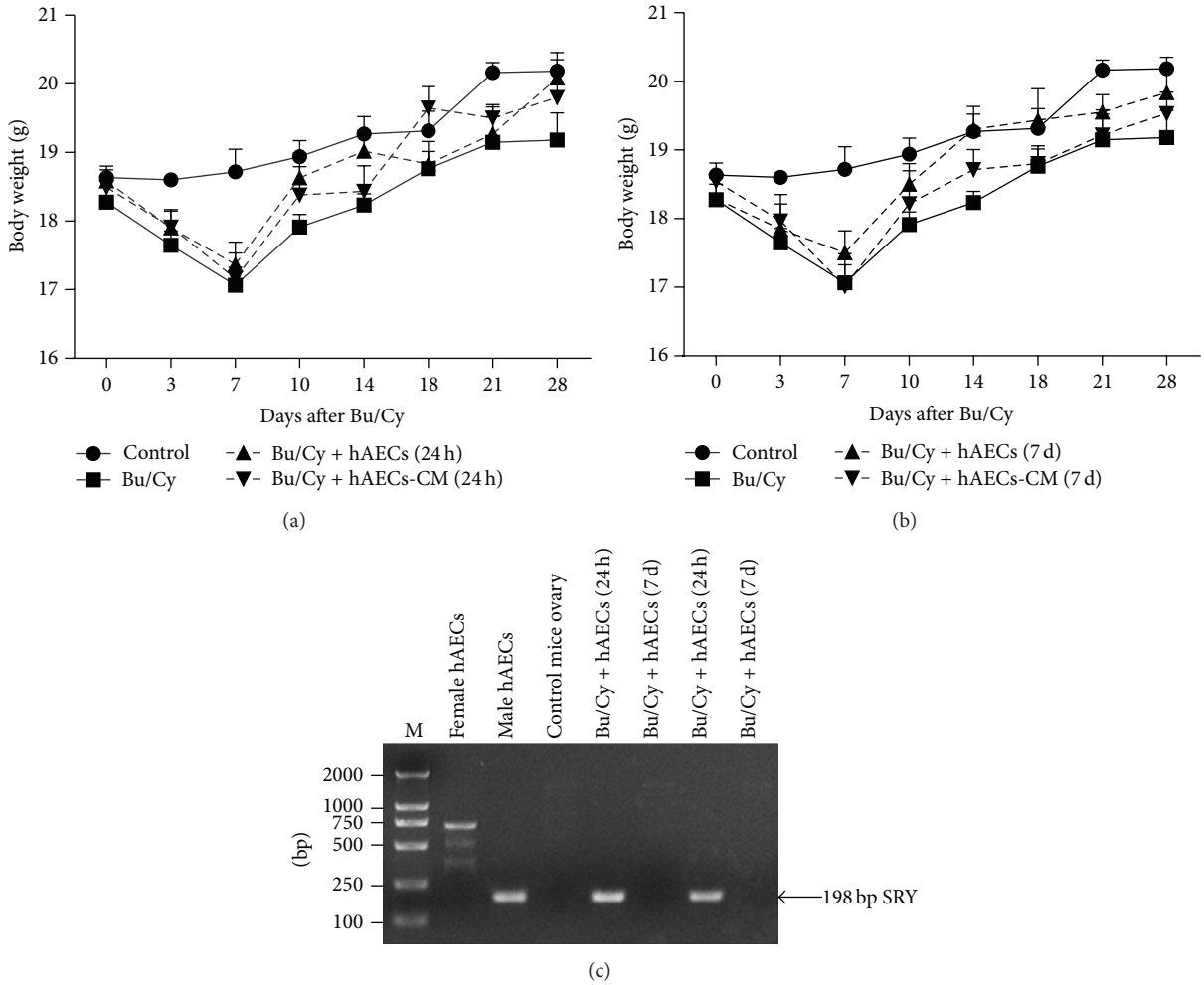

Figure 2: The effect of human hAECs and hAECs-CM administration on mice body weight and the detection of transplanted hAECs. (a) Weight of mice treated with hAECs and hAECs-CM 24 hours after chemotherapy. The weight of Bu/Cy-treated administrated mice decreased significantly 7 days after chemotherapy when compared with mice in the control group ($P < 0.01$). Mice of hAECs- and hAECs-CM-treated groups weighed more compared with Bu/Cy mice treated with Bu/Cy administrated at any time point, although the differences were not significant. (b) The weight of mice that received Bu/Cy treatment and then an IP injection of hAECs or hAECs-CM 7 days later. (c) A representative gel electrophoresis of detection of the *SRY* gene in female mice ovaries treated with male hAECs by a simultaneous nested PCR analysis. The nested amplified product of the *SRY* sequence on the Y chromosome is 198 bp in length.

between Bu/Cy-treated mice and mice that received hAECs or hAECs-CM treatment after Bu/Cy administration at any time point.

3.3. hAECs Transplanted 24 h after Bu/Cy Administration Can Infiltrate into the Damaged Ovarian Tissues. To confirm whether male hAECs could transfer into recipient ovaries, PCR analysis of the *SRY* sequences on the Y chromosome was done. As shown in Figure 2(c), genomic DNA prepared from male hAECs clearly demonstrated the presence of 198 bp *SRY*-specific sequences. Genomic DNA from both female hAECs and C57BL/6 mouse ovaries was used as negative control, with some nonspecific bands and absence of the 198 bp *SRY*-specific sequences. Interestingly, while the 198 bp fragments were identified on the ovarian samples of mice treated with male hAECs 24 hours after chemotherapy, there was no detectable product on the ovarian samples from mice treated with male hAECs 7 days after chemotherapy.

3.4. Both hAECs Transplantation and hAECs-CM Treatment Increase Follicle Number at Varied Stages in POI Mice. To determine whether hAECs transplantation and hAECs-CM treatment via peritoneal cavity could restore ovarian folliculogenesis, the serial sections obtained from ovaries 1 month after hAECs and hAECs-CM treatment were stained with H&E. As shown in Figure 3(a), administration with Bu/Cy induced follicle loss, interstitial fibrosis, and atretic follicles. However, histological evaluations revealed that hAECs or hAECs-CM treatment after chemotherapy increased follicle number in recipient ovaries.

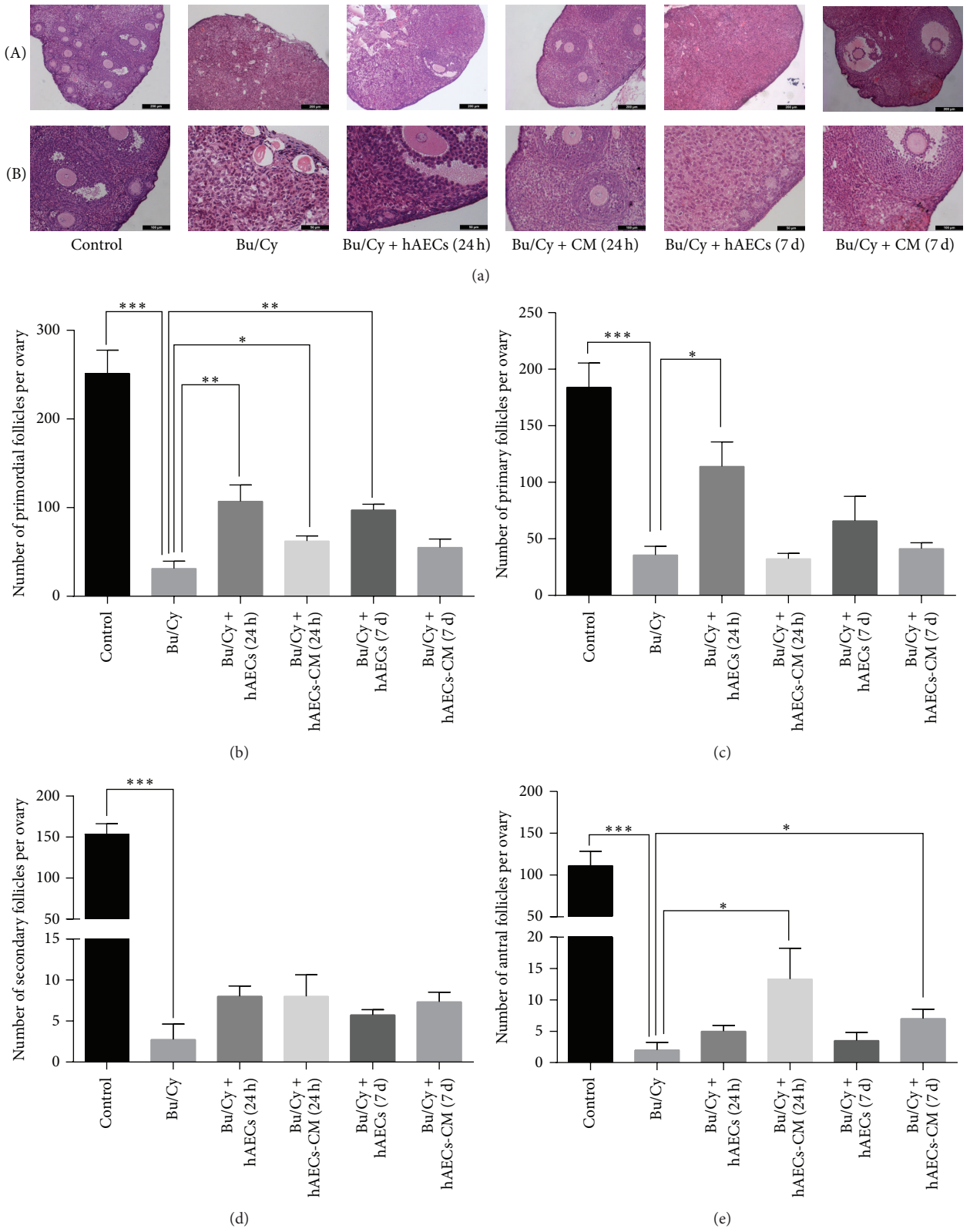

FIGURE 3: Histological analysis of mice ovaries and the follicle number count after treatment with hAECs or hAECs-CM. (a) Ovary tissues from each group were stained with hematoxylin and eosin. Numbers of oocyte-containing follicles at all stages were classified and counted in every fifth section. The primordial follicles (b), primary follicles (c), secondary follicles (d), and antral follicles (e) were identified and calculated. Data are shown as mean ± SEM, $^{*}P < 0.05$, $^{**}P < 0.01$, $^{***}P < 0.001$. Scale bar: 200 μm (Panels (a)(A)) and 50 μm (Panels (a)(B)), respectively.

To further calculate the number of follicles in all stages, every fifth section was analyzed, and the number of primordial, primary, secondary, and antral follicles was counted using light microscopy. Compared with normal control group, the number of primordial (251.25 ± 26.35 versus 31.25±8.5, $P < 0.001$), primary (184±21.57 versus 35.75±7.7, $P < 0.001$), secondary (153.5 ± 12.77 versus 2.75 ± 1.89, $P < 0.0001$), and antral follicles (111.25 ± 17.28 versus 2 ± 1.22, $P < 0.001$) decreased significantly in Bu/Cy-treated mice. In the ovaries of mice treated with hAECs 24 hours after chemotherapy, the number of primordial (107 ± 18.57) and primary follicles (114 ± 21.81) increased significantly compared to those in the Bu/Cy-treated group ($P < 0.05$, Figures 3(b) and 3(c)). However, there is no significant difference in the amounts of secondary and antral follicles between the hAECs-treated group and the Bu/Cy-treated group. In addition, the primordial follicles of mice treated with hAECs-CM 24 hours after Bu/Cy administration and mice transplanted with hAECs 7 days after Bu/Cy administration increased significantly (62.33 ± 5.67 and 97.33 ± 6.44, resp.). Moreover, compared with Bu/Cy-treated mice, the antral follicles of the hAECs-CM-treated group increased significantly, whether they were treated 24 hours or 7 days after chemotherapy (13.33 ± 4.91 versus 2 ± 1.22 and 7 ± 1.52 versus 2 ± 1.22, resp., $P < 0.05$, Figure 3(e)).

3.5. hAECs Transplantation and hAECs-CM Treatment Improve the Fertility of POI Mice. To estimate whether the treatment of hAECs or hAECs-CM via peritoneal cavity could restore the ovarian function, the female mice were naturally mated with male mice of proven fertility four weeks after treatment. The number of litters per pregnancy was calculated. The average number of litters in the group of Bu/Cy-treated mice (1.5 ± 0.29) was significantly lower than that in the normal control group (7 ± 0.58). Treatment of hAECs and hAECs-CM 24 hours after Bu/Cy administration significantly increased the litters per pregnancy (2.7 ± 0.3 and 2.75 ± 0.25, resp.) compared with Bu/Cy-treated mice. The litters per pregnancy in mice treated with hAECs or hAECs-CM 7 days after Bu/Cy administration increased, but there were no significant differences. Therefore, mice fertility can be partly improved by injecting hAECs and hAECs-CM into the abdominal cavity of Bu/Cy-treated mice (Figure 4).

3.6. The VEGFA Pathway Is Involved in the Therapeutic Efficacy of hAECs and hAECs-CM. As it has been reported that VEGFA and its receptors could potentially be involved in the regulation of follicle development [17], we attempted to examine whether VEGFA pathway molecules are involved in ovarian restoration after treatment with hAECs and hAECs-CM by analyzing the RNA and protein expression levels using real-time PCR and immunohistochemistry. As shown in Figures 5(b) and 5(c), the VEGFR2 expression level significantly decreased in the ovaries 2 weeks after chemotherapy ($P < 0.05$), along with increased VEGFA expression ($P < 0.05$) in mRNA levels compared with the normal control group. After treatment with hAECs or hAECs-CM, both VEGFR1 and VEGFR2 were higher expressed than Bu/Cy-treated only mice (Figures 5(a) and 5(b)).

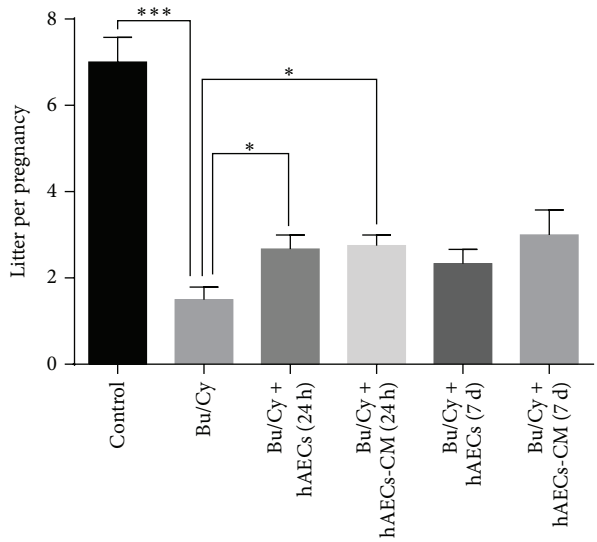

Figure 4: Intraperitoneal injection of hAECs and hAECs-CM could partly restore fertility in mice treated with chemotherapy. The litter size per pregnancy was recorded. Data represent means ± SEM, $^{*}P < 0.05$, $^{***}P < 0.001$.

Immunohistochemical analysis of ovaries 2 weeks after treatment showed that VEGFA and its two receptors had similar expression at the protein level as that of mRNA expression levels (Figures 6–8). Immunohistochemical studies revealed that VEGFA, VEGFR1, and VEGFR2 were frequently observed in the normal control group both at 2 weeks and at 1 month. Interestingly, decreased expression of VEGFA, VEGFR1, and VEGFR2 was observed 1 month after chemotherapy in the Bu/Cy-treated group. However, the expression of these proteins in hAECs- or hAECs-CM-treated mice ovaries was partly restored to the levels of those seen in control group (see Supplemental Figures 1–3 in Supplementary Material available online at http://dx.doi.org/10.1155/2016/4148923).

3.7. hAECs Transplantation and hAECs-CM Treatment Increase the MVD in Ovarian Tissues of POI Mice. CD34, an endothelial marker used in this study for vessel evaluation, was stained by immunohistochemistry in ovarian tissues to evaluate the MVD. Histological evaluations demonstrated that the number of CD34-staining vessels was significantly decreased in ovarian tissues after Bu/Cy administration (Figures 9(a) and 9(c)). As shown in Figures 9(b) and 9(d), compared with normal control group, ovarian MVD was diminished by 34% ($P < 0.01$) and 60% ($P < 0.001$), respectively, in mice ovaries 2 weeks and 1 month after Bu/Cy administration. One month after treatment with hAECs or hAECs-CM, CD34 was significantly higher in all four treatment groups than the Bu/Cy-treated group, regardless of the timing of hAECs or hAECs-CM administration. There were no significant differences among the four treatment groups 2 weeks after treatment (Figures 9(a) and 9(b)).

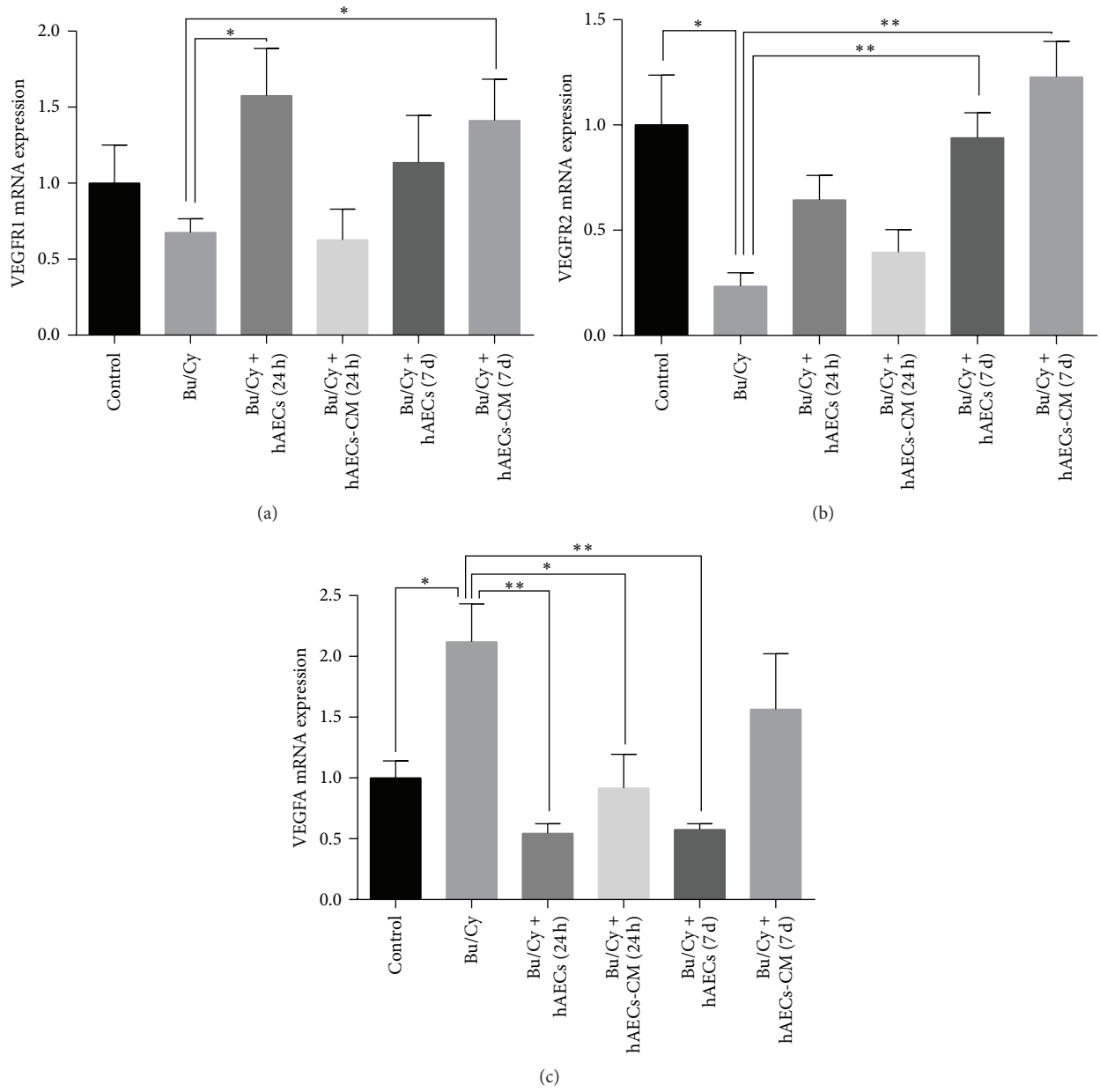

Figure 5: Real-time PCR analysis for VEGFR1, VEGFR2, and VEGFA expression in mice ovaries of different groups 2 weeks after treatment. $^{*}P < 0.05$, $^{**}P < 0.01$.

However, 1 month after treatment, levels of ovarian MVD in the hAECs-CM-treated group were significantly higher than in the hAECs-treated group regardless of time of injection, either 24 hours or 7 days after chemotherapy ($P < 0.05$, Figures 9(c) and 9(d)).

4. Discussion

hAECs have attracted interest for their possible use for regenerative medicine because of their pluripotency, low immunogenicity, nontumorigenicity, and few ethical problems with their usage [8]. There are two possible mechanisms to explain the therapeutic efficiency of hAECs transplantation. One is the differentiation potential of the transplanted cells to damaged cells. The other is the ability to secrete functional or protective factors from the transplanted cells. These factors may stimulate proliferation, inhibit apoptosis of cells residing in the damaged organs, and promote angiogenesis of damaged tissues to improve oxygen delivery and metabolic exchange [25, 26]. To address the mechanism underlying the beneficial effect of hAECs in ovarian restoration, we used a preclinical mouse model of Bu/Cy-induced ovarian failure. Then we injected hAECs and hAECs-CM into the peritoneal cavity of the Bu/Cy-treated mice to investigate

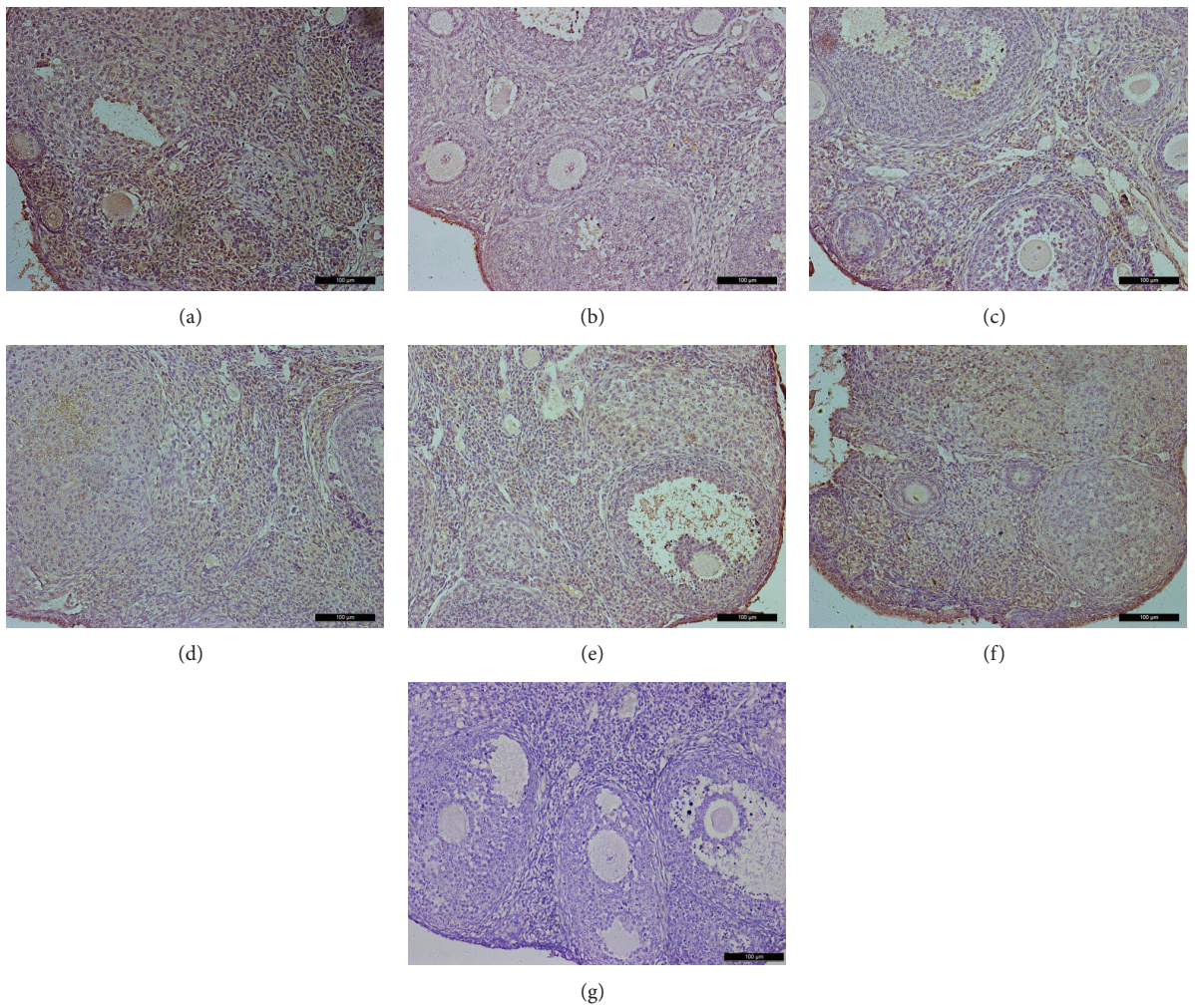

Figure 6: Immunohistochemical analysis for VEGFR1 expression in mice ovaries of different groups 2 weeks after treatment; ovarian sections with no primary antibody were served as negative controls. (a) control group; (b) Bu/Cy-treated group; (c) Bu/Cy + hAECs (24 h) group; (d) Bu/Cy + hAECs-CM (24 h) group; (e) Bu/Cy + hAECs (7 d) group; (f) Bu/Cy + hAECs-CM (7 d) group; (g) negative control. Scale bar: 100 μm.

whether hAECs could migrate to the ovary to revive ovarian function and whether factors secreted by hAECs could also induce similar therapeutic effect.

In 2002, Wang and colleagues [27] reported that real-time PCR was sensitive, species- and sex-specific in detecting the male *SRY* gene after sex-mismatched liver cell transplantation. More recently, PCR detection of the *SRY* gene in the ovaries was suggested as an effective method to investigate whether male marrow-derived mesenchymal stem cells could immigrate into chemotherapy-damaged ovaries to restore ovarian function [3, 28]. Interestingly, in our study, cell tracking experiments using PCR analysis confirmed the presence of donor male hAECs-derived *SRY* gene in ovaries after hAECs were transplanted 24 hours after chemotherapy. However, mice treated with hAECs 7 days after chemotherapy did not have *SRY* gene in any ovary. It was reported that women exposed to a variety of chemotherapy regimes could induce subcapsular focal cortical fibrosis [4], which may inhibit hAECs from immigrating into ovaries 7 days after chemotherapy. In addition, a maximal benefit was achieved when hAECs were transplanted 24 hours (versus 7 days) after Bu/Cy administration. The number of primordial, primary, secondary, and antral follicles was higher in mice transplanted with hAECs 24 hours after chemotherapy than after 7 days, though the difference was not significant. These results suggest that the timing of the transplantation was important and whether hAECs could migrate to the ovary or not could affect the therapeutic effect.

Recently, more and more studies had employed factors released from cells as cellular therapeutics in regenerative medicine. It was demonstrated that conditioned media isolated from adipose-derived stem cells (ADSC) had a similar protective effect as intact ADSC in improving both cardiac function of infarcted hearts and lung vascular protective function after lung tissue microvascular injury [18, 29]. These results strongly support major involvement of paracrine effects in regenerative medicine. Similar to these results, IP injection of hAECs-CM in our study partly restored

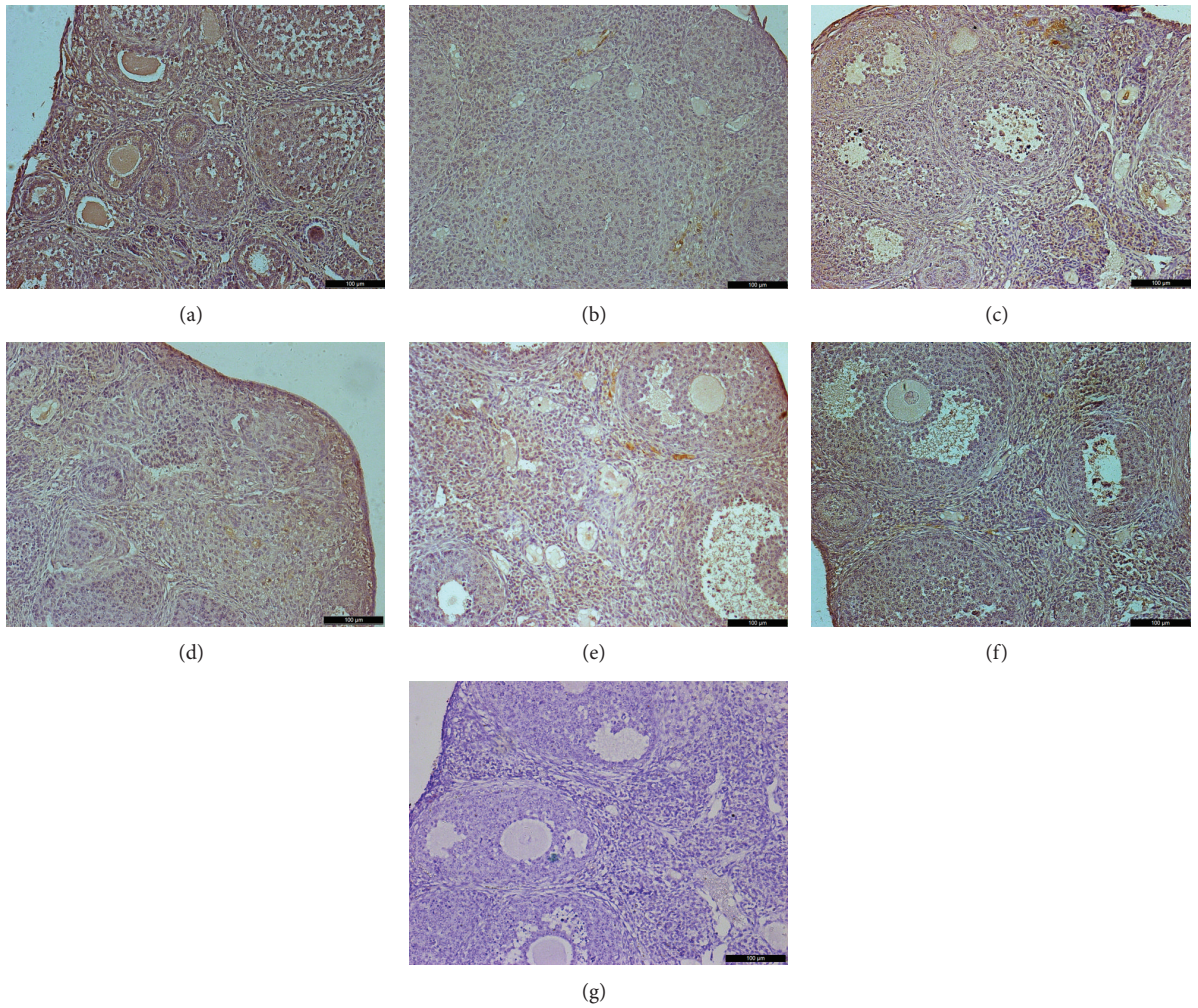

FIGURE 7: Immunohistochemical analysis for VEGFR2 expression in mice ovaries of different groups 2 weeks after treatment; ovarian sections with no primary antibody were served as negative controls. (a) control group; (b) Bu/Cy administrated group; (c) Bu/Cy + hAECs (24 h) group; (d) Bu/Cy + hAECs-CM (24 h) group; (e) Bu/Cy + hAECs (7 d) group; (f) Bu/Cy + hAECs-CM (7 d) group; (g) negative control. Scale bar: 100 μm.

follicle number and improved fertility when compared with Bu/Cy-treated mice. Though treatment 24 hours after Bu/Cy treatment seemed more effective than treatment after 7 days, there is no significant difference. To our surprise, hAECs-CM injection significantly increased the number of antral follicles regardless of the timing of administration. In brief, IP injection of 0.2 mL concentrated hAECs-CM collected from 4×10^6 hAECs (30-fold concentrated) seemed sufficient to improve ovarian function of chemotherapy-induced ovarian damage. Hence, hAECs-CM might be a meaningful treatment strategy for clinical application.

It was reported that VEGF is a factor that acts by stimulating the mitosis of endothelial cells and by increasing vascular permeability [30, 31], which may result in the accumulation of antral fluid, formation of antrum in the growing follicles, and, finally, inducement of follicle rupture [14, 32, 33]. Actually, addition of VEGF to the culture medium improved the development of caprine preantral follicles cultured *in vitro*, allowing the production of mature oocytes [16]. Therefore, the therapeutic effect of hAECs may partly result from hAEC-derived paracrine factors, especially VEGFA.

In the present study, we analysed the expression of VEGFA and its receptors (VEGFR1 and VEGFR2) in the ovaries by real-time PCR and immunohistochemical analysis. Compared with normal control mice, the expression of VEGFR1 and VEGFR2 was decreased 2 weeks after Bu/Cy administration, along with increased VEGFA expression. IP transplantation of hAECs or hAECs-CM into the Bu/Cy-treated mice induced the expression of VEGFR1 and VEGFR2 2 weeks after treatment. We speculated that the increased expression of VEGFA in Bu/Cy-treated mice was transient and caused by autoregulation as a response to the reduction of VEGFR1 and VEGFR2 expression. Actually, the expression of VEGFA, VEGFR1, and VEGFR2 was decreased 1 month after chemotherapy. In addition, the transplantation of hAECs or hAECs-CM into the ovaries that showed decreased angiogenesis due to Bu/Cy treatment resulted in the induction of more CD34-positive cells, namely, more

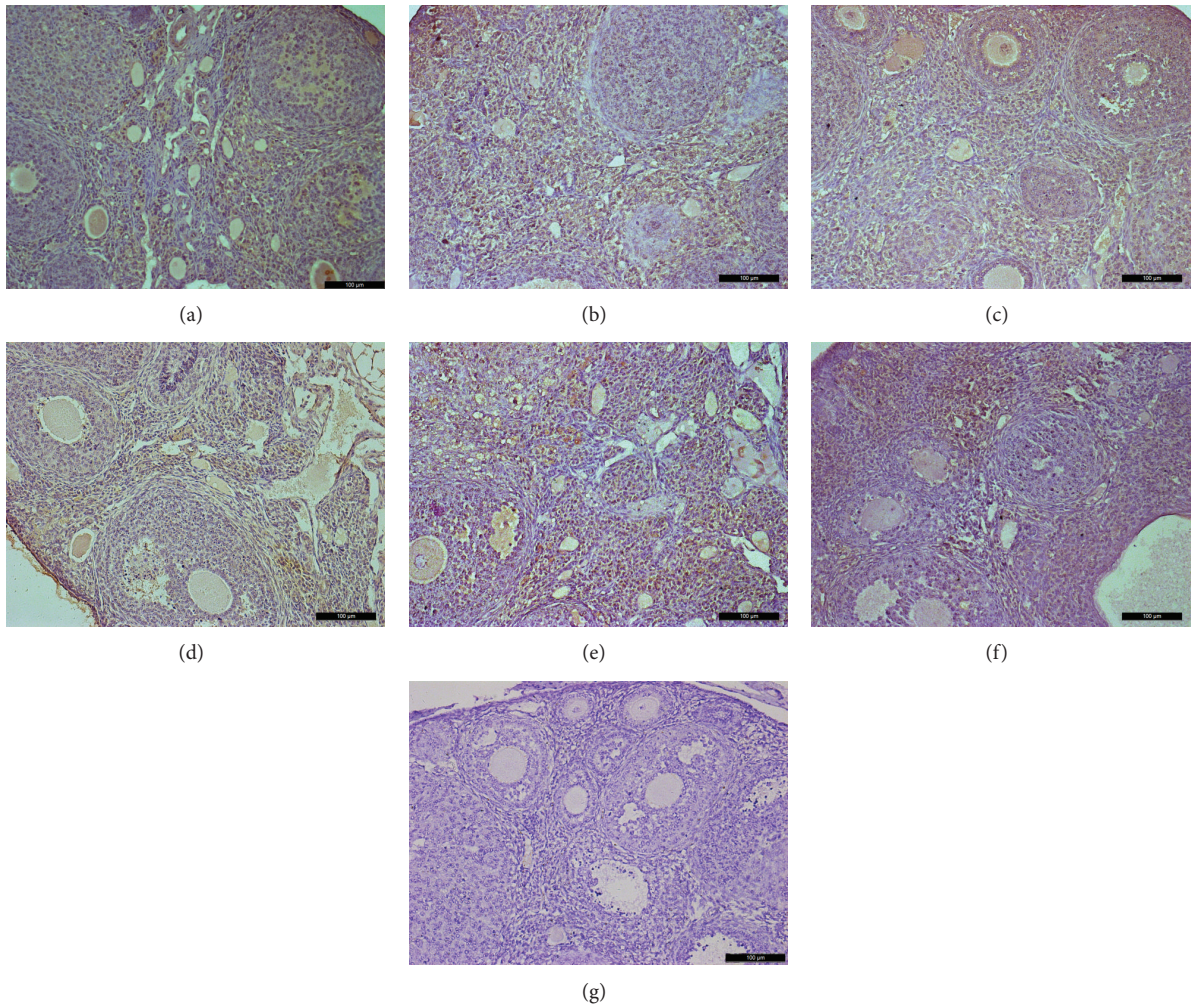

Figure 8: Immunohistochemical analysis for VEGFA expression in mice ovaries of different groups 2 weeks after treatment; ovarian sections with no primary antibody were served as negative controls. (a) control group; (b) Bu/Cy administrated group; (c) Bu/Cy + hAECs (24 h) group; (d) Bu/Cy + hAECs-CM (24 h) group; (e) Bu/Cy + hAECs (7 d) group; (f) Bu/Cy + hAECs-CM (7 d) group; (g) negative control. Scale bar: 100 μm.

angiogenesis. Taken together, hAECs and hAECs-CM may restore ovarian function by regulating expression of VEGFA and its receptors, thus inducing angiogenesis and increasing the follicular growth related to paracrine activity.

So if VEGFA and its receptors played a role in restoring ovarian function, can we just treat POI with administration of VEGFA? Takehara et al. [34] demonstrated that only a small recovery was induced when VEGFA was administered into mouse ovaries. Recently, it has been demonstrated that human hAECs secrete a variety of growth factors, such as epidermal and fibroblast growth factors (HB-EGF, EGF-2, bFGF, FGF-4, FGF-6, and FGF-7), angiogenic growth factors (VEGF, VEGF-D, VEGF-R2, and VEGF-R3), insulin-like growth factors (IGF-1, IGF-ISR, IGFBP-1, and IGFBP-4), and platelet-derived growth factors (PDGF-AA, PDGF-BB, PDGFRa, and PDGFRb) [35]. Therefore, ovaries damaged by chemotherapy needed not only VEGFA for restoration but also other growth factors secreted by hAECs.

5. Conclusion

The present study demonstrates that IP injection of hAECs and hAEC-CM could partly restore ovarian function and hAECs-CM seemed sufficient to improve ovarian function of chemotherapy-induced ovarian damage. In addition, our findings suggest that the possible mechanism by which hAECs participate in reviving ovarian function is by regulating VEGFA and its receptors to induce follicular growth related to paracrine activity. Further investigation is needed to determine whether increasing frequency of IP administration of condition medium from hAECs or direct administration of hAECs-CM into the damaged ovaries could more effectively restore ovarian function.

Conflict of Interests

The authors declare that there is no conflict of interests regarding the publication of this paper.

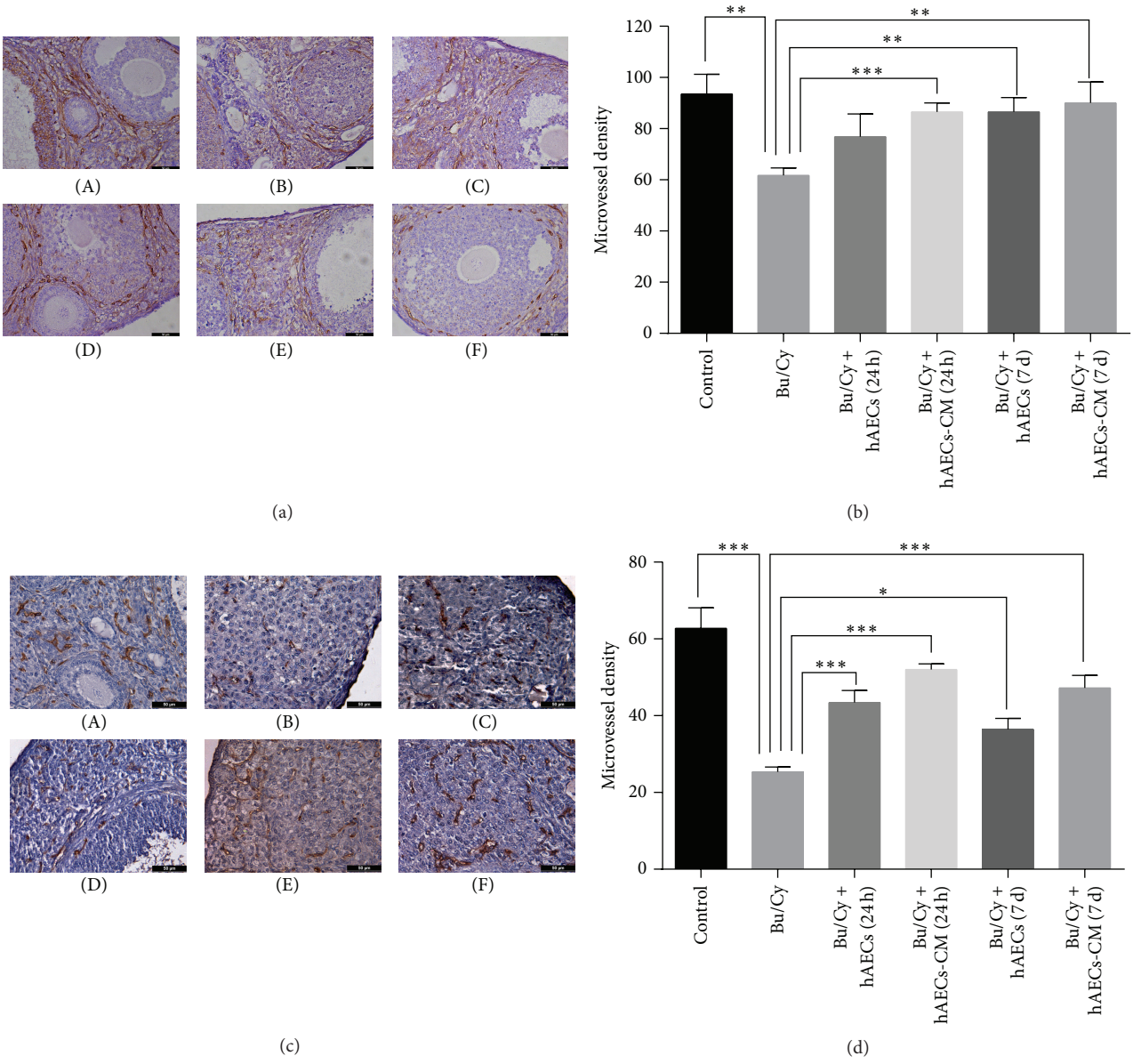

Figure 9: Angiogenesis on Bu/Cy-treated ovaries after intraperitoneal injection of hAECs or hAECs-CM. Immunohistochemistry for CD34 ((a) and (c)) and microvessel density ((b) and (d)) were examined on ovaries obtained 2 weeks ((a) and (b)) or 1 month after treatment ((c) and (d)). Data were given as mean ± SEM. (A): control group; (B): Bu/Cy administrated group; (C): Bu/Cy + hAECs (24 h) group; (D): Bu/Cy + hAECs-CM (24 h) group; (E): Bu/Cy + hAECs (7 d) group; (F): Bu/Cy + hAECs-CM (7 d) group. $^{*}P < 0.05$, $^{**}P < 0.01$, $^{***}P < 0.001$. Scale bar: 100 μm.

Authors' Contribution

Xiaofen Yao and Yuna Guo contributed equally to this work.

Acknowledgments

This work was supported by grants from Shanghai Municipal Health Bureau, Shanghai, China (no. XBR2011069), the NSFC (National Natural Science Foundation of China, no. 81370678), and Shanghai Municipal Council for Science and Technology (no. 12431902201).

References

[1] M. de Vos, P. Devroey, and B. C. Fauser, "Primary ovarian insufficiency," *The Lancet*, vol. 376, no. 9744, pp. 911–921, 2010.

[2] A. N. Hirshfield, "Relationship between the supply of primordial follicles and the onset of follicular growth in rats," *Biology of Reproduction*, vol. 50, no. 2, pp. 421–428, 1994.

[3] S. H. Abd-Allah, S. M. Shalaby, H. F. Pasha et al., "Mechanistic action of mesenchymal stem cell injection in the treatment of chemically induced ovarian failure in rabbits," *Cytotherapy*, vol. 15, no. 1, pp. 64–75, 2013.

[4] D. Meirow, J. Dor, B. Kaufman et al., "Cortical fibrosis and blood-vessels damage in human ovaries exposed to chemotherapy. Potential mechanisms of ovarian injury," *Human Reproduction*, vol. 22, no. 6, pp. 1626–1633, 2007.

[5] M. Sommezer and K. Oktay, "Fertility preservation in female patients," *Human Reproduction Update*, vol. 10, no. 3, pp. 251–266, 2004.

[6] K. Zou, Z. Yuan, Z. Yang et al., "Production of offspring from a germline stem cell line derived from neonatal ovaries," *Nature Cell Biology*, vol. 11, no. 5, pp. 631–636, 2009.

[7] T. Miki, T. Lehmann, H. Cai, D. B. Stolz, and S. C. Strom, "Stem cell characteristics of amniotic epithelial cells," *Stem Cells*, vol. 23, no. 10, pp. 1549–1559, 2005.

[8] A. Toda, M. Okabe, T. Yoshida, and T. Nikaido, "The potential of amniotic membrane/amnion-derived cells for regeneration of various tissues," *Journal of Pharmacological Sciences*, vol. 105, no. 3, pp. 215–228, 2007.

[9] C.-H. Fang, J. Jin, J.-H. Joe et al., "In vivo differentiation of human amniotic epithelial cells into cardiomyocyte-like cells and cell transplantation effect on myocardial infarction in rats: Comparison with cord blood and adipose tissue-derived mesenchymal stem cells," *Cell Transplantation*, vol. 21, no. 8, pp. 1687–1696, 2012.

[10] S. Murphy, R. Lim, H. Dickinson et al., "Human amnion epithelial cells prevent bleomycin-induced lung injury and preserve lung function," *Cell Transplantation*, vol. 20, no. 6, pp. 909–923, 2011.

[11] P. Vosdoganes, R. Lim, E. Koulaeva et al., "Human amnion epithelial cells modulate hyperoxia-induced neonatal lung injury in mice," *Cytotherapy*, vol. 15, no. 8, pp. 1021–1029, 2013.

[12] F. Wang, L. Wang, X. Yao, D. Lai, and L. Guo, "Human amniotic epithelial cells can differentiate into granulosa cells and restore folliculogenesis in a mouse model of chemotherapy-induced premature ovarian failure," *Stem Cell Research and Therapy*, vol. 4, no. 5, article 124, 2013.

[13] E. Geva and R. B. Jaffe, "Role of vascular endothelial growth factor in ovarian physiology and pathology," *Fertility and Sterility*, vol. 74, no. 3, pp. 429–438, 2000.

[14] P. M. Lam and C. Haines, "Vascular endothelial growth factor plays more than an angiogenic role in the female reproductive system," *Fertility and Sterility*, vol. 84, no. 6, pp. 1775–1778, 2005.

[15] D. R. Danforth, L. K. Arbogast, S. Ghosh, A. Dickerman, R. Rofagha, and C. I. Friedman, "Vascular endothelial growth factor stimulates preantral follicle growth in the rat ovary," *Biology of Reproduction*, vol. 68, no. 5, pp. 1736–1741, 2003.

[16] V. R. Araújo, G. M. Silva, A. B. G. Duarte et al., "Vascular endothelial growth factor-A_{165} (VEGF-A_{165}) stimulates the *in vitro* development and oocyte competence of goat preantral follicles," *Cell and Tissue Research*, vol. 346, no. 2, pp. 273–281, 2011.

[17] R. M. McFee, R. A. Artac, R. M. McFee et al., "Inhibition of vascular endothelial growth factor receptor signal transduction blocks follicle progression but does not necessarily disrupt vascular development in perinatal rat ovaries," *Biology of Reproduction*, vol. 81, no. 5, pp. 966–977, 2009.

[18] D. Yang, W. Wang, L. Li et al., "The relative contribution of paracine effect versus direct differentiation on adipose-derived stem cell transplantation mediated cardiac repair," *PLoS ONE*, vol. 8, no. 3, Article ID e59020, 2013.

[19] M. Myers, K. L. Britt, N. G. M. Wreford, F. J. P. Ebling, and J. B. Kerr, "Methods for quantifying follicular numbers within the mouse ovary," *Reproduction*, vol. 127, no. 5, pp. 569–580, 2004.

[20] N. Weidner, "Current pathologic methods for measuring intratumoral microvessel density within breast carcinoma and other solid tumors," *Breast Cancer Research and Treatment*, vol. 36, no. 2, pp. 169–180, 1995.

[21] W. Tungwiwat, G. Fucharoen, T. Ratanasiri, K. Sanchaisuriya, and S. Fucharoen, "Non-invasive fetal sex determination using a conventional nested PCR analysis of fetal DNA in maternal plasma," *Clinica Chimica Acta*, vol. 334, no. 1-2, pp. 173–177, 2003.

[22] J. Nichols, B. Zevnik, K. Anastassiadis et al., "Formation of pluripotent stem cells in the mammalian embryo depends on the POU transcription factor Oct4," *Cell*, vol. 95, no. 3, pp. 379–391, 1998.

[23] I. Chambers, D. Colby, M. Robertson et al., "Functional expression cloning of Nanog, a pluripotency sustaining factor in embryonic stem cells," *Cell*, vol. 113, no. 5, pp. 643–655, 2003.

[24] D. J. Rodda, J.-L. Chew, L.-H. Lim et al., "Transcriptional regulation of Nanog by OCT4 and SOX2," *Journal of Biological Chemistry*, vol. 280, no. 26, pp. 24731–24737, 2005.

[25] T. Miki, "Amnion-derived stem cells: in quest of clinical applications," *Stem Cell Research and Therapy*, vol. 2, no. 3, article 25, 2011.

[26] M. Z. Ratajczak, M. Kucia, T. Jadczyk et al., "Pivotal role of paracrine effects in stem cell therapies in regenerative medicine: can we translate stem cell-secreted paracrine factors and microvesicles into better therapeutic strategies," *Leukemia*, vol. 26, no. 6, pp. 1166–1173, 2012.

[27] L.-J. Wang, Y. M. Chen, D. George et al., "Engraftment assessment in human and mouse liver tissue after sex-mismatched liver cell transplantation by real-time quantitative PCR for Y chromosome sequences," *Liver Transplantation*, vol. 8, no. 9, pp. 822–828, 2002.

[28] S. Kilic, F. Pinarli, C. Ozogul, N. Tasdemir, G. Naz Sarac, and T. Delibasi, "Protection from cyclophosphamide-induced ovarian damage with bone marrow-derived mesenchymal stem cells during puberty," *Gynecological Endocrinology*, vol. 30, no. 2, pp. 135–140, 2014.

[29] K. S. Schweitzer, B. H. Johnstone, J. Garrison et al., "Adipose stem cell treatment in mice attenuates lung and systemic injury induced by cigarette smoking," *American Journal of Respiratory and Critical Care Medicine*, vol. 183, no. 2, pp. 215–225, 2011.

[30] D. A. Redmer and L. P. Reynolds, "Angiogenesis in the ovary," *Reviews of Reproduction*, vol. 1, no. 3, pp. 182–192, 1996.

[31] N. Ferrara, H. P. Gerber, and J. LeCouter, "The biology of VEGF and its receptors," *Nature Medicine*, vol. 9, no. 6, pp. 669–676, 2003.

[32] C. Tamanini and M. de Ambrogi, "Angiogenesis in developing follicle and corpus luteum," *Reproduction in Domestic Animals*, vol. 39, no. 4, pp. 206–216, 2004.

[33] R. C. Zimmermann, T. Hartman, S. Kavic et al., "Vascular endothelial growth factor receptor 2-mediated angiogenesis is essential for gonadotropin-dependent follicle development," *Journal of Clinical Investigation*, vol. 112, no. 5, pp. 659–669, 2003.

[34] Y. Takehara, A. Yabuuchi, K. Ezoe et al., "The restorative effects of adipose-derived mesenchymal stem cells on damaged ovarian function," *Laboratory Investigation*, vol. 93, no. 2, pp. 181–193, 2013.

[35] Z. Grzywocz, E. Pius-Sadowska, P. Klos et al., "Growth factors and their receptors derived from human amniotic cells in vitro," *Folia Histochemica et Cytobiologica*, vol. 52, no. 3, pp. 163–170, 2014.

Hindawi Publishing Corporation
Stem Cells International
Volume 2016, Article ID 8582526, 17 pages
http://dx.doi.org/10.1155/2016/8582526

Research Article

Expression of Genes Related to Germ Cell Lineage and Pluripotency in Single Cells and Colonies of Human Adult Germ Stem Cells

Sabine Conrad,[1] Hossein Azizi,[2,3,4] Maryam Hatami,[2] Mikael Kubista,[5,6] Michael Bonin,[7] Jörg Hennenlotter,[8] Karl-Dietrich Sievert,[8] and Thomas Skutella[2]

[1]*Sabine Conrad, P.O. Box 12 43, 72072 Tübingen, Germany*
[2]*Institute for Anatomy and Cell Biology, Medical Faculty, University of Heidelberg, Im Neuenheimer Feld 307, 69120 Heidelberg, Germany*
[3]*Department of Stem Cells and Developmental Biology, Cell Science Research Center, Royan Institute for Stem Cell Biology and Technology, P.O. Box 19395, Tehran 4644, Iran*
[4]*Faculty of Biotechnology, Amol University of Special Modern Technologies, P.O. Box 46168, Amol 49767, Iran*
[5]*TATAA Biocenter AB, Odinsgatan 28, 41103 Göteborg, Sweden*
[6]*Institute of Biotechnology at the Czech Academy of Sciences Videnska 1083, 14220 Prague 4, Czech Republic*
[7]*Institute of Anthropology and Human Genetics, Microarray Facility, University Clinic, Calwerstraße 7, 72076 Tübingen, Germany*
[8]*Department of Urology, University of Tübingen Hospital, Hoppe-Seyler-Straße 3, 72076 Tübingen, Germany*

Correspondence should be addressed to Thomas Skutella; skutella@ana.uni-heidelberg.de

Received 3 December 2014; Revised 9 February 2015; Accepted 11 February 2015

Academic Editor: Irma Virant-Klun

The aim of this study was to elucidate the molecular status of single human adult germ stem cells (haGSCs) and haGSC colonies, which spontaneously developed from the CD49f MACS and matrix- (collagen−/laminin+ binding-) selected fraction of enriched spermatogonia. Single-cell transcriptional profiling by Fluidigm BioMark system of a long-term cultured haGSCs cluster in comparison to human embryonic stem cells (hESCs) and human fibroblasts (hFibs) revealed that haGSCs showed a characteristic germ- and pluripotency-associated gene expression profile with some similarities to hESCs and with a significant distinction from somatic hFibs. Genome-wide comparisons with microarray analysis confirmed that different haGSC colonies exhibited gene expression heterogeneity with more or less pluripotency. The results of this study confirm that haGSCs are adult stem cells with a specific molecular gene expression profile *in vitro*, related but not identical to true pluripotent stem cells. Under ES-cell conditions haGSC colonies could be selected and maintained in a partial pluripotent state at the molecular level, which may be related to their cell plasticity and potential to differentiate into cells of all germ layers.

1. Background

Human adult germ stem cells (haGSCs) derived from highly enriched spermatogonia isolated from adult human testicular tissue were shown to be highly versatile and having some similarities with human embryonic stem cells (hESCs), including the expression of genes associated with pluripotent cells and the ability to be *in vitro* differentiated into a number of cell lineages comprising the three germ layers [1–6].

In the studies of Mizrak et al. [5], Chikhovskaya et al. [7], and Gonzalez et al. [8], the cells expressing markers of pluripotency were probably derived from mesenchymal stem cells (MSCs) or were more MSC-like. Moreover, it has also been proposed that haGSCs may be low-differentiated testicular fibroblasts [9]. In contrast, Stimpfel et al. [10] demonstrated that both germ- and mesenchyme-derived stem cells were present in stem cell clusters from human testis biopsy, which could differentiate into cells of all three germ

layers. Recently, Lim et al. [6] provided evidence that haGSCs show similarities to hESCs and are being able to generate small teratomas.

The findings of all these studies raised some new questions about the real character of pluripotency in haGSCs. It is generally accepted that pluripotency of cells requires the activation of a transcriptional regulatory network [11], a phenomenon which has been observed in *ex vivo* cultures of early embryonic cells and also in cells of the germ cell lineage, in which members of the pluripotency network are normally active, including embryonic cells during development of morula and blastocyst-stage (inner cell mass) embryo, epiblast, primordial germ cells (PGCs), and germline stem cells.

One main step in analyzing the biology of haGSCs and pluripotency in adult stem cells is to determine their germ cell-specific gene expression profile. The present knowledge regarding the molecular markers that define haGSCs and their pluripotency is significantly limited. Therefore, the goal of this study was to investigate the molecular profile of haGSCs, which are able to comprise both the expression of a residual germ cell profile and genes related to pluripotency, in addition to our previous study on hSSCs [1]. In order to accomplish this goal, we sought to compare the gene expression profiles of haGSCs generated from short-term cultured enriched spermatogonial stem cells (hSSCs) to hFibs and hESCs using (1) single cell nanofluid real-time PCR (Fluidigm) of a representative haGSC colony, (2) microarray analysis, and (3) Fluidigm real-time PCR and immunohistochemistry of haGSC colonies to validate the microarray data. Here, we show that haGSCs are adult stem cells with a specific molecular profile, which is related to spermatogonia. Under hESC culture conditions they can be selected and cultured and maintain a state resembling in part gene expression related to the expression patterns found in pluripotent cells.

2. Results

2.1. Generation of haGSC Colonies from Enriched Fraction of Spermatogonia. Colonies or clusters of haGSC developed spontaneously from the CD49f MACS and matrix (collagen nonbinding, laminin binding) selected fraction of enriched spermatogonia (Figure 1) but not from the negative selected fraction of cells or from patients without spermatogonia. By MACS and matrix selection, the hFibs, which overgrow the primary cell cultures, were depleted and remained in the nonselected populations of cells. The hFibs appeared morphologically completely different compared to haGSCs (Figure 1). In the primary cultures, the first small haGSC colonies/islands started to appear 4–6 weeks after culture of enriched spermatogonia in hGSC medium. The denser haGSC aggregations were manually selected for further propagation and characterization (Figure 1(d)). The typical haGSC colony consisted of central part of colony and outgrowing epithelial cells resembling early cell colonies of hESCs (Figure 1(e)). In the negatively selected cell fraction, no epithelial haGSC colony formation was observed [9]. This typical epithelial morphology is an important distinction to hFibs (Figure 1(g)).

2.2. Single Cell Analysis of hFibs, hESCs and haGSCs. As can be seen from the dendrogram in Figure 2(a), the nanofluid single cell real-time PCR gene expression profiling from a typical single haGSC colony revealed that most cells from the group of haGSCs (72.3%, 34/47 cells) clustered together in a single tree, most closely related to hESCs, where also most of the cells clustered in a single tree (82.6%, 19/23 cells). These two groups were separated from hFibs which clustered in a single tree with several outliner haGSCs (26.7%, 13/47 cells) and a few outliner hESCs (17.4%, 4/23 cells). The majority of single haGSCs clearly separated from hFibs expressing genes of pluripotency, combined with a residual germ cell profile distinct from hFibs (Figures 2 and 3). According to the dendrogram, the haGSCs were divided into two groups: the group of all haGSCs and the group of haGSCs without outliners (group I) for further analysis (Figure 2(b)).

When analysing all the selected germ- and pluripotency-associated genes in more detail, the gene expression profiling showed that the group of all haGSCs expressed a high level of the known germ cell-specific genes *STELLA*, the GDNF-receptor *GFRα1*, *TSPYL,* and *CD9* (haGSCs versus hFibs, t-test and Mann-Whitney test, $P < 0.05$) (Figure 3). In this single cell analysis, the germ cell associated genes *VASA*, *DAZL*, and *LIFR* were not expressed by any group of cells. Furthermore, haGSCs expressed the pluripotency-related genes *NANOS, DNMT3B, TDGF1, STAT3, NANOG, LIN28, GPR125, OCT4A*, and *SOX2* at a significantly higher level than hFibs, while hFibs expressed *KLF4* at a higher level than haGSCs, as revealed by t-test and Mann-Whitney test ($P < 0.05$) (Figure 3, Supplementary Table 3, available online at http://dx.doi.org/10.1155/2016/8582526). In the comparison of haGSC group I and hFibs, the same array group of genes and *DNMT1* were significantly regulated in haGSCs, although at a higher intensity (Figure 3 and Supplementary Table 3). The hFibs did not show any amplification product for *SOX2, UTF1, TDGF1, LIN28B, TERT,* and *CADH1*.

When comparing single hESCs with haGSCs group I (Figure 3 and Supplementary Table 3), hESCs more strongly expressed most of the pluripotency-related genes, including *SOX2, NANOG, LIN28, LIN28B, GDF3, CADH1, OCT4a, TDGF1,* and *UTF1*, while haGSCs more strongly expressed the germ cell-related genes *CD9, GFRα1, NANOS, STAT3, TSPYL, GPR125,* and *MYC* (hESCs versus haGSCs group1, t-test and Mann-Whitney test, $P < 0.05$) (Supplementary Table 3). The analysis of all haGSCs revealed a similar profile with lower expression levels (Figure 3 and Supplementary Table 3). This indicates that the haGSCs expressed the core pluripotency-related genes including *OCT4a*, *NANOG*, *SOX2,* and *LIN28*, while still retaining a partial germ cell-related gene expression profile. The intensity of the expression of the core pluripotency-related genes was lower in haGSCs than in hESCs but significantly higher than in hFibs (Supplementary Table 3).

On a single cell level haGSCs are a heterogeneous population of cells, where there are 12 out of 47 (25.5%) coexpressed

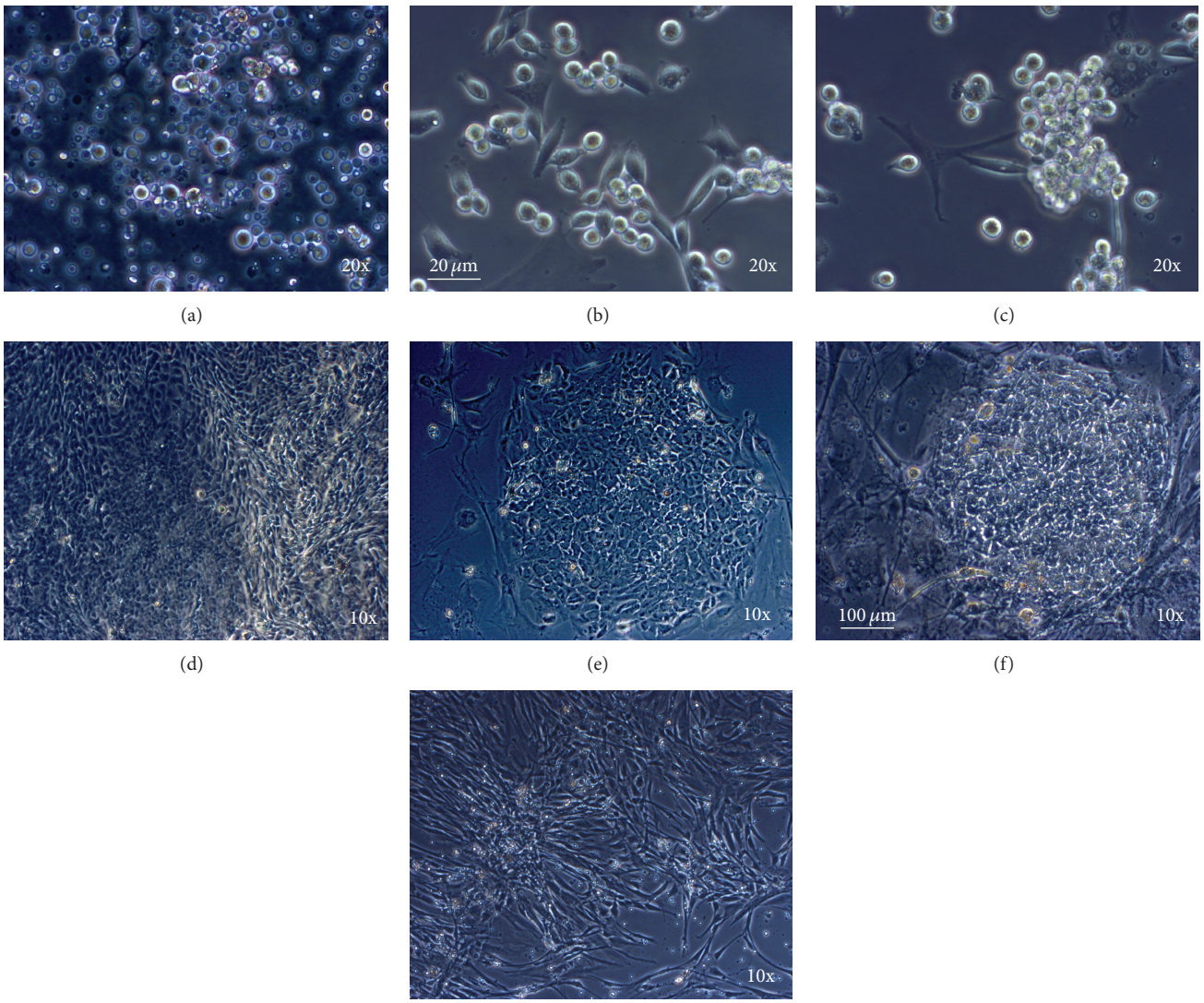

Figure 1: haGSC colonies were derived from enriched spermatogonia and share morphological similarities with early hESC colonies after passaging. Typical representative morphology of spermatogonia and haGSCs from the same patient (157) during culture. (a) Human testis dissociated cells during the first week of culture before selection of spermatogonia. ((b) and (c)) Single, pairs, chains, and groups of round cells with high nucleus/cytoplasm ratio typical of spermatogonia were observable after selection. (d) After 4–6 weeks, some aggregations of the first epithelial haGSCs were observed. (e) Examples of typical early haGSC, (f) early hESC colonies, and (g) typical fibroblasts from testis. Scale bar in ((a)–(c)) 20 μm and ((d)–(g)) 100 μm.

transcripts of core pluripotency genes *OCT4a, NANOG,* and *SOX2* (Figure 2(a)).

These observations encouraged us to have a closer look at the changes in genes global expression and in particular the expression of germ-, pluripotency-, fibroblast-, and mesenchymal-associated genes and genes activated during ESC-like haGSC cluster formation (natural reprogramming of human spermatogonia).

2.3. Microarray Gene Expression Profiling. To this end, we investigated the transcriptome of the following cell types by microarray technology 4 cell groups: hFibs (F161; negative control), hESCs (H1; positive control), short-term cultured hSSCs, and 4 different natural reprogramming trials of single clones of haGSCs.

2.3.1. Sample to Sample Relations. In the first step, we investigated relations between samples especially with regard to different cell types and reprogramming trials. To this end, hierarchical clustering (complete linkage with Euclidean distance) and as well as a principal component analysis (PCA) were performed (Figure 4). For both methods, the set of genes was reduced to the medium variance genes (gene whose standard deviation is higher than the average standard deviation + 2SDs). All the different cell types were clearly separated by the two best principal components, which

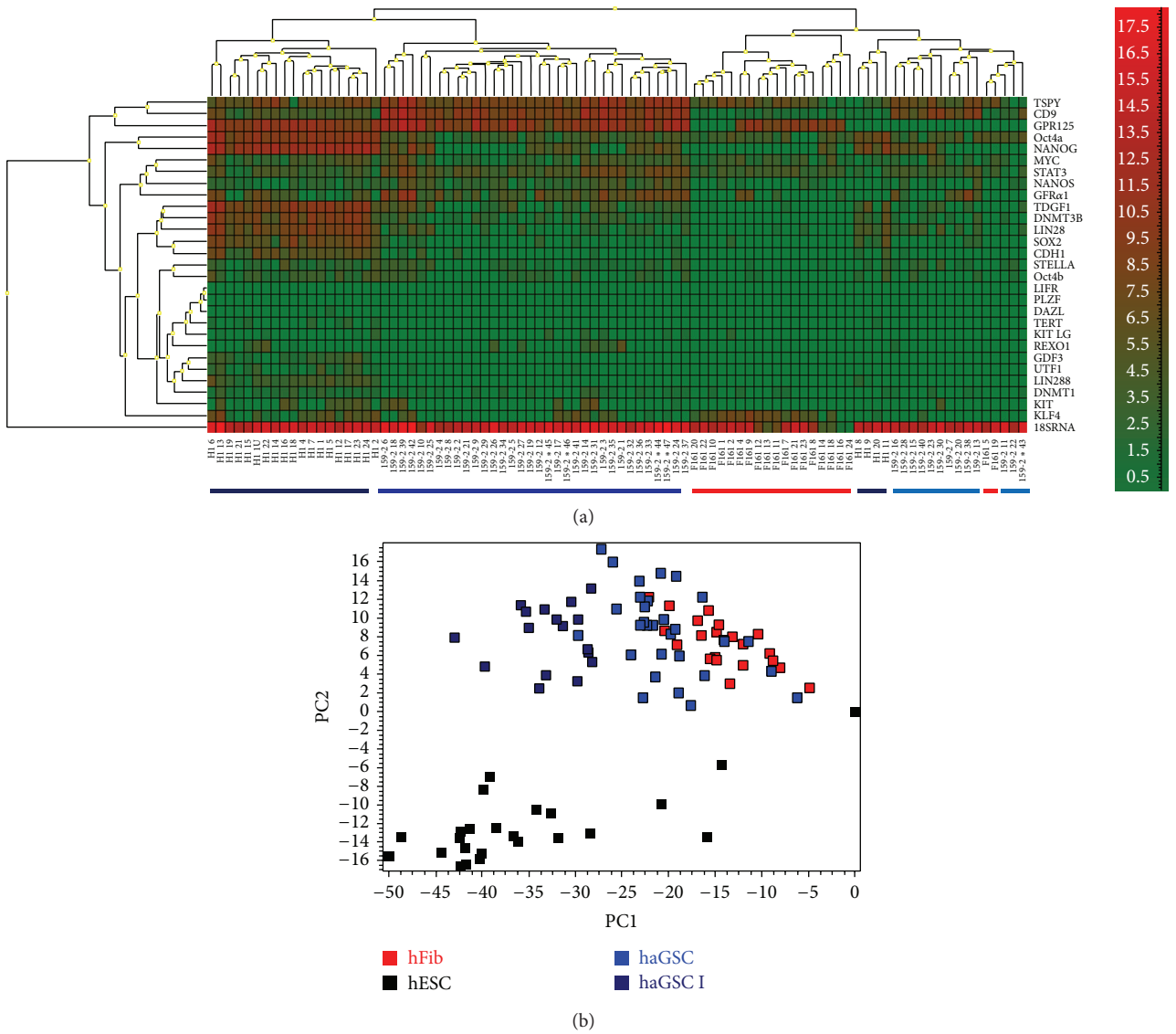

Figure 2: Gene expression profiling of single hESCs, haGSC, and hFibs of germ cell-enriched and pluripotency associated genes. (a) Heat map showing array of pluripotency and germ cell associated genes with each column representing a single cell. Note that haGSCs (coloured blue) are a heterogenic population of cells with more similarities to hESCs (coloured black), while some outliner cluster with hFibs (coloured red). (b) PCA showing the distribution of single cells selected from the separated trees from (a). The group of haGSCs which cluster with hESCs in (a) are named haGSCs I and were coloured dark blue.

explain 79% of the complete variance. The same separation was observed in the cluster dendrogram. In particular, hESCs and hSSCs were aggregated in nicely separated clusters. However, the group of haGSCs was more heterogeneous and the sample 157-23_P5 especially seemed to be more different. The cluster dendrogram was very similar even when the whole transcriptome (all 54K genes) was considered (data not shown).

Then we further investigated the Pearson correlation of the 4 distinct haGSCs to the three other cell types based on the medium variance genes. Three out of the four haGSCs showed their highest correlation to hSSCs with the Pearson correlation coefficient of 0.82–0.85 while the correlation coefficient to hESCs and hFibs was lower between 0.75 and 0.79. Only reprogramming sample 157-30c+d showed the highest correlation coefficient to hFibs.

This analysis clearly pointed that all cell types showed a distinct gene expression pattern and they were clearly distinguishable from each other. This was true for the selected set of genes based on the medium variance genes but was also found for the complete transcriptome.

2.3.2. High Variance Genes. For 150 genes with the highest variances across all samples, we calculated a heatmap (independent clustering of samples and genes) (Figure 5). As already seen in the dendrogram of the median variance genes, all cell types were separated consistently and grouped correctly into subtrees. The high variance genes were clustered

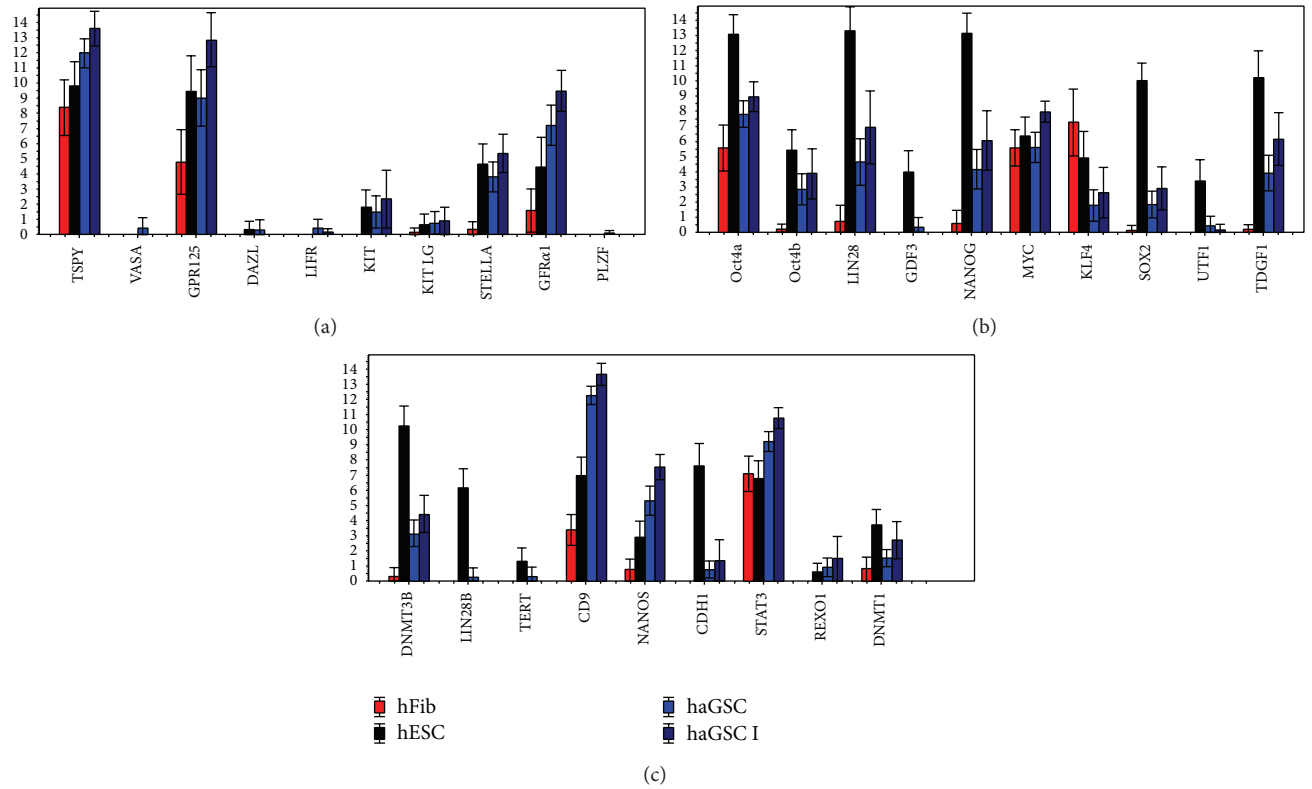

FIGURE 3: Bar plot showing relative expressions of (a) germ- and (b, c) pluripotency-associated genes between haGSCs (coloured light blue), haGSC I (coloured dark blue), hESCs (coloured black), and hFibs (coloured red). For $P < 0.05$ haGSCs versus hFibs and $P < 0.05$ haGSC I versus hFibs, see Supplementary Table 3.

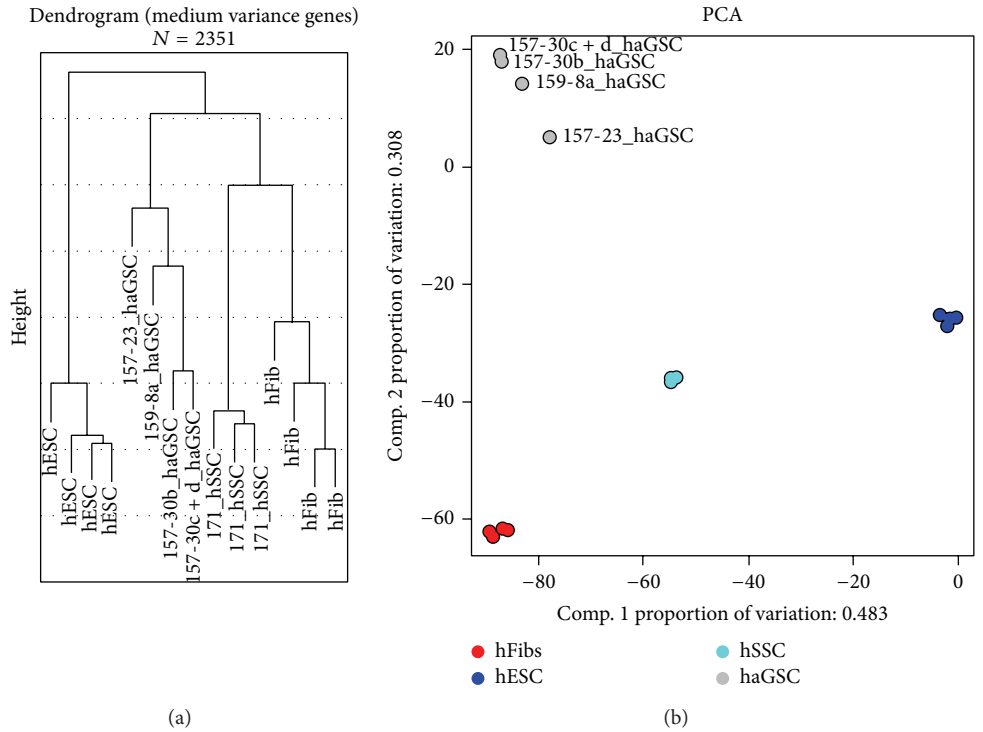

FIGURE 4: (a) Dendrogram using only genes with median variance. Genes with median variance were defined by selecting all genes whose variance is at least 2 SDs away from mean variance (2357 genes). Dendrograms were calculated using average linkage clustering and Euclidean distance. (b) Scatter plot of the first two principle components. The first two components explain 79% of the variance.

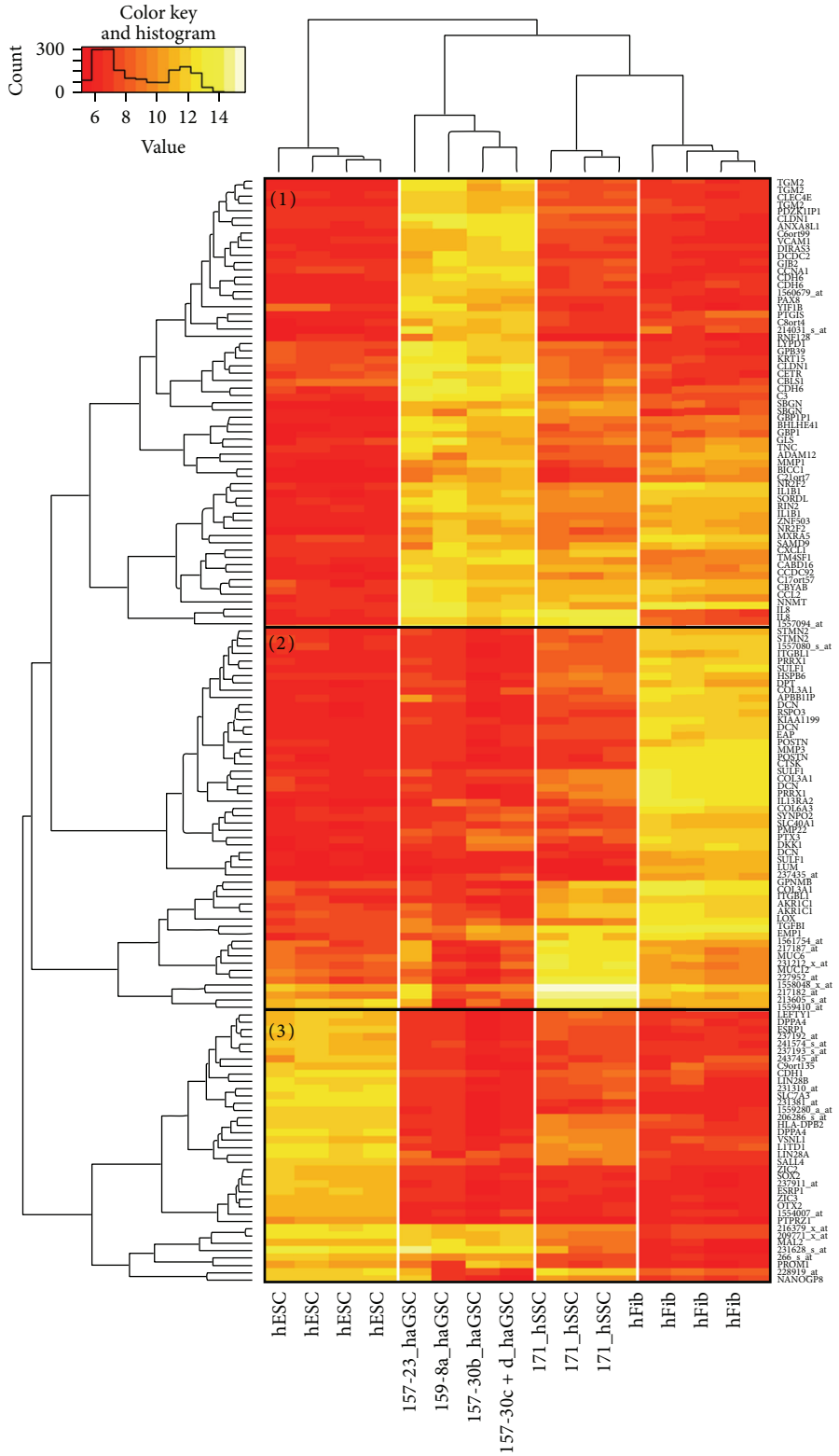

Figure 5: Heatmap of 150 features with the highest variance generated by independent clustering of genes and samples using complete linkage clustering and Euclidean distance. All cell types were separated consistently and grouped correctly into subtrees. Each cell type was characterized by a specific set of highly expressed genes (block pattern). The set of high variance genes could be grouped in 3 classes of genes with high expression: (1) in hESCs (H1), (2) in hFibs, and (3) in haGSCs.

in cell type-specific sets of highly expressed genes (visible as block pattern). The set of high variance genes could be grouped in 3 classes of genes with high expression: (1) in haGSCs, (2) in hFibs, and (3) in both hESCs and haGSCs.

Each of the three groups of genes was searched for enrichment of gene ontology (GO) terms. The 10 most significant GO terms for each group are shown in Supplementary Table 4. Genes highly expressed in hFibs showed typical functional annotation, which involves mainly extracellular matrix production, including collagen and proteoglycan metabolic process. The hESC genes were typically related to embryonic morphogenesis/development and diverse positive regulated cellular processes. In partial overlap with the hESC group, hSSCs and haGSCs expressed several hESC cell-related genes, including *NANOG*, *LIN28,* and *SALL4*. The genes which were highly expressed in haGSCs revealed a heterogeneous enrichment of gene ontology terms including biochemical processes, which partially overlapped with hSSC and hFib mechanisms of cell adhesion and immunological defense responses (Supplementary Table 4).

2.3.3. Analysis of haGSCs with Predefined Gene Sets for Germ-, Pluripotency-, Fibroblast-, and MSC-Associated Genes from the Literature. In an extended approach, we considered different predefined sets of genes: (1) ES cell-specific genes, a gene set containing human pluripotency-related genes specific for ES cells, and (2) hSSC-specific genes, a set of genes specific for germ cells. These two sets reflected the general knowledge from the literature. In addition to these two sets of genes, we used (3) genes which were found to be related to mesenchymal stem cells (MSCs) according to Chikhovskaya et al. [7], (4) hESC-enriched genes, and (5) genes found to be enriched in hFibs. The last two sets of genes (4 and 5) were extracted from the publication of Ko et al. [9] (Figure 1k -Human ES cell-enriched genes). The expression of three different sets of genes 1, 2, and 3 is presented in heatmaps in Supplementary Figures 1 and 2.

The analysis clearly showed that (1) none of the hESC cell-specific genes were expressed in hFibs. The genes *PROM1*, *FOXO1*, and *CD24* had a higher expression in haGSCs and in one of them (157-23_P5) also the genes related to pluripotency *NANOG*, *LIN28A*, *SALL4,* and *POU5F1* were expressed at a higher level than in hFibs. In contrast, the microarray analysis revealed that some genes were highly expressed in hESCs but not in "reprogramming trials" (*SOX2*, *ZIC3*, *DPPA4*, and *LEFTY2*). (2) From the set of hSSC-specific genes, *GFRα1*, *TSPYL*, *GPR125*, and *CD9* showed a higher expression in haGSCs than in hFibs. Some of the MSC-related markers, which are commonly used for the characterization of MSCs, are CD73, CD29, CD90, CD105, CD140b, CD146, and CD166. (3) Most of the set of MSC-related genes which could be detected by microarray analysis (*CD73*, *CD29*, *CD90*, *CD105*, *CD146*, and *CD166*) were not differentially expressed in haGSCs in comparison to hFibs or hESCs (see heatmap, Supplementary Figure 2). The gene *CD146* (*MCAM*) which was used to strengthen the similarity of testicular stem cells to MSCs by Chikhovskaya et al. [7] was also not differentially expressed in haGSCs in comparison to hFibs and hESCs. Furthermore, most of the genes used by Chikhovskaya et al. [7] to demonstrate that their testis-derived stem cells might be MSC-like were also not differentially expressed in haGSCs in comparison to hFibs and hESCs. Additionally, also the genes *CD34* and *CD73* which were used by Choi et al. [12] to isolate their testis-derived fibroblasts were not expressed in haGSCs. In our analysis, the only MSC-specific genes which were differentially expressed in haGSCs were *VCAM1*, *FN1*, *CDCP1*, *TM4SF1,* and *IL6ST*. There were also some other MSC-specific genes such as *NCAM1*, *CD44,* and *BMPR2,* which were expressed in hSSCs or hESCs. A heatmap for the expression of genes for gene sets is shown in Supplementary Figure 2 which corresponded to Figure 1k from the publication of Ko et al. [9]. From this analysis, it was evident that some ESC-enriched genes, like *TERF1*, *CXADR*, *PHC1*, *HOOK1*, *NANOG*, *POU5F1*, *SALL4*, and *LITD1*, were highly expressed in "reprogramming" trials, while others were not. A similar situation was observed for the set of hFibs-enriched genes. Some of them (*NNMT*, *IL1R1*, *NR2F2*, and *GREM1*) were highly expressed in haGSCs, while others did not show any regulation.

Considering the Pearson correlation based on five gene sets, three out of the four haGSC samples showed similar correlation coefficients of 0.48–0.55 to hFibs and to hESCs. But, one "reprogramming" sample (157-23_P5) showed a higher correlation to hESCs (0.68) and lower correlation to hFibs (0.46). Of the four "reprogramming" samples, this sample showed the highest similarity to hESCs.

The expression profiling data support the conclusion that haGSCs were not hFibs or MCSs but instead possess a strong germ-line specific background and a degree of similarity to hESCs.

2.3.4. Extended Profile Search. The differential analysis comparing haGSC samples with hFibs and hESCs allowed to identify differentially expressed genes in these groups of cells. Our special attention went to the comparison of "reprogramming" sample 157-23_P5 to hFibs and hESCs. The haGSC sample 157-23_P5 was selected since it showed the highest similarities to hESCs by other comparisons.

For comparing 157-23_P5 with hFibs and hESC, $\log_2$ ratios of the two corresponding differential analyses (comparisons of reprogramming trials with hFibs and with hESCs) were plotted in a scatter plot. The plot was divided into nine different sectors taking $\log_2$ ratios of −2 and 2 as thresholds which corresponds to a 4-fold differential regulation (see Figure 6(a)).

The majority of genes were not differentially expressed between 157-23_P5, hFibs, and hESCs (49K genes in Sector V). But there were still many genes showing similar expression in 157-23_P5 and hESCs but differential expression between 157-23_P5 and hFibs (454 genes in Sector IV and 855 genes in Sector VI). Considering the expression of these genes, reprogramming sample was similar to hESCs and different from hFibs. On the other hand, there were also many genes, which showed similar expression in both the 157-23_P5 reprogramming sample and hFibs, while they were differentially expressed between 157-23_P5 and hESCs (895

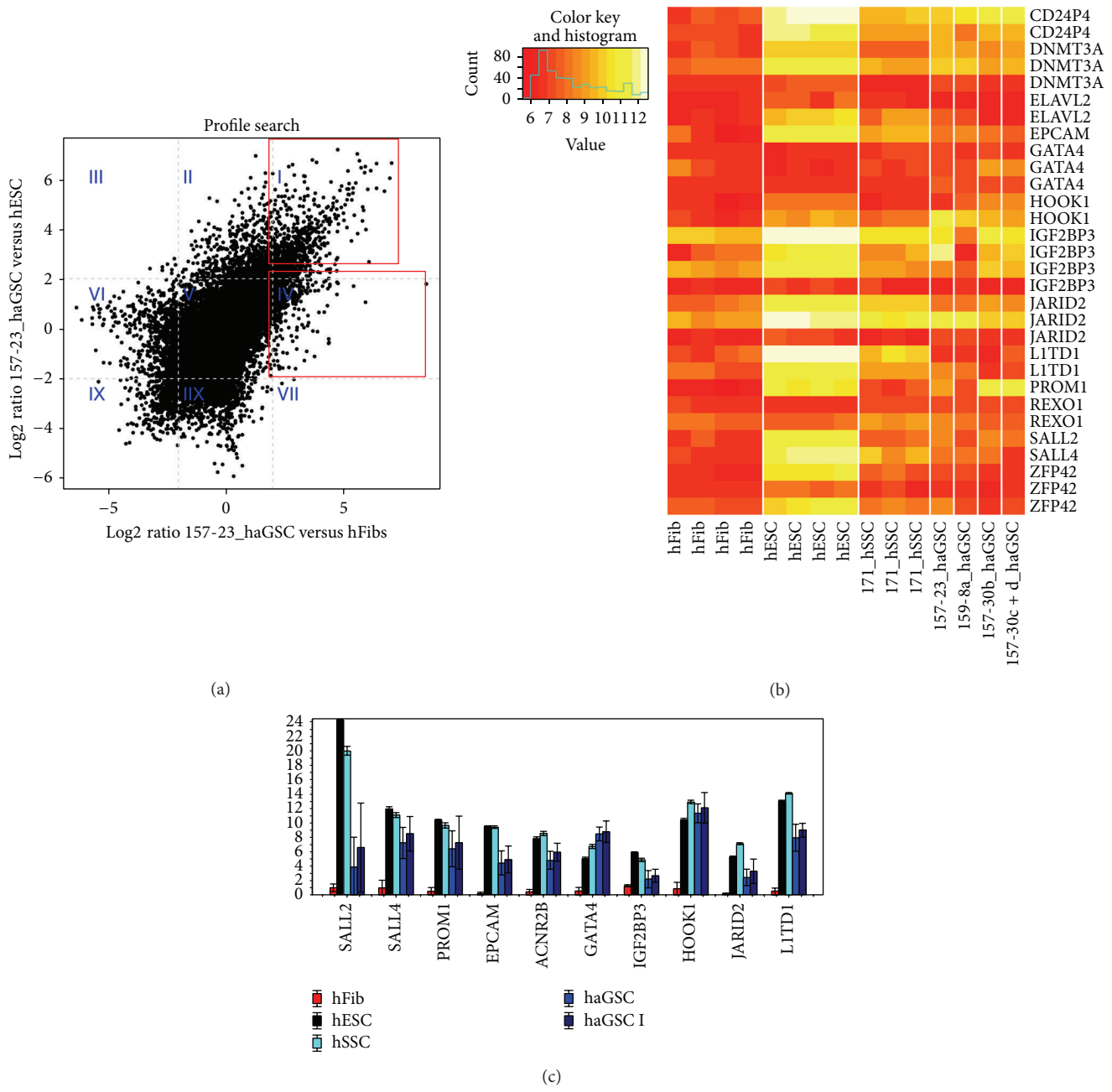

FIGURE 6: (a): Scatter plot of $\log_2$ ratios for the two differential analyses of reprogramming versus hFibs (x-axis) and haGSCs versus hESCs (y-axis). Grey dashed lines represent the thresholds of −2 and 2 used definition of the sectors. Different sectors are labelled with blue-coloured Roman numerals. The plot is divided into nine different sectors taking $\log_2$ ratios of −2 and 2 as thresholds which corresponds to a 4-fold differential regulation. The nine sectors were as follows. Sector I 798 genes were upregulated in 157-23_P5 compared to hFibs and upregulated in 157-23_P5 compared to hESCs. Sector II 895 genes were not differentially regulated in 157-23_P5 compared to hFibs and upregulated in 157-23_P5 compared to hESCs. Sector III 8 genes were downregulated in 157-23_P5 compared to hFibs and upregulated compared to hESCs. Sector IV 454 genes were upregulated in 157-23_P5 compared to hFibs and not differentially regulated in 157-23_P5 compared to hESCs. Sector V 49468 genes are not differentially regulated in 157-23_P5 compared to hFibs and not differentially regulated in 157-23_P5 compared to hESCs. Sector VI 855 genes are downregulated in 157-23_P5 compared to hFibs and not differentially regulated in 157-23_P5 compared to hESCs. Sector VII 2 genes are upregulated in 157-23_P5 compared to hFibs and downregulated in 157-23_P5 compared to hESCs. Sector VIII 1744 genes are not differentially regulated in 157-23_P5 compared to hFibs and downregulated in 157-23_P5 compared to hESCs. Sector IX 451 genes are downregulated in 157-23_P5 compared to hFibs and downregulated in 157-23_P5 compared to hESCs. The majority of the genes were not differentially expressed between 157-23_P5, hFibs, and hESCs (49K gene in Sector V). (b) Heatmap with pluripotency associated genes upregulated by haGSCs in comparison to hFibs according to microarray experiment. (c) Gene expression profiling of hESCs, haGSCs, and hFibs of additional pluripotency associated genes upregulated according to microarray study in haGSCs. (a) haGSCs are a heterogenic population of cells with some similarities to hESCs (coloured black) and hSSCs (coloured aquamarine) but not to hFibs (coloured red).

genes in Sector II and 1744 genes in Sector VIII). According to these genes, the reprogramming sample 157-23_P5 was similar to hFibs but different from hESCs. Additionally, 798 genes in Sector I were upregulated in reprogramming sample in comparison to hFibs and hESCs.

For the genes in Sectors II, IV, VI and IIX, a functional annotation was performed. The 10 GO terms with the most significant *P* values are shown in Supplementary Table 4. The genes in Sector VI were expected to be related to fibroblast-enriched GO terms, since these genes showed a high expression in fibroblasts but low expression in the reprogramming sample 157-23_P7. And indeed these genes were related to the "extracellular region" and "matrix" terms. Analogously the genes in Sector VIII showed high expression in hESCs but low expression in the 157-23_P7 sample. These genes were related to hESC cell-linked GO terms such as "nuclear part" or "cell cycle." The genes, which were upregulated in the sample 157-23_P7 from Sector IV, were mostly linked to GO terms of "nuclear processes."

2.3.5. IPA Ingenuity Analysis. The Sector I genes (upregulated in the haGSCs sample 157-23_P5 compared to hFibs and hESCs) and Sector IV genes (upregulated in the sample 157-23_P5 compared to hFibs and not differentially regulated in 157-23_P5 compared to hESCs) were analyzed by IPA Ingenuity programme.

The results showed that, among Sector I genes which were upregulated in haGSCs in comparison to both hFibs and hESCs, there were gene networks related to (1) amino acid metabolism, small molecule biochemistry, and gene expression (39 genes), (2) cellular assembly and organization, cellular function and maintenance, skeletal and muscular system development and function (37 genes), (3) cell morphology, cellular assembly and organization, and gastrointestinal disease, and (4) cell-to-cell signaling and interaction, cellular assembly and organization, and cellular function and maintenance (28 genes). Among these genes the most expressed canonical pathways were TREM1 signaling, hepatic fibrosis/hepatic stellate cell activation, ILK signaling, IL-17A signaling in airways cells, and production of nitric oxide and reactive oxygen species in macrophages. The main transcription factors were *RELA*, *NFKB* (complex), *CTNNB1*, *NFKBIB*, and *Nfat* (family). In terms of molecular and cellular functions, the highest proportion of upregulated genes was related to cellular growth and proliferation (190 genes), cell death (187 genes), cellular function and maintenance (144 genes), cell morphology (139 genes), and cellular movement (130 genes). In terms of physiological system development and function, the highest proportion of upregulated genes was related to tissue development (180 genes), organismal development (132 genes), tissue morphology (111 genes), cardiovascular system development and function (82 genes), and connective tissue development and function (42 genes). In terms of disease, the highest proportions of upregulated genes were related to cancer (230 genes) and reproductive system disease (133 genes). In comparison to hFibs, the most upregulated genes in haGSCs were *CLDN1*, *LYPD1*, *GPR39*, *PAX8*, *CFTR*, *NCAM1*, *PARD6B*, and *CRLS1*, while the most upregulated genes in comparison to hESCs were *KRT7*, *IL8*, *GBP1*, *C3*, *BHLHE41*, *CLDN1*, *PAX8*, and *CCL2*.

Among Sector IV genes, which were upregulated in haGSCs (157-23_P5) in comparison to hFibs and not differentially regulated in comparison to hESCs, there were gene networks related to (1) RNA posttranscriptional modification, cell morphology, cellular assembly, and organization (57 genes), (2) cellular assembly and organization, cellular compromise, and nervous system development and function (52 genes), (3) gene expression, cellular growth and proliferation, and embryonic development (50 genes), (4) cell-to-cell signaling and interaction, cellular assembly and organization, and tissue development (44 genes), and (5) cancer, hematological disease, DNA replication, recombination, and repair (41 genes). Among these genes the most expressed canonical pathways were Sertoli cell-Sertoli cell junction signaling, tight junction signaling, cell cycle: G1/S checkpoint regulation, Wnt/catenin signaling, and chronic myeloid leukemia signaling. The main transcription regulators were *YY1*, *FOXD3*, *E2F4*, *HOXA9*, and *NPAT*. In terms of molecular and cellular functions, the highest proportion of genes was related to gene expression (83 genes), cellular assembly and organization (46 genes), cellular function and maintenance (34 genes), cell-to-cell signaling and interaction (24 genes), and RNA posttranscriptional modification (23 genes). In terms of physiological system development and function, the highest proportion of genes was related to tissue development (43 genes), nervous system development and function (30 genes), cardiovascular system development and function (28 genes), organ morphology (27 genes), and skeletal and muscular system development and function (7 genes). In terms of disease, the highest proportions of genes were related to cancer (153 genes) and reproductive system disease (76 genes).

Interestingly, among Sector IV genes, which were upregulated in haGSCs (157-23_P5) in comparison to hFibs and not differentially regulated in comparison to hESCs, there was also a network of 50 genes related to gene expression, cellular growth and proliferation, and embryonic development, including the genes related to pluripotency. All these genes were upregulated in the haGSC sample 157-23_P5 in comparison to hFibs. The most upregulated gene in haGSCs was *NANOG*. These results indicated that the haGSC reprogramming sample 157-23_P5 expressed a relatively higher degree of pluripotency genes, which was significantly higher than in hFibs.

2.3.6. Validation of Microarray Results by Real-Time PCR and Immunohistochemistry. In addition to the initial panel of germ cell- and pluripotency-associated genes, the following germ cell- and pluripotency-associated genes were also selected for the Fluidigm real-time PCR analysis (see Figure 6(c) and Supplementary Figure 3) based on microarray results (see Figure 6(b)): *L1TD1*, *SALL4*, *JARID2*, *HOOK1*, *EPCAM*, *PROM1*, *SALL2*, *IGFR2BP3*, *REX1*, and *GATA4*. In similarity to haGSC clones derived from patients 157 and 159, the genes *VASA*, *DAZL*, and *PLZF* were predominantly expressed in haGSCs derived from two additional patients

239 and 240 (Supplementary Figure 3). The haGSCs showed a profound decreased expression of germ cell-specific genes *VASA*, *DAZL*, and *PLZF* in comparison to hSSCs. In contrast, the other two germ cell-specific genes, *STELLA* and *GFRα1*, were strongly expressed in haGSCs. In comparison to hSSCs the genes *REX1*, *LIFR*, and *NANOS* were expressed in haGSCs in a similar range than in hSSCs, while the gene *CD9* was more strongly expressed in haGSCs. The genes *DAZL* and *LIFR* were not expressed in hFibs at all. All germ cell-associated genes were significantly more strongly expressed in hSSCs and haGSCs than in hFibs (t-test, <0.05). In comparison to hSSCs, haGSCs similarly compared to hESCs possessed a rudimentary germ cell- associated gene expression profile. The genes *CD9* and *GFRα1* were more strongly expressed in haGSCs than in hESCs (Supplementary Figure 3).

The expression of pluripotency-associated genes was similar in haGSCs clones from two different patients 239 and 240. All pluripotency-associated genes were significantly upregulated in the best haGSC clones in comparison to hFibs (t-test, <0.05) (Supplementary Figure 3 and Supplementary Figure 4b). From the genes in Sector IV, which were differentially upregulated in the clone 157-23_P5 according to the previous microarray analysis, 8 pluripotency- and germ cell-associated genes were reconfirmed, with the exception of genes *SALL2* and *IGFR2BP3* (Figure 6(c)).

Immunocytochemistry of haGSC clusters in comparison to hESCs and hFibs clearly demonstrated that CD9, CD24, Oct4, and Nanog were expressed by haGSCs and hESCs but not in hFibs (Figure 7). Furthermore immunohistochemical staining with typical germ cell proteins of haGSC clusters in comparison to hESCs and hFibs also clearly demonstrated that VASA, UTF1, TSPYl2, STELLA, and GFRα1 were expressed by haGSCs and in part by hESCs, but not in hFibs (Figure 8).

3. Discussion

The haGSCs displayed a specific gene expression profile, with some properties of both germ cells and hESCs. In general, they showed a higher expression of some ESC-related genes, which were not expressed in hFibs in this study. In the microarray study this distinct gene expression profile was found on all three presented levels: (1) the heatmap of high variance genes showed many pluripotency-related genes which were highly-expressed in haGSCs; (2) in particular one out of four reprogramming samples of haGSCs (157-23_P5) showed a higher similarity to hESCs. However, none of the reprogramming samples exhibited a full pluripotency-related gene expression profile, but only to a degree, as reported by some other groups [13].

According to the microarray experiments in this study, the core pluripotency-related genes *NANOG*, *LIN28*, and *POU5F1* were upregulated in haGSCs in comparison to hFibs, while *SOX2* was not. As revealed by pilot single-cell Fluidigm analysis and also by a reconfirmation experiment with new haGSC clones by the same technology, haGSCs expressed all above mentioned pluripotency-associated genes, including *Sox2, TDGFβ1*, and *UTF1*, and also some germline-associated genes, such as *STELLA*, *CD9*, *GFRα1*, and *TSPY*.

As published by some other groups, the list of significantly regulated genes in haGSCs in comparison to hFibs included several genes which are highly expressed in hESCs, such as *CD24* [14], *EPCAM* [15–18], *L1TD1* [19, 20], *SALL4* [21], *JARID2* [22–24], *DNMT3A* [25, 26], *HOOK1* [27], *ACTIVIN A receptor 1B* [28], and *REX1* [29, 30]. The significant upregulation of these genes in haGSCs, revealed by microarray analyses, was also reconfirmed by Fluidigm RT-PCR and for CD24 by immunohistochemistry.

It is important that there were several genes related to pluripotency, which were regulated in haGSCs. The microarray analysis showed that the cell surface protein-encoding gene *CD24* was strongly expressed in all haGSC clones and to a lesser extent also in the enriched population of spermatogonia. The gene *CD24* was identified as one of the hESC-associated genes proposed by Assou et al. [14] by carrying out a meta-analysis of the hESC transcriptome. This gene encodes a membrane-specific protein, which is strongly expressed in hESCs and enables purifying them by FACS from cocultured fibroblasts.

In this study, we also found that *CD9* and *EPCAM* were also strongly expressed in both haGSCs and hESCs. It is known that the pluripotency-associated epithelial surface marker *EPCAM* is strongly expressed in human fetal gonads and can be effectively used as a selector marker for germ cell enrichment from differentiating ES cells [18]. This molecule has been shown to play a role in progenitor proliferation in the mouse SSC culture system [15]. The gene *EPCAM*, which forms functional complexes with some other genes such as *CLDN7*, *CD44V6*, *TSPAN8*, and *CD9*, might increase the efficiency of transcriptions-factor mediated pluripotency reprogramming by upregulation of *OCT4* and suppression of the p53-p21 pathway [17].

It has already been illustrated that the RNA-binding protein L1TD1, which is highly expressed in haGSCs, is a marker for undifferentiated hESCs [19, 31]. The *L1TD1* gene is also rapidly activated during iPSC generation, but it is dispensable for the maintenance and induction of pluripotency [20]. In these publications it is documented that *L1TD1* interacts with the core pluripotency gene *LIN28* and has an important function in the regulation of stemness, including hESC self-renewal and cancer cell proliferation. The *L1TD1* gene is a downstream target of *NANOG* and represents a useful marker to identify undifferentiated hESCs. Additionally, the *L1TD1* gene is also highly expressed in testicular seminoma, and depletion of *L1TD1* in seminoma cancer cells influences their self-renewal and proliferation [20]. One of genes highly upregulated in haGSCs was also *SALL4*. Hobbs et al. [32] have demonstrated the critical and distinct roles of *SALL4* in development of germ cells during embryonic period of life and differentiation of postnatal spermatogonial progenitor cells. It has further been demonstrated that the stem cell-associated gene *SALL4* suppresses the transcription through recruitment of DNA methyltransferases [21]. There were also some other genes, which were regulated in haGSCs such as *JARID2*/*JUMONJI*, *DNMT3A*, and *HOOK1*. It was shown by Shen et al. [22] that the JARID2/JUMONJI is

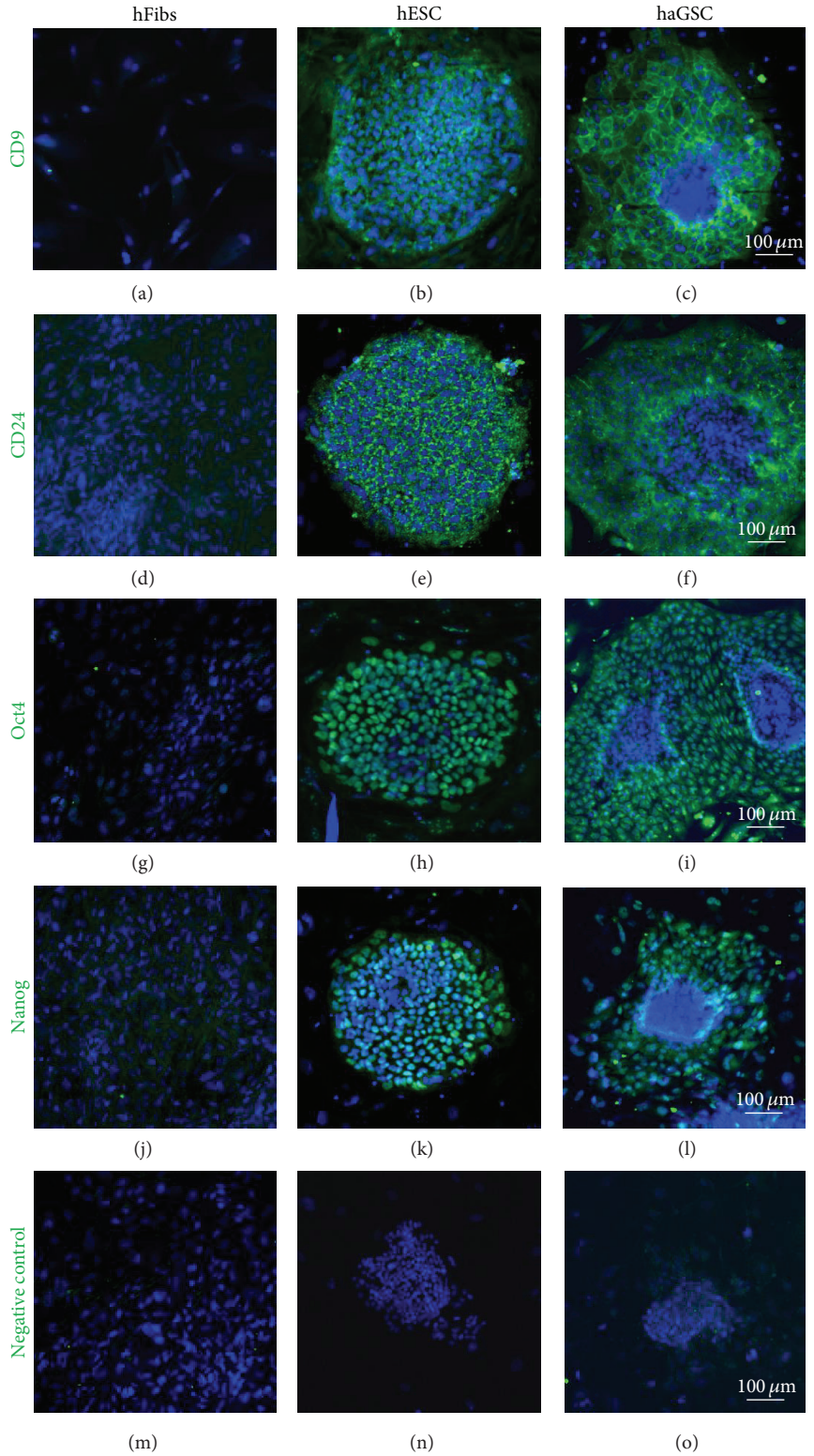

Figure 7: Immunohistochemistry of hESCs, haGSCs, and hFibs with CD9, CD24, Oct4, and Nanog antibodies. The different markers are shown in green and the staining of the nuclei with DAPI in blue. Scale bar is 100 μm.

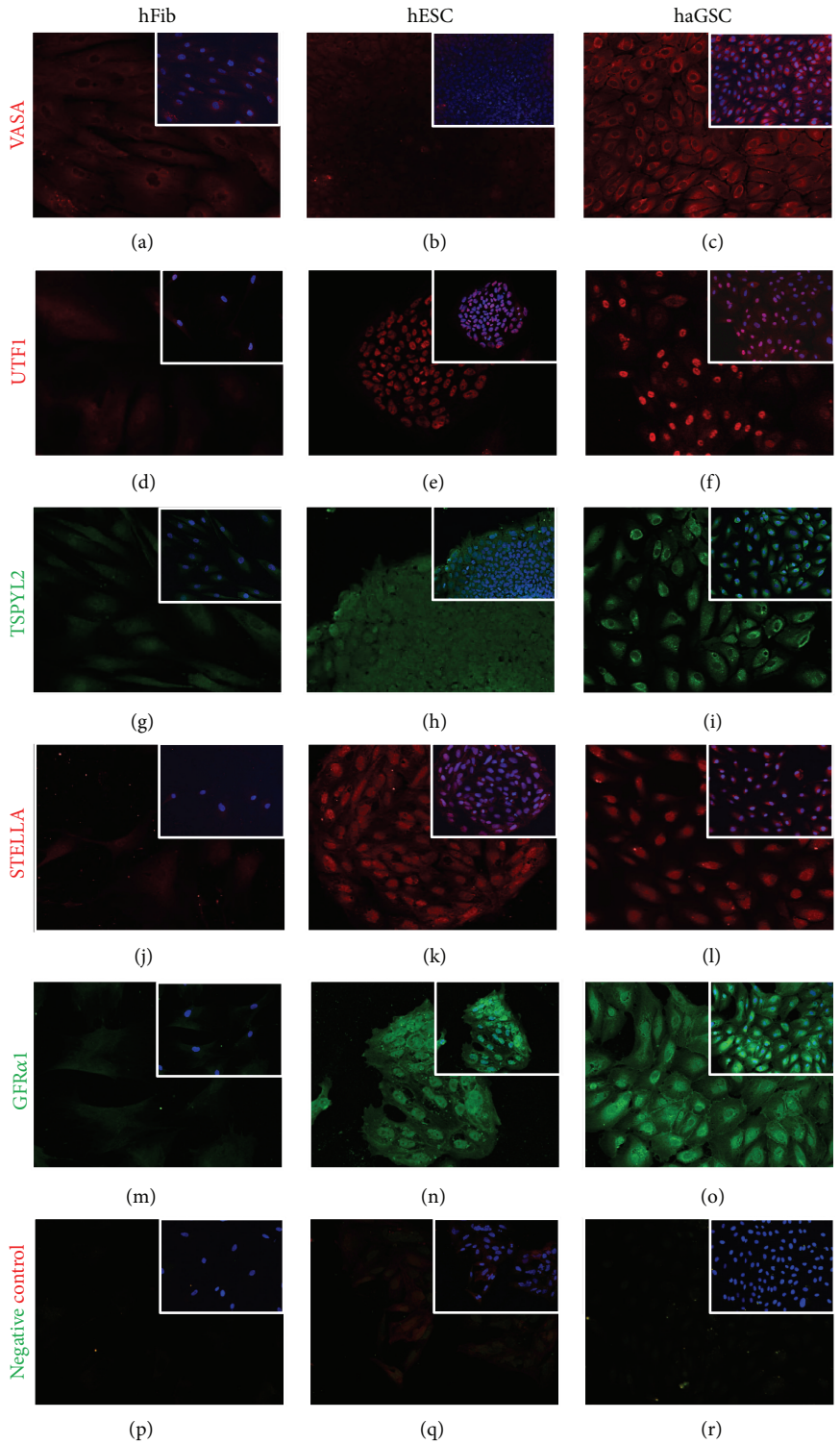

Figure 8: Immunohistochemistry of hFibs, hESCs, and haGSCs with cytoplasmic staining of VASA ((a)–(c)), nuclear staining of UTF1 ((d)–(f)), cytoplasmic staining of TSPYL2 ((g)–(i)), cytoplasmic and nuclear staining of STELLA ((j)–(l)), and cytoplasmic staining of GFRα1 ((m)–(o)). The different germ cell different markers are shown in green (Alexa 488 for TSPYL2 and GFRα1) or red (Alexa 546 for VASA, UTF1, and STELLA) and the staining of the nuclei with HOECHST is shown in blue. Scale bar is 50 μm.

a DNA-binding protein that functions as a transcriptional repressor and modulates POLYCOMB activity and self-renewal versus differentiation of stem cells during embryonic development. This protein facilitates the recruitment of the PRC2 complex to target genes [33]. These authors have also shown that *JARID2* regulates the binding of *POLYCOMB* repressive complex 2 to target genes in ESCs and is therefore responsible for the proper differentiation of ESCs and normal development. It is interesting that epigenetically regulated gene *DNMT3A* was also regulated in haGSCs. In general, the mammalian cells can epigenetically modify their genome by DNA methylation. The protein DNMT3A functions as a *de novo* methyltransferase and was found to be highly expressed in mitotically quiescent human fetal spermatogonia [25, 26]. In addition to the established spermatogonial markers, haGSCs were found to express the ES cell-associated gene *HOOK1*, which is a cytosolic protein attached to the microtubules that mediates the binding to cell organelles. The HOOK1 protein was found to be present at high levels in human testes [27].

There were also some other genes related to pluripotency and ES cells which were regulated in haGSCs, such as *ACTIVIN A* and *ACTIVIN receptors IIA* and *IIB*, *IGFR2BP3*, and *IGF2*. The data from the literature indicate that *ACTIVIN A* and *ACTIVIN receptors IIA* and *IIB* may be involved in the regulation of germ cell proliferation in the human ovary during the period leading up to primordial follicle formation. The insulin growth factors are known to have a key role in maintaining the status of pluripotency [28]. For example, the gene *IGFR2BP3,* which encodes a member of the IGF-II mRNA-binding protein (IMP) family, was also upregulated in haGSCs. The encoded protein binds to the 5′ UTR of the insulin-like growth factor 2 (IGF2) mRNA and thereby regulates the IGF2 translation.

Also *REX1* (*ZFP42*) is another gene whose expression was regulated in haGSCs and is known to be closely associated with pluripotency/multipotency in both mouse and human embryonic stem cells [30]. It was demonstrated that the *REX1* (*ZFP42*) null mice show impaired testicular function, abnormal testis morphology, and aberrant gene expression. Also *BRD7,* a novel PBAF-specific SWI/SNF subunit which was expressed in haGSCs, is known to be required for target gene activation and repression in embryonic stem cells [29]. There were also some reprogramming-related genes which were expressed in haGSCs. Kuo et al. [34] documented the novel role of *miR-302/367* in reprogramming, a process which is normally involved in the early embryonic development and embryonic stem cell formation.

According to the microarray analysis in this study most of ESC-associated genes (including *PROMININ1* and *MYCN*) which were upregulated in haGSCs were also upregulated in enriched population of spermatogonia cultured *in vitro*, but not in hFibs. The correlation analysis of the microarray data showed that haGSCs are more closely related to spermatogonia. This might be related to their cellular origin.

From the single cell population, it became obvious that, under the conditions which we employed to select and maintain long-term culture haGSCs, the cells are a heterogeneous population of cells where most of the cells possess a residual expression of germ cell genes (*TSPY*, *CD9*, *GFRα1*, and *STELLA*), but only 25% of the cells express the core pluripotency genes *OCT4*, *NANOG*, and *SOX2*.

Recently, there were more reports on the presence of MSCs in adult human testicles [10–12]. In contrast to them [10–12], we found that most of the genes, proposed to be expressed in testicular MSCs, were not expressed in the haGSCs presented in this study. In the studies of Mizrak et al. [5], Chikhovskaya et al. [7], and Gonzalez et al. [8], different populations of testicular stem cells might be isolated from the tissue and cultured *in vitro*. It is not excluded that there are different types of stem cells present in adult human testicles, which might interact and reflect the complexity of this reproductive organ.

In conclusion, the molecular analysis in this study confirmed that haGSCs were generated from the enriched population of CD49f MACS and matrix-selected spermatogonia. During the long-term culture *in vitro*, they reexpressed some genes related to developing germ cells in culture, which might be otherwise blocked by their natural niche, testicular tubules, in adult human testicles. The haGSCs are a heterogeneous population of cells that are different from hFibs or MSCs and express a degree of pluripotency. The further research is needed to optimize the culture condition to avoid the molecular block, which prevents the haGSCs from becoming fully molecular pluripotent stem cells.

4. Conclusions

During the cell culture, haGSCs originate in the enriched population of CD49f MACS and matrix-selected spermatogonia, but never in the negatively selected fraction or from patients without spermatogonia [1]. The haGSC colonies were easily distinguishable from hFibs and resembled the early hESC colonies characterized by central cluster with outgrowing "epithelial"-like cells. By single-cell Fluidigm analysis it was found that haGSCs were quite distinct from hFibs in terms of the expression of germ- and pluripotency-associated genes. Only a minority of outliner hESCs and haGSCs shared some similarities with hFibs, but the majority of them did not. It also became clear that haGSC colonies were heterogeneous, displaying more or less similarities to a state of pluripotency. Also in the microarray study different haGSC colonies were confirmed to be relatively heterogeneous in terms of the expression of germ- and pluripotency-associated genes. When analysing the whole transcriptome and the high variance genes in haGSCs in comparison with hESCs and hFibs, it was found that the haGSCs separated from hFibs and represent a specific population of cells.

5. Material and Methods

5.1. Testicular Tissue and Experimental Design. This study was conducted from October 2009 to September 2012 using testicular material from 5 adult men, patients (P157, 159, 171, 239, and 240) with different medical background. The detailed information on patient's data is provided in Supplementary Table 1. All experiments with human material conducted

here were approved by the local ethics councils (University Hospitals of Tübingen and Heidelberg) and informed written consent was obtained from all the human subjects. Age of the patients ranged from 23 to 67 years. Healthy donated tissue included heterogeneous material from patients with different medical background including orchiectomies as part of a reassignment surgery of transsexual patients after hormone therapy (1), orchiectomies of healthy testis in case of penis carcinoma and prostate cancer (2), and biopsies of "healthy" (nonmalignant) peritumoral testicular tissue from patients with seminoma (3). Histopathological examinations of the testicular tissue used in this study were conducted by experts at the Department of Pathology (University Clinic, Tübingen) in routine diagnostics and in case of cancer with more cancer specific diagnostics.

In this study short-term (<2 weeks after matrix selection) SSC cultures and long-term (>2 months, up to 6 months) haGSC cultures from testicular tissues of all 5 men were analyzed on gene expression profile to evaluate the character of testicular adult stem cells. The experimental design of this study can be seen in Supplementary Table 2. The single cells from the different groups of cells were first analyzed on gene expression profile by Biomark Real-Time quantitative PCR (qPCR) system (Fluidigm), followed by microarray analysis in comparison with hESCs and hFibs. The selected group of genes from microarray analysis was validated by Biomark Real-Time quantitative PCR (qPCR) system (Fluidigm). We mainly focused on pluripotency-, germ cell-, fibroblast- and mesenchymal stem cell-associated genes.

5.2. Selection and Cultivation of haGSCs. After removing of the tunica albuginea, the obtained human testicular tissues were mechanically disrupted to dissociate the tubules. In each sample, the dissociated tubules were enzymatically digested with 750 U/mL collagenase type IV (Sigma), 0.25 mg/mL dispase II (Roche), and 5 μg/mL DNase in HBSS buffer with Ca^{++} and Mg^{++} (PAA) for 30 minutes at 37°C, with gentle mixing, to obtain a single-cell suspension. Then the digestion was stopped with 10% ES cell-qualified FBS. The cell suspension was passed through a 100 μm cell strainer and centrifuged for 15 minutes at 1000 rpm. The supernatant was removed and the pellet was washed with HBSS buffer with Ca^{++} and Mg^{++}. After washing, the cells (approximately 2×10^5 cells per cm^2) were plated into culture dishes (d = 10 cm), coated with 0.2% gelatin (Sigma), in hGSC (human germ stem cell) medium consisting of StemPro hESC medium, 1% N2-supplement (Invitrogen), 6 mg/mL D+ glucose (Sigma), 5 μg/mL bovine serum albumin (Sigma), 1% L-glutamine (PAA), 100 μM β-mercaptoethanol (Invitrogen), 1% penicillin/streptomycin (PAA), 1% MEM vitamins (PAA), 1% nonessential amino acids (PAA), 30 ng/mL estradiol (Sigma), 60 ng/mL progesterone (Sigma), 20 ng/mL epidermal growth factor (EGF; Sigma), 10 ng/mL basic fibroblast growth factor (FGF; Sigma), 8 ng/mL glial-derived neurotrophic factor (GDNF; Sigma), 100 U/mL human LIF (Millipore), 1% ES cell qualified FBS, 100 μg/mL ascorbic acid (Sigma), 30 μg/mL pyruvic acid (Sigma), and 1 μL/mL DL-lactic acid (Sigma). In this culture medium, the cells were incubated in a CO_2-incubator for 96 hours at 37°C and 5% CO_2 in air. After 72 hours the half volume of culture medium was replaced with fresh culture medium of the same volume and the cells were further cultured for 4 days. On day 7 the culture medium was carefully removed and the testis cell culture was gently rinsed with 5 mL DMEM/F12 culture medium with L-glutamine (PAA) per plate to harvest the germ cells bound to the monolayer of adherent somatic cells attached to the dish bottom. This procedure was repeated by pipetting 5 mL of DMEM/F12 culture medium. The cell suspension pooled from 5 culture dishes per tissue sample was centrifuged for 5 minutes at 1000 rpm. The pellet was resuspended in 10 mL of MACS buffer and centrifuged again for 5 minutes and the cells were further purified with MACS separation (Miltenyi), CD49f-FITC (α_6-integrin; AbD Serotec), and anti-FITC beads (Miltenyi). After MACS separation, cells were transferred to dishes coated with collagen I (5 $\mu g/cm^2$, Becton & Dickinson) and incubated at 37°C for 4 h. Cells that did not bind to collagen I dishes (Col_{NB} cells) were harvested and pelleted at 1000 rpm. The Col_{NB} cells were suspended in medium and plated at 0.5–1 $\times$ 10^6 cells per mL per well in 12-well plates precoated with laminin (4.4 $\mu g/cm^2$, Sigma). The plated Col_{NB} cells were incubated for 45 min at 37°C and unbound cells (Col_{NB}/Lam_{NB} cells) were removed from bound cells (Lam_B cells) by pipetting and were discarded. The Lam_B cells were rinsed twice with 1 mL media. The Lam_B cells then were harvested by gentle pipetting and were plated onto a 12-well plate with hGSC culture medium, on irradiated CF-1 feeder layer. A half volume of culture medium was removed every 2-3 days and replaced with fresh hGSC culture medium. Under these conditions, the spermatogonia heterogeneously proliferated. The best cell cultures were split 1 : 2 every two to three weeks. It was important not to dilute the cells too much and to keep the appropriate cell number in the wells all the time.

5.3. Cultivation of Human Fibroblasts. The human fibroblasts were obtained from the dermis of the scrotum and a primary cell line was generated in DMEM high glucose, 10% FBS Superior (Biochrom), 200 μM L-glutamine (PAA), 1% nonessential amino acids (PAA), and 100 mM β-mercaptoethanol (Invitrogen).

5.4. Cultivation of hESCs. The H1 human ES cell line from the National Stem Cell Bank were cultured, respectively, according to the protocols from WiCell on CF1 Feeder in DMEM/F12 with L-glutamine (PAA), 20% knockout serum replacement (Invitrogen), 300 μM L-glutamine (PAA), 1% nonessential amino acids (PAA), 100 mM β-mercaptoethanol (Invitrogen), 1 mM HEPES, and 4 ng/mL basic fibroblast growth factor (FGF, Sigma).

5.5. Collection of Single Cells from the Population of Enriched Spermatogonia (hSSCs) with Micromanipulation System. In each sample, the spermatogonial cells were rinsed with the culture medium to remove the spermatogonia from the

attached monolayer of somatic cells or feeder layer in a culture dish. After gentle resuspension, the cells were transferred to a single cell suspension into the top of small culture dish (d = 3.5 cm). The top of dish was placed onto a prewarmed (37°C) working platform of a Zeiss inverted microscope with the micromanipulation system. At magnification 20x, the cells were collected step by step by a micromanipulation pipette. The typical morphology of short-term cultured spermatogonia was clearly observed. This was primarily based on their round shape, diameter of approximately 6–12 μm, and high nucleus-to-cytoplasm ratio, which could be observed by a clear small shining cytoplasmic ring between the round nucleus and the outer cell membrane.

5.6. Collection of Single Cells from Enzymatically Degraded Typical haGSC Colonies, hESCs, and hFibs with a Micromanipulation System. In order to characterize the single cells in the haGSC colony, we enzymatically degraded a typical haGSC and hESC colony or confluent growing hFibs to a single cell level and manually selected individual cells one by one (24 hFibs, 24 hESCs, and 48 haGSCs) with a micromanipulation system for single cell gene expression profiling. With this technique, we aimed to provide information about single cell profiles of important germ- and pluripotency-associated genes in these cells and the homo-/heterogeneity of the selected cells from a typical haGSC colony and to culture further those colonies with the "best" germ- and pluripotency-associated gene expression profile. Single cells per sample probe were collected for Fluidigm analysis and 200 cells per probe for microarray analysis and also for validation of selected pluripotency associated genes by Fluidigm analysis. After collection, the cells were directly transferred into 6.5 μL of cells direct buffer for Fluidigm or 10 μL RNA direct lyses buffer for microarray analysis.

5.7. Gene Expression Analyses by Fluidigm Biomark System. Gene expression analysis of single cells and 200 cells was performed using the Biomark Real-Time quantitative PCR (qPCR) system (Fluidigm) in comparison with hESCs (positive control) and human testis hFibs (F161; negative control). In all cell samples the expression of the following genes was analyzed by Taqman assays: germ cell-specific genes *TSPYL*, *DDX4* (*VASA*), *DAZL*, *ZBTB16* (*PLZF*), *DPPA3* (*STELLA*), *CD9*, *NANOS*, *UTF1*, *GFRα1*, *GPR125*, *REX1*, *KIT*, *KIT LG*, *LIFR*, *STAT3*, pluripotency-associated genes *POU5F1 (OCT4)A*, *POU5F1 (OCT4)B*, *LIN28*, *NANOG*, *SOX2*, *GDF3*, *KLF4*, *MYC*, *TDGF1*, *TERT*, *DNMT3B*, *DNMT1*, *CDH1*, *LIN28B*, *OCT4B*, and the housekeeping genes 18SRNA, *CTNNB1*, *HNBS*, and *GAPDH*.

According to genes upregulated in haGSC clone 157-23_P5 in the microarray experiment, the following further assays were selected: *SALL4* (sal-like 4), *SALL2* (sal-like 2), *PROM1* (prominin 1), *EPCAM* (epithelial cell adhesion molecule), *GATA4* (GATA binding protein 4), *HOOK1* (hook homolog 1), *L1TD1* (LINE-1 type transposase domain containing 1), *JARID2* (JUMONJ), *IGFR2 BP3* (insulin-like growth factor 2 mRNA binding protein 3), *REX1* (zinc finger protein 462), and *ACVAR1B* (activin receptor-like kinase 4).

The inventoried TaqMan assays (Applied Biosystem) were pooled to a final concentration of 0.2x for each of the assays. Cells to be analyzed were harvested directly into 9 μL RT-PreAmp Master Mix consisting of 5.0 μL CellsDirect 2x Reaction Mix (Invitrogen), 2.5 μL 0.2x assay pool, 0.2 μL RT/Taq Superscript III (Invitrogen), and 1.3 μL TE buffer. The harvested cells were immediately frozen and stored at −80°C. Cell lysis and sequence-specific reverse transcription were performed at 50°C for 15 min. The reverse transcriptase was inactivated by heating to 95°C for 2 minutes. In the same tube, cDNA subsequently underwent limited sequence-specific amplification by denaturing at 95°C for 15 seconds and 14 cycle-annealing and amplification at 60°C for 4 minutes. These preamplified products were 5-fold diluted prior to analysis with Universal PCR Master Mix and inventoried TaqMan gene expression assays (ABI) in 96.96 Dynamic Arrays on a Biomark system. Each sample was analyzed in two technical replicates.

5.8. GenEx Statistical Analysis. Ct values obtained from the Biomark system were transferred to the GenEx software (MultiD) for analysis. Missing data in the Biomark system were assigned a Ct of 999 by the instrument software. These were removed in GenEx. Also Ct's larger than a cutoff of 25 were removed, since high Ct's in the Biomark 96 × 96 microfluidic card were expected to be false positives due to baseline drift or formation of aberrant products and since a sample with a single template molecule is expected to generate a lower Ct. The effect of setting cutoff to 25 was tested by repeating the analysis with a slightly different cutoff and was found to have negligible effect on the analysis results. Technical repeats were then averaged and any remaining missing data were replaced by the highest Cq measured + an offset of 1 for each gene separately. Managing missing data is primarily required for downstream multivariate classification of the data. An offset of 1 corresponds to assigning a concentration to the samples with off-scale Cq values, that is, half of the lowest concentration measured for a truly positive sample. The magnitude of the offset does not influence P values calculated with nonparametric methods, which were preferred when there were off-scale data, but it has small influence on P values calculated by t-test and on multivariate classification. In essence, the offset tunes and the weight of the off-scale measurement compared to the positive reading; larger offset gives higher weight to the off-scale measurement. We tested the importance of the offset by repeating the analysis using a higher offset up to +4, which corresponds to a concentration of 6% of a truly positive sample, and found negligible effect on the multivariate results. Linear quantities were calculated relative to the sample having lowest expression and data were then converted to $\log_2$ scale for analysis. Because of the very large and uncorrelated cell-to-cell variation of genes' expressions normalization to the housekeeping genes is not meaningful. Instead, expression levels were presented "per 50-cell" average expression of the genes in different groups was calculated including .95% confidence interval and groups were compared using 1-way ANOVA (Tukey-Kramer pairwise comparison) and unpaired

2-tailed t-test. Expression of genes with multiple off-scale readings was compared with nonparametric Mann-Whitney test. For multivariate analysis to classify the samples based on the combined expression of all the genes data were either mean centred, that is, subtracting the average expression of each gene, or autoscaled, which is mean centre data also divided by the standard deviation (so called z-score). Autoscaling gives all the genes equal weight in the classification algorithms making them equally essential. Hierarchical clustering (Ward's algorithm, Euclidean distance measure) including heatmap and principal component analysis (PCA) were performed.

5.9. Microarray Analysis. The total RNA isolated from short-term spermatogonia and long-term haGSC cultures, hESC line H1 (positive control), and testicular fibroblasts (hFibs; negative control) was prepared using the RNeasy Mini Kit (Qiagen), followed by an amplification step with MessageAmp aRNA Kit (Ambion). In each sample, 200 cells were collected per probe with the micromanipulation system and transferred directly into 10 μL of RNA direct lysis solution and stored at −80°C. Samples were analysed at the microarray facility of the University of Tübingen Hospital, Germany. Gene expression analysis was performed using the Human U133 + 2.0 Genome oligonucleotide array (Affymetrix). The raw data (CEL-files) was provided to the MicroDiscovery GmbH, Berlin, Germany, for normalization and biostatistical analysis.

5.10. Microarray Data Normalisation and Analyses. Microarray data was imported into the R Statistical Environment version 2.12.1 (2010-12-16). Data condensation was performed using Bioconductor package affy version 1.28.0. The condensation criteria were as follows: bg.correct = FALSE, normalize = FALSE, pmcorrect.method = "pmonly," and summary.method = "medianpolish." Additional normalization was performed between samples using multi-lowess algorithm, a multidimensional extension of lowess normalization strategy [15]. The data were analyzed in terms of sample to sample relations, high variance genes, predefined gene sets for germ-, pluripotency-, fibroblast-, and MSC-associated genes from the literature, and extended profile search. A proportion of data was transferred into the IPA Ingenuity program to evaluate the gene functions and pathways. Additional data are provided in the Supplemental Methods section.

5.11. Antibodies and Staining. The following primary antibodies were used as stem cell markers: mouse monoclonal anti-CD9 (R&D System, Stem cell marker kit, SC009), mouse monoclonal anti-CD24 (Abcam, ab31622), rabbit polyclonal anti-OCT4 (Abcam, ab19857), and rabbit polyclonal anti-nanog (Abcam, ab21624). For the staining of germ cells, the following markers were used: rabbit polyclonal anti-VASA (Abcam, ab13840), mouse monoclonal anti-UTF1 (Chemicon, MAB4337), rabbit polyclonal anti-TSPYL2 (Proteintech, 12087-2-AP), rat monoclonal anti-STELLA (R&D Systems, MAB2566), and goat polyclonal anti-GFRα1 (R&D Systems, AF714).

Alexa Fluor-488-conjugated goat anti-mouse IgG, Alexa Fluor-488-conjugated goat anti-rabbit IgG, Alexa Fluor-488-conjugated donkey anti-goat IgG, Alexa Fluor-546 goat anti-mouse IgG, Alexa Fluor-546 goat anti-rabbit IgG, and Alexa Fluor-546-conjugated goat anti-rat IgG were used as secondary antibodies. Nuclear costaining was performed for stem cell markers with DAPI and for germ cell markers with Hoechst.

Conflict of Interests

No financial conflict of interests exists for the data provided within this research paper.

Authors' Contribution

Thomas Skutella and Sabine Conrad conceived and designed the experiments. Sabine Conrad, Hossein Azizi, Maryam Hatami, and Thomas Skutella performed the experiments. Sabine Conrad, Mikael Kubista, and Thomas Skutella analyzed the data. Biostatistics of the microarray data was conducted by MicroDiscovery, Berlin. Michael Bonin, Jörg Hennenlotter, and Karl-Dietrich Sievert contributed reagents/materials/analysis tools. Sabine Conrad, Thomas Skutella, Hossein Azizi, and Mikael Kubista wrote the paper.

Acknowledgments

The authors would like to thank all patients who kindly donated their testis tissue for this research and all other people and institutions supporting this research. This research was funded by the DFG Grant SK 49/10-1 and by BMBF Grant 01GN0821 and was supported by Ministry of Youth, Education and Sports of the Czech Republic RVO:86652036; BIOCEV CZ.1.05/1.1.00/02.0109 from the ERDF.

References

[1] S. Conrad, H. Azizi, M. Hatami et al., "Differential gene expression profiling of enriched human spermatogonia after short- and long-term culture," *BioMed Research International*, vol. 2014, Article ID 138350, 17 pages, 2014.

[2] T. Skutella and S. Conrad, "Generation of germline derived stem cells from adult human testis," in *Regenerative Medicine*, G. Steinhoff, Ed., pp. 207–224, Spinger, Berlin, Germany, 2011.

[3] N. Kossack, J. Meneses, S. Shefi et al., "Isolation and characterization of pluripotent human spermatogonial stem cell-derived cells," *Stem Cells*, vol. 27, no. 1, pp. 138–149, 2009.

[4] N. Golestaneh, M. Kokkinaki, D. Pant et al., "Pluripotent stem cells derived from adult human testes," *Stem Cells and Development*, vol. 18, no. 8, pp. 1115–1126, 2009.

[5] S. C. Mizrak, J. V. Chikhovskaya, H. Sadri-Ardekani et al., "Embryonic stem cell-like cells derived from adult human testis," *Human Reproduction*, vol. 25, no. 1, pp. 158–167, 2010.

[6] J. J. Lim, H. J. Kim, K.-S. Kim, J. Y. Hong, and D. R. Lee, "*In vitro* culture-induced pluripotency of human spermatogonial stem cells," *BioMed Research International*, vol. 2013, Article ID 143028, 9 pages, 2013.

[7] J. V. Chikhovskaya, M. J. Jonker, A. Meissner, T. M. Breit, S. Repping, and A. M. M. van Pelt, "Human testis-derived embryonic stem cell-like cells are not pluripotent, but possess potential of mesenchymal progenitors," *Human Reproduction*, vol. 27, no. 1, pp. 210–221, 2012.

[8] R. Gonzalez, L. Griparic, V. Vargas et al., "A putative mesenchymal stem cells population isolated from adult human testes," *Biochemical and Biophysical Research Communications*, vol. 385, no. 4, pp. 570–575, 2009.

[9] K. Ko, M. J. Araúzo-Bravo, N. Tapia et al., "Human adult germline stem cells in question," *Nature*, vol. 465, no. 7301, pp. E1–E3, 2010.

[10] M. Stimpfel, T. Skutella, M. Kubista, E. Malicev, S. Conrad, and I. Virant-Klun, "Potential stemness of frozen-thawed testicular biopsies without sperm in infertile men included into the *in vitro* fertilization programme," *Journal of Biomedicine and Biotechnology*, vol. 2012, Article ID 291038, 15 pages, 2012.

[11] L. A. Boyer, I. L. Tong, M. F. Cole et al., "Core transcriptional regulatory circuitry in human embryonic stem cells," *Cell*, vol. 122, no. 6, pp. 947–956, 2005.

[12] W. Y. Choi, H. G. Jeon, Y. Chung et al., "Isolation and characterization of novel, highly proliferative human CD34/CD73-double-positive testis-derived stem cells for cell therapy," *Stem Cells and Development*, vol. 22, no. 15, pp. 2158–2173, 2013.

[13] F. J. Muller, B. M. Schuldt, R. Williams et al., "A bioinformatic assay for pluripotency in human cells," *Nature Methods*, vol. 8, no. 4, pp. 315–317, 2011.

[14] S. Assou, T. Le Carrour, S. Tondeur et al., "A meta-analysis of human embryonic stem cells transcriptome integrated into a web-based expression atlas," *Stem Cells*, vol. 25, no. 4, pp. 961–973, 2007.

[15] M. Kanatsu-Shinohara, S. Takashima, K. Ishii, and T. Shinohara, "Dynamic changes in EPCAM expression during spermatogonial stem cell differentiation in the mouse testis," *PLoS ONE*, vol. 6, no. 8, Article ID e23663, 2011.

[16] V. Y. Ng, S. N. Ang, J. X. Chan, and A. B. H. Choo, "Characterization of epithelial cell adhesion molecule as a surface marker on undifferentiated human embryonic stem cells," *Stem Cells*, vol. 28, no. 1, pp. 29–35, 2010.

[17] H.-P. Huang, P.-H. Chen, C.-Y. Yu et al., "Epithelial cell adhesion molecule (EpCAM) complex proteins promote transcription factor-mediated pluripotency reprogramming," *The Journal of Biological Chemistry*, vol. 286, no. 38, pp. 33520–33532, 2011.

[18] C.-Y. Chuang, K.-I. Lin, M. Hsiao et al., "Meiotic competent human germ cell-like cells derived from human embryonic stem cells induced by BMP4/WNT3A signaling and OCT4/EpCAM (epithelial cell adhesion molecule) selection," *The Journal of Biological Chemistry*, vol. 287, no. 18, pp. 14389–14401, 2012.

[19] R. C.-B. Wong, A. Ibrahim, H. Fong, N. Thompson, L. F. Lock, and P. J. Donovan, "L1TD1 is a marker for undifferentiated human embryonic stem cells," *PLoS ONE*, vol. 6, no. 4, Article ID e19355, 2011.

[20] E. Närvä, N. Rahkonen, M. R. Emani et al., "RNA-binding protein L1TD1 interacts with LIN28 via RNA and is required for human embryonic stem cell self-renewal and cancer cell proliferation," *Stem Cells*, vol. 30, no. 3, pp. 452–460, 2012.

[21] J. Yang, T. R. Corsello, and Y. Ma, "Stem cell gene *SALL4* suppresses transcription through recruitment of DNA methyltransferases," *The Journal of Biological Chemistry*, vol. 287, no. 3, pp. 1996–2005, 2012.

[22] X. Shen, W. Kim, Y. Fujiwara et al., "Jumonji modulates polycomb activity and self-renewal versus differentiation of stem cells," *Cell*, vol. 139, no. 7, pp. 1303–1314, 2009.

[23] C. Luzzani, C. Solari, N. Losino et al., "Modulation of chromatin modifying factors' gene expression in embryonic and induced pluripotent stem cells," *Biochemical and Biophysical Research Communications*, vol. 410, no. 4, pp. 816–822, 2011.

[24] Z. Zhang, A. Jones, C.-W. Sun et al., "PRC2 complexes with JARID2, MTF2, and esPRC2p48 in ES cells to modulate ES cell pluripotency and somatic cell reprograming," *Stem Cells*, vol. 29, no. 2, pp. 229–240, 2011.

[25] Y. Yanagisawa, E. Ito, Y. Yuasa, and K. Maruyama, "The human DNA methyltransferases DNMT3A and DNMT3B have two types of promoters with different CpG contents," *Biochimica et Biophysica Acta—Gene Structure and Expression*, vol. 1577, no. 3, pp. 457–465, 2002.

[26] D. Galetzka, E. Weis, T. Tralau, L. Seidmann, and T. Haaf, "Sex-specific windows for high mRNA expression of DNA methyltransferases 1 and 3A and methyl-CpG-binding domain proteins 2 and 4 in human fetal gonads," *Molecular Reproduction and Development*, vol. 74, no. 2, pp. 233–241, 2007.

[27] I. Mendoza-Lujambio, P. Burfeind, C. Dixkens et al., "The *Hook1* gene is non-functional in the abnormal spermatozoon head shape (*azh*) mutant mouse," *Human Molecular Genetics*, vol. 11, no. 14, pp. 1647–1658, 2002.

[28] L. Wang, T. C. Schulz, E. S. Sherrer et al., "Self-renewal of human embryonic stem cells requires insulin-like growth factor-1 receptor and ERBB2 receptor signaling," *Blood*, vol. 110, no. 12, pp. 4111–4119, 2007.

[29] M. D. Kaeser, A. Aslanian, M.-Q. Dong, J. R. Yates III, and B. M. Emerson, "BRD7, a novel PBAF-specific SWI/SNF subunit, is required for target gene activation and repression in embryonic stem cells," *The Journal of Biological Chemistry*, vol. 283, no. 47, pp. 32254–32263, 2008.

[30] N. C. Rezende, M.-Y. Lee, S. Monette, W. Mark, A. Lu, and L. J. Gudas, "Rex1 (Zfp42) null mice show impaired testicular function, abnormal testis morphology, and aberrant gene expression," *Developmental Biology*, vol. 356, no. 2, pp. 370–382, 2011.

[31] R. Brandenberger, H. Wei, S. Zhang et al., "Transcriptome characterization elucidates signaling networks that control human ES cell growth and differentiation," *Nature Biotechnology*, vol. 22, no. 6, pp. 707–716, 2004.

[32] R. M. Hobbs, S. Fagoonee, A. Papa et al., "Functional antagonism between Sall4 and Plzf defines germline progenitors," *Cell Stem Cell*, vol. 10, no. 3, pp. 284–298, 2012.

[33] D. Pasini, M. Malatesta, H. R. Jung et al., "Characterization of an antagonistic switch between histone H3 lysine 27 methylation and acetylation in the transcriptional regulation of Polycomb group target genes," *Nucleic Acids Research*, vol. 38, no. 15, pp. 4958–4969, 2010.

[34] C.-H. Kuo, J. H. Deng, Q. Deng, and S.-Y. Ying, "A novel role of miR-302/367 in reprogramming," *Biochemical and Biophysical Research Communications*, vol. 417, no. 1, pp. 11–16, 2012.

Hindawi Publishing Corporation
Stem Cells International
Volume 2016, Article ID 7651645, 8 pages
http://dx.doi.org/10.1155/2016/7651645

Research Article

Human Very Small Embryonic-Like Stem Cells Are Present in Normal Peripheral Blood of Young, Middle-Aged, and Aged Subjects

Hanna Sovalat, Maurice Scrofani, Antoinette Eidenschenk, and Philippe Hénon

Institut de Recherche en Hématologie et Transplantation, Hôpital du Hasenrain, 87 avenue d'Altkirch, 68100 Mulhouse, France

Correspondence should be addressed to Hanna Sovalat; hsovalat@yahoo.fr

Received 17 February 2015; Accepted 27 March 2015

Academic Editor: Mariusz Z. Ratajczak

The purpose of our study was to determine whether the number of human very small embryonic-like stem cells (huVSELs) would vary depending on the age of humans. HuVSELs frequency was evaluated into the steady-state (SS) peripheral blood (PB) of healthy volunteers using flow cytometry analysis. Their numbers were compared with volunteers' age. Blood samples were withdrawn from 28 volunteers (age ranging from 20 to 70 years), who were distributed among three groups of age: "young" (mean age, 27.8 years), "middle" (mean age, 49 years), and "older" (mean age, 64.2 years). Comparing the three groups, we did not observe any statistically significant difference in huVSELs numbers between them. The difference in mRNA expression for PSC markers as SSEA-4, Oct-4, Nanog, and Sox2 between the three groups of age was not statistically significant. A similar frequency of huVSELs into the SS-PB of young, middle-aged, and aged subjects may indicate that the VSELs pool persists all along the life as a reserve for tissue repair in case of minor injury and that there is a continuous efflux of these cells from the BM into the PB.

1. Introduction

Under steady-state conditions, small amounts of hematopoietic stem cells (HSCs) constantly leave the bone marrow (BM), penetrate the tissues, and return to the BM or peripheral niches via the blood or the lymphatic system [1–3]. Thus, the peripheral blood (PB) may be envisioned as a highway by which HSC can relocate between distant stem cell niches to keep the pool of BM stem cells in balance. In adult organisms, circulating stem/progenitor cells show a circadian rhythm with a peak occurring early in the morning and a nadir at night. Their number increases modestly during minor hematopoietic stresses, such as infection or strenuous exercise, [4–6]. In addition to HSCs, some rare other stem/progenitor cells such as mesenchymal stem cells (MSCs) [7], fibrocytes [8, 9], skeletal progenitors [10, 11], and endothelial progenitor cells (EPCs) [12–14] may also circulate into the PB after tissue/organ injury. Recently, a population of very small embryonic-like stem cells (VSELs) was identified in murine adult bone marrow [15]. Murine VSELs (muVSELs) are small, nonhematopoietic cells with high nuclear/cytoplasm ratio and unorganized euchromatin and express markers of pluripotent embryonic and primordial germ cells. MuVSELs have been identified in most tissues [16]. These cells circulate in a very few number into the PB under steady-state (SS) conditions and in much larger numbers after administration of granulocyte-colony stimulating factor (G-CSF) [17]. It was demonstrated that, either under steady-state conditions or after response to G-CSF, circulating VSELs numbers were lower in older animals than in younger ones [18, 19]. Human VSELs (huVSELs) have been firstly identified in umbilical cord blood as $CXCR4^+$, $CD34^+$, $CD133^+$, Lin^-, and $CD45^-$ cells enriched for Oct-4 and SSEA-4 [20]. We have recently shown that a similar population of huVSELs was present in both adult BM and PB and could be harvested by leukapheresis after G-CSF administration [21].

However, whether the number of VSELs would also vary in humans depending on the age has to be determined. In the present study, we have both assessed the presence of huVSELs into the steady-state PB of healthy volunteers and compared their numbers in function of age.

2. Material and Methods

2.1. Human Healthy Volunteers. 28 healthy volunteers (12 females and 16 males; mean age, 41.9±15.4 years; range 20–70 years), not taking any medication, were enrolled in this study after informed consent.

20 mL of SS-PB was withdrawn by venous puncture from each subject early in the morning to avoid the impact of any physical effort on PB cell counts, collected on EDTA, and immediately processed. The absolute number of white blood cells (WBC) was determined at the same time using a Coulter A^{c}T diff cell counter (Beckman Coulter, Roissy, France).

2.2. Flow Cytometry (FCM) Analysis. Staining and FCM analysis were performed as previously described [21]. Briefly, samples of whole PB were lysed in hypotonic ammonium chloride buffer (IOTest lysing solution, Beckman Coulter, Roissy, France) to remove red blood cells. Total nucleated cells (TNC) were stained with a mixture of lineages (Lin) associating monoclonal antibodies (MoAbs) conjugated with fluorescein isothiocyanate (FITC). At the same time, phycoerythrin (PE) conjugated-CD45 MoAb clone J33 (Beckman Coulter, Roissy, France) and a combination of allophycocyanin (APC) conjugated MoAbs, CD133 clone AC133 (Miltenyi Biotec, Paris, France), CD34 clone 8G12, or CD184 (CXCR4) clone 12G5 (BD, Le Pont de Claix, France), were added for 30 minutes on ice. Cells were then washed and fixed with 4% formaldehyde (FA) for 20 minutes. Finally, 7-aminoactinomycin D (7-AAD; BD, Le Pont de Claix, France) was added to stain nucleated cells.

FCM analyses were performed using a FACSVantage DIVA fluorescence-activated cell sorting device (BD Biosciences, Erembodegem, Belgium). At least 10^6 small events ranging from 2 to 10 μm were included in the gate after comparison with five different size beads calibrated at standard diameters of 1, 2, 4, 6, and 10 μm (Flow Cytometry Size Calibration, Invitrogen/ThermoFischer Scientific, Illkirch, France). CXCR4$^+$ Lin$^-$ CD45$^-$, CD34$^+$ Lin$^-$ CD45$^-$, or CD133$^+$ Lin$^-$ CD45$^-$ cell subset amounts were counted among the nucleated 7-AAD$^+$ cells.

Cell subpopulations absolute numbers were calculated in 1 mL of PB.

2.3. Reverse Transcription-Quantitative-Polymerase Chain Reaction (RT-qPCR) Analysis. RNA extraction from total PB-NC and analysis of *Oct-4*, *Nanog*, and *Sox2* mRNA were carried out as previously described [21]. Primer sequences of *Oct-4*, *Nanog*, *Sox2*, and β_2 are summarized in Table 1. RNA isolated from H9 and HUES 3 hESC lines [22, 23], kindly provided by the "Plateforme Cellules Souches Embryonnaires Humaines" (Inserm U602 Villejuif, France), was used as reference sample for each PCR reaction.

2.4. Immunofluorescence Staining. The expression of pluripotency antigens was determined for each healthy volunteer. NC were stained for 2 hours with antibodies against SSEA-4 (clone MC-813-70, mouse monoclonal IgG), Tumor Rejection Antigen (TRA-1-81, clone TRA-1-81, mouse monoclonal IgM), OCT-4A/4B (clone 9E3.2, mouse monoclonal IgG), and NANOG (goat polyclonal) (Millipore, Molsheim, France), as previously described in detail [21]. Appropriate secondary FITC or tetramethylrhodamine-5-isothiocyanate (TRITC) goat anti-mouse IgG or IgM and FITC-goat anti-rabbit (Beckman Coulter, Marseille, France) were added for 1 h. The nuclei were labelled with 4′,6-Diamidino-2-phenylindole (DAPI) complemented with Vectashield (Vector Laboratories, Abcys, Paris, France). Cells stained with secondary antibodies only were used as negative controls. Slides with H9 and/or HUES3 hESC lines were stained similarly and used as positive controls. Fluorescence images were recorded with the AxioVision 4.7 "Full support" system attached to a fluorescent microscope Axiostar Plus Zeiss and captured by AxioCam ICC 1 R3 Cameras (Lordil, Villers-les-Nancy, France).

2.5. Statistical Analysis. Data were expressed as mean ± standard deviation (SD). To verify the difference in expression of each marker between the different age groups, normality data were tested by the Shapiro test. Once normality is verified, one-way ANOVA was chosen to carry out this comparison; on the contrary, the Kruskal-Wallis test was chosen when normality was not verified. *t*-test pairwise analysis was performed when previous tests were significant.

3. Results

3.1. VSELs Numbers Do Not Decrease with Aging. Enumeration of circulating VSELs requires FACS-unique gating strategies to focus on very rare and small events (Figures 1(a) and 1(b)).

We applied here the identification strategy which was published in detail by Zuba-Surma and Ratajczak [24]. Three different subpopulations of huVSELs (diameter ranging from 3 to 6 μm) have thus been detected into SS-PB but in very low numbers. Considering altogether the healthy adult volunteers enrolled in this study, 290 ± 150 CD133$^+$ Lin$^-$ CD45$^-$ cells, 80±60 CD34$^+$ Lin$^-$ CD45$^-$ cells, and 300 ± 260 CXCR4$^+$ Lin$^-$ CD45$^-$ cells were counted on average per mL of total blood.

When volunteers were distributed among three groups of age, "young" (mean age, 27.8 years, range from 20 to 39 years; $n = 13$), "middle," (mean age, 49 years, range from 40 to 59 years; $n = 10$), and "older" (mean age, 64.2 years, range from 60 to 70 years; $n = 5$) groups, not any statistically significant difference in huVSELs frequency (expressed as number of cells/mL) in PB was observed between these three groups ($P > 0.05$; one-way analysis of variance (ANOVA)) (Figure 2).

However, in the older group, all VSELs subset numbers were lower in 3 of the subjects compared to the other 2, but this decline was not statistically significant. It may be due to the low number of "old" patients ($n = 5$) compared to the number of "young" and "middle-aged" groups. It is clearly important to increase the number of patients in the "old" group to have a clear data. This low number of aged healthy volunteers is due to our difficulty to find people with advanced age taking any drug. In fact, in our future investigations, by increasing our collaborations with other laboratories we hope to resolve this problem.

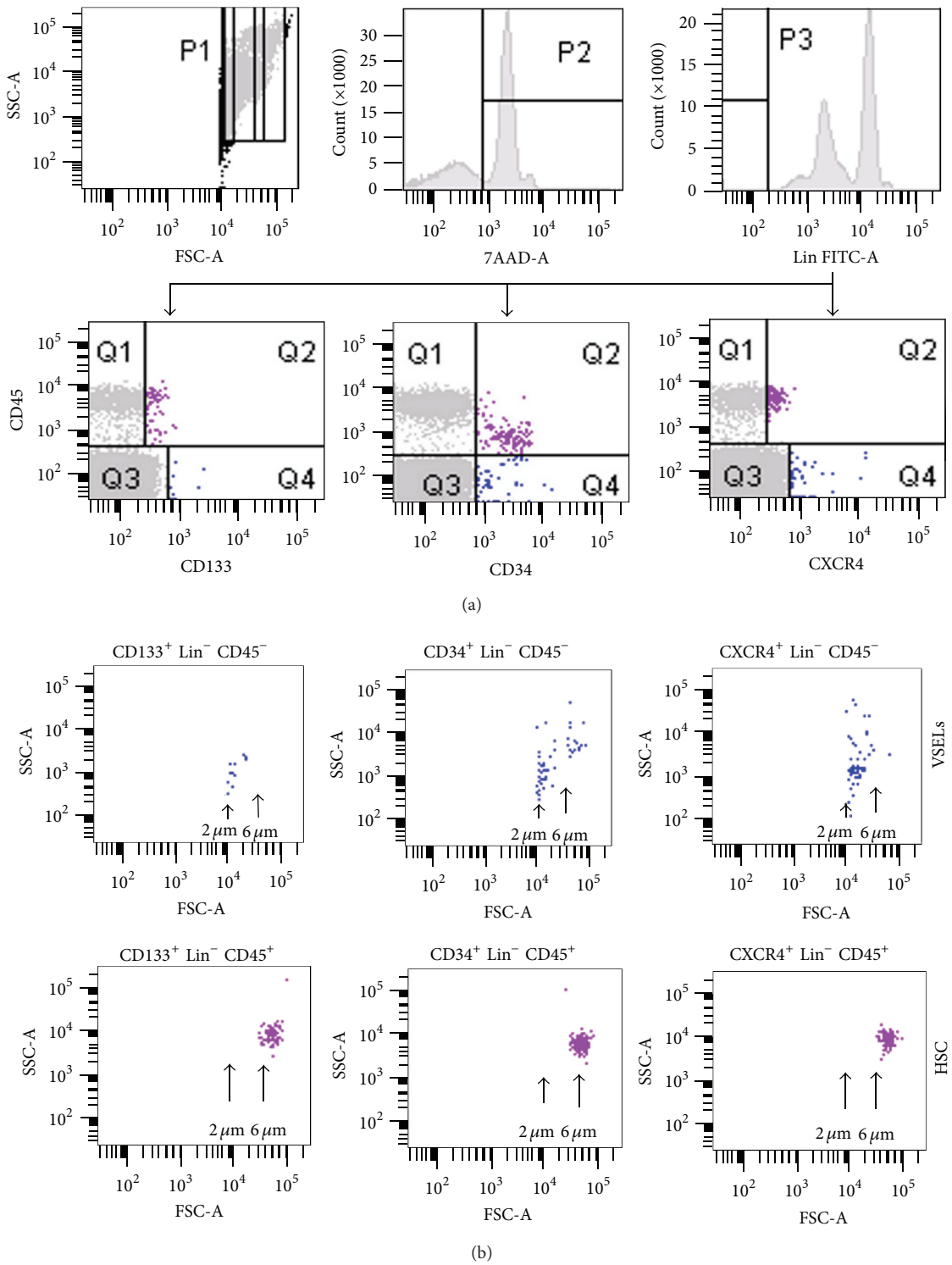

Figure 1: FCM analysis of PB-derived VSELs. Erythrocytes were removed by hypotonic lysis and PB NCs were stained with fluorescein isothiocyanate-lineage markers (Lin), phycoerythrin-CD45 and allophycocyanin-CD133, CD34, or CXCR4 mAbs. (a) Left dot plot: 10^6 events ranging from 2 to 10 μm were included in the P2 gate. Right histogram: Lin^- cells were included in the P1 analysis gate. Middle histogram: P1 gated cells stained with 7-aminoactinomycin D (7-AAD) were included in the P2 gate. Right histogram: Lin^- cells were included in the P3 gate and were analyzed for CD45 coexpression with CD133, CD34, or CXCR4 antigens. (b) Dot plots showing the size of analyzed $CD133^+$, $CD34^+$, or $CXCR4^+$, Lin^-, $CD45^-$ VSELs (upper row) and $CD133^+$, $CD34^+$, or $CXCR4^+$, Lin^-, $CD45^+$ HSC (lower row).

Table 1: Sequences of the forward and reverse primers employed for qPCR.

	Forward	Reverse
Oct-4	GAT GTG GTC CGA GTG TGG TTC T	TGT GCA TAG TCG CTG CTT GAT
Nanog	GCA GAA GGC CTC AGC ACC TA	AGG TTC CCA GTC GGG TTC A
Sox2	TAC AGC ATG TCC TAC TCG CAG	GAG GAA GAG GTA ACC ACA GGG
Beta-2-microglobuline	AAT GCG GCA TCT TCA AAC CT	TGA CTT TGT CAC AGC CCA AGA TA

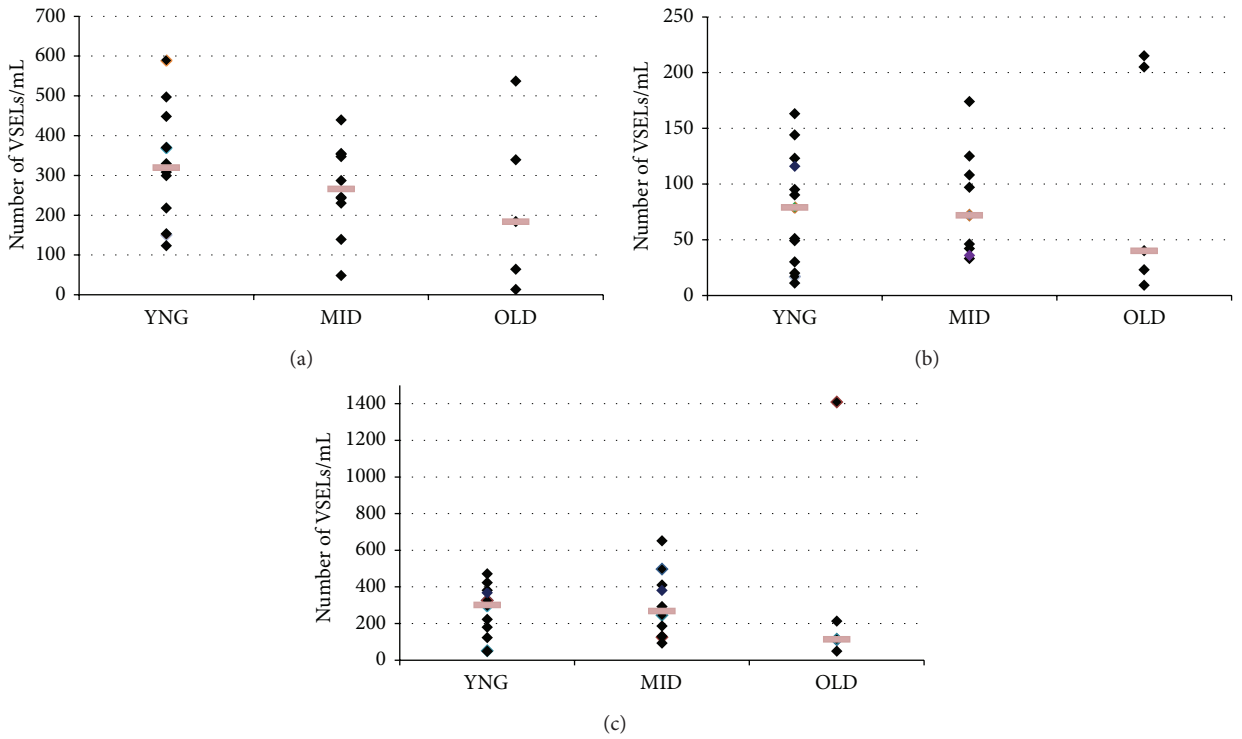

Figure 2: Age-dependent frequency of $Lin^-/CD45^-$ cell subsets expressing (a) CD133, (b) CD34, and (c) CXCR4 into the PB. Three groups of healthy human volunteers were designed according to their age: "young" (20–39 years; $n = 13$), "middle" (40–59 years; $n = 10$), and "older" (60–70 years; $n = 5$). Frequency of Lin^- $CD45^-$ cell subsets was calculated per mL of PB. Each square represents the number of VSELs/mL per volunteer in each group. The difference between the three groups of volunteers is not statistically significant ($P > 0.05$; one-way analysis of variance (ANOVA)).

3.2. A Population of Small $CD45^-$ Cells Expressing Several Pluripotent Stem Cell Markers Is Present in SS-PB of Young, Middle, and Older Subjects. Immunofluorescence staining showed that $CD45^-$ cell subsets express both specific pluripotent stem cell (PSC) markers such as SSEA-4 and TRA-1-81 on their surface and OCT-4 and NANOG transcription factors at the protein level (Figure 3).

Expression of PSC markers was confirmed by RT-qPCR. The differences in mRNA expression for those markers between the three groups of age were not statistically significant ($P > 0.05$, Kruskal-Wallis test) (Figure 4).

4. Discussion

The PB could be envisioned as a highway by which stem cells are trafficking in the body to keep in balance a pool of stem cells located in different niches in peripheral tissues. In this context, the BM has been proposed to be a main reservoir for these circulating cells [25]. In addition to HSCs, several other types of stem/progenitor cells have been described in the adult BM, such as mesenchymal stem cells (MSCs) [26], marrow-isolated adult multilineage inducible (MIAMI) cells [27], and multipotent adult stem cells (MASCs) [28]. A population of VSELs was first identified in the murine BM by the group of Ratajczak [15]. These cells express several markers characteristics for embryonic stem cells (ESCs), such as Oct-4, Nanog, and SSEA-1. MuVSELs circulate at very low numbers (~150–300/mL) into the murine SS-PB. Wojakowski et al. have also recently shown that very small numbers of VSELs (80–1300 cells/mL) could be detected under steady-state condition into the SS-PB of healthy humans, aged from 30 to 50 years, thus reflecting a continuous efflux of these cells from the BM [29]. Our present study, performed in a population of healthy adults with a larger age range (from 20 to 70 years), confirms that huVSELs actually circulate at very low levels (80–300/mL) into the SS-PB, in young and in older

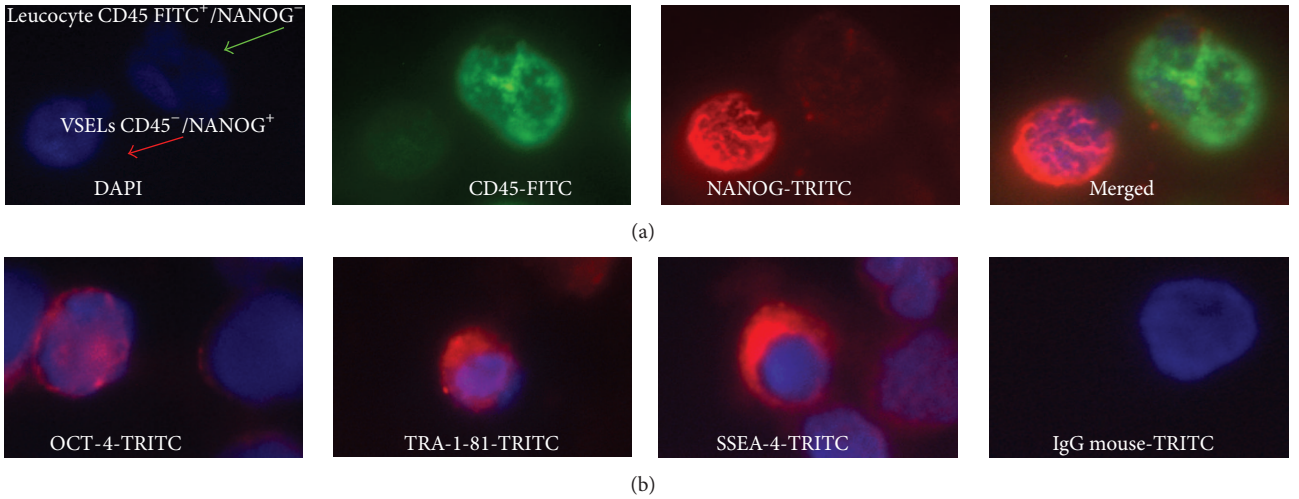

Figure 3: Immunofluorescence analysis of PB-derived VSELs. A typical triple-staining with 4′,6-diamidino-2-phenylindole (DAPI) (blue: nuclei), fluorescein isothiocyanate- (FITC-) CD45 (green fluorescence), and tetramethylrhodamine-5-isothiocyanate- (TRITC-) SSEA-4$^-$, TRA-1-81, OCT-4, or NANOG (red) shows (a) VSELs: small CD45$^-$ cells NANOG$^+$ and leukocytes: greater CD45$^+$ NANOG$^-$ cells and (b) VSELs: CD45$^-$ cells which express OCT-4 in nuclei or TRA-1-81 and SSEA-4 on the surface.

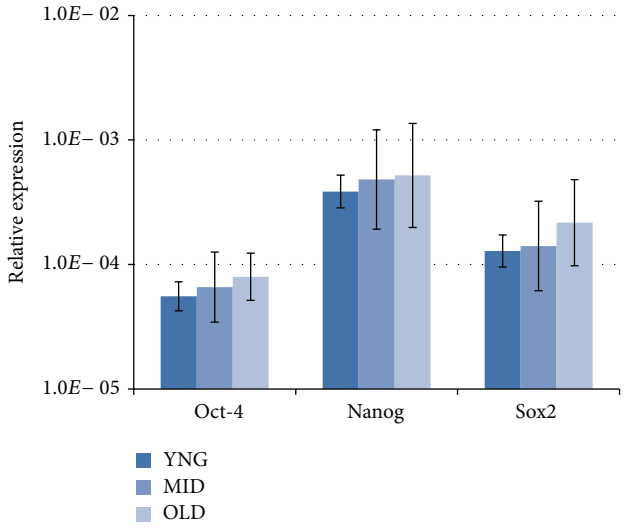

Figure 4: Relative expressions of PSC markers, Oct-4, Nanog, and Sox2, were measured by RT-qPCR and compared using equal amounts of mRNA isolated from CNT PB of young, middle, and older healthy volunteers. The relative expression of each PSC marker is calculated according to a positive control PCR (RNA isolated from H9 and HUES 3 hESC lines). Data represent the mean ± standard deviation for each age group. The difference in mRNA expression of these markers between the three groups of age was not statistically significant ($P > 0.05$, Kruskal-Wallis test).

subjects. Furthermore, they can be physiologically mobilized in order to participate in tissue/organ repair. Indeed, in several pathological situations, both in mice and in humans (e.g., heart infarct, stroke, skin burn injury, Crohn's disease, etc.), VSELs are released into the PB and their circulating numbers thus significantly increase [30–34]. However, when VSELs are released from the BM as a physiological response to tissue/organ injuries, even if they are able to home to the damaged areas, it is likely that they can only participate in the regeneration of minor tissue injuries and not of the largest ones, because of their too small amounts. To improve their potential regenerative impact, murine and huVSELs could then be mobilized by G-CSF administration [17, 21]. We have thus observed that circulating huVSELs amounts increase up to 2–4-fold after 4 days of G-CSF administration [35].

In case of myocardial infarct, it was also noticed that the intensity of the pic of VSELs spontaneous mobilization correlates with the extend of the ischemic [36, 37] or stroke lesion [32]. The knowledge of time occurrence of the mobilization pic might thus allow the determination of a therapeutic "window" useful for clinical application. On the other hand, the spontaneous (equal to physiological) mobilization rate could reflect the overall "regenerative potential" of an adult organism. Reduced spontaneous stem cell mobilization has been associated with poor prognosis in patients with myocardial infarction [37]. Thus, we suggest that the mean steady-state level of circulating huVSELs determined from a large enough cohort of healthy subjects might serve as a reference value which could be used as a baseline from which the physiopathological VSEL mobilization rate following an organ injury (e.g., heart infarct or stroke) would be correlated with its severity and its prognosis.

We also focused our study on the potential effect of aging on the amounts of huVSELs circulating in PB under steady-state conditions. The effects of aging on the HSC compartment have been extensively studied in mice. In the murine HSC system, several studies have reported an increase in the absolute number of phenotypically defined HSCs, although elderly animals have a reduced repopulation potential when compared to younger organisms [38–42]. Additionally, other investigators interestingly showed in mice that the frequency of the HSC subpopulation phenotypically defined as lineage

negative Sca-1$^+$, c-kit$^+$, Thy-1$^+$, CD135$^-$ side population (SP) steadily increased in the BM of the femurs and tibias with age. But, although long-term repopulation assays indicated that SP cells are still present and capable of self-renewal and differentiation in older mice, they have shown a lower homing efficiency than those from younger mice [43].

A little study on age-related changes in HSC number and function has been reported in humans. Although indirectly demonstrated through clinical data, there is evidence that human HSC function declines with age. For example, hematopoietic engraftment following HSCs transplantation is often faster and better sustained when the donor (in the autologous as well in the allogeneic setting) is young. Also, elderly people frequently and specifically develop hematological disorders due to acquired HSCs abnormalities, as, for example, myelodysplastic syndromes (MDS). Marley et al. have also found clear *in vitro* correlations between the relative numbers and function of clonogenic myeloid progenitors (CFU-GM) and age of the donor: *in vitro* colony formation study has indeed revealed that, although the absolute number of colony forming cells increases with age, their individual self-renewal capacity decreases [44].

Regarding VSELs, it was recently demonstrated in steady-state mice that, unlike HSC and SP, the number of muVSELs in the BM and the PB gradually decreases with age, in parallel with their ability to form VSEL-derived spheres (VSEL-DS) containing primitive stem cells, which may explain why the regenerative processes are less efficient in advanced age [18, 19]. Moreover, the number of VSELs is much higher in the BM of long-lived (C57BL/6) as compared to short-lived (DBA/2) mice [15], which allows supposing a positive correlation between high VSEL numbers and a greater length of life.

The effects of aging on the VSELs compartment had never been evaluated in humans until our present study. In response to G-CSF administration, we did not observe age-dependent huVSELs release into leukapheresis products from adult cancer patients aged from 34 to 71 years [35]. Here, we interestingly show for the first time that the numbers of circulating huVSELs in healthy subjects aged from 20 to 70 years were not statistically different whichever the age bracket is and thus would not seem to decline significantly with age. However, as we observed that the number of the all VSELs subpopulations was lower, while not significantly, in 3 subjects in the older group, this would nevertheless suggest that the frequency of CD133$^+$, CD34$^+$, or CXCR4$^+$ VSELs subpopulations could progressively run out with aging. A study including more number of older subjects is necessary in future to support this hypothesis.

On the other side, it is supposed that, as we age, stem cells likely progressively lose at least a part of their self-renewal and/or differentiation capabilities, which would lead to reduce their cell tissue regeneration potential and consequently contribute to the global somatic senescence. Thus, it would be crucial to demonstrate whether the proliferation potential of huVSELs also depends on age in humans. However, while murine VSELs proliferation and differentiation has been well demonstrated *in vitro*, we and others had failed to demonstrate such proliferative capacities of huVSELs by *in vitro* studies up to now. The major difficulty is that these cells stay in dormant state and nobody had already identified the combination of factors necessary to trigger the expansion/differentiation processes in purified huVSELs *ex vivo* cultures. Hopefully, the Taichman's group has very recently shown that huVSELs are able to generate multiple tissues within an osseous wound in immune-deficient mouse when cocultured with the C2C12 cell line [45], thus demonstrating for the very first time *in vitro* that huVSELs have actually the capacity to self-renew.

5. Conclusions

In this study, we demonstrate that huVSELs circulate at a similar frequency into the SS-PB of young, middle-aged, and aged subjects. This may indicate that the pool of VSELs *persists along the life* as a reserve for tissue repair in case of minor injury, and that there is a continuous efflux of these cells from the BM into the PB. We hypothesize that in case of major health complications (e.g., heart infarct, stroke) circulating VSELs could be isolated even from elderly patients, *ex vivo* expanded, and reinjected back into the same recipients for therapeutic purposes. Of course, such a strategy should be first tested in animal models. First and foremost, the actual VSELs' ability to self-renew and to differentiate has to be determined before they could be used for cell-based clinical therapies. In the recent study, the Taichman's group now opens the way for future huVSEL-based regenerative therapies at least for osseous, neural, and connective tissue disorders.

Conflict of Interests

The authors declare that there is no conflict of interests regarding the publication of this paper.

Acknowledgments

This work was supported by a grant from the REUNICA Group (Mulhouse, France). The authors thank A. Merlin from CellProthera SAS, Mulhouse, France, for statistical consultation.

References

[1] J.-P. Lévesque, I. G. Winkler, S. R. Larsen, and J. E. J. Rasko, "Mobilization of bone marrow-derived progenitors," in *Bone Marrow-Derived Progenitors*, vol. 180 of *Handbook of Experimental Pharmacology*, pp. 3–36, Springer, Berlin, Germany, 2007.

[2] P. J. Quesenberry, G. Colvin, G. Dooner, M. Dooner, J. M. Aliotta, and K. Johnson, "The stem cell continuum: cell cycle, injury, and phenotype lability," *Annals of the New York Academy of Sciences*, vol. 1106, pp. 20–29, 2007.

[3] S. Massberg and U. H. von Andrian, "Novel trafficking routes for hematopoietic stem and progenitor cells," *Annals of the New York Academy of Sciences*, vol. 1176, pp. 87–93, 2009.

[4] B. Bittira, D. Shum-Tim, A. Al-Khaldi, and R. C.-J. Chiu, "Mobilization and homing of bone marrow stromal cells in

myocardial infarction," *European Journal of Cardio-Thoracic Surgery*, vol. 24, no. 3, pp. 393–398, 2003.

[5] A. M. Leone, S. Rutella, G. Bonanno et al., "Mobilization of bone marrow-derived stem cells after myocardial infarction and left ventricular function," *European Heart Journal*, vol. 26, no. 12, pp. 1196–1204, 2005.

[6] D. C. Hess and C. V. Borlongan, "Stem cells and neurological diseases," *Cell Proliferation*, vol. 41, supplement 1, pp. 94–114, 2008.

[7] G. Y. Rochefort, B. Delorme, A. Lopez et al., "Multipotential mesenchymal stem cells are mobilized into peripheral blood by hypoxia," *Stem Cells*, vol. 24, no. 10, pp. 2202–2208, 2006.

[8] R. Bucala, L. A. Spiegel, J. Chesney, M. Hogan, and A. Cerami, "Circulating fibrocytes define a new leukocyte subpopulation that mediates tissue repair," *Molecular Medicine*, vol. 1, no. 1, pp. 71–81, 1994.

[9] R. J. Phillips, M. D. Burdick, K. Hong et al., "Circulating fibrocytes traffic to the lungs in response to CXCL12 and mediate fibrosis," *Journal of Clinical Investigation*, vol. 114, no. 3, pp. 438–446, 2004.

[10] M. A. Long, S. Y. Corbel, and F. M. V. Rossi, "Circulating myogenic progenitors and muscle repair," *Seminars in Cell and Developmental Biology*, vol. 16, no. 4-5, pp. 632–640, 2005.

[11] S. A. Kuznetsov, M. H. Mankani, S. Gronthos, K. Satomura, P. Bianco, and P. G. Robey, "Circulating skeletal stem cells," *The Journal of Cell Biology*, vol. 153, no. 5, pp. 1133–1140, 2001.

[12] Q. Shi, S. Rafii, M. H. Wu et al., "Evidence for circulating bone marrow-derived endothelial cells," *Blood*, vol. 92, no. 2, pp. 362–367, 1998.

[13] S. Rafii, "Circulating endothelial precursors: mystery, reality, and promise," *The Journal of Clinical Investigation*, vol. 105, no. 1, pp. 17–19, 2000.

[14] F. Dignat-George, A. Blann, and J. Sampol, "Circulating endothelial cells in acute coronary syndromes," *Blood*, vol. 95, no. 2, p. 728, 2000.

[15] M. Kucia, R. Reca, F. R. Campbell et al., "A population of very small embryonic-like (VSEL) CXCR4(+)SSEA-1(+)Oct-4+ stem cells identified in adult bone marrow," *Leukemia*, vol. 20, no. 5, pp. 857–869, 2006.

[16] M. Z. Ratajczak, B. Machalinski, W. Wojakowski, J. Ratajczak, and M. Kucia, "A hypothesis for an embryonic origin of pluripotent Oct-4(+) stem cells in adult bone marrow and other tissues," *Leukemia*, vol. 21, no. 5, pp. 860–867, 2007.

[17] M. J. Kucia, M. Wysoczynski, W. Wu, E. K. Zuba-Surma, J. Ratajczak, and M. Z. Ratajczak, "Evidence that very small embryonic-like stem cells are mobilized into peripheral blood," *Stem Cells*, vol. 26, no. 8, pp. 2083–2092, 2008.

[18] M. Z. Ratajczak, E. K. Zuba-Surma, D.-M. Shin, J. Ratajczak, and M. Kucia, "Very small embryonic-like (VSEL) stem cells in adult organs and their potential role in rejuvenation of tissues and longevity," *Experimental Gerontology*, vol. 43, no. 11, pp. 1009–1017, 2008.

[19] E. K. Zuba-Surma, W. Wu, J. Ratajczak, M. Kucia, and M. Z. Ratajczak, "Very small embryonic-like stem cells in adult tissues-Potential implications for aging," *Mechanisms of Ageing and Development*, vol. 130, no. 1-2, pp. 58–66, 2009.

[20] M. Kucia, M. Halasa, M. Wysoczynski et al., "Morphological and molecular characterization of novel population of $CXCR4^+$ $SSEA\text{-}4^+$ $Oct\text{-}4^+$ very small embryonic-like cells purified from human cord blood—preliminary report," *Leukemia*, vol. 21, no. 2, pp. 297–303, 2007.

[21] H. Sovalat, M. Scrofani, A. Eidenschenk, S. Pasquet, V. Rimelen, and P. Hénon, "Identification and isolation from either adult human bone marrow or G-CSF-mobilized peripheral blood of $CD34^+/CD133^+/CXCR4^+/ Lin^-CD45^-$ cells, featuring morphological, molecular, and phenotypic characteristics of very small embryonic-like (VSEL) stem cells," *Experimental Hematology*, vol. 39, no. 4, pp. 495–505, 2011.

[22] C. A. Cowan, I. Klimanskaya, J. McMahon et al., "Derivation of embryonic stem-cell lines from human blastocysts," *The New England Journal of Medicine*, vol. 350, no. 13, pp. 1353–1356, 2004.

[23] J. A. Thomson, J. Itskovitz-Eldor, S. S. Shapiro et al., "Embryonic stem cell lines derived from human blastocysts," *Science*, vol. 282, no. 5391, pp. 1145–1147, 1998.

[24] E. K. Zuba-Surma and M. Z. Ratajczak, "Unit 9.29. Overview of very small embryonic-like stem cells (VSELs) and methodology of their identification and isolation by flow cytometric methods," in *Current Protocols in Cytometry*, J. P. Robinson, Ed., chapter 9, 2010.

[25] T. Papayannopoulou, "Bone marrow homing: the players, the playfield, and their evolving roles," *Current Opinion in Hematology*, vol. 10, no. 3, pp. 214–219, 2003.

[26] Y. Jiang, B. N. Jahagirdar, R. L. Reinhardt et al., "Pluripotency of mesenchymal stem cells derived from adult marrow," *Nature*, vol. 418, no. 6893, pp. 41–49, 2002.

[27] G. D'Ippolito, G. A. Howard, B. A. Roos, and P. C. Schiller, "Isolation and characterization of marrow-isolated adult multilineage inducible (MIAMI) cells," *Experimental Hematology*, vol. 34, no. 11, pp. 1608–1610, 2006.

[28] Y. Jiang, B. Vaessen, T. Lenvik, M. Blackstad, M. Reyes, and C. M. Verfaillie, "Multipotent progenitor cells can be isolated from postnatal murine bone marrow, muscle, and brain," *Experimental Hematology*, vol. 30, no. 8, pp. 896–904, 2002.

[29] W. Wojakowski, M. Kucia, R. Liu et al., "Circulating very small embryonic-like stem cells in cardiovascular disease," *Journal of Cardiovascular Translational Research*, vol. 4, no. 2, pp. 138–144, 2011.

[30] W. Wojakowski, M. Tendera, M. Kucia et al., "Mobilization of bone marrow-derived $Oct\text{-}4^+$ $SSEA\text{-}4^+$ very small embryonic-like stem cells in patients with acute myocardial infarction," *Journal of the American College of Cardiology*, vol. 53, no. 1, pp. 1–9, 2009.

[31] E. K. Zuba-Surma, M. Kucia, B. Dawn, Y. Guo, M. Z. Ratajczak, and R. Bolli, "Bone marrow-derived pluripotent very small embryonic-like stem cells (VSELs) are mobilized after acute myocardial infarction," *Journal of Molecular and Cellular Cardiology*, vol. 44, no. 5, pp. 865–873, 2008.

[32] E. Paczkowska, M. Kucia, D. Koziarska et al., "Clinical evidence that very small embryonic-like stem cells are mobilized into peripheral blood in patients after stroke," *Stroke*, vol. 40, no. 4, pp. 1237–1244, 2009.

[33] J. Drukała, E. Paczkowska, M. Kucia et al., "Stem cells, including a population of very small embryonic-like stem cells, are mobilized into peripheral blood in patients after skin burn injury," *Stem Cell Reviews and Reports*, vol. 8, no. 1, pp. 184–194, 2012.

[34] W. Marlicz, E. Zuba-Surma, M. Kucia, W. Blogowski, T. Starzynska, and M. Z. Ratajczak, "Various types of stem cells, including a population of very small embryonic-like stem cells, are mobilized into peripheral blood in patients with Crohn's disease," *Inflammatory Bowel Diseases*, vol. 18, no. 9, pp. 1711–1722, 2012.

[35] H. Sovalat, M. Scrofani, A. Eidenschenk, M. Ojeda-Uribe, and P. Hénon, "G-CSF Administration induces mobilization of human very small embryonic like (VSEL) stem cells into peripheral blood of cancer patients," *Experimental Hematology*, vol. 40, no. 8, pp. S59–S60, 2012.

[36] W. Wojakowski, M. Tendera, A. Zebzda et al., "Mobilization of CD34(+), CD117(+), CXCR4(+), c-met(+) stem cells is correlated with left ventricular ejection fraction and plasma NT-proBNP levels in patients with acute myocardial infarction," *European Heart Journal*, vol. 27, no. 3, pp. 283–289, 2006.

[37] A. Abdel-Latif, E. K. Zuba-Surma, K. M. Ziada et al., "Evidence of mobilization of pluripotent stem cells into peripheral blood of patients with myocardial ischemia," *Experimental Hematology*, vol. 38, no. 12, pp. 1131–1142, 2010.

[38] S. J. Morrison, A. M. Wandycz, K. Akashi, A. Globerson, and I. L. Weissman, "The aging of hematopoietic stem cells," *Nature Medicine*, vol. 2, no. 9, pp. 1011–1016, 1996.

[39] K. Sudo, H. Ema, Y. Morita, and H. Nakauchi, "Age-associated characteristics of murine hematopoietic stern cells," *Journal of Experimental Medicine*, vol. 192, no. 9, pp. 1273–1280, 2000.

[40] M. Kim, H.-B. Moon, and G. J. Spangrude, "Major age-related changes of mouse hematopoietic stem/progenitor cells," *Annals of the New York Academy of Sciences*, vol. 996, pp. 195–208, 2003.

[41] D. E. Harrison, "Long-term erythropoietic repopulating ability of old, young, and fetal stem cells," *Journal of Experimental Medicine*, vol. 157, no. 5, pp. 1496–1504, 1983.

[42] D. J. Rossi, D. Bryder, J. M. Zahn et al., "Cell intrinsic alterations underlie hematopoietic stem cell aging," *Proceedings of the National Academy of Sciences of the United States of America*, vol. 102, no. 26, pp. 9194–9199, 2005.

[43] D. J. Pearce, F. Anjos-Afonso, C. M. Ridler, A. Eddaoudi, and D. Bonnet, "Age-dependent increase in side population distribution within hematopoiesis: implications for our understanding of the mechanism of aging," *Stem Cells*, vol. 25, no. 4, pp. 828–835, 2007.

[44] S. B. Marley, J. L. Lewis, R. J. Davidson et al., "Evidence for a continuous decline in haemopoietic cell function from birth: application to evaluating bone marrow failure in children," *British Journal of Haematology*, vol. 106, no. 1, pp. 162–166, 1999.

[45] A. M. Havens, H. Sun, Y. Shiozawa et al., "Human and murine very small embryonic-like cells represent multipotent tissue progenitors, in vitro and in vivo," *Stem Cells and Development*, vol. 23, no. 7, pp. 689–701, 2014.

Hindawi Publishing Corporation
Stem Cells International
Volume 2016, Article ID 5069857, 14 pages
http://dx.doi.org/10.1155/2016/5069857

Research Article

Identification of New Rat Bone Marrow-Derived Population of Very Small Stem Cell with Oct-4A and Nanog Expression by Flow Cytometric Platforms

Anna Labedz-Maslowska, Elzbieta Kamycka, Sylwia Bobis-Wozowicz, Zbigniew Madeja, and Ewa K. Zuba-Surma

Department of Cell Biology, Faculty of Biochemistry, Biophysics and Biotechnology, Jagiellonian University, 30-387 Krakow, Poland

Correspondence should be addressed to Ewa K. Zuba-Surma; ewa.zuba-surma@uj.edu.pl

Received 13 May 2015; Revised 5 July 2015; Accepted 8 July 2015

Academic Editor: Irma Virant-Klun

Very small embryonic-like stem cells (VSELs) represent a unique rare population of adult stem cells (SCs) sharing several structural, genetic, biochemical, and functional properties with embryonic SCs and have been identified in several adult murine and human tissues. However, rat bone marrow- (BM-) derived SCs closely resembling murine or human VSELs have not been described. Thus, we employed multi-instrumental flow cytometric approach including classical and imaging cytometry and we established that newly identified population of nonhematopoietic cells expressing CD106 (VCAM-I) antigen contains SCs with very small size, expressing markers of pluripotency (Oct-4A and Nanog) on both mRNA and protein levels that indicate VSEL population. Based on our experience in both murine and human VSEL isolation procedures by fluorescence-activated cell sorting (FACS), we also optimized sorting protocol for separation of $CD45^-/Lin^-/CD106^+$ rat BM-derived VSELs from wild type and eGFP-expressing rats, which are often used as donor animals for cell transplantations in regenerative studies *in vivo*. Thus, this is a first study identifying multiantigenic phenotype and providing sorting protocols for isolation VSELs from rat BM tissue for further examining of their functional properties *in vitro* as well as regenerative capacity in distinct *in vivo* rat models of tissue injury.

1. Introduction

Flow cytometric platforms have been well established as valuable tools for identification and isolation of several cell populations based on their multiantigenic profile [1–4]. Based on advanced modified and optimized FACS protocols, we have identified and sorted new fractions of rare stem cells (SCs) including very small embryonic-like stem cells (VSELs) that reside predominantly in bone marrow (BM) but also in other tissues such fetal liver, umbilical cord blood (UCB), and multiple adult specimens harvested from various organs and tissues [2, 3, 5]. The major impact of our experience in this subject was the implementation of challenging methods for purification of such unique rare fractions of SCs based on their multiantigenic profile by modern flow cytometric platforms.

Recently, numerous reports have shown that adult murine as well as human specimens such as BM, peripheral blood (PB), solid organs, and UCB may contain primitive stem cell fractions with multi- and pluripotent characteristics. Such SCs populations include unrestricted somatic stromal cells (USSCs) [6], multilineage-differentiating stress-enduring (Muse) cells [7, 8], marrow-isolated adult multilineage inducible cells (MIAMI) [9], multipotent adult progenitor cells (MAPCs) [10], multipotent adult stem cells (MASCs) [11], and a population of VSELs [12–14].

VSELs represent a unique rare population of adult SCs sharing several structural, genetic, biochemical, and functional properties with embryonic SCs and have been identified in several adult murine and human tissues including ovaries and testes [15–22]. Murine VSELs defined representing small-sized cells expressing Sca-1 antigen but not expressing CD45 and hematopoietic lineages markers ($FSC^{low}/SSC^{low}/CD45^-/Lin^-/Sca\text{-}1^+$) have been initially identified in murine BM and subsequently found in several

other adult murine organs as rare population of SCs [23–25]. Genetic analysis such as real-time RT-PCR in sorted murine $FSC^{low}/SSC^{low}/CD45^{-}/Lin^{-}/Sca\text{-}1^{+}$ cells has showed the increased levels of mRNA for embryonic stem cells markers such as SSEA-1, Oct-4, Nanog, and Rex-1 (Rexo1) that was also confirmed on protein level using immunofluorescent staining and ImageStream system imaging (ISS) [23, 26]. Importantly, detailed molecular and genetic analysis of these cells reveled their (1) hypomethylated promoters for Oct-4 and Nanog transcription factors and (2) unique epigenetic status including hypomethylation of growth-repressive H19 gene along with hypermethylation of growth-promoting Igf-2 gene that leads to in inhibition of proliferation of these cells and limits their tumorigenic and blastocyst complementation capacity [27]. Importantly, the presence of VSELs in several other murine and human tissues including ovaries and testes has been also confirmed by other investigators [17–19, 21, 22, 28–30].

Human UCB- and PB-derived VSELs are phenotypically similar to those described in adult murine BM and may be also identified within nonhematopoietic compartments ($CD45^{-}/Lin^{-}$) of such specimens, especially among small-sized objects (FSC^{low}/SSC^{low}). Human VSELs are also very small in diameter and are smaller than red blood cells (RBCs), which is a unique feature for these stem cells along all investigated species. The population of Oct-4-, Nanog-, and SSEA-4-expressing VSELs in humans is enriched among $CD45^{-}/Lin^{-}$ fraction carrying CD133/1 (AC133), CD34, or partially CXCR4 [3, 4, 14]. Although the human VSELs have been initially characterized as cells expressing CXCR4 receptor, we further established that the fraction enriched in Oct-4, SSEA-4 expressing cells that possess very small size and high N/C ration, may be predominantly found in $CD45^{-}/Lin^{-}/CD133^{+}$ population of UCB-derived cells [3, 31]. Such cell expressed early embryonic transcription factors as Oct-4 and Nanog, at both mRNA and protein levels as confirmed by quantitative RT-PCR and imaging cytometry, respectively [31]. Since then, we consider the $CD45^{-}/Lin^{-}/CD133^{+}$ population as mostly enriched in VSELs. Importantly, cytometric characteristics of UCB-derived SCs revealed normal diploid (2n) content of DNA in both VSELs and HSCs fractions in the G0/G1 phase of the cell cycle [32].

Distinct "positive markers" have been identified for VSELs isolated from different species. In our previous studies, we have identified only limited number of such selection markers present on VSEL surface including Sca-1 antigen in mice and CD34 or CD133 in humans [32]. These findings indicate that the expression of these markers is species-related and there is no VSEL-specific surface antigen identified for all species up to today. Moreover, Sca-1 antigen representing murine VSELs selection marker is not present on human or rat cell, while CD34 antigen commonly present on human stem and progenitor cells has been rarely identified on murine or rat stem cells. Importantly, the positive selection markers for VSELs have not been identified within MSC-specific markers such as CD29 and CD105 [1, 7]. However, our long term observations of murine and human VSELs in *in vitro* culture strongly suggest their high adhesive properties. Such functional properties correspond to the expression of several adhesion molecules and receptors including CD54, CD106, and members of α-integrin family (e.g., CD49f) that were detected on murine VSEL surface by our group and also by Professor Ratajczak and his colleagues, but these important data are still unpublished. However these findings may suggest that the adhesion molecules and receptors may be group harboring selection markers for VSEL isolation that was considered in this study.

Although both murine and human VSELs have been well characterized on phenotypical and genetic levels, such primitive SCs in other mammals including rats have been poorly investigated. The first study questing for VSELs counterpart in rat BM was performed by Wu and colleagues who described a population of $CD45^{-}/Lin^{-}$ ($Ter\text{-}119^{-}$, $CD11b^{-}$, and $Gr\text{-}1^{-}$)/$SSEA\text{-}1^{+}$ cells in this tissue. Although the Sca-1 antigen has been identified specifically on murine, but not rat or human cells, the authors reported existence of such rat $SSEA\text{-}1^{+}$ VSELs expressing Sca-1 and also PSC transcriptional factors such as Oct-4, Nanog, Rex-1, Sox-2, and Fgf-4 in murine bone marrow [33].

Thus, the aim of our study was to identify and purify enriched population of rat VSELs (rVSELs) derived from adult rat BM based on phenotypic and antigenic similarity to murine VSELs and selected antigen expression (CD54 and CD106) with using only specifically anti-rat reagents and by employing both classical and imaging flow cytometry (ImageStream X system, ISS-X). Moreover, the goal was to optimize flow cytometric sorting strategies for purification of rVSELs derived from wild type (WT) and eGFP-expressing transgenic Wistar rats that may be further employed in *in vitro* and preclinical studies identifying their functional potential.

2. Materials and Methods

2.1. Animals. Experimental procedures involving animal material were performed in accordance with the national and European legislation following approval by the First Local Ethical Committee on Animal Testing at the Jagiellonian University in Krakow (approval number: 56/2009). Two strains of Wistar rats, (1) WT (Crl: WT) and (2) transgenic eGFP-expressing rats (Wistar-TgN(CAG-GFP)184Ys), were purchased from National Bio Resource Project for the Rat in Japan, Kyoto University, and supplied by the experimental animal facility from Nencki Institute of Experimental Biology, Polish Academy of Sciences, Warsaw, Poland.

2.2. BM Cells Preparation. BM tissue was isolated from adult (8–12-week-old) WT and transgenic eGFP-expressing Wistar rats by flashing of cavities of tibias and femurs. BM cell suspensions were collected and filtered through a 70-μm strainer (BD Bioscience). Total nucleated cells (TNCs) were obtained following lysis of red blood cells (RBCs) with 1x BD Pharm Lyse Buffer (BD Pharmingen) for 10 minutes. TNCs were subsequently washed with phosphate buffered saline (DPBS; w/o Ca^{2+}, Mg^{2+}; Life Technologies) and resuspended in DMEM-based staining medium (Sigma-Aldrich, St. Louis,

MO) containing 2% of fetal bovine serum (FBS) (Lonza, Basel, Switzerland) for further analyses.

2.3. Staining for Flow Cytometric Analysis and FACS Sorting. TNCs harvested from both Wistar strains were immunolabeled with the following monoclonal antibodies: Alexa Fluor 647- or PE-Cy7-conjugated anti-CD45 (clone: OX-1; BioLegend), Alexa Fluor 647- or FITC-conjugated anti-hematopoietic lineages markers cocktail—"Lin" markers, including anti-TCR$\alpha\beta$ (clone: R73), anti-CD3 (clone: 1F4), anti-CD11b/c (clone: OX-42), and anti-CD45RA (clone: OX-33); BD Pharmingen and BioLegend, PE-conjugated anti-CD54 (clone: 1A29; BD Pharmingen), and PE- or biotin-conjugated anti-CD106 (PE, clone: MR-106; BioLegend). Streptavidin with PerCp-Cy5.5 (BD Pharmingen) was added to the samples to visualize the binding of biotin-conjugated anti-CD106 antibody. All antibodies were used according to manufacturer's protocols and staining was performed for 30 min at 4°C. Cells were subsequently washed and resuspended in DMEM with 2% FBS for further flow cytometric analysis (LSR II; Becton Dickinson) or sorting procedure (MoFlo XDP; BeckmanCoulter).

Rat BM-derived VSEL population was considered to be enriched in $FSC^{low}/SSC^{low}/CD45^{-}/Lin^{-}$ cells expressing CD54 or/and CD106 antigens.

To compare the status of the sorted rVSELs with $CD45^{-}/Lin^{-}/SSEA\text{-}1^{+}$ population identified by Wu et al. [33], TNC fraction was stained for CD45 and Lin markers (as described above) and additionally with directly conjugated anti-mouse/human SSEA-1 antibody (PE, clone: MC-480, BioLegend). We used directly conjugated anti-SSEA-1 antibody to prevent nonspecific background staining crucial to be avoided in sorting of rare cell populations. All used antibodies are described in Table 1.

2.4. Staining for ImageStream X System (ISS-X) Analysis. For rVSELs identification by ImageStream X system (Amnis Corp.), TNCs derived for WT Wistar rats were prepared according to the protocol described above. Based on the detection channels available for the ISS-X, the following directly conjugated monoclonal antibodies were used for identification of small $CD45^{-}/Lin^{-}/CD106^{+}$ and/or $CD45^{-}/Lin^{-}/CD54^{+}$ cells: (i) anti-CD45 (Alexa Fluor 647, clone: OX-1), (ii) FITC-conjugated Lin markers (including anti-TCR$\alpha\beta$ (clone: R73), anti-CD3 (clone: 1F4), anti-CD11b/c (clone: OX-42), anti-CD45RA (clone: OX-33)) (BD Pharmingen), and (iii) CD106 (PE, clone: MR-106; BioLegend) or (iv) CD54 (PE, clone: 1A29) (BD Pharmingen). Staining was performed according to manufacturers' protocols for 30 min at 4°C. Samples were subsequently washed and fixed with 4% of paraformaldehyde solution (Sigma) for 20 min (RT). Fixed cells were resuspended in saline (DPBS; w/o Ca^{2+}, Mg^{2+}; Life Technologies) in concentration of 2×10^{6}/mL for further analysis with ImageStream X system (Amnis Corp.); Hoechst 33342 (Hoe; 2 μM) was added for 10 min prior to analysis to visualize nuclei.

In order to analyze intranuclear expression of pluripotent markers such as Oct-4A and Nanog and to further identify $Oct\text{-}4A^{+}$ and/or $Nanog^{+}$ rat BM-derived VSELs, freshly isolated TNCs were initially fixed with 4% paraformaldehyde (Sigma) for 20 min (RT) and subsequently permeabilized with 0.1% Triton X-100 solution (Sigma) for 10 min (RT). Cells were further washed and stained either with (i) primary anti-Oct-3/4 antibody (rabbit polyclonal IgG, Santa Cruz Biotechnology, sc-9081, CA, USA, 1 : 100) that specifically stains Oct-4A isoform identifying PSCs or (ii) primary anti-Nanog antibody (rabbit polyclonal IgG, Santa Cruz Biotechnology, sc-33760, 1 : 100) for 2 h at 37°C. Secondary goat anti-rabbit IgG antibody conjugated with Alexa Fluor 488 or Alexa Fluor 647 (Invitrogen, Molecular Probes, Carlsbad, Ca, USA, 1 : 200) was added for 2 h (37°C). Cells were washed following the staining for Oct-4A and Nanog and subsequently incubated with directly conjugated antibodies against (i) CD106-PE, CD45-PE-Cy7, or FITC-conjugated Lin markers (including TCR$\alpha\beta$, CD3, CD11b, and CD45RA) for 30 min at 4°C. Cells were further washed and resuspended in DPBS (w/o Ca^{2+}, Mg^{2+}; Life Technologies). Nuclei were stained with Hoechst 33342 (Hoe) directly before analysis and samples were further analyzed with ImageStream X system (Amnis Corporation, Seattle, WA, USA). Analyses of morphological features of selected BM-derived populations were performed based on the collected images with IDEAS analytical software (Amnis Corporation, Seattle, WA, USA).

Table 1: Antibodies employed in staining for identification and sorting of rat BM-derived populations including rVSELs.

Antibody (anti-rat antigen)	Clone	Fluorochrome	Source
Anti-CD45	OX-1	PE-Cy7/Alx647	BioLegend
Anti-$\alpha\beta$-TCR	R73	FITC Alx 647	BD Biosciences BioLegend
Anti-CD2	OX-34	FITC	BD Bioscience
Anti-CD3	1F4	FITC Alx 647	BD Bioscience BioLegend
Anti-CD11b/c	OX-42	FITC Alx 647	BD Bioscience BioLegend
Anti-CD45RA	OX-33	FITC APC	BD Bioscience BioLegend
Anti-CD54	1A29	PE	BD Bioscience
Anti-CD106	MR-106 eBioMR106	PE Biotin	BioLegend eBioscience
Streptavidin	—	PerCp-Cy5.5	BD Bioscience
Anti-SSEA-1	MC-480	PE	BioLegend

2.5. Gene Expression Analysis by Real-Time RT-PCR. Total RNA from sorted subpopulations of $CD45^{-}/Lin^{-}/CD106^{+}/CD54^{+}$, $CD45^{-}/Lin^{-}/CD106^{+}$, and $CD45^{-}/Lin^{-}/SSEA\text{-}1^{+}$ cells as well as from their hematopoietic counterparts ($CD45^{+}/Lin^{-}/CD106^{+}/CD54^{+}$ and $CD45^{+}/Lin^{-}/CD106^{+}$) was isolated using the RNeasy Micro Kit (Qiagen, Valencia, CA). mRNA was further reversely transcribed into cDNA with TaqMan Reverse Transcription Reagents (Applied Biosystems, Foster City, CA, USA) and the reactions were performed under the following conditions: 1 cycle at

25°C for 10 min, 1 cycle at 48°C for 30 min, and finally 1 cycle at 95°C for 5 min. mRNA harvested from unfractionated TNCs was used as control (called "input"). 50 ng of total RNA was used for each reverse transcription reaction.

Detection of expression of the following rat genes β-actin, Oct-4, Nanog, and Rexo1 was performed by real-time RT-PCR using an ABI PRISM 7000 sequence detection system (Applied Biosystems). A 25-μL reaction mixture contained 12.5 μL SYBR Green PCR Master Mix (Applied Biosystems), cDNA template (2,5 ng), and both forward (1 μM) and reverse (1 μM) primers (Tib MolBiol, Poznan, Poland). The following sequences of primers were used: β-actin: (F) 5′- TGA CCC AGA TCA TGT TTG AGA -3′, (R) 5′- CAA GGT CCA GAC GCA GGA T-3′; Oct-4: (F) 5′- CCC AGC GCC GTG AAG TTG GA -3′, (R) 5′- AGA ACG CCC AGG GTG AGC CC -3′; Nanog: (F) 5′- CCC TTG CCG TTG GGC TGA CA -3′, (R) 5′- AAG GCG GAG GAG AGG CAG TCT -3′; Rexo-1 (F) 5′- GCT CCG GCG GAA TCG AGT GG -3′, (R) 5′- GCA CGT GTT GCT TGG CGA CC -3′.

Real-time RT-PCR reactions were performed under the following conditions: 1 cycle at 50°C for 2 min, 1 cycle at 95°C for 10 min, followed by 40 cycles at 95°C for 15 s, and 60°C for 1 min. Relative quantification of Oct-4, Nanog, and Rexo1 mRNA expression was calculated using the comparative Ct method. The relative quantitative value of the target, normalized to an endogenous control (β-actin gene) and relative to a calibrator, was expressed as $2^{-\Delta\Delta Ct}$ (i.e., fold difference), where ΔCt = [Ct of target genes] − [Ct of endogenous control gene] and $\Delta\Delta$Ct = [ΔCt of samples for target genes] − [ΔCt of calibrator for target gene].

To avoid the possibility of amplifying contaminating DNA, the following steps were taken: (i) all primers were designed with an intron sequence inside the cDNA to be amplified; (ii) all reactions were performed with an appropriate negative controls (template-free controls); (iii) a uniform amplification of the products was rechecked by analyzing the melting curves of the amplified products (dissociation graphs).

2.6. Immunocytochemistry. To evaluate Oct-4A and Nanog expression in purified BM subpopulation, the limited number of sorted cells (10×10^3) was seeded on poly-L-lysine (Sigma) coated glass-bottom plates (Willco-dish, Willco Wells B.V.) in medium DMEM with 2% FBS (Lonza) and was incubated overnight in standard culture conditions. The medium was subsequently removed and the attached cells were gently fixed with 4% paraformaldehyde (Sigma) for 20 min (RT) and subsequently permeabilized with 0.1% Triton X-100 solution (Sigma) for 10 min (RT). Cells were washed and stained either with (i) primary anti-Oct-3/4 antibody (rabbit polyclonal IgG, Santa Cruz Biotechnology, sc-9081, CA, USA, 1 : 100) that specifically stains Oct-4A isoform identifying PSCs or (ii) primary anti-Nanog antibody (rabbit polyclonal IgG, Santa Cruz Biotechnology, sc-33760, 1 : 100) for 16 h at 4°C. Secondary goat anti-rabbit IgG antibody conjugated with Alexa Fluor 488 or Alexa Fluor 546 (Invitrogen, Molecular Probes, Carlsbad, Ca, USA, 1 : 200) was added for 2 h (37°C). Cells were washed and nuclei were stained with 4′, 6-diamidino-2-phenylindole (DAPI, 2 μM, Life Technologies, Molecular Probes) for 15 min (37°C) and plates were closed with VECTASHIELD Mounting Medium (Vector Laboratories, CA, USA) and cover slips. Sorted $CD45^+/Lin^-/CD106^+$ subpopulation of BM cells that represents hematopoietic counterpart of purified $CD45^+/Lin^-/CD106^+$ VSELs was also stained for Oct-4A and Nanog and was used as negative control in this setting. The labeled cells were subsequently analyzed with Leica DMI6000B (ver. AF7000) fluorescent microscope under total 945x magnification (Leica Microsystems GmbH, Germany).

2.7. Statistical Analysis. Data were expressed as the mean ± standard deviation (SD). A value of $P < 0.05$ was considered significant. All statistical analyses were performed using the Origin (ver. 5.0) statistical software (Microcal Software, Northampton, MA).

3. Results

3.1. Rat BM Harbors a Population of Very Small Nonhematopoietic SCs Expressing CD54 and CD106 Antigen. Our previously published data have indicated murine and human VSELs represent populations of nonhematopoietic stem cells with very small cells size which do not express markers of hematopoietic lineages such as CD45 and major hematopoietic lineage specific antigens [2, 3, 5]. Thus, in this study, we started our quest for rat BM-derived VSELs focusing on cells with corresponding characteristics by employing multiparameter flow cytometric platforms. We focused on $CD45^-/Lin^-$ cells with small size and low cytoplasmic complexity and volume, indicated as FSC^{low} and SSC^{low} objects, respectively. Our second step was focused on "positive selection" marker that would optimally define these unique SCs. We have previously reported only limited number of markers present on VSEL surface that may distinguish them from other cell types such as Sca-1 antigen in mice and CD34 or CD133 in humans [2, 3, 5]. Therefore, the expression of VSEL "positive selection" markers is distinct in different species and VSEL-specific surface antigen has not been identified. However, our long term observations of murine and human VSELs in *in vitro* culture indicate their high adhesive properties which correspond to the expression of several adhesion molecules and receptors including, for example, CD54, CD106, and CD49f (unpublished data). Thus, we focused on two molecules involved in cell adhesion as potential markers for rVSELs including CD54 (ICAM-I) and CD106 (VCAM-I).

We initially isolated BM cells from adult WT Wistar rats and stained total nucleated cells obtained following RBCs lysis to identify presence of $CD45^-/Lin^-/CD54^+$ or $CD45^-/Lin^-/CD106^+$ cells by classical as well as imaging cytometry (ISS-X) that allows for distinguishing real rare cellular objects from artifacts.

By using both flow cytometric platforms, we found that rat BM tissue contains both rare populations of very small nonhematopoietic ($CD45^-/Lin^-$) cells expressing CD54 and CD106 antigens (0.003 ± 0.001% and 0.011 ± 0.005%, resp.) (Figure 1). Since we expected rVSELs to be small size cells, we focused on gating events including those with

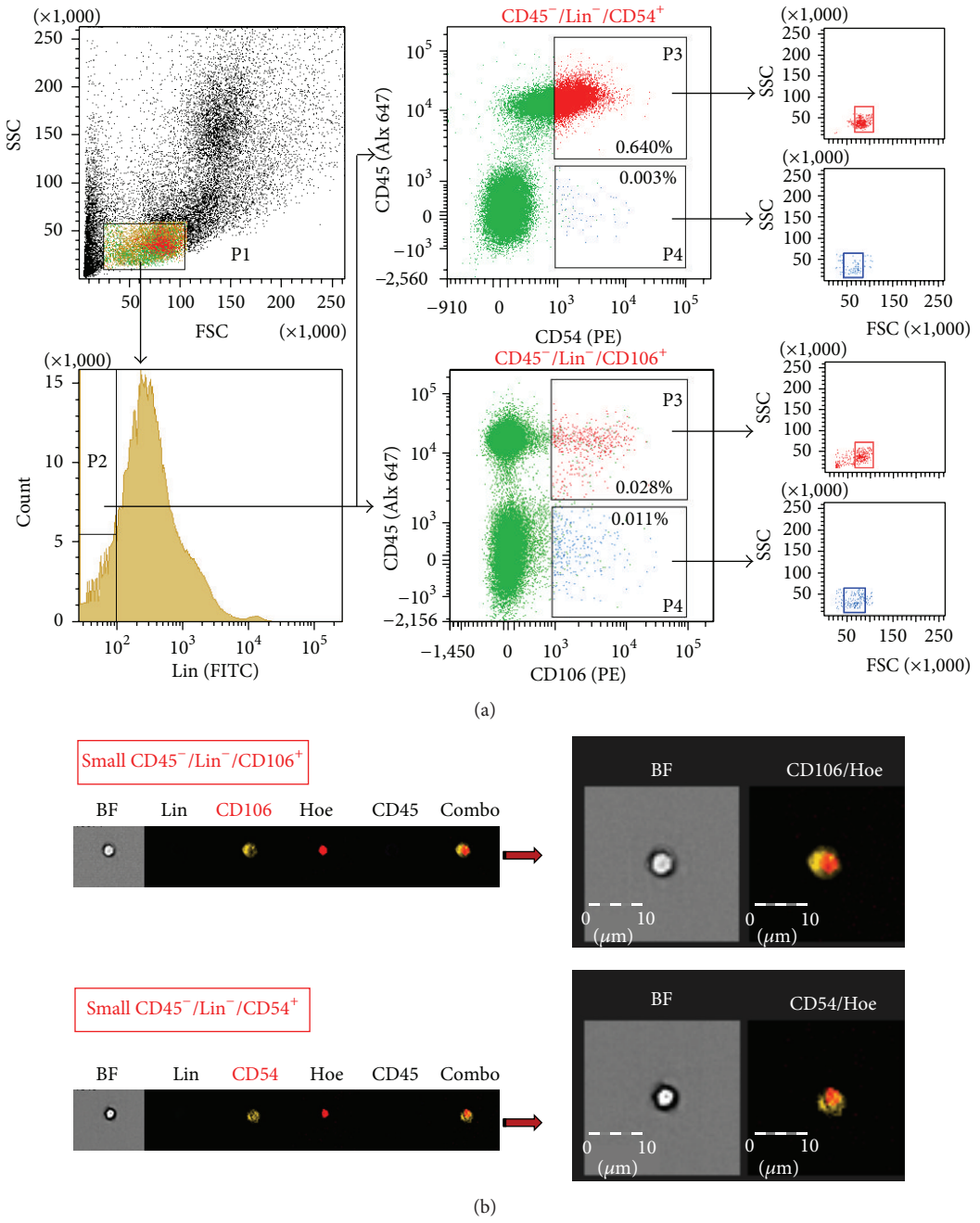

FIGURE 1: Expression of CD54 (ICAM-I) and CD106 (VCAM-I) on rat BM cells. (a) Gating strategy for identification of $CD54^+$ and $CD106^+$ populations by classical flow cytometry. Total nucleated cells (TNCs) derived from WT rat BM were stained for CD45 (PE-Cy7), hematopoietic lineages markers (Lin: TCR$\alpha\beta$, CD3, CD11b, CD45RA; FITC), and CD54 (PE) or CD106 (PE) and further analyzed by LSR II (Becton Dickinson). BM cells are visualized on dot-plot showing FSC versus SSC signals, which are related to the size and granularity/complexity of the cell, respectively. 2% of total 1×10^6 of analyzed TNCs is only displayed in this dot-plot to visualize the population distribution. Objects from region P1 (lymphgate including FSC^{low}/SSC^{low} objects) were further analyzed for Lin markers expression and only Lin^- events are included into region P2. *Upper, middle dot-plot* cells stained for CD54, derived from gate P2, and analyzed for CD54 versus CD45 expression. Two fractions of cells potentially enriched in stem/progenitor cells are gated: rHSCs, $CD45^+/Lin^-/CD54^+$ (region P3), and rVSELs, $CD45^-/Lin^-/CD54^+$ (region P4). Both populations are further "back-gated" on FSC versus SSC dot-plot to visualize cell size distribution. *Lower, middle dot-plot* cells stained for CD106, derived from gate P2, and analyzed for CD106 versus CD45 expression; rHSC, $CD45^+/Lin^-/CD106^+$ (region P3), and rVSELs, $CD45^-/Lin^-/CD106^+$ (region P4). Both populations are further "back-gated" on FSC versus SSC dot-plot to visualize cell size distribution. Percentages show content of each subpopulation among TNCs in representative sample. Total 1×10^6 of TNCs was typically collected for each sample to identify the SC populations. (b) Representative images of nonhematopoietic cells expressing CD54 and CD106 by ImageStream X system (ISS-X). TNCs were stained for Lin markers (FITC, green), CD45 (Alexa Fluor 647, blue), CD54 (PE, orange), or CD106 (PE, orange). Cells were fixed and nuclei were stained with Hoechst 33342 prior to analysis by ISS. Extracellular expression of CD106 and CD54 is shown on combo as well as on magnified images (right panels). The scale bars indicate 10 μm.

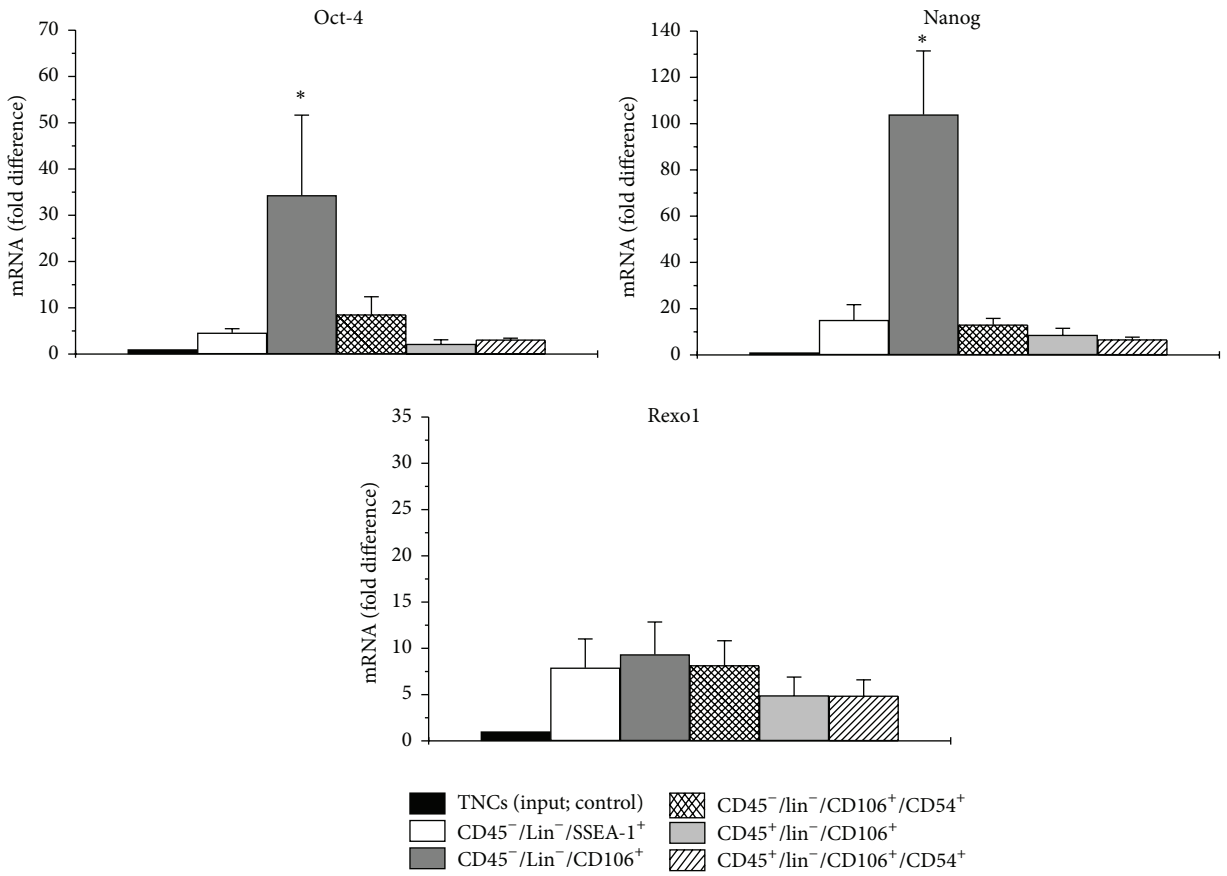

Figure 2: Expression of mRNA for Oct-4, Nanog, and Rexo-1 by real-time RT-PCR in sorted fractions of BM cells. Indicated populations of nonhematopoietic ($CD45^-/Lin^-/CD106^+$, $CD45^-/Lin^-/CD106^+/CD54^+$, and $CD45^-/Lin^-/SSEA\text{-}1^+$) and hematopoietic ($CD45^+/Lin^-/CD106^+$, $CD45^+/Lin^-/CD106^+/CD54^+$) cells were sorted with MoFlo XDP. The graphs show the fold difference in concentration of mRNA for Oct-4, Nanog, and Rexo-1 in sorted fractions when compared to unfractionated TNCs (shown as 1). Results are presented as mean ± SD. Statistically significant differences ($P < 0.05$) are shown when compared with TNCs. Analysis was performed three times with samples prepared from three independent sorts.

low values of FSC and SSC parameters (Figure 1(a)). We found that especially $CD45^-/Lin^-/CD106^+$ fraction exhibited morphology of very small cells in comparison with its hematopoietic counterpart ($CD45^+/Lin^-/CD106^+$) when "back-gated" on FSC versus SSC dot-plot (Figure 1(a)). Moreover, we confirmed the existence of such small cellular objects within both identified populations of $CD45^-/Lin^-/CD54^+$ or $CD45^-/Lin^-/CD106^+$ cells by ImageStream system (Figure 1(b)).

3.2. Rat BM-Derived $CD45^-/Lin^-/CD106^+$ Population Contains Developmentally Early rVSELs Expressing Oct-4 and Nanog Pluripotency Markers. Thus, by employing two staining and gating strategies on MoFlo XDP cell sorter, we focused on two subpopulations expected to potentially contain rVSELs: (1) $CD45^-/Lin^-/CD106^+$ and (2) $CD45^-/Lin^-/CD106^+/CD54^+$. We further evaluated the expression of selected VSEL-related genes (Oct-4, Nanog, and Rexo1) whose expression we consider as indicator for the potential presence of rVSELs in such sorted fractions (Figure 2). Additionally to hematopoietic counterparts ($CD45^+/Lin^-/CD106^+/CD54^+$ and $CD45^+/Lin^-/CD106^+$ cells), we also purified nonhematopoietic fraction ($CD45^-/Lin^-$) of rat BM cells expressing SSEA-1 which has been recently reported as rat VSEL population by Wu et al. [33]. We planned to pursue this fraction further in our experiments if enrichment in mRNA for VSEL-related genes is found within these cells. We found significantly greater concentration in mRNA for both vast transcription factors regulating cell pluripotency (Oct-4A and Nanog) in purified $CD45^-/Lin^-/CD106^+$ population of rat BM cells when compared to unfractionated BM cells (TNCs; input cells) and also to $CD45^-/Lin^-/SSEA\text{-}1^+$ fraction (Figure 2, Table 2). However, opposite to our initial expectations, the expression of Oct-4 and Nanog in highly purified subfraction of $CD45^-/Lin^-/CD106^+/CD54^+$ cells was lower than in $CD45^-/Lin^-/CD106^+$ population (Figure 2, Table 2). These results indicated that CD54 was not a selection marker for Oct-4-expressing rVSELs and other markers need to be found to be coexpressed with CD106 and to enrich for rVSELs during sorting procedure.

We could also notice some upregulation in mRNA expression for Oct-4 and Nanog in $CD45^-/Lin^-/SSEA\text{-}1^+$ cells when compared to unpurified BM cells, but it was rather negligible and significantly lower when compared with

Table 2: Quantitative real time RT-PCR analysis of mRNA expression for genes related to pluripotency in purified populations of rat BM-derived populations.

Cells fractions	Pluripotent stem cells markers		
	Oct-4	Nanog	Rexo1
	Mean ± SD	Mean ± SD	Mean ± SD
Unfractionated TNCs (control)	1.00	1.00	1.00
$CD45^-/Lin^-/SSEA\text{-}1^+$	4.58 ± 0.91	15.08 ± 6.67	7.90 ± 3.11
$CD45^-/Lin^-/CD106^+$	34.30 ± 17.35	103.89 ± 27.56	9.34 ± 3.51
$CD45^+/Lin^-/CD106^+$	2.16 ± 0.91	8.63 ± 2.88	4.90 ± 2.00
$CD45^-/Lin^-/CD106^+/CD54^+$	3.11 ± 0.31	13.07 ± 2.72	8.15 ± 2.66
$CD45^+/Lin^-/CD106^+/CD54^+$	8.54 ± 3.85	6.69 ± 0.99	4.87 ± 1.73

Results are presented as values of ΔΔCt (average data based on 3 independent experiments; mean ± SD) when compared with whole unfractionated BM tissue (control; computed as 1.00).

purified $CD45^-/Lin^-/CD106^+$ population (Figure 2, Table 2). The level of mRNA expression for Rexo1 that also represents transcription factor expressed in pluripotent cells occurred to be the least discriminative for the tested populations and was fairly enriched in all three sorted nonhematopoietic populations (Figure 2, Table 2). Thus, the results indicate that the expression of CD106, but not CD54 and SSEA-1 antigens, defines developmentally early population of SCs in rat bone marrow.

Since our data from gene expression analysis indicated that the fraction of $CD45^-/Lin^-/CD106^+$ cells may be enriched in primitive SCs, we evaluated expression of Oct-4 and Nanog on protein level within (i) $CD45^-/Lin^-/CD106^+$ subpopulation gated on whole BM cells by ImageStream X system and we calculated morphological features of these cells (Figures 3 and 4) as well as in (ii) FACS-purified $CD45^-/Lin^-/CD106^+$ fraction by immunocytochemistry (Figure 5). Importantly, in terms of identification of expression of Oct-4, we employed exclusively antibodies that bind Oct-4A isoform related to stem cell pluripotency to focus entirely on SCs with such characteristics (Santa Cruz Biotechnology, sc-9081, CA, USA).

Both imaging platforms confirmed the existence of subpopulation of stem cells expressing Oct-4A and Nanog among $CD45^-/Lin^-/CD106^+$ fraction of rat BM cells (Figures 3 and 5). On the other hand, we did not observe any cells expressing Oct-4 or Nanog among sorted hematopoietic counterparts (Figure 5). We also directly measured several morphological features of Oct-4 expressing $CD45^-/Lin^-/CD106^+$ rVSELs when compared to other cells including diameter of individual cells (cell size) as well as N/C ratio and cytoplasmic area that confirmed primitive stem cell phenotype of rVSELs (Figure 4). We found that $CD45^-/Lin^-/CD106^+/Oct\text{-}4^+$ rVSELs possess the smallest size, the highest N/C ratio, and the smallest cytoplasmic area when compared to $CD45^-/Lin^-/CD106^+$ rHSCs and TNC population (Figure 4).

Importantly, only subfraction of $CD45^-/Lin^-/CD106^+$ cells stained positively for Oct-4A (Figure 5) indicating the need for further purification of these cells leading eventually to further enrichment in pluripotent rVSELs.

3.3. Optimized Protocol for Isolation of Rat BM-Derived rVSELs-Technical Hints. Since we established that $CD45^-/Lin^-/CD106^+$ population of rat BM cells exhibit higher concentration of mRNA for pluripotent stem cell markers such as Oct-4 and Nanog which was also confirmed on protein level, we moved to fine-tuning the sorting protocol for such SCs that would be applicable for isolation of these cells from both WT and eGFP-expressing rat BM tissue (Figure 6). We focused on BM tissue derived not only from WT, but also from transgenic eGFP-expressing rats, since the potential donor eGFP+ rVSELs may be tracked following transplantation into WT animals, which would be important for further studies of their biological properties *in vivo*.

Thus, we employed the following directly conjugated antibodies prior to sorting procedures to avoid any nonspecific binding: (i) Alexa Flour 647/APC-conjugated antibodies against Lin markers (anti-TCR$\alpha\beta$, anti-CD3, anti-CD11b/c, and anti-CD45RA); (ii) PE-Cy7-conjugated antibody for CD45, and (iii) PE-conjugated antibody for CD106 (all antibodies listed in Table 1) that allow for compensation and sorting also eGFP-expressing cells (Figure 6).

In the first gating step, all events including lymphocytes and sublymphocyte fraction with FSC^{low}/SSC^{low} parameters (enclosing small cell and debris) were included into sorting gate R1 ("*lymphgate extended into lower values of FSC*"; Figure 6(a)). In the next step of such gating strategy, doublets were excluded from sorting by employing gating on FSC-Width versus FSC-Height dot-plot (Figure 6(b)). Single cells from gate R2 were subsequently analyzed based on hematopoietic lineages (Lin) markers expression and Lin^- fraction derived from gate R3 (Figure 6(c)) was further visualized based on CD106 expression (Figure 6(d)). $CD106^+$ cells were finally gated based on CD45 expression on CD45 versus FSC-H dot-plot which allowed us to distinguish two populations of (1) rat VSELs ($FSC^{low}/SSC^{low}/CD45^-/Lin^-/CD106^+$) and (2) hematopoietic $CD45^+/Lin^-/CD106^+$ cells consisting of smaller and larger subfractions (Figure 6(e)). Importantly, the established new protocol for FACS sorting of CD106-expressing very small cells from rat bone marrow allows for isolation of developmentally early SCs expressing

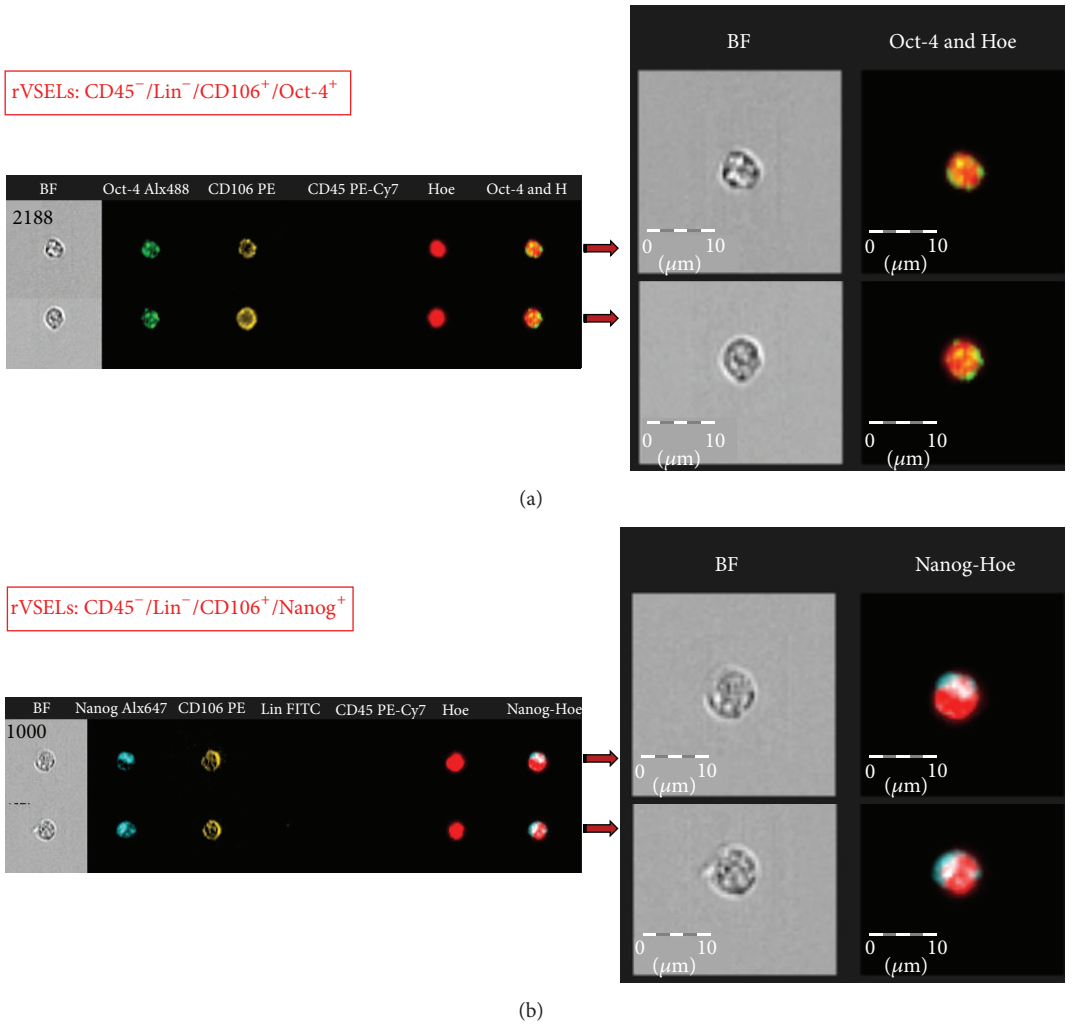

Figure 3: Expression of Oct-4A and Nanog in selected BM populations on protein level. Representative images of Oct-4A- and Nanog-expressing $CD45^-/Lin^-/CD106^+$ cells by ImageStream X system. TNCs were stained for (1) Oct-4A (Alexa Fluor 488, green), CD45 (PE-Cy7, magenta), and CD106 (PE, orange) (a) and (2) Nanog (Alexa Fluor 647, blue), Lin markers (FITC, green), CD45 (PE-Cy7, magenta), and CD106 (PE, orange) (b). Cell were stained with Hoechst 33342 to visualize nuclei and analyzed by ISS to detect intranuclear expression of Oct-4A (a) and Nanog (b) as shown in magnified, combined images. The scale bars indicate 10 μm.

Oct-4 and Nanog antigens from tissues of both WT and GFP animals.

4. Discussion

Recent evidence indicates that adult murine BM harbors a multitude of nonhematopoietic stem and progenitor cells in addition to well described HSCs [34, 35]. Such SC populations belonging to nonhematopoietic compartment of BM tissue include mesenchymal stem cells (MSC) [36], multipotent adult progenitor cells (MAPC) [10], marrow-isolated adult multilineage inducible cells (MIAMI) [9], multipotent adult stem cells (MASC) [11], and very small embryonic-like stem cells (VSEL) [31].

BM-derived murine VSELs have been isolated and characterized based on surface antigens as well as gene expression as a population of $Sca\text{-}1^+/Lin^-/CD45^-/Oct\text{-}4^+/Nanog^+$ cells [23]. VSELs morphology and ultrastructure have been also described indicating their very small size (smaller than erythrocytes) and higher N/C ratio which supports their primitive nature [24]. Importantly, several groups have reported the presence of such SCs in other murine and human tissues including ovaries and testes [16–22, 28, 29].

In this study, we isolated and antigenically defined in adult rat BM a population of stem cells with developmentally early characteristics that we may define as $FSC^{low}/SSC^{low}/CD45^-/Lin^-/CD106^+$ cells. Due to a very small size and the presence of other stem cell-related morphological features accompanied with expression of markers related to pluripotency including expression of Oct-4 and Nanog, we consider this population as rat counterpart of BM-derived murine VSELs. As such we called these cells rat VSELs (rVSELs).

In the first step, we tested and optimized two different protocols for sorting rVSELs by flow cytometry. The unique small size of VSELs requires optimized strategy for sorting

	ISS-X (IDEAS feature):	Area_Erode (M01, 2), mean	Area_Erode (M01, 2), std. dev.	Minor Axis_Erode (M01, 2), mean	Minor Axis_Erode (M01, 2), std. dev.	Nuclear_ Area_Erode (M07, 2), mean	Nuclear_ Area_Erode (M07, 2), std. dev.	Area_Erode(M01, 2) – Nuclear_Area_Erode (M07, 2), mean	Area_Erode(M01, 2) – Nuclear_Area_Erode (M07, 2), std. dev.	Nuclear_Area_Erode(M07, 2)/ [Area_Erode(M01, 2) – Nuclear_Area_Erode(M07, 2)], mean	Nuclear_Area_Erode(M07, 2)/ [Area_Erode(M01, 2) – Nuclear_Area_Erode(M07, 2)], std. dev.
Populations:	Corresponding cellular feature:	Cellular area (μm^2)	SD	Cell diameter (μm^2)	SD	Nuclear area (μm^2)	SD	Cytoplasmic area (μm^2)	SD	N/C ratio	SD
rVSELs	Lin^- $CD45^-CD106^+Oct\text{-}4^+$	25.99	2.56	5.32	0.39	18.32	3.00	7.88	2.63	2.326	0.776
rHSCs	Lin^- $CD45^+CD106^+Oct\text{-}4^-$	60.49	5.33	8.39	0.47	33.86	4.79	29.57	4.43	1.145	0.565
rTNCs	All cells (singlets)	56.49	20.07	7.79	1.45	30.91	13.4	22.71	10.52	1.361	0.691

	ISS-X (IDEAS feature):	Area_Erode (M01, 2), mean	Area_Erode (M01, 2), std. dev.	Minor Axis_Erode (M01, 2), mean	Minor Axis_Erode (M01, 2), std. dev.	Nuclear_ Area_Erode (M07, 2), mean	Nuclear_ Area_Erode (M07, 2), std. dev.	Area_Erode(M01, 2) – Nuclear_Area_Erode (M07, 2), mean	Area_Erode(M01, 2) – Nuclear_Area_Erode (M07, 2), std. dev.	Nuclear_Area_Erode(M07, 2)/ [Area_Erode(M01, 2) – Nuclear_Area_Erode(M07, 2)], mean	Nuclear_Area_Erode(M07, 2)/ [Area_Erode(M01, 2) – Nuclear_Area_Erode(M07, 2)], std. dev.
Populations:	Corresponding cellular feature:	Cellular area (μm^2)	SD	Cell diameter (μm^2)	SD	Nuclear area (μm^2)	SD	Cytoplasmic area (μm^2)	SD	N/C ratio	SD
rVSELs	Lin^- $CD45^-CD106^+Nanog^+$	29.62	5.79	5.70	0.67	18.94	4.16	10.72	4.46	1.767	0.735
rHSCs	Lin^- $CD45^+CD106^+Nanog^-$	57.91	7.80	8.23	0.60	30.94	2.55	27.03	7.94	1.145	0.336
rTNCs	All cells (singlets)	65.56	17.05	8.42	1.21	36.35	12.75	29.25	9.13	1.243	0.388

(a)

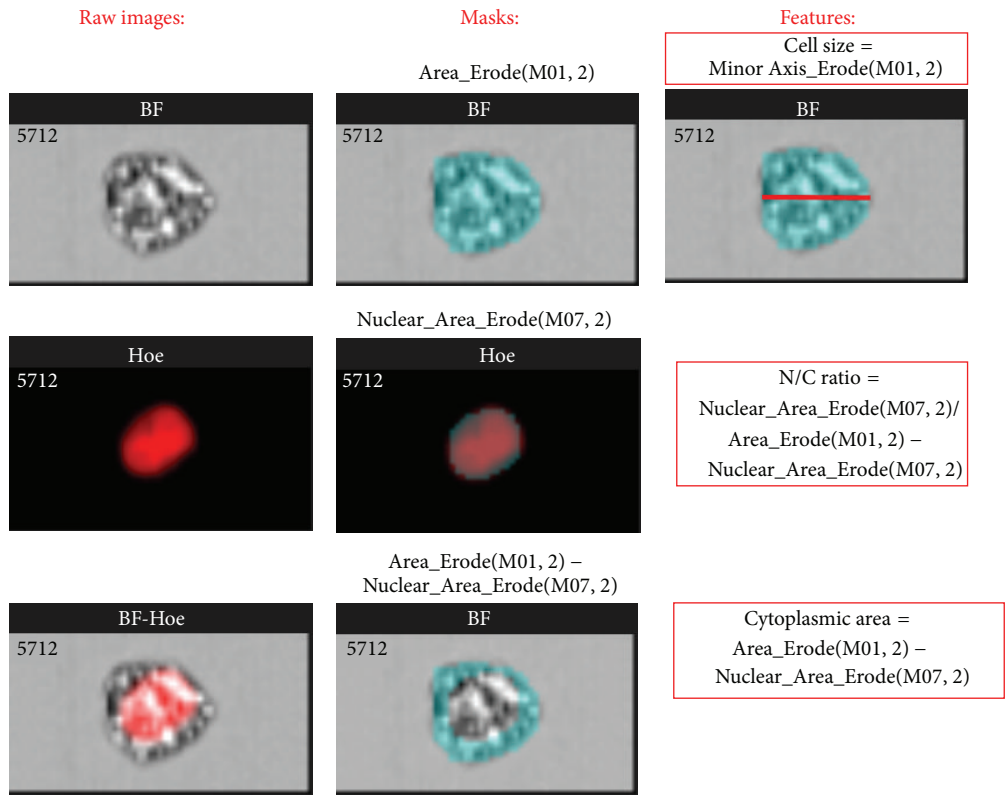

(b)

Figure 4: Quantitative analysis of morphological features of selected rat BM populations by ImageStream X system. (a) Quantitative analysis of cell size, nuclear to cytoplasmic (N/C) ratio, and cytoplasmic area of rVSELs when compared to other cell types. Analysis was performed based on the collected images of following rat BM populations: (i) rVSELs: $CD45^-/Lin^-/CD106^+$ cells expressing Oct-4A or Nanog (upper and lower table, resp.); (ii) rHSCs: $CD45^+/Lin^-/CD106^+$ cells with no expression of Oct-4A and Nanog, and (iii) TNCs (gated as singlets during the analysis). Analyses were performed with IDEAS software (Amnis Corp.). Data are shown as average values of each indicated feature within the cell population (mean ± SD). (b) Analytical approach for masking and feature calculation by IDEAS. Images show brightfield (BF), nuclear (Hoe), and combined (BF-Hoe) images of one example rat BM cell as well as exact masks (cyan) and features (formulas based on the defined masks) that were optimized and used for the analysis shown in (a). Cell size was expressed as minor cell axis computed within the mask covering BF image, while cytoplasmic area and N/C ratio were calculated based on the areas of BF and nuclear images (as indicated in red boxes). All masks and features including their nomenclature represent standard parameters provided by IDEAS software (Amnis Corp.)

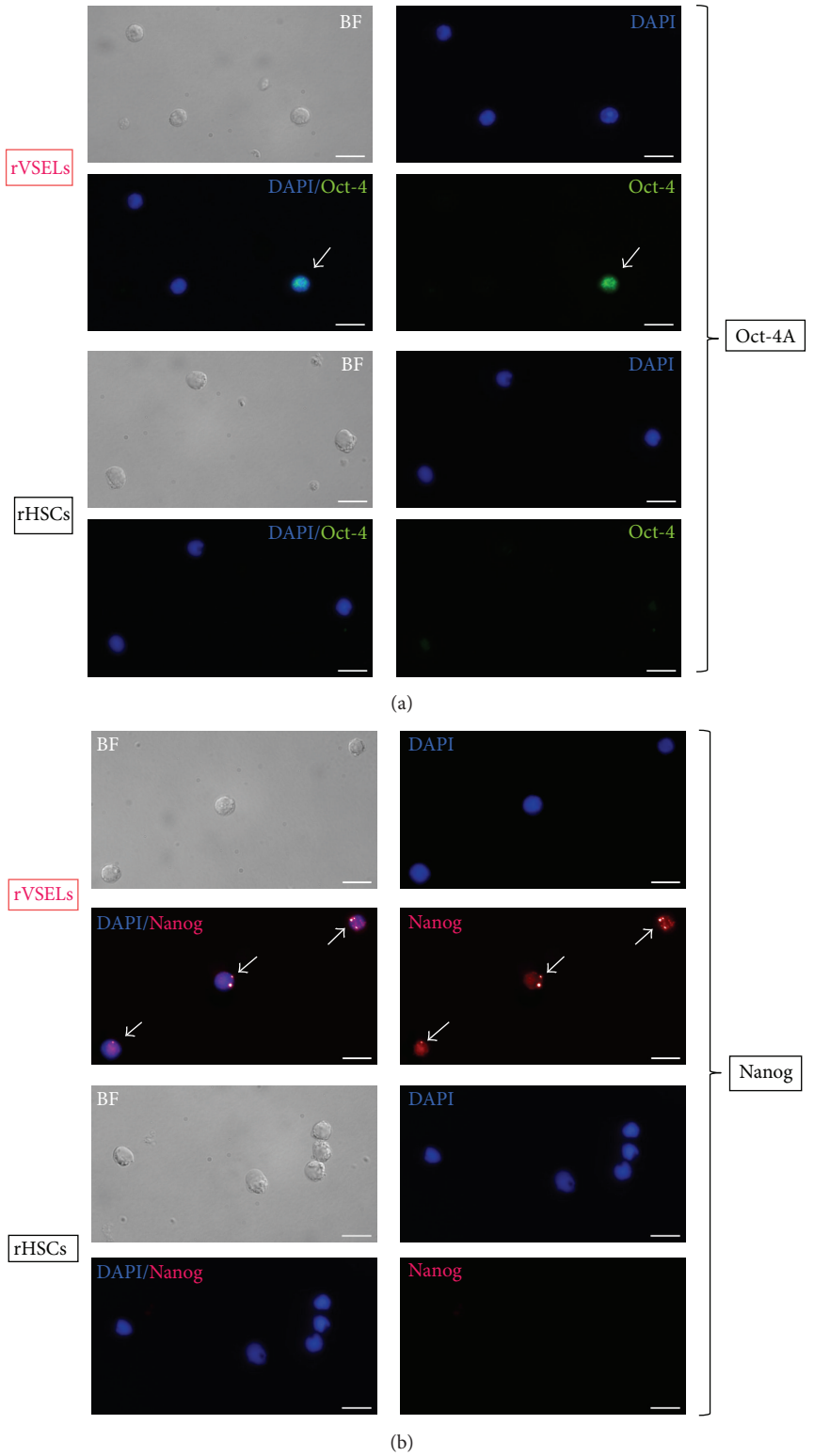

Figure 5: Expression of Oct-4A and Nanog in sorted fractions of rVSELs ($CD45^-/Lin^-/CD106^+$) and rHSCs ($CD45^+/Lin^-/CD106^+$) by immunocytochemistry. Both fractions were sorted with MoFlo XDP cell sorter (Beckman Coulter) and further stained for Oct-4A (Alexa Fluor 488, green) (a) or Nanog (Alexa Fluor 546, red) (b) and analyzed with Leica DMI6000B (ver. AF7000) fluorescent microscope. Nuclei are stained with DAPI. Intranuclear staining for both transcription factors is visualized on combo images. The scale bars indicate 10 μm.

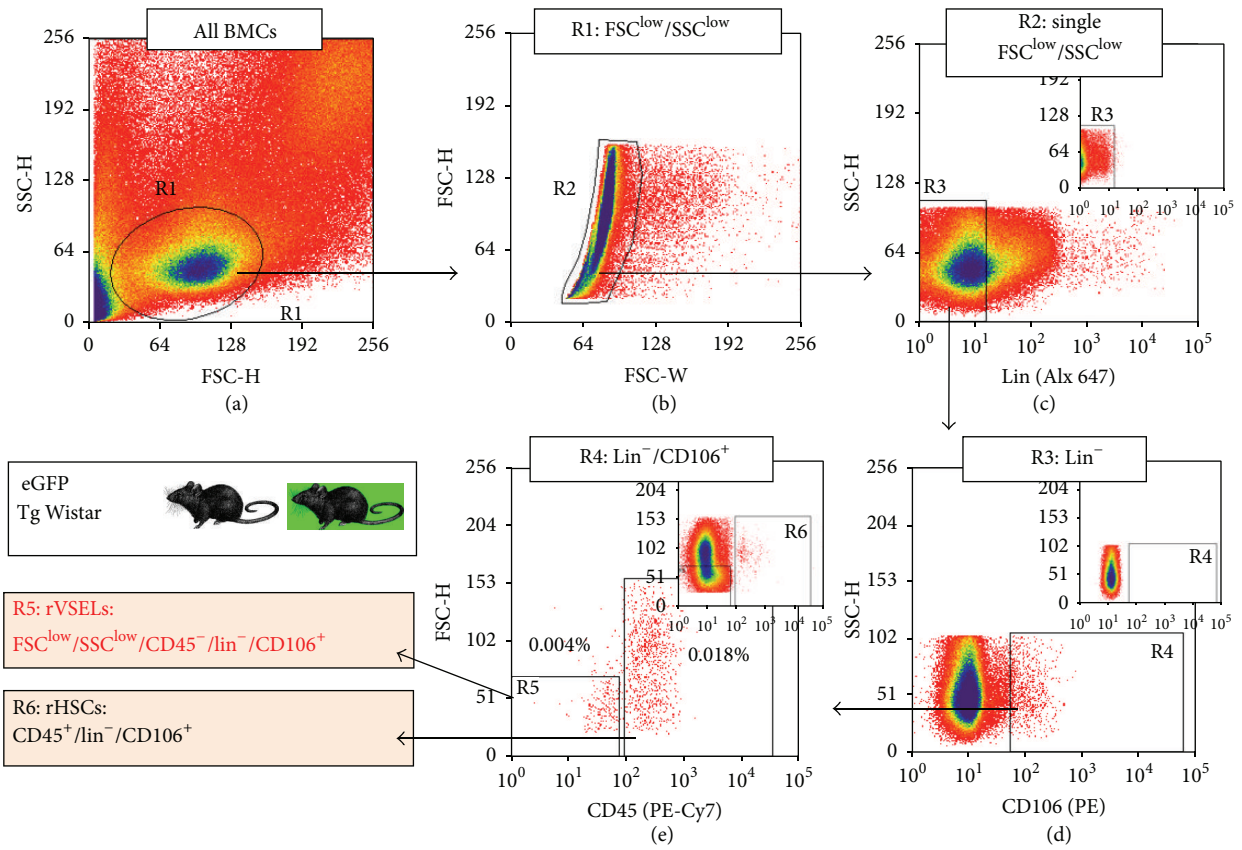

Figure 6: Optimized protocol for isolation of rVSELs from WT and eGFP-expressing rat BM tissue. Rat BM-derived VSELs were isolated from full population of BM cells stained for CD45 (PE-Cy7), Lin markers (TCR$\alpha\beta$, CD3, CD11b, and CD45RA; Alexa Fluor 647), and CD106 (PE) by MoFlo XDP cell sorter (Beckman Coulter). (a) Total nucleated cells (TNCs) are visualized on dot-plot showing FSC-H versus SSC-H. (b) Small agranular cells from gate R1 (with extension of lymphgate into low values of FSC; Figure 5(a)) are plotted on FSC-W versus FSC-H dot-plot to exclude doublets. (c) Single cells from gate R2 are subsequently analyzed for Lin markers expression. (d) Lin^- events included in region R3 are further plotted on dot-plot showing CD106 expression versus side scattered characteristics (SSC-H) of these cells. (e) $CD106^+$ cells from gate R4 are eventually visualized on dot-plot based on their CD45 expression and FSC signal (FSC-H). Rat HSCs are identified as $CD45^+/Lin^-/CD106^+$ (region R6), while rVSELs as $FSC^{low}/SSC^{low}/CD45^-/Lin^-/CD106^+$ cells (region R5).

that includes minimal threshold on instrument and extension the "lymphgate" into lowest values of FSC signal as described in several previous studies where VSELs were isolated [14, 25]. Based on the established protocols, we focused in our sorting gating strategy exclusively on small objects including lymphocytes and sublymphocyte fraction with FSC^{low}/SSC^{low} parameters that may enclose very small stem cells. Such approach in isolation of VSEL from murine and human specimens has been previously employed and successfully used by several groups [3, 15, 17, 25, 29] and represents a crucial step for successful isolation of these rare cells.

In the next step, we selected potential markers for purification of rat VSELs including CD54 and CD106 representing vast surface antigen potentially expressed on subset on murine VSELs. Although CD54 (ICAM-1) antigen has been found to be expressed on activated endothelial cells, T and B cells, monocytes/macrophages, granulocytes, and dendritic cells [37], it may also be expressed on stem cells [38, 39]. Similarly, CD106 (VCAM-1) may be expressed not only on mature myeloid cells, splendid dendritic cells, or induced endothelial cells, but also on more primitive bone marrow stem/stromal cells [40]. CD106 represents a counterreceptor for VLA-4 ($\alpha_4\beta_1$ integrin) [41] and the interactions between these molecules may play an important role in binding of leukocytes to activated endothelial cells and leukocyte extravasation at inflammatory sites as well as in stem cell migration [41, 42].

By employing multi-instrumental flow cytometric analysis, quantitative RT-PCR, and immunochemistry, we established that FACS-sorted population of $FSC^{low}/SSC^{low}/CD45^-/Lin^-/CD106^+$ rat VSELs expresses several markers of pluripotency including Oct-4, Nanog, and Rexo1. We established that isolation protocol described in this study may be more effective in isolation of developmentally early SCs when compared to $FSC^{low}/SSC^{low}/CD45^-/Lin^-/CD54^+$ population or $CD45^-/SSEA\text{-}1^+$ cells described by Wu and colleagues [33]. Here, for the first time we report that highly purified adult rat BM-derived $CD45^-/Lin^-/CD106^+$ cells may be enriched in fraction of SCs expressing markers of pluripotent cells such as Oct-4 and Nanog. Importantly, such

Table 3: Comparison of major features and phenotype of human and murine VSELs with rat BM-derived VSELs.

Feature	Human VSELs [3, 4, 12, 46]	Murine VSEL [1, 5, 12, 15, 23–25]	Rat VSELs
Morphology of "very small SCs" Cells smaller than red blood cells in researched typical species contain large nuclei surrounded by a narrow rim of cytoplasm	+	+	+
Size (by ISS)	6.75 ± 1.04 μm	3.63 ± 0.27 μm	5.32 ± 0.39 μm
Frequency (% of TNCs)	0.01%	0.02%	0.03%
Phenotype currently used for purification (FACS)*	$CD45^-/Lin^-/CD133/1^+$ $CD45^-/Lin^-/CD34^+$	$CD45^-/Lin^-/Sca\text{-}1^+$	$CD45^-/Lin^-/CD106^+$
Other surface antigen expression	$CD133/1^+$ ($AC133^+$), $CD34^+$, $SSEA\text{-}4^+$, AP^+, $c\text{-}Met^+$, $LIF\text{-}R^+$, $CXCR4^+$, $CD45^-$, Lin^-	$Sca\text{-}1^+$, $SSEA\text{-}1^+$, AP^+, $c\text{-}Met^+$, $LIF\text{-}R^+$, $CXCR4^+$, $CD45^-$, Lin^-, $HLA\text{-}DR^-$, MHC I^- $CD90^-$, $CD29^-$, $CD105^-$	$CD106^+$, $CD54^{+/-}$, $SSEA\text{-}1^+$, $CD45^-$, Lin^-
Expression of pluripotent SC transcription factors: Oct-4A and Nanog	+	+	+

(*) Lin – abbreviation indicating major markers characterizing main fractions of hematopoietic cell lineages present in BM tissue such as erythrocytes, monocytes, granulocytes, and subfractions of lymphocytes.

$CD45^-/Lin^-/CD106^+$ population remains still heterogeneous in terms of the expression of both markers indicating that further phenotypic characterization has to be performed. Interestingly, coexpression of CD54 does not indicate the population of rVSELs with greater Oct-4 and Nanog expression. Although single small cellular objects were found within $CD45^-/Lin^-/CD54^+$ population by ISS, we lost enrichment in early Oct-4- and Nanog-expressing rVSELs in $CD45^-/Lin^-/CD106^+/CD54^+$ fraction. The data indicates that other surface markers will be required in the future to enrich purification of the Oct-4- and Nanog-expressing rVSELs.

Importantly, since some cellular debris may be also sorted during rVSELs purification due to the very small size expected from stem cells, the imaging cytometry (ImageStream X; ISS-X) was also employed in our study to confirm that isolated rVSELs represent cellular nucleated objects. The ISS technology allows for statistical analysis of a variety of cellular parameters and for visualization of cells in suspension during flow analysis via high-resolution brightfield, darkfield, and fluorescence images collected with the high resolution [43–45]. Importantly, we have previously employed imaging cytometry for identification and characterization of VSELs from other specimens proving this technology as an optimal tool distinguishing real cellular objects such as small SCs from debris and artifacts present in different specimens [24, 25].

Interestingly, we confirmed that very small embryonic-like $CD45^-/SSEA\text{-}1^+$ stem cells described by Wu et al. are also enriched in mRNA for transcription factor (Oct-4, Nanog, and Rexo1) but the expression was lower when compared with purified $CD45^-/Lin^-/CD106^+$ rVSELs isolated in our study. Wu et al. described nonhematopoietic $CD45^-/SSEA\text{-}1^+$ cells, which were characterized by small size (4-5 μm), large nucleus, small amount of cytoplasm, expression of PSC transcription factors, and ability to differentiate into the cells from 3-germ layer under special conditions [33]. Thus, these observations may strongly suggest that rat $CD45^-/SSEA\text{-}1^+$ and $CD45^-/Lin^-/CD106^+$ may overlap that would need to be further investigated.

5. Conclusions

In conclusion, we identified and characterized in adult rat bone marrow a population of very small stem cells expressing Oct-4A and Nanog markers that shares phenotypic features of previously identified VSELs. The newly identified fraction of rat VSELs ($FSC^{low}/SSC^{low}/CD45^-/Lin^-/CD106^+$) may in fact correspond to murine and human VSELs based on their morphology and expression of pluripotent markers such as Oct-4, Nanog, and Rexo1 on mRNA level and protein levels. Comparison of human and murine VSELs as well as newly identified rVSELs is shown in Table 3.

Although our results indicated CD106 as a first positive selection marker for Oct-4A-expressing rat VSELs, further antigens need to be found to enrich these unique stem cells during isolation procedures, when used in coexpression with CD106. Thus, further efforts are needed to exactly define multiantigenic profile of BM-derived rVSELs as well as to further characterize biological properties and functionality of these newly identified rat stem cells.

However, this is the first study optimizing flow cytometric sorting strategies for purification of rat BM-derived $Oct\text{-}4A^+$ VSELs from both wild type (WT) and eGFP-expressing animals for further experimental purposes in this species. The described phenotype may be employed for further studies of rVSELs in multiple other rat tissues and organs including ovaries and testes. Importantly, the donor eGFP-expressing rVSELs may be followed after transplantation which would

allow for further studies of biological properties of these cells *in vivo*.

Importantly, this study opens new perspectives for studying VSELs in several rat tissues and organs in normal healthy conditions as well as for examining their potential regenerative capacity in several unique rat tissue injury models. This would provide a new impact on current knowledge about VSELs including potential regenerative capacity of these unique SCs, which still need to be investigated in *in vitro* as well as *in vivo* studies.

Conflict of Interests

The authors declare no conflict of interests. No competing financial interests exist.

Acknowledgments

This work was supported by POIG.01.01.02-00-109/09 Grant and in part by Grant no. N N302 177338 to Ewa K. Zuba-Surma. The authors would like to thank Dr. Malgorzata Zawadzka and Dr. Bartosz Wylot from Nencki Institute of Experimental Biology, Polish Academy of Sciences, Warsaw, Poland, for providing rats and for designing primer sequences used in this study. The authors thank Jagiellonian Centre for Experimental Therapeutics (JCET) for access to flow cytometric facility. Faculty of Biochemistry, Biophysics and Biotechnology, JU, is a partner of the Leading National Research Center (KNOW) supported by the Ministry of Science and Higher Education.

References

[1] M. Kucia, M. Wysoczynski, J. Ratajczak, and M. Z. Ratajczak, "Identification of very small embryonic like (VSEL) stem cells in bone marrow," *Cell and Tissue Research*, vol. 331, no. 1, pp. 125–134, 2008.

[2] W. Wojakowski, M. Tendera, M. Kucia et al., "Mobilization of bone marrow-derived Oct-4+ SSEA-4+ very small embryonic-like stem cells in patients with acute myocardial infarction," *Journal of the American College of Cardiology*, vol. 53, no. 1, pp. 1–9, 2009.

[3] E. K. Zuba-Surma, I. Klich, N. Greco et al., "Optimization of isolation and further characterization of umbilical cord blood-derived very small embryonic/ epiblast-like stem cells (VSELs)," *European Journal of Haematology*, vol. 84, no. 1, pp. 34–46, 2010.

[4] E. K. Zuba-Surma and M. Z. Ratajczak, "Overview of very small embryonic-like stem cells (VSELs) and methodology of their identification and isolation by flow cytometric methods," *Current Protocols in Cytometry*, chapter 9: Unit 9.29, 2010.

[5] E. K. Zuba-Surma, M. Kucia, L. Rui et al., "Fetal liver very small embryonic/epiblast like stem cells follow developmental migratory pathway of hematopoietic stem cells," *Annals of the New York Academy of Sciences*, vol. 1176, pp. 205–218, 2009.

[6] G. Kögler, S. Sensken, J. A. Airey et al., "A new human somatic stem cell from placental cord blood with intrinsic pluripotent differentiation potential," *Journal of Experimental Medicine*, vol. 200, no. 2, pp. 123–135, 2004.

[7] S. Wakao, M. Kitada, Y. Kuroda et al., "Multilineage-differentiating stress-enduring (Muse) cells are a primary source of induced pluripotent stem cells in human fibroblasts," *Proceedings of the National Academy of Sciences of the United States of America*, vol. 108, no. 24, pp. 9875–9880, 2011.

[8] Y. Kuroda, S. Wakao, M. Kitada, T. Murakami, M. Nojima, and M. Dezawa, "Isolation, culture and evaluation of multilineage-differentiating stress-enduring (Muse) cells," *Nature Protocols*, vol. 8, no. 7, pp. 1391–1415, 2013.

[9] G. D'Ippolito, S. Diabira, G. A. Howard, P. Menei, B. A. Roos, and P. C. Schiller, "Marrow-isolated adult multilineage inducible (MIAMI) cells, a unique population of postnatal young and old human cells with extensive expansion and differentiation potential," *Journal of Cell Science*, vol. 117, no. 14, pp. 2971–2981, 2004.

[10] Y. Jiang, B. N. Jahagirdar, R. L. Reinhardt et al., "Pluripotency of mesenchymal stem cells derived from adult marrow," *Nature*, vol. 418, no. 6893, pp. 41–49, 2002.

[11] A. P. Beltrami, D. Cesselli, N. Bergamin et al., "Multipotent cells can be generated in vitro from several adult human organs (heart, liver, and bone marrow)," *Blood*, vol. 110, no. 9, pp. 3438–3446, 2007.

[12] W. Wojakowski, M. Kucia, E. Zuba-Surma et al., "Very small embryonic-like stem cells in cardiovascular repair," *Pharmacology and Therapeutics*, vol. 129, no. 1, pp. 21–28, 2011.

[13] M. Z. Ratajczak, E. K. Zuba-Surma, B. MacHalinski, J. Ratajczak, and M. Kucia, "Very small embryonic-like (VSEL) stem cells: purification from adult organs, characterization, and biological significance," *Stem Cell Reviews*, vol. 4, no. 2, pp. 89–99, 2008.

[14] M. Z. Ratajczak, E. Zuba-Surma, W. Wojakowski et al., "Very small embryonic-like stem cells (VSELs) represent a real challenge in stem cell biology: recent pros and cons in the midst of a lively debate," *Leukemia*, vol. 28, no. 3, pp. 473–484, 2014.

[15] E. K. Zuba-Surma, M. Kucia, J. Ratajczak, and M. Z. Ratajczak, "'Small stem cells' in adult tissues: very small embryonic-like stem cells stand up!," *Cytometry Part A*, vol. 75, no. 1, pp. 4–13, 2009.

[16] A. M. Havens, H. Sun, Y. Shiozawa et al., "Human and murine very small embryonic-like cells represent multipotent tissue progenitors, in vitro and in vivo," *Stem Cells and Development*, vol. 23, no. 7, pp. 689–701, 2014.

[17] H. Sovalat, M. Scrofani, A. Eidenschenk, S. Pasquet, V. Rimelen, and P. Hénon, "Identification and isolation from either adult human bone marrow or G-CSF-mobilized peripheral blood of $CD34^+/CD133^+/CXCR4^+/Lin\text{-}CD45^-$ cells, featuring morphological, molecular, and phenotypic characteristics of very small embryonic-l," *Experimental Hematology*, vol. 39, no. 4, pp. 495–505, 2011.

[18] I. Virant-Klun, T. Skutella, M. Hren et al., "Isolation of small ssea-4-positive putative stem cells from the ovarian surface epithelium of adult human ovaries by two different methods," *BioMed Research International*, vol. 2013, Article ID 690415, 15 pages, 2013.

[19] I. Virant-Klun, T. Skutella, M. Kubista, A. Vogler, J. Sinkovec, and H. Meden-Vrtovec, "Expression of pluripotency and oocyte-related genes in single putative stem cells from human adult ovarian surface epithelium cultured in vitro in the presence of follicular fluid," *BioMed Research International*, vol. 2013, Article ID 861460, 18 pages, 2013.

[20] K. Sriraman, D. Bhartiya, S. Anand, and S. Bhutda, "Mouse ovarian very small embryonic-like stem cells resist chemotherapy and retain ability to initiate oocyte-specific differentiation," *Reproductive Sciences*, vol. 22, no. 7, pp. 884–903, 2015.

[21] S. Anand, H. Patel, and D. Bhartiya, "Chemoablated mouse seminiferous tubular cells enriched for very small embryonic-like stem cells undergo spontaneous spermatogenesis in vitro," *Reproductive Biology and Endocrinology*, vol. 13, article 33, 2015.

[22] A. M. Havens, Y. Shiozawa, Y. Jung et al., "Human very small embryonic-like cells generate skeletal structures, in vivo," *Stem Cells and Development*, vol. 22, no. 4, pp. 622–630, 2013.

[23] M. Kucia, R. Reca, F. R. Campbell et al., "A population of very small embryonic-like (VSEL) CXCR4$^+$SSEA-1$^+$Oct-4$^+$ stem cells identified in adult bone marrow," *Leukemia*, vol. 20, no. 5, pp. 857–869, 2006.

[24] E. K. Zuba-Surma, M. Kucia, W. Wu et al., "Very small embryonic-like stem cells are present in adult murine organs: ImageStream-based morphological analysis and distribution studies," *Cytometry Part A*, vol. 73, no. 12, pp. 1116–1127, 2008.

[25] E. K. Zuba-Surma, M. Kucia, A. Abdel-Latif et al., "Morphological characterization of very small embryonic-like stem cells (VSELs) by ImageStream system analysis," *Journal of Cellular and Molecular Medicine*, vol. 12, no. 1, pp. 292–303, 2008.

[26] M. Kucia, E. Zuba-Surma, M. Wysoczynski et al., "Physiological and pathological consequences of identification of very small embryonic like (VSEL) stem cells in adult bone marrow," *Journal of Physiology and Pharmacology*, vol. 57, supplement 5, pp. 5–18, 2006.

[27] D. M. Shin, E. K. Zuba-Surma, W. Wu et al., "Novel epigenetic mechanisms that control pluripotency and quiescence of adult bone marrow-derived Oct4$^+$ very small embryonic-like stem cells," *Leukemia*, vol. 23, no. 11, pp. 2042–2051, 2009.

[28] D. Bhartiya, A. Mundekar, V. Mahale, and H. Patel, "Very small embryonic-like stem cells are involved in regeneration of mouse pancreas post-pancreatectomy," *Stem Cell Research and Therapy*, vol. 5, no. 5, article 106, 2014.

[29] S. H. Kassmer, H. Jin, P.-X. Zhang et al., "Very small embryonic-like stem cells from the murine bone marrow differentiate into epithelial cells of the lung," *Stem Cells*, vol. 31, no. 12, pp. 2759–2766, 2013.

[30] R. Iwaki, R. Nakatsuka, Y. M. Matsuoka et al., "Development of a highly efficient method for isolating very small embryonic-like stem cells identified in adult mouse bone and their stem cell characteristics," *ASH Annual Meeting Abstracts*, vol. 120, abstract 2345, 2012.

[31] M. Kucia, E. K. Zuba-Surma, M. Wysoczynski et al., "Adult marrow-derived very small embryonic-like stem cells and tissue engineering," *Expert Opinion on Biological Therapy*, vol. 7, no. 10, pp. 1499–1514, 2007.

[32] M. Z. Ratajczak, D.-M. Shin, R. Liu et al., "Very Small Embryonic/Epiblast-Like stem cells (VSELs) and their potential role in aging and organ rejuvenation—an update and comparison to other primitive small stem cells isolated from adult tissues," *Aging*, vol. 4, no. 4, pp. 235–246, 2012.

[33] J.-H. Wu, H.-J. Wang, Y.-Z. Tan, and Z.-H. Li, "Characterization of rat very small embryonic-like stem cells and cardiac repair after cell transplantation for myocardial infarction," *Stem Cells and Development*, vol. 21, no. 8, pp. 1367–1379, 2012.

[34] M. Kucia, R. Reca, V. R. Jala, B. Dawn, J. Ratajczak, and M. Z. Ratajczak, "Bone marrow as a home of heterogenous populations of nonhematopoietic stem cells," *Leukemia*, vol. 19, no. 7, pp. 1118–1127, 2005.

[35] S. H. Orkin and L. I. Zon, "Hematopoiesis and stem cells: plasticity versus developmental heterogeneity," *Nature Immunology*, vol. 3, no. 4, pp. 323–328, 2002.

[36] F. Anjos-Afonso and D. Bonnet, "Nonhematopoietic/endothelial SSEA-1$^+$ cells define the most primitive progenitors in the adult murine bone marrow mesenchymal compartment," *Blood*, vol. 109, no. 3, pp. 1298–1306, 2007.

[37] T. A. Springer, "Adhesion receptors of the immune system," *Nature*, vol. 346, no. 6283, pp. 425–434, 1990.

[38] S. Arkin, S. Ferrone, and J. M. Lipton, "Modulation of adhesion molecule CD54 expression on CD34$^+$ hematopoietic progenitors," *Experimental Hematology*, vol. 23, no. 7, pp. 588–596, 1995.

[39] S. Arkin, B. Naprstek, L. Guarini, S. Ferrone, and J. M. Lipton, "Expression of intercellular adhesion molecule-1 (CD54) on hematopoietic progenitors," *Blood*, vol. 77, no. 5, pp. 948–953, 1991.

[40] P. A. Koni, S. K. Joshi, U.-A. Temann, D. Olson, L. Burkly, and R. A. Flavell, "Conditional vascular cell adhesion molecule 1 deletion in mice: impaired lymphocyte migration to bone marrow," *Journal of Experimental Medicine*, vol. 193, no. 6, pp. 741–753, 2001.

[41] T. Kinashi, Y. S. Pierre, and T. A. Springer, "Expression of glycophosphatidylinositol-anchored and -non-anchored isoforms of vascular cell adhesion molecule 1 in murine stromal and endothelial cells," *Journal of Leukocyte Biology*, vol. 57, no. 1, pp. 168–173, 1995.

[42] A.-M. Perdomo-Arciniegas and J.-P. Vernot, "Co-culture of hematopoietic stem cells with mesenchymal stem cells increases VCAM-1-dependent migration of primitive hematopoietic stem cells," *International Journal of Hematology*, vol. 94, no. 6, pp. 525–532, 2011.

[43] D. A. Basiji, W. E. Ortyn, L. Liang, V. Venkatachalam, and P. Morrissey, "Cellular image analysis and imaging by flow cytometry," *Clinics in Laboratory Medicine*, vol. 27, no. 3, pp. 653–670, 2007.

[44] T. C. George, D. A. Basiji, B. E. Hall et al., "Distinguishing modes of cell death using the ImageStream multispectral imaging flow cytometer," *Cytometry A*, vol. 59, no. 2, pp. 237–245, 2004.

[45] W. E. Ortyn, B. E. Hall, T. C. George et al., "Sensitivity measurement and compensation in spectral imaging," *Cytometry Part: A*, vol. 69, no. 8, pp. 852–862, 2006.

[46] M. Kucia, M. Halasa, M. Wysoczynski et al., "Morphological and molecular characterization of novel population of CXCR4$^+$ SSEA-4$^+$ Oct-4$^+$ very small embryonic-like cells purified from human cord blood: preliminary report," *Leukemia*, vol. 21, no. 2, pp. 297–303, 2007.